SYMPOSIUM ON SURFACE SCIENCE 2024

St. Christoph am Arlberg, Austria
March 10 - 16, 2024

CONTRIBUTIONS

EDITORS
Friedrich Aumayr, Ulrike Diebold and Christoph Lemell
TU Wien

The Competence **C**enter for **E**lectrochemical **S**urface **T**echnology (CEST) is THE research center for electrochemistry and surface technology in Austria. We are carrying out fundamental and industrial research projects to set future standards for electrochemical surface and interface engineering. Within three areas, we work on technological transformations from fundamental research to future applications, thanks to value chain advantages in research, infrastructure and our partner network.

Electrochemical energy conversion

Bringing together sustainability, recycling, and organic electrochemistry to optimize energy storage, create new high value products from waste, and capture & convert CO_2.

- **Sustainability** - Lifecycle improvement of batteries and electronics, as well as the development and optimization of energy storages (e.g. for H_2).
- **Recycling** - High value product generation from plastic or organic waste.
- **Organic electrochemistry** - We develop technologies for capturing and converting CO_2 itself into a resource for producing chemicals and additives.

Analytical infrastructure

CEST's in-house high-end infrastructure and its skilled researchers are the key for our success in fundamental and industrial projects.

- **ELSA -** combined XPS and scanning auger setup.
- **LEIS -** Low energy ion spectroscopy. This technique enables in-depth chemical and structural profiling of atomic layers on surfaces.
- **SEM -** Scanning electron microscope withenergy-dispersive X-ray spectroscopy (**EDX**).
- **GD-OES** – in-depth investigation of the composition and structure of bulk materials via glow discharge optical emission spectroscopy.
- **HPLC & HPLC-MS –** With the possibility for real time in-line monitoring of gases such as CO_2 within electrochemical conversion towards chemicals.

Dry and sustainable surface technology

Development of novel surfaces to improve functionality, lifetime and their specific application range. We deliver solutions across:

- **Novel surface processes** - Organic, dry, and hazard free surface modifications ranging from chemical to Plasma, Laser, PVD and electrochemical processes.
- **Adhesive bonding** - Developing bonding solutions for hybrid and polymer materials ranging from polymeric liners to automotive industry.

Semiconductors and high-power electronics

We work on new surface technologies for semiconductor devices. Future high-power electronics require new processing solutions to meet the demands of sustainable infrastructures. CEST creates and adapts processes to suit these needs and solve high-power materials-related challenges.

Collaborations

We are open for all kind of partnerships ranging from EU to national project applications and subcontracting to ensure the successful realization of research projects.

Center for Electrochemical Surface Technology - **CEST**
Viktor-Kaplan-Straße 2, 2700 Wr. Neustadt, Austria

Mail: office@cest.at

Electrochemical energy conversion

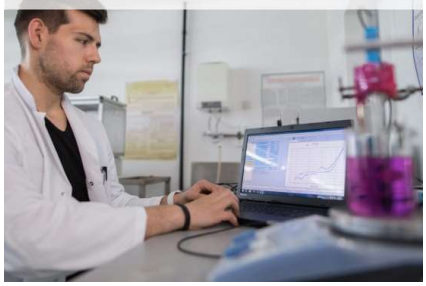

Surface technology

Adhesive bonding / testing

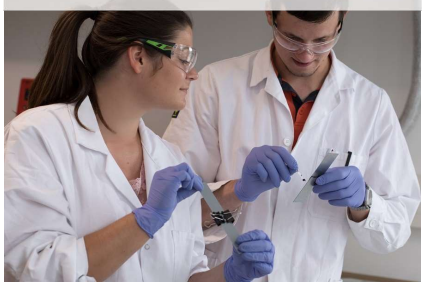

AEOLOS 150 | **µFOCUS** 450

THE MOST VERSATILE ELECTRON ANALYZER | X-RAY SOURCE COMBINATION FOR CUTTING EDGE XPS, HAXPES AND NAP-XPS

µFOCUS 450

- Multiple photon energies of 1487 eV, 2984 eV, 5415 eV
- Variable spot size from <100 µm to >1000 µm
- Ultimate photon flux densities
- Complete software control

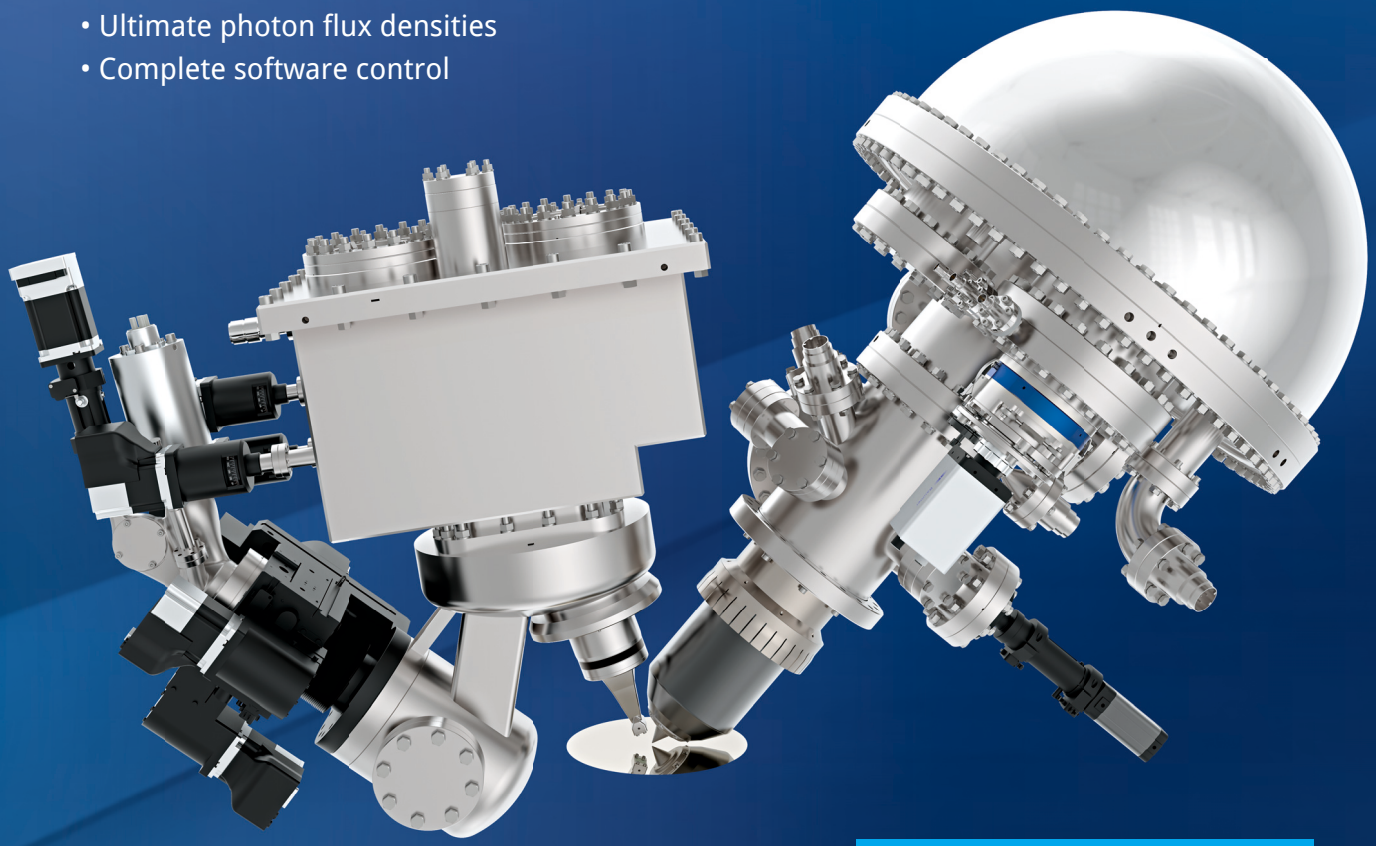

AEOLOS 150

- Transmission-optimized design
- Parallel angle detection, over 60°
- Puls counting AD-CMOS detector
- Optimized UHV and NAP modes

SPECS Surface Nano Analysis GmbH

T +49 30 46 78 24-0
E info@specs.com
H www.specs-group.com

SPECS™
A member of SPECSGROUP

SYMPOSIUM ON SURFACE SCIENCE 2024

St. Christoph am Arlberg, Austria
March 10 - 16, 2024

CONTRIBUTIONS

EDITORS
Friedrich Aumayr, Ulrike Diebold and Christoph Lemell
TU Wien

This symposium is organized by

Friedrich Aumayr, Ulrike Diebold & Markus Valtiner
TU Wien, Institute of Applied Physics (IAP)
Wiedner Hauptstr. 8-10/E134
1040 Vienna, Austria
https://ions.science/wp/3s24/

International Scientific Committee
A. Arnau, Donostia, ES
F. Aumayr, Vienna, AT
U. Diebold, Vienna, AT
H. Dil, London, Lausanne, CH
P. M. Echenique, Donostia, ES
K.-H. Ernst, Zürich, CH
S. Hasegawa, Tokyo, JP
J. Kunze-Liebhäuser, Innsbruck, AT
E. Lundgren, Lund, SE
M. Messing, Lund, SE
K. Morgenstern, Bochum, DE
P. Müller, Marseille, FR
F. Netzer, Graz, AT
K. Reuter, Berlin, DE
M. Rocca, Genova, I
W. D. Schneider, Lausanne, CH
T. Šikola, Brno, CZ
M. Valtiner, Vienna, AT

Organizing Committee
F. Aumayr (IAP, TU Wien)
U. Diebold (IAP, TU Wien)
C. Lemell (ITP, TU Wien)
M. Valtiner (IAP, TU Wien)

Venue
Ski Austria Academy, St. Christoph 10,
6580 St. Anton am Arlberg, Austria
www.skiakademie.at

Medieninhaber: F. Aumayr, U. Diebold, M. Valtiner, Institut für Angewandte Physik, Technische Universität Wien, Adresse: Wiedner Hauptstr. 8-10/E134, A-1040 Wien
Druck: R. & W. Smutny OEG, A-1110 Wien

PREFACE

We welcome all participants and accompanying persons to the 36th Symposium on Surface Science (3S). The 3S was founded in 1983 as a winter school by members of the Institute of Applied Physics of TU Wien in Vienna, Austria The conference seeks to promote the growth of scientific knowledge and its effective exchange among scientists in the field of surface physics and chemistry and related areas, including applied topics. Its format is similar to that of Gordon Conferences, with ample time for discussions and joint outdoor activities. Attendance is kept below 100 to ensure active communication among all participants.
Originally, the 3S was held exclusively in Austria and took place every other year. It became an annual event in 1990, and the site started to alternate between locations in France and Austria. From 1998 on, the 3S evolved into a truly global conference, with venues in the US, Canada, Bulgaria, Japan, Switzerland, Spain, France, Sweden and very recently also Italy, always returning to Austria in alternate years. Only once, in 2021, the 3S had to be cancelled due to the Covid-19 pandemic.

We hope that all participants will again experience a lively and successful in-person meeting in this beautiful mountain region of Austria.

Fritz Aumayr Ulrike Diebold Markus Valtiner

Peter Varga 3S-Poster Prize

In memory of one of the founding fathers of the 3S workshop series, Peter Varga (1946 – 2018), the *Peter Varga 3S-Poster Prize* is awarded every year starting with 3S*19.

List of prize winners

3S*19	Ales Cahlik (CAS, Praha, Czech Republic)
3S*20	Anna Niggas (TU Wien, Vienna, Austria)
3S*21	Wolf Dieter Schneider (Lausanne, Switzerland)
3S*22	Johannes Brötzner (TU Wien, Vienna, Austria)
3S*23	Giada Franceschi (TU Wien, Vienna, Austria)

Dates and locations of 3S conferences:

1983	(31.01.-04.02.)	Obertraun	AT
1985	(27.01.-02.02.)	Obertraun	AT
1988	(22.05.-28.05.)	Kaprun	AT
1990	(11.03.-17.03.)	La Plagne	FR
1991	(10.02.-16.02.)	Obertraun	AT
1992	(15.03.-21.03.)	La Plagne	FR
1993	(09.05.-15.05.)	Kaprun	AT
1994	(06.03.-12.03.)	Les Arcs	FR
1995	(23.04.-29.04.)	Kaprun	AT
1997	(26.01.-31.01.)	Aussois	FR
1998	(29.03.-04.04.)	Park City	US
1999	(21.02.-27.02)	Pamporova	BG
2000	(15.02.-18.02.)	Kananaskis	CA
2001	(07.01.-13.01.)	Furano	JP
2002	(03.03.-09.03.)	St.Christoph/Arlberg	AT
2003	(30.03.-05.04.)	La Plagne	FR
2004	(29.02.-06.03.)	St.Christoph/Arlberg	AT
2005	(13.03.-19.03.)	Les Arcs 1800	FR
2006	(05.03.-11.03.)	St. Christoph/Arlberg	AT
2007	(11.03.-17.03.)	Les Arcs 2000	FR
2008	(02.03.-08.03.)	St. Christoph/Arlberg	AT
2009	(08.03.-14.03.)	St. Moritz	CH
2010	(07.03.-13.03.)	St. Christoph/Arlberg	AT
2011	(06.03.-12.03.)	Baqueira Beret	ES
2012	(11.03.-17.03.)	St. Christoph/Arlberg	AT
2013	(03.03.-09.03.)	Åre	SE
2014	(09.03.-15.03.)	St. Christoph/Arlberg	AT
2015	(22.03.-28.03.)	Les Arcs 1800	FR
2016	(21.02.-27.02.)	St. Christoph/Arlberg	AT
2017	(05.03.-10.03.)	St. Moritz	CH
2018	(25.02.-03.03.)	St. Christoph/Arlberg	AT
2019	(10.03.-16.03.)	Baqueira Beret	ES
2020	(01.03.-07.03.)	St. Christoph/Arlberg	AT
2021	Cancelled due to Covid-19 pandemic		
2022	(13.03.-19.03.)	St. Christoph/Arlberg	AT
2023	(12.03.-18.03.)	Courmayeur/AostaValley	IT
2024	(10.03.-16.03.)	St. Christoph/Arlberg	AT

SYMPOSIUM ON SURFACE SCIENCE 2024

St. Christoph am Arlberg, Austria
March 10 – 16, 2024

Time Schedule

Sunday, 10 March 2024

16:00 – 18:30	**Registration**
20:00 – 20:20	**Opening**
	Chair: F. Aumayr
20:25 – 20:45	**S. Maier** *Atomically precise vacancy lattices in epitaxially grown $FeBr_2$ and $CoBr_2$ on Au(111)*
20:45 – 21:05	**O.M. Magnussen** *In situ studies of Cu surface restructuring during electrochemical CO_2 reduction*
21:05 – 21:25	**J.V. Barth** *Surface-confined metalated graphdiyne sheet*

Monday, 11 March 2024

Chair: F. Netzer

08:00 – 08:20 **K. Reuter**
Exploring Mesoscopic Mass Transport Effects on Electrocatalytic Selectivity

08:20 – 08:40 **E. Lundgren**
Probing the electrode-liquid interface using surface sensitive x-ray absorption spectroscopy

Chair: U. Diebold

16:40 – 17:00 **W.D. Schneider**
A short history of spectroscopic manifestations of the Kondo effect

17:00 – 17:20 **A. Odobesko**
Experimental evidence of new many-body spinaron excitations in Co atoms on Cu(111)

17:20 – 17:40 **D. Sánchez-Portal**
Kondo Effect of Co-Porphyrin: Remarkable Sensitivity to Adsorption Sites and Orientations

17:40 – 18:00 **A.L. Vázquez de Parga**
Probing the phase transition to a coherent 2D Kondo lattice

18:00 – 18:20 **H. Dil**
Altermagnetism; a new surface science playground?

Chair: R. Bliem

19:30 – 19:50 **K. Morgenstern**
Single-molecule visualization of electron solvation induced kinetics within ammonia

19:50 – 20:10 **F.J. Giessibl**
Atomic Scale Manipulation with an Unexpected Intermediate State

20:10 – 20:30 **F. Moresco**
Translation and rotation of a single molecule on Au(111) between thermal and electronic inelastic excitations

20:30 – 20:50 **H. Brune**
Electron Spin Resonance of Individual Rare-Earth Ions

20:50 – 21:10 **N. Zaiats**
Time-resolved photoemission electron microscopy of the near-field dynamics in nanowires excited by few-cycle short-wave infrared pulses

Tuesday, 12 March 2024

Chair: C. Lemell

08:00 – 08:20 **M. Willinger**
Graphene folding and fabrication of twisted layer graphene

08:20 – 08:40 **U. Starke**
Epitaxial Graphene Nanoribbons: One-dimensional confinement and pn-junction array

Chair: A. Niggas

16:40 – 17:00 **V. Chesnyak**
From Single Atoms to Clusters: Co nanostructures on C-Modified Ni Supports

17:00 – 17:20 **M. Jugovac**
Single-spin flat bands in cobalt-supported graphene

17:20 – 17:40 **J. Yuhara**
Continuous growth of germanene and stanene lateral heterostructures

17:40 – 18:00 **A. Molle**
Two-Dimensional Epitaxial Silicene: Synthesis, and Processing Paths for Technology Applications

18:00 – 18:20 **D. Akinwande**
Two-dimensional atomic surfaces for defect-mediated resistive switching phenomenon

Chair: F. Mittendorfer

19:30 – 19:50 **S.-X. Liu**
Chemical principles for N-doped graphene nanostructures of different dimensionality

19:50 – 20:10 **D.G. de Oteyza**
On-surface synthesis and characterization of [19]-starphene

20:10 – 20:30 **A. Vestergaard**
Covalent M-Porphyrin Networks: Synthesis, ORR/OER Performance and Stability

20:30 – 20:50 **M. Baljozović**
Successive on-surface synthesis of fused anthracenyl-porphyrins

20:50 – 21:10 **M. Buck**
Beyond dense packing: supramolecular interactions as a design element in self-assembled monolayers

Wednesday, 13 March 2024

Chair: S. Decurtins

08:00 – 08:20 **V. Vonk**
The Dirty Surface Science of Niobium

08:20 – 08:40 **Z. Jakub**
How the support defines properties of 2D metal-organic frameworks: Fe-TCNQ on graphene vs. Au(111)

Chair: D. Miano

16:40 – 17:00 **D. Rath**
Setup for Angle-Selective IRAS – Investigation of CO and D_2O on TiO_2 (110)

17:00 – 17:20 **J. Pavelec**
Unveiling the Complexity of Single-Atom Catalysts on Rh-decorated TiO_2 (110) via Infrared Absorption Reflection Spectroscopy

Chair: P. Jelinek

17:25 – 18:20 **Poster Introduction**

R. Bliem
The role of defects in the initial oxidation of Ru(0001) and their effect on surface chemistry

C. Bocaniciu
Matrix dependence analysis enabling quantitative application of Low-Energy Ion Spectroscopy for wide bandgap semiconductor materials

A.T. Celebi
Ion-specific and concentration-dependent adsorption on mica surfaces: A molecular dynamics study

U. Diebold
The reconstructed Al_2O_3 (0001)- ($\sqrt{31}\times\sqrt{31}$)±R9° Surface: An ideal case for non-contact AFM

J. Doležal
Magnetism of single Tb atoms on MgO

M. Fellinger
Laboratory studies on sputtering of structured tungsten model surfaces

M. Hedevang
Exploring the oxygen poisoning of the MoS_2 catalyst at Near-Ambient Pressures of H_2O

L.A. Hellberg
Photon, electron, ion and atom emission kinetics from the $Cl_2^{gas} + K^{solid}$ reaction

P. Jelínek
On-surface synthesis of radical 2D supramolecular assemblies and metalorganic frameworks

P. Kocán
Diffusion of polarons in transition metal oxides – how far must the polaron fly?

U. Küst
Temperature-dependent reaction pathway selectivity and detection of a hidden carbon deposition channel in hydrocarbon oxidation

A. Lagin
Advancing Single-Atom Catalysis: Development of an Apparatus for Reactions at Near-Ambient Pressure

C. Lemell
Model for Nanopore Formation in Two-Dimensional Materials by Impact of Highly Charged Ions

F.J. Lewis
Extended support structure dictates the reactivity of model single-atom catalysts for dissociative oxygen adsorption

L. Lezuo
Atomic-scale imaging of K-feldspar surfaces and their interaction with water

D. Miano
Understanding interaction forces at silicon wafer interfaces to optimize nanoscale cleaning processes

F. Mittendorfer
The intrinsic short-range ordering of K^+ ions on cleaved muscovite mica

T. Moser
Au(111) Oxidation Imaged in Oxygen Free Alkaline Media with Electrochemical Scanning Tunneling Microscopy

E.I. Neziri
Ferromagnetism in a Monolayer 2D Metal-Organic Framework

A. Niggas
On the low-energy secondary electron emission from surfaces

A. Odobesko
The double-functionalized STM probe reveals the interference of Bogoliubov quasiparticles around magnetic Fe atoms on the superconducting Nb(110) surface

A. Rank
Towards lightwave driven magnetic field scanning tunneling microscopy

V.M. Silkin
Electronic states and collective electronic excitations in sub-atomic-thick slots

R. Spachtholz
Towards mid-Infrared Lightwave Scanning Tunneling Microscopy

M. Valtiner
Towards understanding interfacial thermodynamics: visualising and quantifying competitive adsorption on muscovite mica with AFM

19:30 – 21:30 **Postersession**

Thursday, 14 March 2024

Chair: V.M. Silkin

08:00 – 08:20 **K.-H. Ernst**
Enantioselective adsorption on ferromagnetic surfaces

08:20 – 08:40 **G.B. Vonbun-Feldbauer**
Calculating core-level binding energies for small molecules on magnetite (111)

Chair: A.T. Celebi

16:40 – 17:00 **J. Kunze-Liebhäuser**
Laboratory based NAP-XPS for probing the electrified solid-liquid interface

17:00 – 17:20 **A. Larsson**
The Oxygen Evolution Reaction Drives Passivity Breakdown of Ni-Cr-Mo alloys

17:20 – 17:40 **M.E. Messing**
Tuning the magnetic properties of Co-Ni bimetallic nanoparticles and turning them into $NiCo_2O_4$

17:40 – 18:00 **J. Ibañez-Azpiroz**
Bulk photovoltaic effect in nanotubes and layered Weyl semimetals

18:00 – 18:20 **P. Müller**
Experimental determination of forces on adatoms in external fields

Chair: M. Valtiner

19:30 – 19:50 **T. Berghaus**
Comeback of JT-Cooling for Low Temperature SPM: the new USM1200-JT

19:50 – 20:10 **F. Mirabella**
Enriching Photoelectron Spectroscopy Instrumentation: New Developments in NAP-XPS Analysis

20:10 – 20:30 **F. Altmann**
Computationally efficient model for the transport of multi-component electrolytes in chemically active nano-tubes

20:30 – 20:50 **J. Brötzner**
Sputtering yields of lunar soils under solar wind ion impact

20:50 – 21:10 **M. Kogler**
Using High Sensitivity – Low Energy Ion Scattering Spectroscopy (HSLEIS) to unravel the complex nature of multi principal element alloys

Friday, 15 March 2024

Chair: P. Kocan

08:00 – 08:20 **M. Setvin**
Structure of copper oxide films solved by noncontact AFM and machinelearning methods

08:20 – 08:40 **J. Libuda**
Atomic layer deposition of 2D semiconductors on atomically defined oxide surfaces: Insights from surface science

Chair: L.A. Hellberg

16:30 – 16:50 **M.A. Schneider**
C_{60} layers on epitaxial $CsPbBr_3$ films on Au(100)

16:50 – 17:10 **H. Sjö**
Spatially resolved surface X-ray diffraction on polycrystalline surfaces

17:10 – 17:30 **T. Šikola**
Strong coupling between surface excitations observed by STEM - EELS

17:30 – 17:50 **G. Zamborlini**
Probing the molecular conformation via photoemission orbital tomography

17:50 – 18:10 **D. Baranowski**
Angle-resolved photoemission mapping of hybrid states characteristic of metal-organic nanostructures

Chair: W. Swiech

18:30 – 18:50 **G. Rupprechter**
Single particle catalysis: Lanthanum effect on a Rh nanotip in hydrogen oxidation

18:50 – 19:10 **J.E. Ortega**
Simulating high-pressure surface reactions with molecular beams

19:10 – 19:50 **Giant Slalom Race Award Ceremony**

20:00 **Conference Dinner**

More Than You Expect

Use the Optimal Technology for All Vacuum Ranges

Your added value

- **Technological:** Pumps for vacuum generation down to ultra-high vacuum
- **Precise:** Vacuum measurement and analysis equipment
- **Safe:** Leak detectors and tightness control
- **Extensive:** Complete range with chambers, components and valves
- **Individual:** Customized vacuum solutions
- **Sustainable:** Pumps with energyefficient IPM motors and standby function

Pfeiffer Vacuum Austria GmbH
Businesspark 1B, 2100 Korneuburg
T +43 2262 72 777
office.at@pfeiffer-vacuum.com

PFEIFFER VACUUM

Your Success. Our Passion.

www.pfeiffer-vacuum.com

Content

Advanced Ion Beam Technology for Surface Analysis

M6

Superior SIMS Performance

The M6 is the latest generation of high-end TOF-SIMS instruments developed by IONTOF. Its design guarantees superior performance in all fields of SIMS applications.

M6 Plus

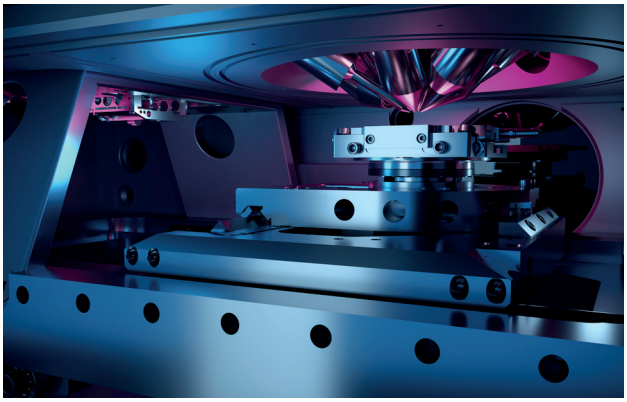

SIMS and SPM in situ

The M6 Plus is the tool for nano characterisation. Combining high-end performance SIMS and SPM, true in situ 3D chemical imaging becomes possible.

M6 Hybrid SIMS

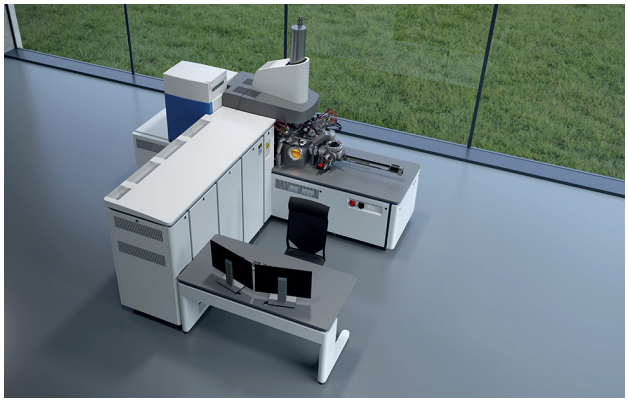

High-end Mass Spectrometry

With the Orbitrap™ extension for the M6, IONTOF introduces the first commercial SIMS instrument combining highest mass resolution and mass accuracy with high resolution cluster SIMS imaging.

Qtac

Top Atomic Layer Analysis

The Qtac is a high sensitivity low energy ion scattering (LEIS) instrument. It is extremely surface sensitive, providing small spot quantitative elemental characterisation of the top atomic layer.

CONTRIBUTIONS

Sunday

Atomically precise vacancy lattices in epitaxially grown $FeBr_2$ and $CoBr_2$ on Au(111)

F. Xiang[1], N. Bisht[2], B. Da[1], Ch. Neiss[2], A. Görling[2], S. Maier[1]

Department of Physics, Friedrich-Alexander-Universität Erlangen-Nürnberg, Germany
(corresponding author: S. Maier, e-mail: sabine.maier@fau.de)

[1] *Department of Physics, Friedrich-Alexander-Universität Erlangen-Nürnberg, Germany*

[2] *Department of Chemistry and Pharmacy, Friedrich-Alexander-Universität Erlangen-Nürnberg, Germany*

The generation of extensive 2D periodic patterns of point defects in 2D materials, such as vacancy lattices, has been a challenging task until now. Therefore, constructing atomically precise antidot lattices made of monovacancies has been constrained in size, whether assembled through bottom-up methods or through artificial structures created by manipulating individual atoms with low-temperature scanning tunneling microscopy.

Here, we report on 2D transition metal dihalides grown epitaxially on Au(111) featuring periodically assembled halogen vacancies that can function as antidot lattices.[1] Transition metal halides (TMHs) gained significant interest since the recent discovery of intrinsic ferromagnetism in these 2D van der Waals materials. For 2D transition metal dihalides, only a limited number of experimental surface science studies that provide atomic-scale insights into these materials' structure, growth, and defects have been presented so far.

Using low-temperature scanning tunneling microscopy, non-contact atomic force microscopy, and low-energy electron diffraction, we observe a periodic superstructure of Br vacancies in the top halide layer in $FeBr_2$ and $CoBr_2$ monolayers grown epitaxially on Au(111). Interestingly, the periodic arrangement of halogen vacancies results in a large number of atomically defined undercoordinated and stabilized transition metal atom sites, giving rise to an alternating 6-fold and 5-fold coordination of the transition metal atom across the film. Density-functional theory indicates

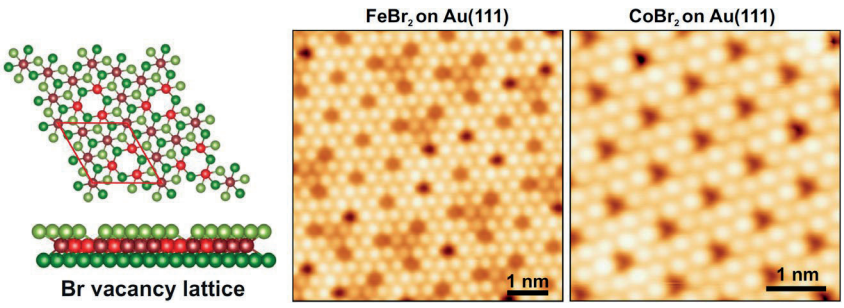

that Br-vacancies are favored due to low formation energies, and the formation of a vacancy lattice substantially reduces the lattice mismatch with the underlying Au(111). We demonstrate that interfacial strain engineering presents a versatile strategy for controlled patterning in 2D with atomic precision over several hundred nanometers to solve a longstanding challenge of growing atomically precise antidot lattices.

This work was funded by the German Research Foundation (DFG) through the SFB 953 Synthetic Carbon Allotropes (project number 182849149) and the Interdisciplinary Center for Molecular Materials (ICMM) at the Friedrich-Alexander-Universität Erlangen-Nürnberg.

[1] F. Xiang, et al. arXiv preprint arXiv:2305.06489, 2023.

In situ studies of Cu surface restructuring during electrochemical CO_2 reduction

R. Amirbeigiarab, J. Tian, A. Herzog[1], C. Qiu, A. Bergmann[1], B. Roldan Cuenya[1], O.M. Magnussen

Institut für experimentelle und angewandte Physik, Christian-Albrechts-Universität zu Kiel, D-24098 Kiel, Germany (corresponding author: O.M. Magnussen, e-mail: magnussen@physik.uni-kiel.de)

[1] 2Department of Interface Science, Fritz-Haber Institute of the Max-Planck Society, Berlin, Germany

The electrochemical reduction of carbon dioxide holds great promise for sustainable production of base chemicals and synthetic fuels. Copper catalysts are of particular interest, as they enable formation of multi-carbon compounds. Here, we present *in situ* scanning tunnelling microscopy (STM), surface X-ray diffraction (SXRD), and surface-enhanced Raman spectroscopy (SERS) studies of well-defined Cu(100) electrodes in CO_2-satured 0.1 M $KHCO_3$, which is one of the most common electrolytes for CO_2 electroreduction (CO_2RR).
For Cu(100) in the double layer potential range, coexistence of two ordered (bi)carbonate adlayer phases was observed [1]. These adlayer phases have a highly complex structure, exhibit dynamic fluctuations, and undergo a potential dependent order-disorder transition at about 0 V vs. the reversible hydrogen electrode. Detailed density functional calculations reveal the observed layer is composed of carbonate and water that coadsorb on the electrode surface, underlining the key role of water in the stabilization of the (bi)carbonate adlayers.
Upon decreasing the potential to the onset of CO_2RR, the formation of Cu nanoclusters is found on the Cu(100) surface by *in situ* STM [2]. This surface restructuring can be assigned to the influence of CO intermediates formed in the CO_2RR, as verified by *in situ* SERS. In situ SXRD allows to verify the presence of the nanoclusters down to -1.1 V, i.e. deep into the CO_2RR regime. Upon subsequently increasing the potential back into the double layer range, the clusters disperse, resulting in a highly disordered interface structure that contains Cu adatoms, (bi)carbonates, and further molecular adsorbates. This irreversible change of the molecular-scale electrode surface is supported by spectroscopic data. Our results demonstrate the spontaneous formation of low-coordinated surface species at the very onset of carbonate electroreduction which needs to be considered for a fundamental understanding and rational design of electrocatalysts for CO2RR.

The Authors gratefully acknowledge financial support by the Deutsche Forschungsgemeinschaft (DFG, German Research Foundation) via SPP 2080, project no. 327886311.

[1] R. Amirbeigiarab, A. Bagger, J. Tian, J. Rossmeisl, O.M. Magnussen, Angew. Chem. Int. Ed., 61, e202211360 (2022)

[2] R. Amirbeigiarab, J. Tian, A. Herzog, C. Qiu, A. Bergmann, B. Roldan Cuenya, O.M. Magnussen, Nature Catalysis, 6, 837 (2023)

Surface-confined metalated graphdiyne sheet

Ignacio Piquero-Zulaica[1], Yi-Qi Zhang[2,1], Wenqi Hu[2] , Ari Paavo Seitsonen[3], Felix Haag[1], Johannes Küchle[1], Francesco Allegretti[1], Yuanhao Lyu[2], Lan Chen[2], Kehui Wu[2], Zakaria M. Abd El- Fattah[4], Ethem Aktürk[5], Svetlana Klyatskaya[6], Mario Ruben[6], Matthias Muntwiler[7], Johannes V. Barth[1,*]

[1]Physics Department E20, Technical University of Munich, D-85748 Garching, Germany [2]Institute of Physics, Chinese Academy of Sciences, 100190 Beijing, China [3]Département de Chemie, École Normale Supérieure, 24 rue Lhomond, F-75005 Paris, France [4]Physics Department, Faculty of Science, Al-Azhar University, Nasr City, E-11884, Cairo, Egypt [5]Department of Physics, Adnan Menderes University, 09100 Aydin, Turkey [6]Institute of Nanotechnology, Karlsruhe Institute of Technology, 76344 Eggenstein-Leopoldshafen, Germany [7]Paul Scherrer Institute, Forschungsstrasse 111, 5232 Villigen PSI, Switzerland

Extended organometallic honeycomb alkynyl−silver networks representing metalated graphdiyne sheets have been synthesized on a noble metal surface under ultrahigh vacuum conditions via a gas- mediated surface reaction protocol. Specifically, the controlled exposure to molecular oxygen efficiently deprotonates terminal alkyne moieties of 1,3,5-tris(4-ethynylphenyl)benzene (Ext-TEB) precursors adsorbed on Ag(111), whereby long-range ordered alkynyl−silver networks incorporating substrate atoms are fabricated, featuring Ag-bis-acetylide motifs, high structural quality and a regular arrangement of nanopores with a van der Waals cavity of ≈8.3 nm^2 [1].

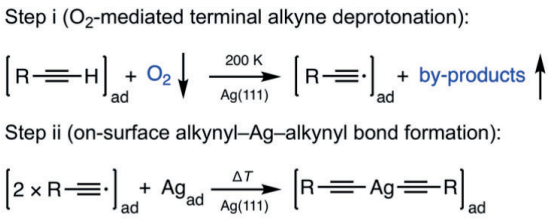

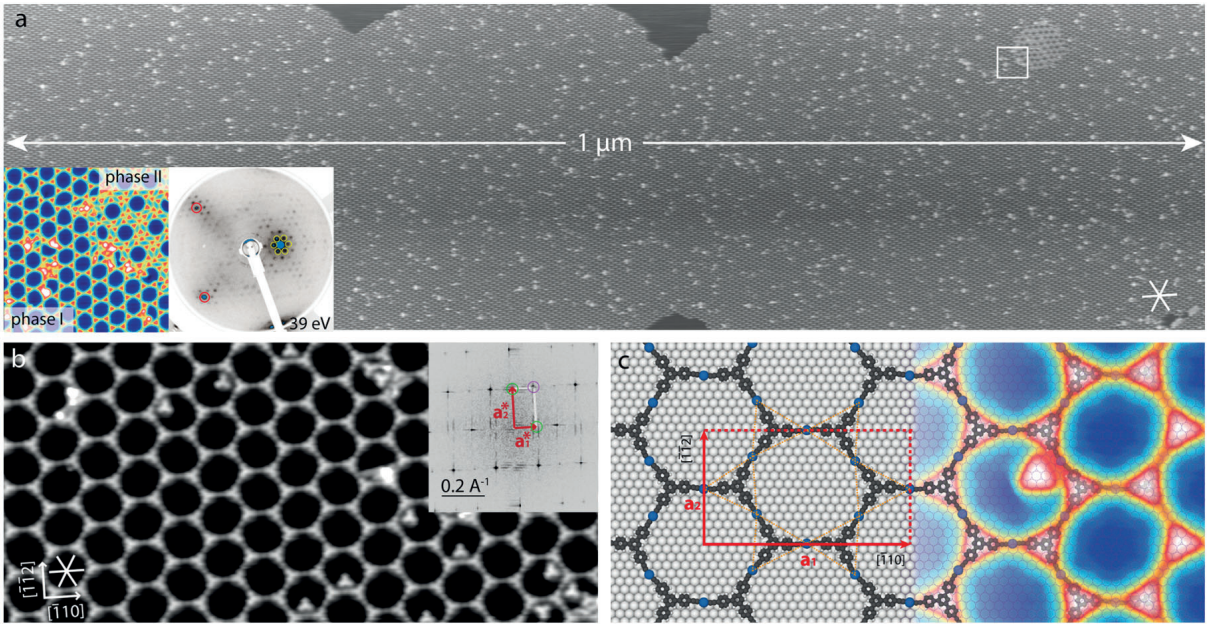

Upper panel: Large-scale STM image of sample annealed at 375 K, featuring a uniform, regular Ag-GDY sheet on Ag(111) extending at the micrometer scale. Lower panels: High-resolution STM image and DFT calculated unit cell with the network molecular registry superposed on experimental data.

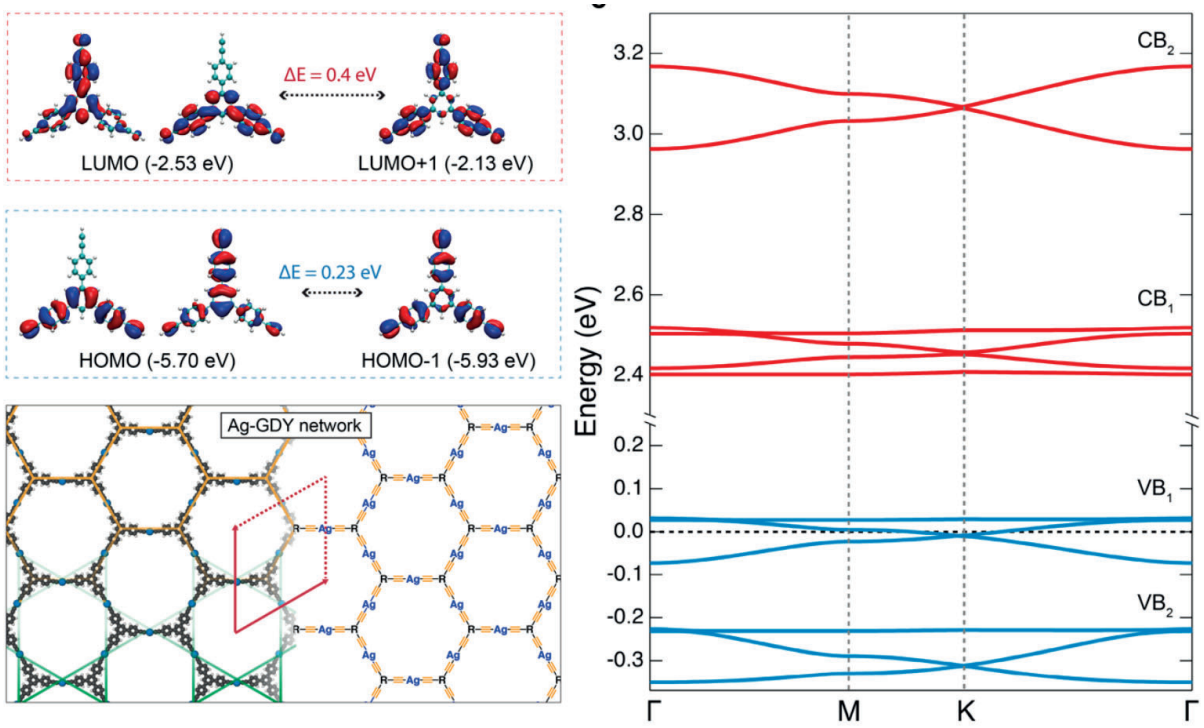

Left panels: DFT calculated frontier molecular orbitals of isolated Ext-TEB molecule | Model and chemical scheme of freestanding Ag-GDY sheet with rhombic unit cell; honeycomb and Kagome lattices occupied by molecules and Ag atoms are highlighted, respectively. Right panel: Band structure around the Fermi level and above the band gap of freestanding network.

The electronic features of the adsorbed layer are revealed by complementary scanning tunnelling and angle-resolved photoemission spectroscopies, demonstrating electronic band structure formation with an appreciable gap [2]. Extensive density functional theory calculations substantiate the experimental findings in line with recent theoretical insights on the proper combination of frontier molecular orbital and lattice symmetries to generate unconventional band structures. Finally, the transmetalation of the alkynyl-Ag-alkynyl linkages with copper atoms is recognized and implemented as a means to obtain a more robust Ag-GDY sheet with modified electronic properties [3].

[1] Y.-Q. Zhang et al., J. Am. Chem. Soc. 141 (2019), 5087.
[2] I. Piquero-Zulaica, A.P. Seitsonen, Y.-Q. Zhang et al., arXiv:2308.16049 (2023).
[3] W. Zhao, I. Piquero-Zulaica, B. Yang, F. Allegretti et al., subm. (2024).

Monday

Exploring Mesoscopic Mass Transport Effects on Electrocatalytic Selectivity

H.H. Heenen, H.S. Pillai, V.J. Bukas, and K. Reuter

Fritz-Haber-Institut der Max-Planck-Gesellschaft, Faradayweg 4-6, D-14195 Berlin, Germany
(corresponding author: K. Reuter, e-mail: reuter@fhi.mpg.de)

The rational design of more efficient electrocatalysts hinges upon improving our fundamental understanding of the underlying reaction mechanisms. At the microscopic level, these mechanisms are currently almost exclusively discussed through the lens of the catalytically active site [1]. The emerging mechanistic picture is one that is entirely focused on surface-bound reaction intermediates and the simple assumption that catalytic rates are directly controlled through the adsorption strength of these intermediates. Subsequent catalyst design strategies therefore revolve around tuning the nature of the active site, e.g. through doping or alloying.

This approach has been met with tremendous success in predicting activity trends across different catalysts in computational screening studies for e.g. the electrochemical oxygen reduction reaction (eORR), CO_2 reduction reaction (eCO2RR), and many others [1]. It has been known to fail, however, when it comes to more subtle aspects of the electrochemical kinetics. Such aspects can be decisive in determining the reaction path that is being followed and thus the final product that is being formed. Increasing experimental evidence, for example, shows electrocatalytic selectivity change with catalyst loading or reactor design in a non-obvious way that cannot be simply rationalized through considerations of the active site and its immediate chemical environment [2,3].

Such puzzling effects bring the active site model into perspective and suggest a possibly important mechanistic role for mesoscopic mass transport phenomena. In this talk, we discuss one particular such transport effect: the kinetic competition that arises from exchanging volatile reaction intermediates between the electrocatalyst surface and bulk electrolyte. This reaction model was first proposed by Behm and coworkers and coined the “desorption–re-adsorption-reaction” mechanism [4]. Basis for the underlying mechanism is the desorption of a specific surface-bound and usually closed-shell reaction intermediate, whose subsequent fate creates a bifurcation in the reaction pathway: either to re-adsorb onto the surface toward full conversion, or to entirely diffuse away and thus be detected as an early partially-converted product. Electrocatalytic selectivity is thus driven by the competition between surface kinetics and diffusion. Given this competition, descriptors of a catalyst’s morphology such as the catalyst loading or inter-particle distance become critical as they directly affect the probability of re-adsorption, i.e. the probability that the diffusing species returns to the surface for continued reaction rather than escaping as an early intermediate product.

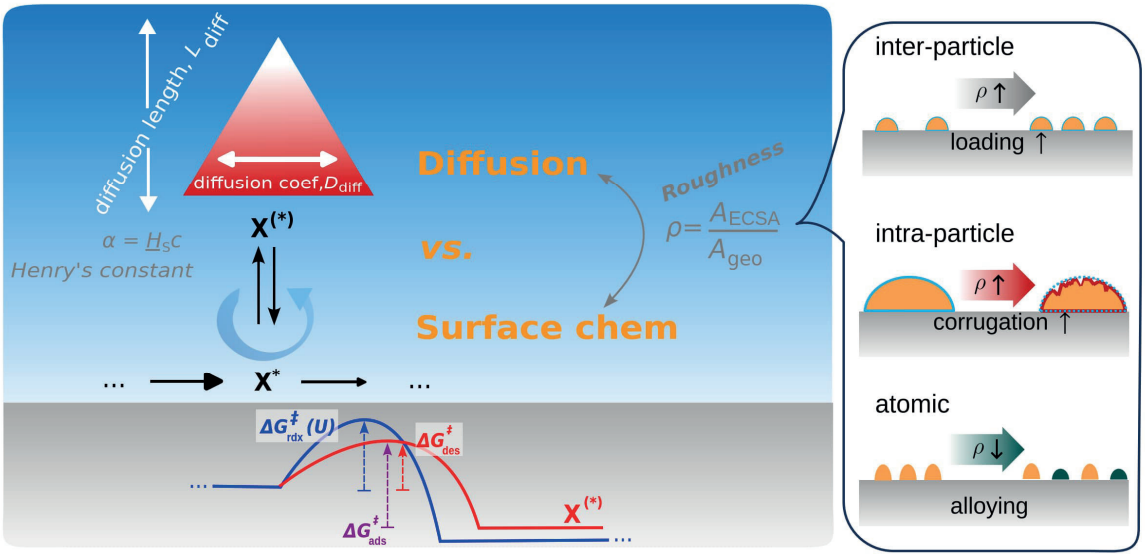

Figure 1: Schematic representation of the "desorption–re-adsorption-reaction" mechanism. A surface-bound, closed shell intermediate X^* faces the kinetic competition between a forward surface redox step vs. desorption. Following desorption, if diffusion is fast enough, near-surface $X^{(*)}$ species will escape into the bulk electrolyte and be detected as an early, partially-converted product. Our model couples diffusion with the surface kinetics via the surface roughness ρ which effectively captures the influence of catalyst morphology across multiple length-scales.

We explore the role of mesoscopic mass transport in determining electrocatalytic selectivity for a number of technologically important processes, including the eORR and different products of eCO2RR on Cu. Quantitative understanding of the underlying "desorption–re-adsorption-reaction" mechanism is established by developing a simple multi-scale model that couples diffusion to the electro-chemical surface kinetics. Our model correctly reproduces a series of trends found in the experimental literature, while providing an alternative or, at least, complementary explanation to changes in electrocatalytic selectivity beyond the active site model. Within this picture, the electrode surface roughness emerges as a descriptor of selectivity that effectively captures the influence of catalyst morphology across multiple length-scales: the mesoscopic scale at the inter-particle level, microscopic scale at the intra-particle level, and nanoscopic scale at the atomic level, cf. Fig. 1. Our analysis finally highlights the relevance of the "desorption–re-adsorption-reaction" mechanism in catalyst degradation as morphological changes over time (e.g. due to nanoparticle agglomeration) induce corresponding changes in electrocatalytic selectivity.

[1] Z.W. Seh, J. Kibsgaard, C.F. Dickens, I. Chorkendorff, J.K. Nørskov, and J.T. Jaramillo, Science 355, eaad4998 (2017).

[2] R. Kas, K. Yang, D. Bohra, R. Kortlever, T. Burdyny, and W.A. Smith, Chem. Sci. 11, 1738 (2020).

[3] N. Govindarajan, G. Kastlunger, H.H. Heenen, and K. Chan, Chem. Sci. 13, 14 (2022).

[4] Y.E. Seidel, A. Schneider, Z. Jusys, B. Wickman, B. Kasemo, and R.J. Behm, Faraday Discuss. 140, 167 (2009).

Probing the electrode-liquid interface using surface sensitive x-ray absorption spectroscopy

Andrea Grespi[1], Alfred Larsson[1], G. Abbondanza[1], E. Lira[1],
L. R. Merte[2], and Edvin Lundgren[1]

[1]*Division of synchrotron radiation research, Lund University, Lund, Sweden,*
[2]*Materials Science and Applied Mathematics, Malmö University, Malmö, Sweden.*
Edvin.Lundgren@sljus.lu.se

The electrified electrode electrolyte interface is notoriously difficult to study during electrochemical reactions. Most traditional surface science techniques are disqualified due to the use of electrons, an exception being Electro Chemical X-ray Photoelectron Spectroscopy (ECXPS) utilizing the so-called dip and pull method [1]. This approach is not without serious complications, such as the electrolyte film thickness reproducibility on the electrode surface, and issues with the EC properties in this thin liquid film. Scanning Tunneling Microscopy (STM) and Atomic Force Microscopy (AFM) has also been used but is limited due to lack of order and chemical sensitivity [2,3]. Photon-in-photon-out techniques, such as High Energy Surface X-Ray Diffraction (HESXRD) [4] and EC-IRAS [5] has frequently been used, however the former is not sensitive to amorphous structures often encountered in EC systems, while the latter probes molecular species at the surface and is less sensitive to the chemical composition of the electrode surface.

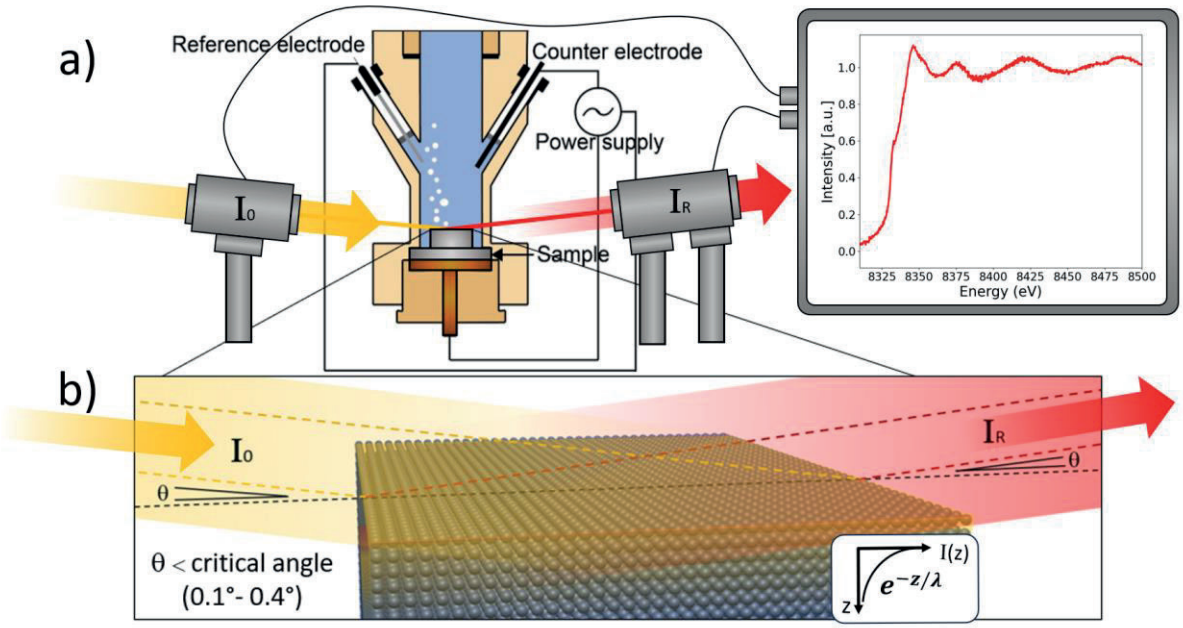

Figure 1 a) The incoming and reflected x-ray beam penetrating the EC-cell and impinges on the sample (working electrode) at an angle of incidence below the critical angle, resulting in total external reflection. The change in the intensity between the incident (I_0) and reflected beam (I_R) is then measured across the Ni k-edge. **b)** Illustration of the GIXAS experiment.

In this contribution we present an alternative approach. By using a combination of Grazing Incidence X-ray Absorption Spectroscopy (GIXAS) [6], 2D Surface Optical Reflectance (2D-

SOR) [7] and Cyclic Voltammetry (CV) from a Au(111) electrode surface, direct surface information during real-time CV can be obtained. A schematic of the GIXAS experimental setup and the experiment are shown in Fig. 1, including an absorption spectrum from the Ni k-edge.

The experiments were performed at the beamline Balder at MAXIV, providing a 30μ large and brilliant x-ray beam with extraordinary high stability, properties necessary to perform these experiments. Using H_2SO_4 as an electrolyte, our study demonstrate that a thin, passive Au oxide is formed at potentials corresponding to the oxidation peak in the Au CV. This oxide prevents further oxidation of the surface, and not until the onset of the Oxygen Evolution Reaction (OER), further oxidation of the Au surface occur leading to the formation of a thick Au oxide. The reduction peak in the CV coincide with the reduction of the Au oxide, and the potential for the reduction is shown to be dependent on the thickness of the oxide, in other words how far the potential is taken into the OER. The measurements also show that the degree of oxidation is dependent on the CV scanning speed. For NaOH, only the thin Au oxide is observed to form on the surface, no thicker Au oxide is formed despite the onset of the OER at high potentials, under the present conditions.

The 2D-SOR data confirm the GIXAS data, since the SOR signal is sensitive to the oxidation and reduction of the Au surface, confirming our previous 2D-SOR observations [8]. The thickness of the thin, passive oxide can be estimated to be 2-3 Å based on the Fresnel equations, using normal incidence of the 660 nm wavelength light and the complex refactive index of H_2O, Au and Au_2O_3 [9].

[1] S. Axnanda et al, Sci. Rep. **5** (2016) 9788.
[2] A. A. Gewirth, B. K. Niece, Chem. Rev. **97** (1997) 1129
[3] K. Itaya, Prog. Surf. Sci. **58** (1998) 121
[4] M. Ruge et al, J. Electrochem. Soc. **164** (2017) 608
[5] T. Iwasita, F. C. Nart, Prog. Surf. Sci. **55** (1997) 271
[6] H. Abe, Y. Niwa, M. A. Kimura, Phys. Chem. Chem. Phys. **22** (2020) 24974.
[7] S. Pfaff et al, ACS Appl. Mater. Interfaces **13** (2021) 19530.
[8] W. Linpe et al, E. Lundgren, Rev. Sci. Instrum., **91** (2020) 044101.
[9] J. Horkans, B.D. Cahan, E. Yeager, Surf. Sci. **46** (1974) 1

A short history of spectroscopic manifestations of the Kondo effect

Wolf-Dieter Schneider[1,2]

[1]*Ecole Polytechnique Fédérale de Lausanne (EPFL), Switzerland*
(e-mail: wolf-dieter.schneider@epfl.ch)

[2]*School of Physics, Institute of Basic Science (IBS), Center for Quantum NanoScience (QNS), Ewha Womans University, Seoul, Republic of Korea*

In 1930, a resistance minimum observed in dilute magnetic alloys [1,2], was the first experimental evidence for a new scattering mechanism of conduction electrons at magnetic impurities at low temperatures. More than 30 years later, J. Kondo developed a theory that described the effect as a consequence of the spin-flip scattering of conduction electrons at a localised magnetic moment [3,4]. The term "Kondo effect" was born for this phenomenon. About the same time P. W. Anderson developed his "single impurity model" [6] where he calculated the implications of this scattering mechanism for the local density of electronic states. Anderson, Suhl, Nagaoka, and Abrikosov [6-9] predicted a strong singularity at the Fermi level, later termed "Kondo resonance". This conjecture triggered numerous experimental physicists to search for and finally to discover this resonance in transition metal and rare earth elements as well in their alloys using techniques such as photoelectron [10], point contact [11], electronic transport [12,13], and scanning tunneling spectroscopies (STS) [14-16]. The latter technique revealed the presence of Kondo resonances also in molecular systems containing unpaired electron spins [17-19]. These discoveries opened the door for a detailed study of electronic transport and molecular magnetism on the molecular scale.

In the context of magnetic molecules, a microscopic magnetic sensor has been fabricated by attaching a single nickelocene molecule to the tip apex of a scanning tunneling microscope (STM) [20,21]. Here we present a similar method of single-atom spin sensing. We detect the magnetic moment of an individual Ce adatom adsorbed on a Cu_2N ultrathin film on Cu (100) by using a sensor tip that has its apex functionalized with a Kondo screened spin system, a small Ce cluster containing only a few Ce atoms [22]. We calibrate the sensor tip by deliberately coupling it to a well characterised Fe surface atom. Subsequently, we use the increasing splitting of the tip's Kondo resonance when approaching a spectroscopically dark Ce atom [23] to sense its spin, which is found to have the smallest possible value allowed by quantum mechanics: S=1/2. Thus, without applying an external magnetic field, the functionalised tip is used as a spin detector for single Ce-adatoms. This technique should be applicable to atoms of other rare earth elements and it may lead to applications such as the use

of rare earth atoms in ultra-dense magnetic storage, spintronics computers, and quantum information technologies.

Addendum: Recently, a new view on the origin of zero-bias anomalies of Co atoms atop noble metal surfaces, as detected by STS, has been presented: *"These features originate from gapped spin-excitations induced by a finite magnetic anisotropy energy, in contrast to the usual widespread interpretation relating them to Kondo resonances. Resting on relativistic time-dependent density functional and many-body perturbation theories, we furthermore unveil a new many-body feature, the spinaron, resulting from the interaction of electrons and spin-excitations localizing electronic states in a well-defined energy."* (quoted from Ref. 24). Experimental evidence for the existence of these theoretically predicted spinarons in Co adatoms has been reported very recently [25].

[1] W. Meissner and B. Voigt, Ann. Phys., Lpz. 7**,** 761 (1930).
[2] W. J. de Haas, J. de Boer, and G. J. van d'en Berg, Physica 34, 1115 (1934).
[3] J. Kondo, Prog. Theor. Phys. 32**,** 37 (1964).
[4] J. Kondo, Phys. Rev. 169, 437 (1968).
[6] P. W. Anderson, Phys. Rev. 124, 41 (1961).
[7] H. Suhl, Phys. Rev. 138, A 515 (1965); Physica 2, 39 (1965).
[8] Y. Nagaoka, Phys. Rev. B 138, A1112 (1965).
[9] A. A. Abrikosov, Physics 2, 5 (1965).
[10] F. Patthey, B. Delley, W.-D. Schneider, Y. Baer, Phys. Rev. Lett. 55, 1518 (1985).
[11] D. C. Ralph and R. A. Buhrman, Phys. Rev. Lett. 72, 3401 (1994).
[12] D. Goldhaber-Gordon *et al*., Nature 391, 156 (1998).
[13] S. M. Cronenwett, T. H. Oosterkamp, L. P. Kouwenhoven, Science 281, 540 (1998).
[14] J. Li, W.-D. Schneider, R. Berndt, B. Delley, Phys. Rev. Lett. 80, 2893 (1998).
[15] V. Madhavan, W. Chen, T. Jamneala, M. F. Crommie, N. S. Wingren, Science 280, 567 (1998).
[16] M. Ternes, A. J. Heinrich, and W.-D. Schneider, J. Phys.: Cond. Matter 21, 053001 (2009).
[17] I. Fernandez-Torrente, K. J. Franke, and J. I. Pascual, Phys. Rev. Lett. 101, 217203 (2008).
[18] P. Stoll *et al*., J. Phys.: Cond. Matter 30, 454002 (2018).
[19] S. Mishra *et al*., Nature 598, 287 (2021).
[20] G. Czap *et al*., Science 364, 670 (2019).
[21] Verlhac *et al*., Science 366, 623 (2019).
[22] M. Ternes, C. P. Lutz, A. J. Heinrich, W.-D. Schneider, Phys. Rev. Lett. 124, 167202 (2020).
[23] Up to now, a Kondo resonance on a single Ce adatom has not been observed.
As reported in Ref.16, the Kondo resonance observed for Ce/Ag (111) and published in Ref.14, has been measured on small Ce ad-clusters containing only a few atoms.
[24] J. Bouaziz, F. Souza Mendes Guimarães, S. Lounis, Nature Comm. 11:6112 (2020).
[25] F. Friedrich, A. Odobesko, J. Bouaziz, S. Lounis, M. Bode,
Nature Physics, Published Online: 2023-10-26, DOI link: https://doi.org/10.1038/s41567-023-02262-6

Experimental evidence of new many-body spinaron excitations in Co atoms on Cu(111)

Artem Odobesko,[1] Felix Friedrich,[1] Juba Bouaziz,[2] Samir Lounis, [2] and Matthias Bode[1]

[1]Physikalisches Institut, Experimentelle Physik II,
Julius-Maximilians-Universität Würzburg, Würzburg, Germany
(corresponding author: A. Odobesko, e-mail: artem.odobesko@uni-wuerzburg.de)

[2]Peter Grünberg Institut and Institute for Advanced Simulation,
Forschungszentrum Jülich, Jülich, Germany

The collective screening of an impurity spin by conduction electrons in the Kondo effect is one of the most fundamental manifestations of many-body phenomena in physics. The experimental identification of the Kondo effect in individual atoms is linked to the rise of a local electronic state at the Fermi level with a characteristic temperature and field dependence. Corresponding spectroscopic signature with a zero- bias anomaly (ZBA) in the differential conductance signal was for the first time observed in scanning tunneling spectroscopy (STS) experiments on Co atoms on Cu(111) surface [1] and is explained by a Fano resonance caused by interfering tunneling paths into the Kondo state and atomic orbitals. Recent first-principle calculations [2] suggest, however, that the experimentally observed spectroscopic ZBA should be interpreted in terms of excitations of the Co atom's spin and the formation of a novel quasiparticle, the spinaron, a magnetic polaron resulting from the interaction of spin excitations with conduction electrons, rather than in terms of a Kondo resonance.

Here we present state-of-the-art spin-averaged and spin-polarized scanning tunneling spectroscopy measurements on Co atoms on the Cu(111) surface in magnetic fields of up to 12T. We observe a field-induced energy shift and experimentally determined spin character of the spectral features, showing a completely opposite behaviour, as expected for the Kondo, but predicted for the spinaron. Our careful study of the responses of the ZBA on Co atoms on Cu(111) to an external magnetic field in combination with spin-polarized STS allowed us to discriminate between the different theoretical models and to invalidate the prevailing Kondo-based interpretation of the ZBA in favor of spinaron and for the first time experimentaly detect this novel many-body excitation [3].

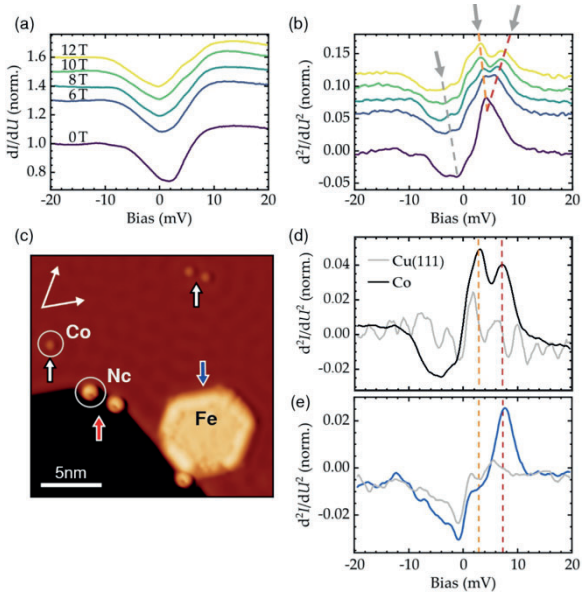

Figure 1. (a) Magnetic field-dependent splitting of the zero-bias anomaly on Co atoms on Cu(111) and (b) numerically calculated derivative. (c) Topography image of the Cu(111) surface decorated with Fe islands, Nc molecules and Co atoms. After picking up a small magnetic Fe cluster, the tip polarization is determined by measuring the SE signal on top of a Nc molecule. (d) d^2I/dU^2 signal measured at B = 12T with spin-averaged tip atop a Co atom (black) and the bare Cu(111) surface. Dashed orange and red lines indicate the position of the low-and high- energy spectral features shifting to low- and high-energies with increasing magnetic field respectively. (e) Same Co atom as in (d) measured with a majority spin-polarised tip. The data attribute high-energy spectral feature to a majority spin channel, and low-energy spectral feature to a minority spin channel with a magnetic field dependence oppposite to a Kondo picture but consistent with a spinaron.

Support by DFG through SFB1170 “ToCoTronics” and the Würzburg-Dresden Cluster of Excellence ct.qmat.

[1] V. Madhavan et al., Science **280**, 567 (1998)
[2] J. Bouaziz et al., Nat. Comm. **11**, 6112 (2020)
[3] F. Friedrich et al., Nat. Phys. (2023)

Kondo Effect of Co-Porphyrin: Remarkable Sensitivity to Adsorption Sites and Orientations

Xiangzhi Meng[1], Jenny Möller[2], Rodrigo E. Menchón[3,4,5], Alexander Weismann[1], Daniel Sánchez-Portal[3,6], Aran Garcia-Lekue[3,7], Rainer Herges[2], and Richard Berndt[1]

[1]*Institut für Experimentelle und Angewandte Physik, Christian-Albrechts-Universität, 24098 Kiel, Germany*

[2]*Otto-Diels-Institut für Organische Chemie, Christian-Albrechts-Universität, 24098 Kiel, Germany*

[3]*Donostia International Physics Center (DIPC), 20018 Donostia-San Sebastián, Spain*

[4]*Instituto de Física Rosario (IFIR), 2000 Rosario, Argentina*

[5]*Universidad Nacional de Rosario (UNR), 2000 Rosario, Argentina*

[6]*Centro de Física de Materiales CSIC-UPV/EHU, 20018 Donostia-San Sebastián, Spain*

[7]*Ikerbasque, Basque Foundation for Science, 48013 Bilbao, Spain*

(corresponding author: X. Meng, e-mail: meng@physik.uni-kiel.de)

We investigated the Kondo effect of Cobalt(II)-5-15-bis(4'-bromophenyl)-10,20-bis(4'-iodophenyl)porphyrin ($CoTPPBr_2I_2$) molecules on Au(111) using low-temperature scanning tunneling microscopy under ultrahigh vacuum conditions and density functional theory calculations [1]. The molecules exhibit four adsorption configurations at the top and bridge sites of the surface with different molecular orientations. The Kondo resonance shows extraordinary sensitivity to the adsorption configuration. By switching the molecule between different configurations, the Kondo temperature is varied over a wide range from ~8K up to ~250K. Density functional theory calculations reveal that changes of the adsorption configuration lead to distinct variations of the hybridization between the molecule and the surface. Furthermore, experiments show that the surface reconstruction plays a significant role for the molecular Kondo effect.

DSP, AGL and REM acknowledge financial support from Grants PID2019-107338RB-C66, PID2022-140845OB-C66 and TED2021-132388B-C41 funded by MCIN/AEI/10.13039/501100011033, the European Union (EU) H2020 program through the FET Open project SPRING (Grant Agreement No. 863098), the Basque Department of Education (Grant IT1569-22), as well as the financial support received from the IKUR Strategy under the collaboration agreement between Ikerbasque Foundation and DIPC on behalf of the Department of Education of the Basque Government.

[1] X. Meng, J. Möller, R. E. Menchón, A. Weismann, D. Sánchez-Portal, A. Garcia-Lekue, R. Herges, and R. Berndt, Nano Letters (accepted, 2023), DOI: 10.1021/acs.nanolett.3c03669

Probing the phase transition to a coherent 2D Kondo lattice

C.G. Ayani[1,2], M. Pisarra[3], I.M. Ibarburu[1], M. Garnica[2,6], R. Miranda[1,2,4,6], F. Calleja[2], F. Martín[2,4,5], and A.L. Vázquez de Parga[1,2,4,6]

[1] *Departamento de Física de la Materia Condensada, Universidad Autónoma de Madrid, Cantoblanco 28049, Madrid, Spain*
(corresponding author: A.L. Vázquez de Parga, e-mail: al.vazquezdeparga@uam.es)
[2] *IMDEA Nanociencia, Calle Faraday 9, Cantoblanco 28049, Madrid; Spain*

[3] *Dipartimento di Fisisca, Universittà della calabria, Via P. Buci, Cubo 3C, 87036 Rende, Italy*

[4] *IFIMAC, Universidad Autónoma de Madrid, Cantoblanco 28049, Madrid, Spain*

[5] *Departamento de Química, Módulo 13, Universidad Autónoma de madrid, Cantoblanco 28049, Madrid, Spain*

[6] *Instituto Nicolás Cabrea, Universidad Autónoma de madrid, Cantoblanco 28049, Madrid, Spain*

Solids containing strongly correlated electrons are the cradle of quantum states with unusual collective properties. When the system's dimensionality is reduced from 3D to 2D, the Coulomb interaction between electrons becomes even more relevant. Consequently, many-body effects that do not exist or manifest in 3D are expected to prevail in highly correlated 2D systems, and a paradigmatic example of these effects is the formation of two-dimensional Kondo lattices.

When a magnetic impurity is placed in a metallic host, the screening of the magnetic moment by the conduction electrons is known as Kondo effect [1-3]. The presence of several localized magnetic moments (as opposed to just one) in a metallic host can further modify the physics of the system. The same spin-exchange coupling that induces the Kondo effect can also induce a magnetic interaction between the localized spins. The resulting ground state can be either magnetically ordered or a paramagnetic Fermi liquid, depending on the relative strength of the Kondo coupling and the Ruderman-Kittel-Kasuya-Yosida interaction, as discussed by Doniach [4].

Theoretical predictions of the possible existence of Kondo lattices and the physics behind this phenomenon date from as early as the 1980s [5,6]. In Kondo lattices, at temperatures below a characteristic value, T_{KL}, the Kondo clouds of the individual impurities are coherently superimposed and acquire the periodicity of the crystal. Bloch's theorem ensures the formation of a renormalized flat band of width of the order of T_{KL}. The electrons originally

localized at the magnetic impurities are thus delocalized becoming part of the new Fermi surface, while at the same time the conduction electrons of the crystal acquire very large effective masses due to the hybridization of the new flat band with the existing conduction bands [7]. The corresponding LDOS at the Fermi level is expected to exhibit a more complex gap-like structure [5], in contrast with the single peak related to the single Kondo impurity regime. The characteristic temperature T_{KL} associated to the energy scale for the formation of the coherent Kondo lattice is expected to be lower than T_K because, once the localized magnetic moments are lost, the magnetic interaction between impurities is no longer in operation [8].

In this work we follow by means of low temperature Scanning Tunneling Microscopy and Spectroscopy, the buildup of a 2D Kondo lattice in a system composed by a Mott insulator, a single 1T-TaS_2 layer, stacked on the surface of a metallic crystal, 2H-TaS_2). We unambiguously demonstrate the existence of the resulting collective quantum coherent phase by measuring the characteristics of the Kondo-lattice gap that develops within the Kondo resonance at the Fermi level. Upon ramping up the temperature across T_{KL}, we follow the evolution of this gap during the phase transition from the Kondo lattice regime to the single-Kondo impurity regime. When the sample temperature is lower than 27K, the magnetic moments present in the Mott insulator start to experience the Kondo screening by the conduction electrons of the metal, leading to the appearance of a Kondo resonance at the Fermi level. By further lowering the temperature down to 11 K, the strength of the Kondo screening increases, as demonstrated by the increase in the intensity of the Kondo resonance. Below 11 K, a gap opens within the Kondo resonance, which is the signature of the formation of a coherent quantum state that extends all over the sample, i.e., a Kondo lattice [9]. This state results from the overlap between the Kondo clouds associated with the local magnetic moments in the Mott insulator layer. The observed modifications in the LDOS are well explained by state-of-the-art Density Functional Theory calculations.

This work was supported by Ministerio de Ciencia, Innovación y Universidades through grants, PID2021-128011NB-I00 and PID2019-105458RB-I00. Ministerio de Ciencia e Innovación and Comunidad de Madrid through grants “Materiales Disruptivos Bidimensionales (2D)” (MAD2D-CM)-UAM and “Materiales Disruptivos Bidimensionales (2D)” (MAD2D-CM)-IMDEA-NC funded by the Recovery, Transformation and Resilience Plan, and by NextGenerationEU from the European Union..

[1] P.W. Anderson, Phys. Rev. 124, 41 (1961).

[2] J. Kondo, Prog. Theor. Phys. 32, 37 (1964)

[3] J.R. Schrieffer, P.A. Wolf, Phys. Rev. 149, 491 (1996)

[4] S. Doniach, Physica B & C 91, 231 (1977).

[5] R.M. Martin, Phys. Rev. Lett. 48, 362 (1982).

[6] A.C. Hewson, Cambridge University Press, Cambridge, UK, (1993)

[7] A. R. Schmidt, M. H. Hamidian, P. Wahl, F. Meier, A. V. Balatsky, J. D. Garret, T. J. Williams, G. M. Luke, J. C. Davis. Nature 465, 570 (2010)

[8] P. Fulde, J. Keller, G. Zwicknagl, Solid State Phys. 41, 1 (1988).

[9] C.G. Ayani, M. Pisarra, I.M. Ibarburu, M. Garnica, R. Miranda, F. Calleja, F. Martín, A.L. Vázquez de Parga, Small 2303275 (2023) doi: 10.1002/smll.202303275.

Altermagnetism; a new surface science playground?

J Krempasky[1], L Šmejkal[2], G Springholz[3], J Minar[4], T Jungwirth[2], and Hugo Dil[1,5]
[1]*Photon Science Division, Paul Scherrer Institut, Villigen, Switzerland*
[2] *Institute of Physics, Czech Academy of Sciences, Prague, Czech Republic*
[3]*Institut für Halbleiter-und Festkörperphysik, Johannes Kepler Universität, Linz, Austria*
[4]*New Technologies-Research Center, University of West Bohemia, Plzeň, Czech Republic*
[5]*Institute of Physics, Ecole Polytechnique Fédérale de Lausanne, Switzerland*
(corresponding author: H. Dil, e-mail: hugo.dil@epfl.ch)

Kramers spin degeneracy refers to the fact that in a nonmagnetic and centrosymmetric bulk crystal the states with opposite spin coincide. To be able to make use of the electron spin in applications, this degeneracy has to be lifted. This can be done by either breaking the time-reversal symmetry, or by breaking space inversion symmetry in combination with spin-orbit coupling (SOC). The latter forms the basis of Rashba- or Dresselhaus-type spin splitting, and ultimately also of the spin-polarised surface states of topological materials. Time-reversal symmetry is broken in materials with magnetic order, but this does not necessarily lift the Kramers spin degeneracy. In a ferromagnet (FM) there is one spin lattice and the Zeeman effect lifts the degeneracy of the spin states (anti)parallel to the magnetisation direction. However, in an antiferromagnet (AFM) the two spin sublattices are connected by translation or inversion symmetry and this maps the electronic structures of the two sublattices on top of each other, thereby restoring the degeneracy. Until the recent introduction of altermagnets (AM) [1,2], these were generally considered to be the two main band structure possibilities for commensurate magnetic order. Here we will present experimental results of the third possibility and show that also in altermagnets the Kramers spin degeneracy is lifted [3].

One of the first things one learns with respect to spin is that, whereas for charge a phase of 2π brings the system back to the same point, for spin this only happens after a phase of 4π. In other words, spin and charge respond differently to rotations. Therefore, if two spin sublattices are coupled by rotational symmetry, and not by translation or inversion, their band structures do not map back to each other and Kramers spin degeneracy is lifted. Thus, an altermagnet has, similar to an AFM, fully compensated magnetic order, but the spin sublattices are connected by rotation and not translation or inversion. This seemingly minor difference has far-reaching consequences and rightfully places AM in a distinct category [4]. In essence, it shows many of the properties of ferromagnetism, but without any stray fields.

Whereas the AM response in transport measurements was observed in various experiments soon after the concept was introduced [5], the lifting of the Kramers spin degeneracy, which forms the basis of all further results, was not shown. The main difficulty is that the interesting physics occurs in the bulk bands, which can be easily overshadowed by surface states in a typical angle-resolved photoemission (ARPES) experiment. Based on our experience with bulk Rashba systems [6] we used soft X-ray ARPES to suppress surface contributions and enhance the visibility of pure bulk states. The simple structure and large predicted spin

splitting made MnTe the ideal choice and experiments were performed both on MBE films that were transferred in-situ and on cleaved single crystals. Apart from differences in the magnetic domain structure, these samples show similar results. In the figure below the measured band structure is shown and a clear degeneracy lifting, in accordance with calculations can directly be observed.

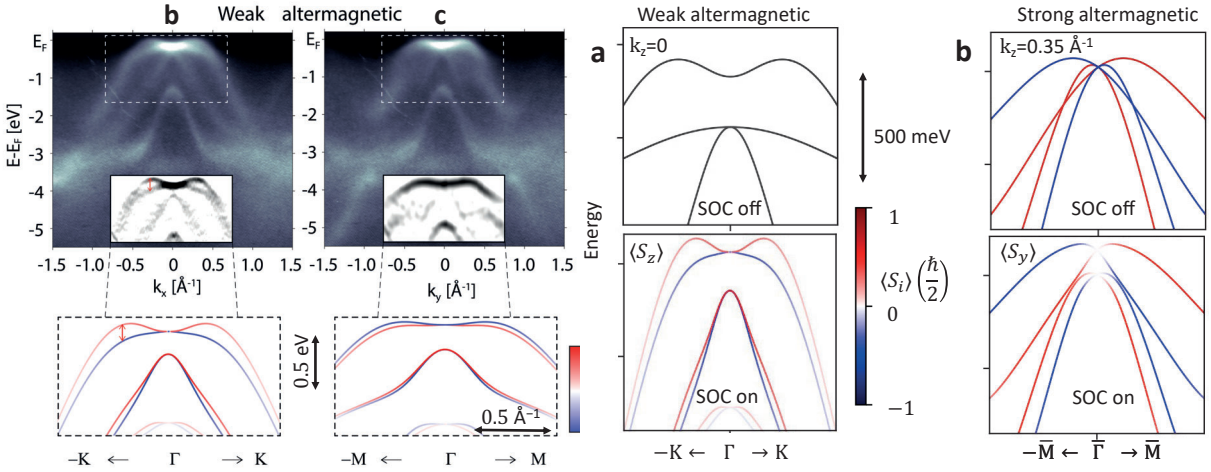

These results also highlight further unique and intriguing properties of the altermagnetic band structure. The mirror planes of the crystal structure form nodal planes in k-space where the degeneracy is enforced. However, in the presence of SOC also here the degeneracy is lifted and we refer to this as weak lifting. The strong degeneracy lifting is independent of SOC and occurs in regions in reciprocal space away from the nodal planes. The distinction between these mechanisms and how asymmetries in the measured electronic structure can be used to determine the Néel vector will be discussed in more detail during the presentation.

The final proof of the non-relativistic lifting of the spin degeneracy is in the measured spin polarisation signal. These extremely challenging experiments were performed at low photon energies after having identified the bulk bands. The obtained symmetry of the spin texture is directly in line with the altermagnetic order and corresponds to calculations. However, further developments both in sample preparation and measurement technique are required to explore the details of the spin texture.

Given the bulk nature of the relevant band structure, the interest of the surface science community in altermagnetic systems might be limited for now, hence the question mark in the title. However, it can be foreseen that this classification will have a similar impact as the consideration of band topology almost two decades ago. It can therefore be expected that, similar to band topology, it will become a standard item in our toolbox in several years.

[1] Smejkal, L., Sinova, J. & Jungwirth, T. Physical Review X 12, 031042 (2022).
[2] Smejkal, L., Sinova, J. & Jungwirth, T. Physical Review X 12, 040501 (2022).
[3] J. Krempasky et al. Nature (in press). arXiv:2308.10681
[4] I. Mazin, Physical Review X 12, 040002 (2022).
[5] Feng, Z.et al. Nature El. 5, 735 (2022); Bai, H. et al. PRL 128, 197202 (2022) (and others).
[6] J. Krempasky et al. Physical Review B 94, 205111 (2016).

Single-molecule visualization of electron solvation induced kinetics within ammonia

Prashant Srivastava, Hussain Mazhar, Morgan Redington[1], Quinlan Crossley[2], Daniel P. Miller[2], Karina Morgenstern

Physical Chemistry I, Department of Chemistry and Biochemistry, Ruhr-Universität Bochum, Universitätstr. 150, D-44801 Bochum, Germany
[1]Department of Chemistry, State University of New York at Buffalo, Buffalo, New York 14260, United States
[2]Department of Chemistry, Hofstra University, Hempstead, New York 11549, United States

Electron solvation in ammonia has fascinated scientists since the first description of blue-colored alkali metal-ammonia solutions [1]. Today's high relevance of electron solvation in several branches of chemistry and environmental science [2] arises from its potential of driving reactions in molecular solvents as a strong reducing agent, in particular in liquid water and ammonia. Despite 200 years of research, the enhancement in various reactions that involve electron solvation remains elusive. Most studies so far have focused on deciphering the initial steps of electron-induced reactions, i.e., the solvation dynamics of the electron, its stabilization, and relaxation.

We designed an experiment to explore the impact of solvated electrons on the solvent structure in liquid-like ammonia on the molecular scale. Hydrogen bonding in a liquid-like environment is mimicked by placing ammonia clusters on an ammonia support, supported itself by a metal, Cu(110). Electrons are provided from a hot electron gas generated in the metal by femtosecond laser pulses, extending a route employed successfully to understand the initial electron solvation dynamics in water [3]. We extend this approach to the molecular scale by following the nanoscale motion of individual molecules by a unique combination of a femtosecond laser with low-temperature scanning tunneling microscopy (termed fs-STM [4]). By imaging the exact same molecular clusters before and after their exposure to laser-generated electrons, we identify several distinct processes resulting from electron-solvent interactions (Fig. 1), while unraveling their origin using density functional theory (DFT) calculations and first-principles molecular dynamics (FPMD) simulations that account for dispersion forces. Enhanced molecular kinetics reflect hydrogen bond rearrangement and cleavage for differently bonded molecules. We explain which electron-solvent interactions induce what kind of mobility for individual molecules and how. Beyond general knowledge, the solvent structure is altered more than transiently by subsequent solvation of two electrons, non-linear dynamics with implications for enhanced reactivity in electron-solvation-driven chemical reactions beyond ammonia. The gained understanding will impact the reactions catalytically enhanced by the presence of solvated electrons. The molecular-scale approach

could play a role in studying the impact of solvated electrons in other solvents beyond ammonia.

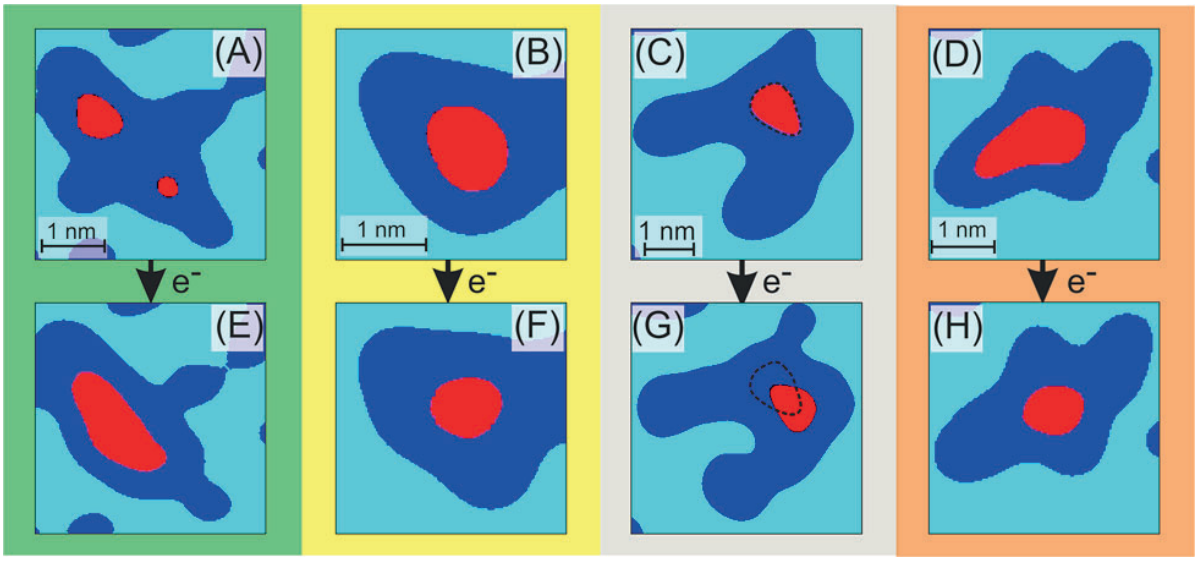

Fig. 1: Laser-induced processes in liquid like ammonia clusters: STM images (**A to D**) before and (**E to H**) after illumination of ammonia clusters (red) on ammonia support (blue) with a single pulse peak fluence of F = 0.235 mJ/cm^2 at a wave length of 400 nm and a pulse length of 36 fs; for details see supplementary materials, Materials and methods and S2: (A to E, green) upward mass transport; the two red clusters are joined to one cluster by additional material (B to F, yellow) downward mass transport; the blue support increases in size while the red clusters decreases in size (C to G, grey) mass transport on the support; the dashed line marks the original position of the cluster and is at the same position in both images (D to H, orange) desorption; the red cluster decreases in size while the area of the blue support remains approximately constant. The number of pulses was (A to E) 12 · 10^6 (B to F) 2 · 10^6 pulses (C to G) 4 · 10^6, and (D to H) 9 · 10^6 pulses. The images were recorded at 100 mV and 9.6 pA at 5 K.

This work was funded by the Deutsche Forschungsgemeinschaft (DFG, German Research Foundation) under Germany's Excellence Strategy - EXC 2033 - 390677874 - RESOLV (PS, HM, KM), the Faculty Research and Development Grants (FRDG) from Hofstra University (DPM), and the Presidential Research Awards Program (PRAP) from Hofstra University (DPM).

[1] W. Weyl, Über Metallammonium-Verbindungen. *Ann. Phys.* **197**, 601–612 (1864). doi: 10.1002/andp.18641970407

[2] T. Buttersack, P. E. Mason, R. S. McMullen, H. C. Schewe, T. Martinek, K. Brezina, M. Crhan, A. Gomez, D. Hein, G. Wartner, R. Seidel, H. Ali, S. Thürmer, O. Marsalek, B. Winter, S. E. Bradforth, P. Jungwirth, Photoelectron Spectra of Alkali Metal–Ammonia Microjets: From Blue Electrolyte to Bronze Metal. *Science* **368**, 1086–1091 (2020). doi: 10.1126/science.aaz7607

[3] J. Stähler, U. Bovensiepen, M. Meyer, M. Wolf, A Surface Science Approach to Ultrafast Electron Transfer and Solvation Dynamics at Interfaces. *Chem. Soc. Rev.* **37**, 2180–2190 (2008). doi: 10.1039/B800257F

[4] M. Mehlhorn, H. Gawronski, L. Nedelmann, A. Grujic, K. Morgenstern, An Instrument to Investigate Femtochemistry on Metal Surfaces in Real-Space. *Rev. Sci. Instrum.* **78**, 033905 (2007). doi: 10.1063/1.2432244

Atomic Scale Manipulation with an Unexpected Intermediate State

Norio Okabayashi,[1] Thomas Frederiksen,[2,3] Alexander Liebig,[4] and Franz J. Giessibl[4]

[1]*Graduate School of Nat. Science and Technology, Kanazawa University, Ishikawa 920-1192, Japan*

[2]*Donostia International Physics Center (DIPC), San Sebastián 20018, Spain*

[3]*IKERBASQUE, Basque Foundation for Science, Bilbao 48013, Spain*

[4]*Institute of Experimental and Applied Physics, University of Regensburg, Regensburg D-93053, Germany, e-mail: Franz.Giessibl@ur.de*

The pervasive phenomenon of friction has been studied at the nanoscale via a controlled manipulation of single atoms and molecules with a metallic tip, which enabled a precise determination of the static friction force necessary to initiate motion. However, little is known about the atomic dynamics during atomic manipulation [1,2]. Here, we reveal the complete manipulation process of a CO molecule on a Cu(110) surface at low temperatures using a combination of noncontact atomic force microscopy and density functional theory simulations. We found that an intermediate state, inaccessible for the far-tip position, is enabled in the reaction pathway for the close-tip position, which is crucial to understanding the manipulation process, including dynamic friction.

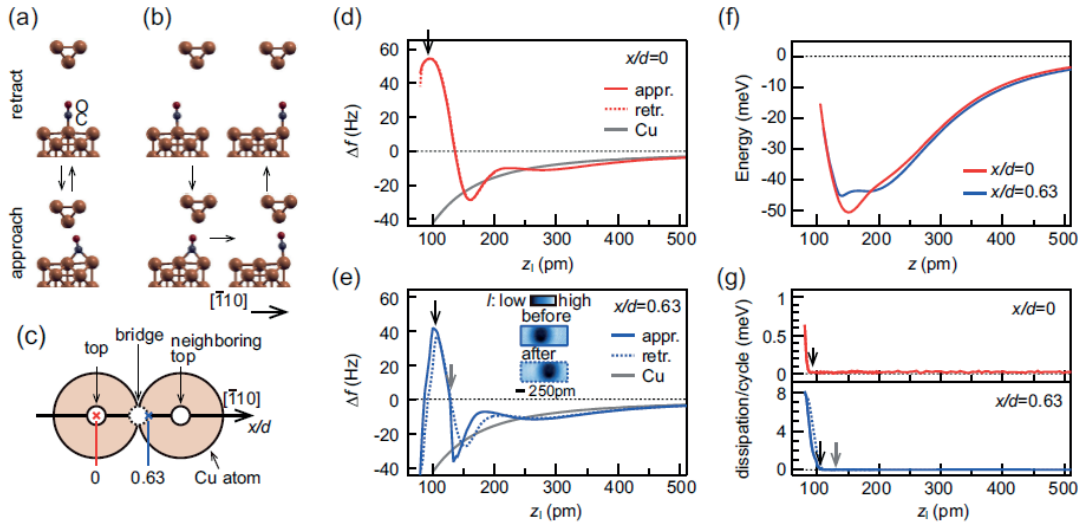

Fig.1 (a) Schematic of CO manipulation on Cu(110) between top and bridge sites by a metallic tip over the top site. The thin arrows indicate the reaction processes of CO for tip approach and retract. (b) Same as (a), but for CO manipulation from top to neighboring top site when the tip approach and retract occurs for a tip position laterally closer to the neighboring top site. (c) Definition of lateral tip positions along Cu [1̄10] (d = 255 pm): x/d = 0 (top site) and x/d = 0.63 (outside of bridge). (d) Measured frequency shift (Δf) as a function of vertical tip position (z_l) for the tip-on-top-site case (x/d = 0). The Δf curves for tip approach and retraction are depicted by red solid and dotted lines, respectively. The Δf curve for the tip on Cu is also depicted by a gray line. (e) Same as (d), but for the lateral tip position x/d = 0.63 (outside of bridge). In the inset, typical STM images of CO before and after the manipulation are shown. (f) Measured potential energy between the tip and CO up to the point of manipulation. (g) Energy dissipation per cycle of the vertically oscillating tip, where both cases of tip approach and retract are depicted.

Figure 1 shows that the journey of a CO molecule between two neighboring adsorption sites includes a bridge site that is only occupied in the close presence of the tip. With the tip

oscillating over the CO molecule at a lateral distance of 63% of the way between two final adsorption sites, a bridge site is temporarily occupied that shows up in the dissipation channel in Fig. 1 (g) [3,4].

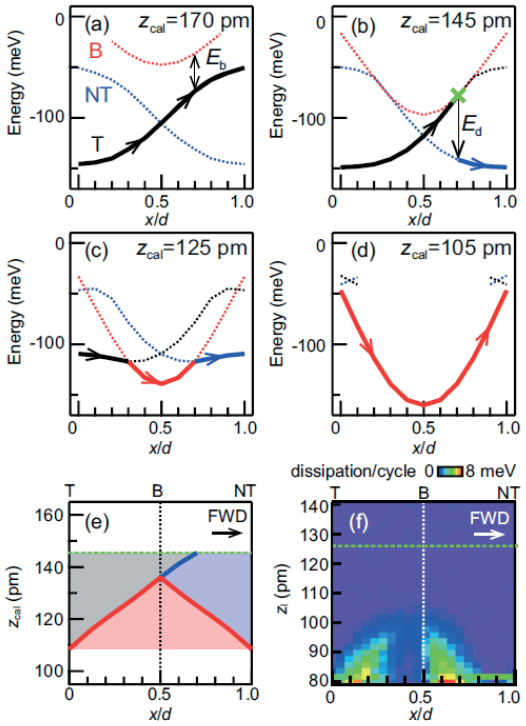

(a) Calculated potential energy between the Cu11 tip and CO as a function of lateral tip position (at a constant tip height of 170 pm) for CO in top (T), bridge (B), and neighboring top (NT) configurations. The thick path represents the CO configuration during the lateral tip scan. (b)–(d) Same as (a) but for tip heights: (b) 145 pm, (c) 125 pm, and (d) 105 pm. (e) Calculated CO configuration as a function of tip height and lateral position during the forward tip scan. The gray, light red, and light blue regions represent CO in top (T), bridge (B), and neighboring top (NT) sites, respectively. The thick lines indicate the transition points. (f) Energy dissipation per cycle of the vertically oscillating tip, experimentally measured during the lateral CO dragging. In (e) and (f), the onset of dragging is indicated by the dashed green line.

Density functional theory calculations confirm the existence of this intermediate bridge site occupation (Fig. 2).

The spirit of these investigations, i.e. finding useful new applications of old ideas goes along well with the work of young and rising female [5] as well as established male Austrians [6].

[1] D.M. Eigler, E.K. Schweizer, *Nature* **344,** 524 (1990).
[2] M. Ternes, C.P. Lutz, C. Hirjibehedin, F. J. Giessibl, A.J. Heinrich, *Science* **319,** 1066 (2008).
[3] N. Okabayashi, T. Frederiksen, A. Liebig, and F. J. Giessibl, *Phys. Rev. B* **108**, 165401 (2023).
[4] N. Okabayashi, T. Frederiksen, A. Liebig, and F. J. Giessibl, *Phys. Rev. Lett.* **131,** 148001 (2023).
[5] Andrea Auer, B. Eder, F. J. Giessibl, *J. Chem. Phys.* **159,** 174201 (2023).
[5] Arnold Schwarzenegger, *Be Useful: Seven tools for life*, Ebury Edge (2023).

Translation and rotation of a single molecule on Au(111) between thermal and electronic inelastic excitations

Kwan Ho Au-Yeung, Suchetana Sarkar, Dmitry A. Ryndyk[1], Roberto Robles[2], Nicolas Lorente[2], Franziska Lissel[3], Christian Joachim[4] and Francesca Moresco

Center for Advancing Electronics Dresden, TU Dresden, 01062 Dresden, Germany (corresponding author: F. Moresco, e-mail: francesca.moresco@tu-dresden.de)

[1] Institute for Materials Science and Theoretical Chemistry, TU Dresden, 01062 Dresden, Germany

[2] Centro de Física de Materiales CFM/MPC (CSIC-UPV/EHU), 20018 Donostia-San Sebastián, Spain

[3] Leibniz-Institut für Polymerforschung Dresden e.V., 01069 Dresden, Germany, and Faculty of Chemistry and Food Chemistry, TU Dresden, 01062 Dresden, Germany

[4] CEMES, CNRS, 29 rue J. Marvig, 31055 Toulouse, France

We will present the investigation of single DMNI-P zwitterionic molecules adsorbed on the Au(111) surface by scanning tunneling microscopy and tip-induced manipulation. Thanks to the possibility to both chemisorb and physisorb on the Au(111) surface, this class of molecules represents an ideal model system to study inelastic electron tunneling based manipulation, allowing the comparison of unidirectional rotations and translations on the same compound [1].

Tunneling electrons originated from the STM tip can inelastically excite specific conformational or vibrational molecular degrees of freedom of adsorbed molecules, producing controlled rotations or translations. Even if the excitation mechanisms are probably similar, rotation requires a strong local molecule-substrate interaction providing a rotational axle, while a translation is possible if the adsorption is weak. It is therefore unusual that the same species presents both functionalities. On the other hand, the thermal excitation of the substrate also induces movements in adsorbed molecules, showing that some molecular degrees of freedom can be addressed also thermally.

Depending on its adsorption conformation on the Au(111) surface, the zwitterionic molecule works in two different ways under bias voltage pulses. It is a unidirectional rotor while anchored on the surface. It is a fast drivable molecule vehicle (nanocar) while physisorbed. By tuning the surface coverage, the conformation of the molecule can be selected to be either rotor or nanocar. The inelastic tunneling excitation producing the movement can be therefore

compared in the same experimental conditions for both the unidirectional rotation of the rotor and the directed movement of the nanocar.

Furthermore, combining long-time electronic excitations with the slow controlled increasing of the substrate temperature, we could explore the limits of the microscopic reversibility principle, investigating the interplay between thermal and electron tunneling excitations for the unidirectional rotation of the DMNI-P molecule-rotor on the Au(111) surface [2]. We identified a range of moderate voltages and temperatures where heating the surface enhances the unidirectional rotational rate of the rotor. At higher voltage inelastic tunneling effects dominate, while at higher temperature the process becomes stochastic.

This work has received funding from the European Innovation Council (EIC) under the project ESiM (grant agreement no. 101046364) and the Horizon 2020 research and innovation program under the project MEMO, grant agreement no. 766864.

[1] J K. H. Au-Yeung, S. Sarkar, T. Kühne, O. Aiboudi, D. A. Ryndyk, R. Robles, N. Lorente, F. Lissel, C. Joachim, F. Moresco. ACS Nano 17, 3128 (2023)

[2] K. H. Au-Yeung, S. Sarkar, T. Kühne, O. Aiboudi, D. A. Ryndyk, R. Robles, F. Lissel, N. Lorente, C. Joachim, F. Moresco, J. Phys. Chem. 127, 16989 (2023)

Electron Spin Resonance of Individual Rare-Earth Ions

Harald Brune,[1,2] Greg Czap,[2] Jairo Valesco Jr.,[2,3] Roger M. Macfarlane,[2] Chris Lutz[2]

(corresponding author: H. Brune, e-mail: harald.brune@epfl.ch)

[1]*Institute of Physics, École Polytechnique Fédérale de Lausanne (EPFL), CH-1015 Lausanne, Switzerland*

[2]*IBM Almaden Research Center, 650 Harry Road, San Jose, CA 95120, USA*

[3]*Department of Physics, University of California, Santa Cruz CA 95064, USA*

The magnetic properties of individual surface adsorbed atoms and molecules can be accessed as a function of their adsorption site and charge state by means of STM. For many years, rare-earth atoms have remained an exception since their strongly localized *f*–electrons don't contribute to the tunnel current. However, indirect access becomes possible once these atoms exhibit spin-polarization in their valence electrons. The resulting valence spin strongly couples via intra-atomic exchange to the *f*–moment and thereby makes its orientation accessible to spin-polarized STM [1–5]. In addition, the dipolar stray field of individual rare-earth atoms can be accessed by the change in electron spin resonance (ESR) frequency of "spectator" atoms placed at various distances, enabling the determination of their magnetic moment with high precision [2,5]. Finally, the magnetic level scheme can be derived from recording the magnetic switching rate as a function of tunnel voltage. Each threshold voltage marks the opening of a new path for magnetization reversal and thereby unravels the energies and symmetries of the wavefunctions describing the projections of the total angular momentum onto the quantization axis [2–5].

Altogether, this has created a fairly good understanding of the fascinating thermal and magnetic field stability [3,5] of the magnetization of individual surface adsorbed rare-earth atoms. The next step is to unravel the coherence time of their magnetic quantum states. This is motivated by individual rare-earth atoms in solids exhibiting exceptionally long coherence times, reaching several hours for the nuclear spin states [6]. The strong coupling between the magnetic degrees of freedom and entangled photons enables quantum repeaters for long distance quantum communication [7] and schemes for universal quantum computing with the electron-nuclear wavefunction of individual rare-earth atoms were proposed [8].

We show the first step towards addressing the quantum coherence of electron and nuclear spin states in surface adsorbed rare-earth atoms. The only technique offering this access on an individual atom basis is ESR-STM [9]. We place Eu and Sm atoms on adsorption sites where they are cations making their electron spin resonance accessible to the STM. The figure below

shows spectra for Eu/MgO/Ag(100). They reveal several hyperfine branches giving access to the isotope, hyperfine coupling, the magneto-crystalline anisotropy, and electron *g*-factor. Comparison with tabulated optical spectroscopy data of gas-phase ions shows remarkable agreements but also important differences between the free and surface adsorbed species [10].

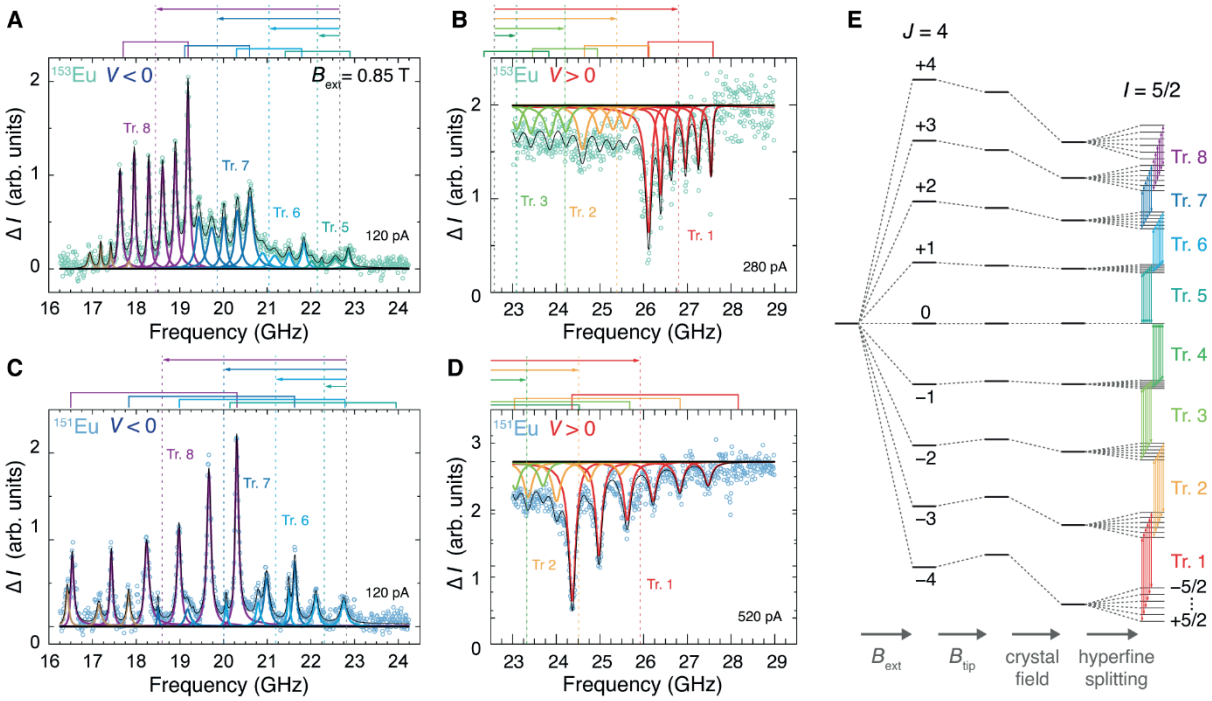

A–D ESR spectra of ^{153}Eu and ^{151}Eu (nuclear spin $I = 5/2$) adsorbed on MgO/Ag(100) bridge sites (set-point before opening the feedback loop $V_t = \pm 50$ mV, $I_t = 120$ pA, $V_{RF} = 20$ mV, $T = 1.2$ K, $B_{ext} = 0.85$ T). **E** Magnetic energy levels of the ground-state multiplet, split by Zeeman energy due to B_{ext} and B_{tip}, shifted due to magneto-crystalline anisotropy $D < 0$ normal to the surface, and hyperfine splitting with $A > 0$ (exaggerated), to yield eight trees of transitions (colored lines) labeled Tr. 1 through Tr. 8.

[1] M. Pivetta, F. Patthey, I. D. Marco, A. Subramonian, O. Eriksson, S. Rusponi, and H. Brune, Phys. Rev. X **10**, 031054 (2020).

[2] F. D. Natterer, K. Yang, W. Paul, P. Willke, T. Choi, T. Greber, A. J. Heinrich, and C. P. Lutz, Nature **543**, 226 (2017).

[3] F. D. Natterer, F. Donati, F. Patthey, and H. Brune, Phys. Rev. Lett. **121**, 027201 (2018).

[4] A. Curcella, D. Sblendorio, S. Rusponi, M. Pivetta, F. Patthey, and H. Brune, Phys. Rev. Lett. **130**, 106702 (2023).

[5] A. Singha, P. Willke, T. Bilgeri, X. Zhang, H. Brune, F. Donati, A. J. Heinrich, and T. Choi, Nat. Communic. **12**, 4179 (2021).

[6] M. Zhong, M. P. Hedges, R. L. Ahlefeldt, J. G. Bartholomew, S. E. Beavan, S. M. Wittig, J. J. Longdell, and M. J. Sellars, Nature **517**, 177 (2015).

[7] N. Sangouard, C. Simon, H. d. Riedmatten, and N. Gisin, Rev. Mod. Phys. **83**, 33 (2011).

[8] M. Grimm, A. Beckert, G. Aeppli, and M. Müller, PRX Quantum **2**, 010312 (2021).

[9] S. Baumann, W. Paul, T. Choi, C. P. Lutz, A. Ardavan, and A. J. Heinrich, Science **350**, 417 (2015).

[10] G. Czap, J. Valesco Jr., R. M. Macfarlane, C. Lutz, and H. Brune, to be published.

Time-resolved photoemission electron microscopy of the near-field dynamics in nanowires excited by few-cycle short-wave infrared pulses

Nelia Zaiats[1], Lukas Wittenbecher[1], Ivan Sytcevich[2], Chandni Babu[3], Eduardo J. C. Dias[4], Chen Guo[2], J. García de Abajo[4], Cord L. Arnold[2], Jan Vogelsang[1], Anne L'Huillier[2], Anders Mikkelsen[1]

1 Department of Physics and NanoLund, Lund University, Sweden
(corresponding author: Nelia Zaiats, e-mail: nelia.zaiats@sljus.lu.se)

2 Department of Physics and Lund Laser Center, Lund University, Sweden

3 Department of Chemistry, Lund University, Sweden

4 ICFO - The Institute of Photonic Sciences, Spain

Ultrafast photoemission electron microscopy (PEEM) is a powerful technique for studying the dynamics of surface plasmons and other electronic excitations, allowing space and time coherent imaging of plasmonic phenomena at the sample, irradiated by pulsed light with high temporal and spatial resolution [1].

Short-wave infrared (SWIR) light is used for optical communication as well as in a wide range of sensor applications [2]. Femtosecond SWIR sources can also be used for generating high-order harmonics in the water window [3]. Silver nanowires, which can be synthesized with high crystal perfection [4], present a pronounced plasmonic resonance in the SWIR range, allowing them to act as efficient light concentrators.

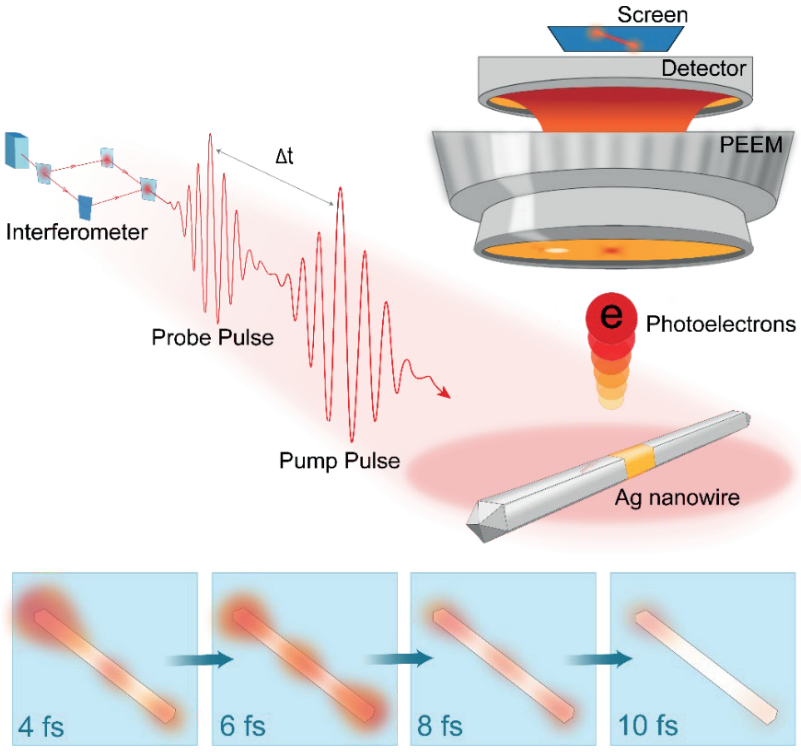

Fig 1: Schematic representation of TR-PEEM experiment on Ag nanowires.

While detailed interferometric time-resolved photoemission electron microscopy (ITR-PEEM) measurements have been carried out on Ag nanoparticles in the visible and near-infrared range [5,6], few such PEEM studies have been reported in the SWIR range [1].

Here, we investigate the near-field dynamics in Ag nanowires excited by SWIR pulses with a duration of ~17 fs (2.3 optical cycles) and wavelengths in the 1600-2400 nm range using ITR-PEEM. We study the nanowire response for different light polarizations and intensities as well as for different orientations and geometrical shapes of the wires. We excite the dipolar longitudinal plasmon mode of the nanowire and investigate the near-field dynamics on the femtosecond time scale using two SWIR pump-probe pulses separated in time. The study shows the use of ITR-PEEM in the SWIR wavelength regime, revealing the dynamics of a model plasmonic system.

[1] E. Mårsell, et al, “Photoemission electron microscopy of localized surface plasmons in silver nanostructures at telecommunication wavelengths”, J. of Appl. Phys. 117, 083104 (2015).

[2] M. P. Hansen and D. S. Malchow "Overview of SWIR detectors, cameras, and applications", Proc. SPIE 6939, Thermosense XXX, 69390I (2008).

[3] J. Li, J. Lu, A. Chew, et al, ”Attosecond science based on high harmonic generation from gases and solids”, Nat Commun 11, 2748 (2020).

[4] M. Mayer, et al, “Controlled Living Nanowire Growth: Precise Control over the Morphology and Optical Properties of AgAuAg Bimetallic Nanowires”, Nano Lett 15(8), 5427 (2015).

[5] D. Bayer, et al, “Time and Space Resolved Studies on Metallic Nanoparticles”, in: D.T. Cat, A. Pucci, K. Wandelt. (eds) Physics and Engineering of New Materials. Springer Proceedings in Physics 127. Springer, Berlin, Heidelberg (2009).

[6] E. Mårsell, et al, “Nanoscale imaging of local few-femtosecond near-field dynamics within a single plasmonic nanoantenna”, Nano Lett. 15(10), 6601 (2015).

Tuesday

Graphene folding and fabrication of twisted layer graphene

M. Willinger

Lehrstuhl für Elektronenmikroskopie mit Forschungsschwerpunkt Energiematerialien,
TUM School of Natural Sciences, Technische Universität München,
85748 Garching b. München
(e-mail: marc.willinger@tum.de)

The properties of two-dimensional (2D) van der Waals (vdW) materials can be tuned through nanostructuring or by controlled stacking and modification of the electronic coupling between layers. Depending on the sacking angle, interlayer hybridization can induce exotic electronic states and transport phenomena. In my talk I will describe a viable mechanism for assisted self-assembly of twisted layer graphene. The process, which can be implemented in standard chemical vapour deposition (CVD) growth, is best described using the analogy to Origami and Kirigami of paper [1]. It involves controlled induction of wrinkle formation in single-layer graphene and subsequent wrinkle folding, tearing, and adlayer-growth. Inherent to the process is the formation of intertwined graphene spirals and conversion of the chiral angle of one-dimensional (1D) wrinkles into a 2D twist angle between layers in a three-dimensional (3D) superlattice. Seeded growth and substrate engineering can be used for tailored formation of layer stacks with pre-defined twist angles. The underlying principle is universal and can be extended to other foldable 2D materials and facilitates the production of miniaturized electronic components, including capacitors, resistors and inductors. The mechanistic insights were obtained through direct observation of CVD growth inside the chamber of a modified environmental scanning electron microscope [2-4].

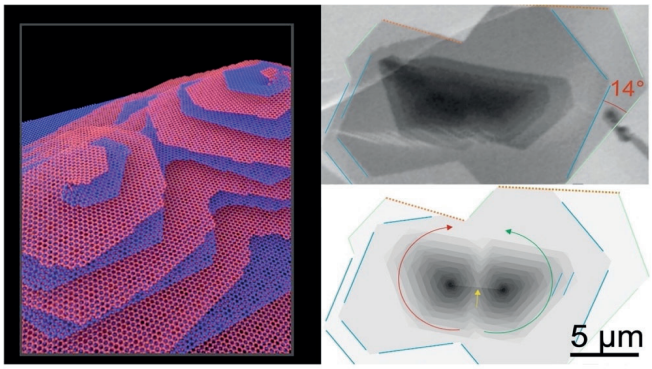

***Fig.1**. Spirals of twisted layer graphene with pre-defined twist-angle. Comparison between simulation and in-situ observation during CVD growth.*

[1] ZJ Wang *et al*., Nature Materials, *Nat. Mater*. (2023)
[2] ZJ Wang *et al*., Nat Commun **7** (2016), p. 13256
[3] ZJ Wang *et al*. *ACS Nano* 2015, 9, 2, 1506–1519
[4] ZJ Wang *et al*. *Adv. Mater. Interfaces 2018, 5, 1800255*

Epitaxial Graphene Nanoribbons: One-dimensional confinement and pn-junction array

U. Starke, H. Karakachian, P. Rosenzweig, B. Matta, T.T.N. Nguyen[1], J. Aprojanz[1,2], A.A. Zakharov[3], R. Yakimova[4], T. Balasubramanian[3], Z. Mamiyev[1], S.R. Power[5], C. Tegenkamp[1,2], and C.M. Polley[3]

Max-Planck-Institut für Festkörperforschung, D-70569 Stuttgart, Germany
(corresponding author: U.Starke, e-mail: u.starke@fkf.mpg.de)

[1]*Institut für Physik, Technische Universität Chemnitz, 09126, Chemnitz, Germany*

[2]*Institut für Festkörperphysik, Leibniz Universität Hannover, 030167 Hannover, Germany*

[3]*MAX IV Laboratory, Lund University, 22484 Lund, Sweden*

[4]*IFM, Linköping University, 58183 Linköping, Sweden*

[5]*School of Physical Sciences, Dublin City University, 9 Dublin, Ireland*

Wafer scale epitaxial graphene grown on Silicon Carbide (SiC) is regarded as a suitable candidate for carbon based electronics. In recent years, our group has demonstrated many possibilities to tune the electronic properties of this two-dimensional (2D) material by controlled doping schemes or intercalation between the SiC substrate and the graphene layer. However, for application in logical electronics, the necessity to define an off state is a key ingredient, which – due to the absence of an electronic bandgap – is so far impossible in conventional pristine graphene layers. Spatial constriction of the material can provide a way to circumvent this problem. Indeed, arm-chair graphene nanoribbons (AGNRs) were theoretically predicted to display a bandgap. However, lithographical patterning of the graphene creates irregular edges. The self-assembly of molecular precursors is restricted to metallic substrates which introduce an electrical short-circuit. Here, we grow high-quality AGNRs on the sidewalls of 6H-SiC mesa structures, a semi-insulating substrate (see Fig. 1a,b). Angle-resolved photoelectron spectroscopy (ARPES) and scanning tunneling spectroscopy measurements reveal the development of a width-

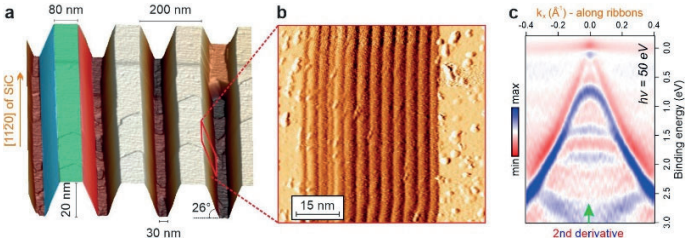

Figure 1: a) Perspective AFM view of the mesa structures with a periodicity of 200 nm. The trench depth is 20 nm and the facet inclination is around 26°. **b)** First derivative of a STM topography image taken on a single facet displaying the "ladder structure" **c)** High-resolution ARPES energy-momentum cut taken along the ribbons using a photon energy of 50 eV and its second derivative plot along the energy axis.

dependent semiconducting gap driven by quantum confinement effects. Furthermore, ARPES demonstrates an ideal one-dimensional (1D) electronic behavior that for the first time is realized in a graphene-based environment, consisting of well-resolved subbands (Fig. 1c), dispersing and non-dispersing along and across the ribbons, respectively [1]. Our experimental findings, coupled with tight-binding calculations [2], set the grounds for a deeper exploration of quantum confinement phenomena and may open intriguing avenues for new low-power electronics.

On the facets, the nano-sized AGNRs are defined by a periodic ladder of nano-buffer stripes and free-standing ribbons as demonstrated by low-energy electron diffraction (LEED), spot-profile analysis (SPA)-LEED and scanning tunneling microscopy (STM), cf. Fig. 1b. By hydrogen intercalation the buffer stripes become decoupled, so that the series of 1D confined nanoribbons is transformed into a single 2D graphene sheet rolling over the 6H-SiC mesa structures. Simultaneously, the buffer layer sheets on the mesas and trenches are also decoupled and turn into the well-known quasi-free standing monolayer graphene (QFMLG). The different constituents of the graphene-SiC interface are identified using X-ray photoelectron spectroscopy (XPS). Due to the different surface terminations of the basal and vicinal SiC planes constituting the mesa structures, different types of charge carriers are locally induced into the graphene layer. By ARPES, we can selectively measure the electronic band structure of the two graphene regions, finding two symmetrically doped phases with p-type being located on the basal planes and n-type on the facets, cf. Fig. 2. Our results demonstrate that through a careful structuring of the substrate, combined with H-intercalation, an array of graphene pn-junctions could be engineered at the nanoscale [3]. Such graphene pn-junctions represent potential building-blocks for a broad spectrum of future technologies, ranging from electronic lenses analogous to metamaterials in optics, to high-performance photodetectors important for a variety of optoelectronic applications.

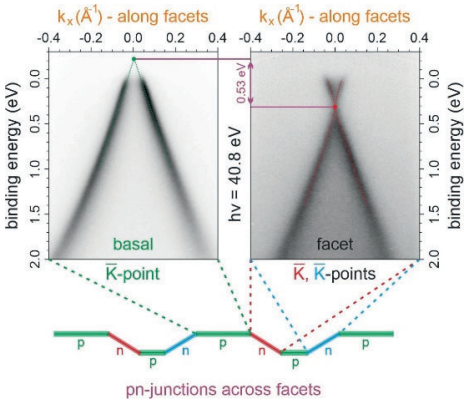

Figure 2: ARPES energy-momentum cuts acquired at the K-points of basal and facet QFMLGs, respectively, as indicated in the schematic side-view of the mesa structure.

This work was supported by the Deutsche Forschungsgemeinschaft (DFG) through Sta315/9-1, Te386/12-1, Te386/13-1 and within FOR5242. We would like to thank Ulrike Waizmann and Thomas Reindl for performing e-beam lithography and reactive ion etching at the Nanostructuring lab of MPI-FKF. We acknowledge MAX IV and HZB/Bessy for the allocation of synchrotron radiation beamtime and the support by their beamline staff. S.R.P. acknowledges funding from the Irish Research Council under the Laureate awards program.

[1] H. Karakachian, T.T. Nhung Nyuyen, J. Aprojanz, A.A. Zakharov, R. Yakimova, P. Rosenzweig, C.M. Polley, T. Balasubramanian, C. Tegenkamp, S.R. Power, U. Starke, Nat. Commun. **11**, 6380 (2020). *One-dimensional confinement and width-dependent bandgap formation in epitaxial graphene nanoribbons.*

[2] T. T. N. Nguyen, S. R. Power, H. Karakachian, U. Starke, and C. Tegenkamp, ACS Nano 17, 20345-20352 (2023). *Quantum Confinement in Epitaxial Armchair Graphene Nanoribbons on SiC Sidewalls.*

[3] H. Karakachian, P. Rosenzweig, T.T. Nhung Nyuyen, B. Matta, A.A. Zakharov, R. Yakimova, T. Balasubramanian, Z. Mamiyev, C. Tegenkamp, C.M. Polley, and U. Starke, Adv. Funct. Mater. 2109839 (2022). *Periodic Nanoarray of graphene pn-junctions on silicon carbide obtained by hydrogen intercalation.*

From Single Atoms to Clusters: Co nanostructures on C-Modified Ni Supports

Valeria Chesnyak[1,2], Srdjan Stavrić[1,3], Mirco Panighel[2], Daniele Povoledo[1], Alessandro Namar[1], Simone del Puppo[1], Daniele Perilli[4], Alexander Markevich[5], Thuy An Bui[5], Aldo Ugolotti[4], Ayesha Farooq[1,2], Matus Stredansky[2], Clara Kofler[5], Cinzia Cepek[2], Jani Kotakoski[5], Maria Peressi[1], Giovanni Comelli[1], Cristina Africh[2]

[1] *Physics Department, University of Trieste, via A. Valerio 2, Trieste 34127, Italy*
(corresponding author: V. Chesnyak, e-mail: chesnyak@iom.cnr.it)

[2] *CNR-IOM, Laboratorio TASC, S.S. 14 Km 163.5, Basovizza, Trieste, 34149, Italy*

[3] *Vinča Institute of Nuclear Sciences – National Institute of the Republic of Serbia, University of Belgrade, P. O. Box 522, RS-11001 Belgrade, Serbia*

[4] *Dipartimento di Scienza dei Materiali, Università di Milano-Bicocca, via R. Cozzi 55, I-20125, Milano, Italy*

[5] *Faculty of Physics, University of Vienna, Boltzmanngasse 5, 1090 Vienna, Austria*

The manipulation of matter at the nanometer scale has introduced transformative possibilities for diverse functionalities in nanoscience and -technology. Stability stands as a cornerstone in the synthesis and application of nanostructures, particularly in (electro-)catalysis, where extreme conditions challenge their endurance [1].

Strategies employing suitable supports to stabilize and enhance the activity of nanostructures have been pivotal. However, the intricate relationship between structural variations and support interactions profoundly influences their properties. Investigations aimed at identifying optimal supports reveal the superiority of C-containing materials, such as graphene, owing to their mechanical and electronic attributes, offering promising avenues in catalysis and as electrode materials [2,3]. Yet, their synthesis complexity and property dependency on the quality of the nanostructured material pose significant challenges.

Within this context, Co nanostructures on C-based supports emerge as versatile tools addressing multidisciplinary realms from physics and chemistry to sustainability challenges like energy storage and catalysis. Despite their potential, the translation of functionalized

graphene-based nanomaterials beyond fundamental research encounters efficiency limitations in resource utilization [4].

This study presents Co nanostructures, starting from single atoms, stabilized in combination with graphene grown on Ni substrates. It comprehensively assesses their synthesis, characterization and stability under diverse conditions mainly by variable temperature scanning tunneling microscopy accompanied by ab initio calculations.

A highly efficient single-step bottom-up synthesis method introduces single Co atoms, alongside Ni, as active sites within the graphene layer grown on Ni supports. The synthesis is inspired by the catalytic activity of transition metals at the growing graphene step edge [5]. These incorporated metal atoms exhibit exceptional stability while preserving their properties as single active sites [6,7]. Notably, the transfer onto another support is presented enabling scanning transmission electron microscopy and electron energy loss spectroscopy measurements on the so produced functionalized layers demonstrating the stability and versatility of the material. Furthermore, such single active sites present a method to efficiently stabilize Co clusters on graphene. The resulting relatively small Co structures exhibit remarkable stability even at elevated temperatures and under CO gas exposure. Finally, selective adsorption of small gas molecules at the single active sites is presented and promising for applications in catalysis, gas sensing and electronics.

These results are relevant in fields such as materials science, catalysis and nanotechnology, presenting an efficient and sustainable approach to stabilize transition metal nanostructures, aiming to go a step forward in fundamental research towards practical applications, emphasizing sustainability, versatility and material efficiency.

We acknowledge financial support from the Italian Ministry of Education, Universities and Research (MIUR) through the program PRIN 2017 - Project no. 2017NYPHN8.

[1] X. Shan, et al. Nat. Nanotech., 7.10, 668-672 (2012)

[2] C. Dong, Y. Li, D. Cheng, M. Zhang, J. Liu, Y. G. Wang, ...& D. Ma, ACS Catal., 10, 11011-11045 (2020)

[3] B. Zhang, et al., In Nanotechnology for Sustainable Development, Springer International Publishing, 371-390, (2014)

[5] L. L. Patera et al., Science, 359, 1243–1246 (2018)

[6] A. Baby, L. Trovato, C. Di Valentin, Carbon, 174, 772-788, (2021)

[7] V. Carnevali et al., Nanoscale, 11, 10358-10364 (2019)

Single-spin flat bands in cobalt-supported graphene

M. Jugovac[1], I. Cojocariu[1,2], J. Sánchez-Barriga[3], P. Gargiani[4], M. Valvidares[4], V. Feyer[2], S. Blügel[5], G. Bihlmayer[5], and P. Perna[3]

[1] Elettra – Sincrotrone Trieste, S.S. 14 – km 163.5, Basovizza, 34149 Trieste, Italy
(corresponding author: M. Jugovac, e-mail: matteo.jugovac@elettra.eu)
[2] Peter Grünberg Institute (PGI-6), Forschungszentrum Jülich GmbH, 52425 Jülich,Germany
[3] IMDEA Nanociencia, Campus de Cantoblanco, c/ Faraday 9, 28049 Madrid, Spain
[4] ALBA Synchrotron Light Source, 08290 Barcelona, Spain
[5] Peter Grünberg Institut and Institute for Advanced Simulation, Forschungszentrum Jülich and JARA, 52425 Jülich,Germany

Due to the fundamental and technological implications in driving the appearance of non-trivial, exotic topological spin textures and emerging symmetry-broken phases, flat electronic bands in 2D materials, including graphene, are a hot topic in the field of spintronics.

By means of spin-resolved angle-resolved photoemission spectroscopy (ARPES) experiments combined with density functional theory (DFT) calculations, we investigated the role of europium in modifying the spin-dependent electronic properties of monolayer Gr on Co(0001). Manifold effects can be revealed: i) an enhancement of the charge transfer into Gr via Eu doping (Fig. 1 top right); ii) the existence of a spin-polarized Gr-Co hybrid state formed by positioning Eu on top or beneath the Gr monolayer in both cases with a single spin (majority) character. While in the former case, the low-dispersive parabolic Gr-Co hybrid band is observed close to Fermi energy (Fig. 1 top right), extending all over the surface Brillouin zone (SBZ), when Eu is intercalated, the π* band becomes flat (Fig. 1 bottom left); iii) the large exchange coupling due to the presence of Eu induces the splitting of the π band that crosses the 4f states into minority and majority branches bending towards higher and lower binding energies respectively, accompanied by a bandgap opening at the Dirac point of about 0.36 eV [1].

In addition, if graphene is sandwiched between two Eu layers, the europium 5d majority bands from the uppermost layer hybridize with graphene, forming single-spin electron pockets, while the hybridization of the minority Eu bands induces hybridization gaps in the π* bands of graphene. Additionally, the spin-resolved measurements reveal a noteworthy single-spin dispersionless contribution near the Fermi level, hinting at the intriguing coupling between the single-spin polarized bands of graphene and optical phonons [2]. This observation expands the understanding of the electronic structure of heavily doped graphene and suggests avenues for exploring novel optical and electronic functionalities.

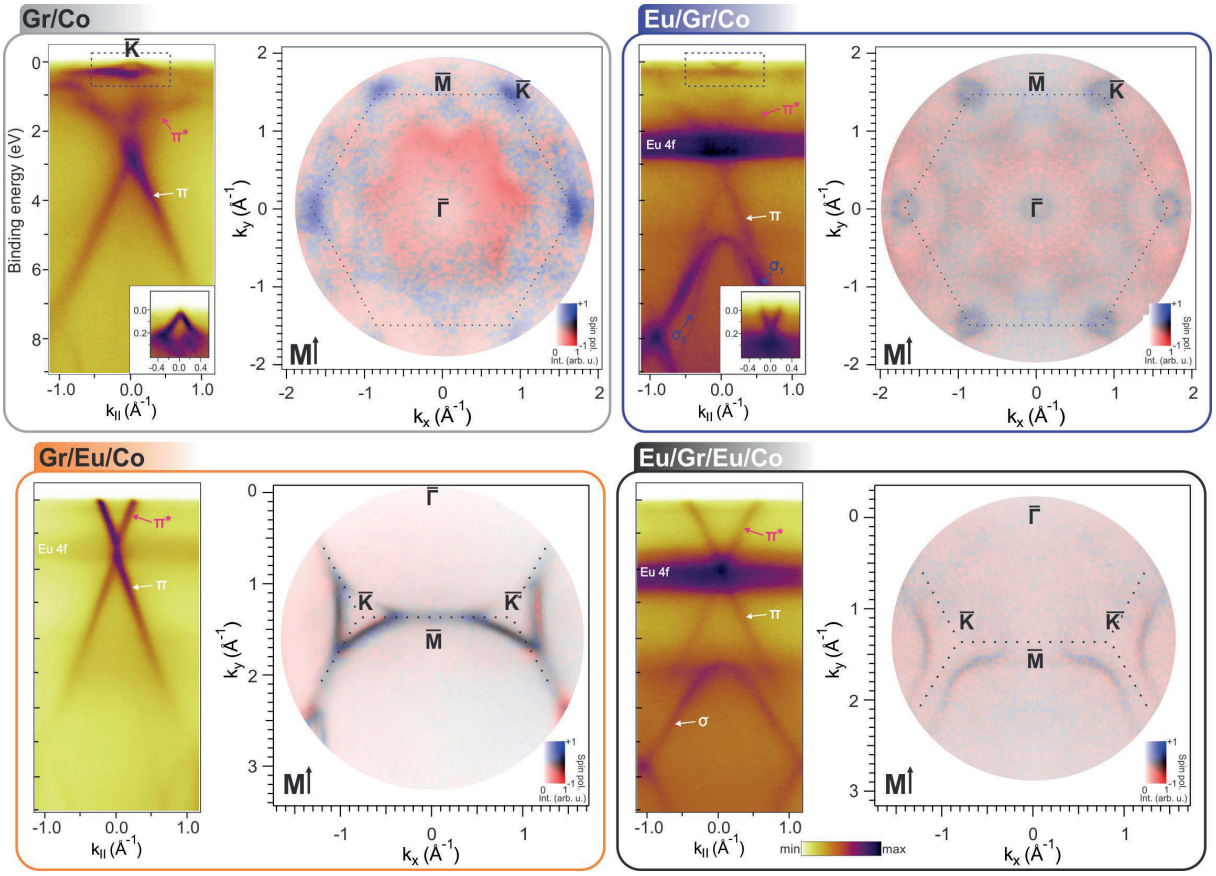

Figure 1. ARPES energy vs. momentum map acquired at the K point of the first Brillouin zone and 2D spin resolved momentum map at the Fermi level of: monolayer graphene/cobalt (top left), Eu deposited on Gr/Co (top right), intercalated Eu at the Gr/Co interface (bottom left) graphene sandwiched between two Eu layers (bottom right).

This research is supported by the FLAG-ERA grant SOgraphMEM Project PCI2019-111867-2 and PCI2019-111908-2 by Spanish AEI and by German DFG. IMDEA team acknowledges support by the Regional Government of Madrid through Project P2018/NMT-4321 (NANOMAGCOST-CM) and by the Spanish MICINN Projects RTI2018-097895-B-C42 (FUN-SOC), PID2021-122980OB-C52 (ECLIPSE-ECoSOx) and the "Severo Ochoa" Programme for Centres of Excellence in R&D (CEX2020-001039-S). S.B. acknowledges funding from Deutsche Forschungsgemeinschaft (DFG) through the Collaborative Research Center SFB 1238 (Project No. C01). G.B. gratefully acknowledges the computing time granted through JARA-HPC on the supercomputer JURECA at Forschungszentrum Jülich.

[1] M. Jugovac, I. Cojocariu, J. Sánchez-Barriga, P. Gargiani, M. Valvidares, V. Feyer, S. Blügel, G. Bihlmayer, and P. Perna, Adv. Mater. 35, 2301441 (2023)

[2] M. Jugovac, I. Cojocariu, V. Feyer, S. Blügel, G. Bihlmayer, and P. Perna, *in preparation*

Continuous growth of germanene and stanene lateral heterostructures

J. Yuhara, T. Ogikubo, H. Shimazu, Y. Fujii, A. Ohta, M. Araidai[1], M. Kurosawa, G. Le Lay[2]

Graduate School of Engineering, Nagoya University, Nagoya 464-8603, Japan

[1]Institute of Materials and Systems for Sustainability, Nagoya University, Nagoya 464-8601, Japan

[2]Aix-Marseille Université, CNRS, PIIM UMR 7345, 13397 Marseille Cedex, France

Group 14 elemental post-graphene materials have received much attention recently because of their outstanding properties, typically, as robust two-dimensional topological insulators. Their heterostructures are one of the next main targets in view of disruptive technological applications. Here, we show the realization of striking in-plane lateral heterostructures between germanene and stanene, which are sustainable 2D Ge- and Sn-based graphene analogs, but with a strong intrinsic spin-orbit coupling. We use a unique combination of atomic segregation epitaxy (ASE) and molecular beam epitaxy (MBE) for the in-situ continuous fabrication of nearly atomically precise lateral multi-junction heterostructures, respectively consisting of atom-thin germanene and stanene on a Ag(111) thin film (Fig.1). Scanning tunneling microscopy (STM) observations down to atomic scale and low-energy electron diffraction testify that germanene and stanene sheets without intermixing are prepared simultaneously on the same terraces at wide scale; remarkably, tin and germanium atoms neither exchange their sites nor adsorb on the germanene and stanene sheets. The atomic structure of the boundary between germanene and stanene is directly derived from atomic-scale STM images (Fig.2), while scanning tunneling spectroscopy reveals key features of the electronic structure at the heterojunction (Fig.3) [1-3]. Our innovative approach of ASE and MBE growths combined in synergy offers great flexibility for the realization of unprecedented lateral 2D heterostructures.

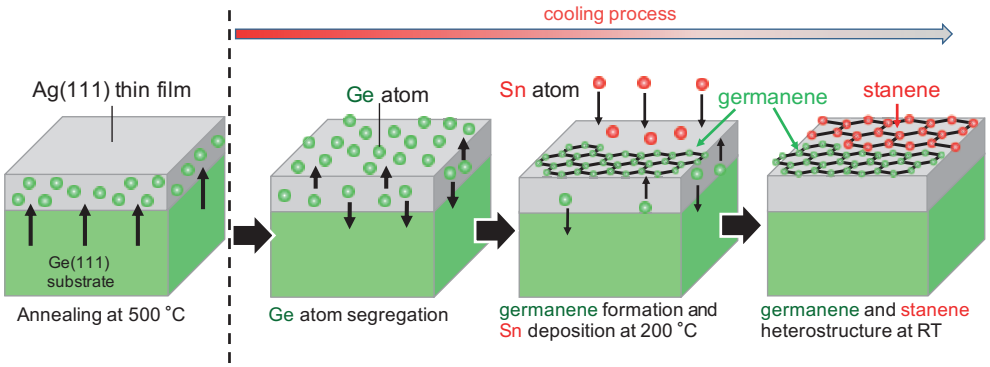

Fig.1. Illustration of the sequential formation of lateral heterostructures of s germanene and stanene, prepared on a Ag(111) thin film grown on a Ge(111) substrate after annealing at 500°C, followed by slow cooling. A Sn deposition is performed at 200°C during the Ge segregation and germanene formation processes while cooling, resulting in the growth of lateral heterostructures of germanene and stanene observed at room temperature.

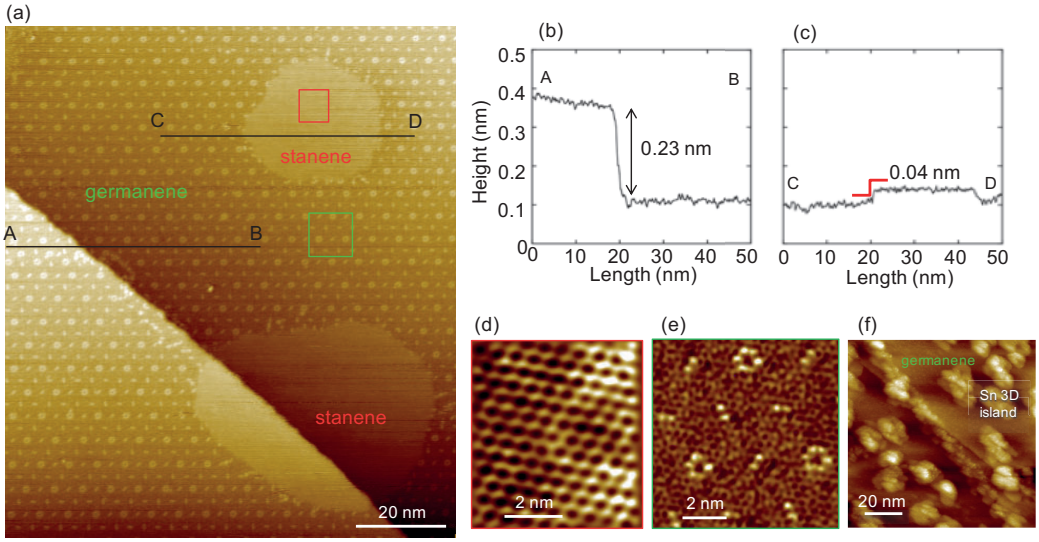

Fig. 2. Lateral heterostructures of germanene and stanene observed at RT. They were prepared on a Ag(111) thin film grown on a Ge(111) substrate after annealing at the substrate temperature of 500 ºC. During the cooling process, where Ge segregation takes place, a Sn deposition of 0.3 ML at 200 ºC was performed. (a) Large-scale STM image (Us = + 1.5 V, I = 200 pA). (b) Section profile along the A-B black line in (a). (c) Section profile along the C-D black line in (a). (d) Atomic-scale STM image of the embedded stanene island within the red square in (a) (Us = + 0.4 V, I = 200 pA). (e) Atomic-scale STM image of the surrounding germanene sheet within the green square in (a); the white circle signals the strongest protrusions in (a) (Us = + 1.0V, I = 200 pA). (f) Wide-scale STM image prepared on a Ag(111) thin film grown on a Ge(111) substrate after annealing at the substrate temperature of 500 ºC with a Sn deposition of 0.3 ML at 150 ºC during the cooling process. (Us = + 1.5 V, I = 200 pA), showing Sn 3D islanding at this too low temperature.

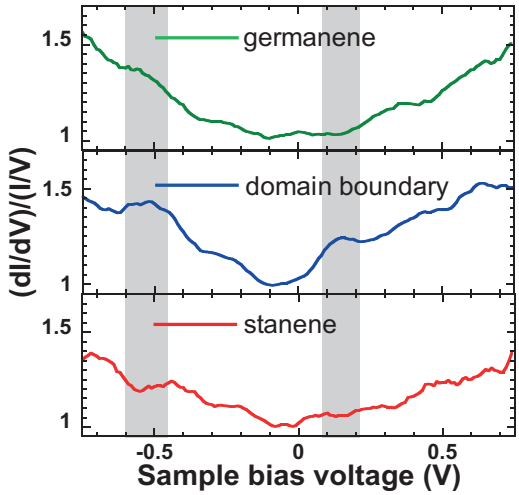

Fig. 3. STS spectra of a germanene zone, a zigzag domain boundary region, and a stanene zone of the heterostructure on the same terrace of the Ag(111) thin film.

[1] J. Yuhara, H. Shimazu, K. Ito, A. Ohta, M. Araidai, M. Kurosawa, M. Nakatake, G. Le Lay, ACS Nano 2018, 12, 11632.

[2] J. Yuhara, Y. Fujii, K. Nishino, N. Isobe, M. Nakatake, L. Xian, A. Rubio, G. Le Lay, 2D Mater. 2018, 5, 025002.

[3] T. Ogikubo, H. Shimazu, Y. Fujii, K. Ito, A. Ohta, M. Araidai, M. Kurosawa, G. Le Lay, J. Yuhara, Adv. Mater. Interfaces, 7, 1902132 (2020)

Two-Dimensional Epitaxial Silicene: Synthesis, and Processing Paths for Technology Applications

Alessandro Molle, Christian Martella, Carlo Grazianetti

CNR-IMM, unit of Agrate Brianza, via C. Olivetti 2, I-20864 Agrate Brianza, Italy
(corresponding author: alessandro.molle@cnr.it)

Isolation of graphene paved the way to an unprecedented fashion of two-dimensional (2D) materials. While many of them can be readily derived by mechanical exfoliation in the form of single-crystal flakes, a synthetic approach to 2D materials production is functional to have scalability and atomic control as enabling factors for applications. Xenes, namely 2D single-element crystals beyond graphene, are a representative case in this respect [1]. A first generation of Xenes started from group IV elements of the periodic table, so called silicene, germanene, stanene, and more recently plumbene as counterpart of silicon, germanium, tin, and lead, respectively. The list of synthetic Xenes progressively encompassed a second generation made of elements from the group III (B group), V (pnictognes), and VI (chalcogens). Xenes display a characteristic electronic variability from Dirac semimetals to metals and semiconductors. Heavier Xenes, with stronger spin-orbit coupling interaction, incorporate a non-trivial topological texture, i.e. a 2D topological insulators state [2]. Here we focus on silicene, namely 2D Si, as paradigmatic case of Xene from its synthesis by template and interface engineering up to the technology transfer. Silicene is epitaxially grown on a (111) terminated Ag surface [3]. As epitaxial material, silicene is thus qualified by a large-area coverage that is conformal with the underlying surface morphology, see the scanning tunneling microscopy (STM) image of epitaxial silicene in **Figure 1a**. Self-organization of silicene is kinetically driven, and stable forms of silicene are made possible by the simultaneous emergence of diffrently buckled arrangements of the surface atoms giving rise to a structural polymorphism in the same layer (**Figure 1b**) [4]. By template and interface engineering through atomic Sn [5], we recently demonstrated single phase selection in a silicene monolayer via Sn decoration of the Ag(111) surface, and silicene decoupling from ist host substrate via stannene (2D Sn) buffering [7]. The latter case is a prototypical example of an epitaxial silicene-stannene

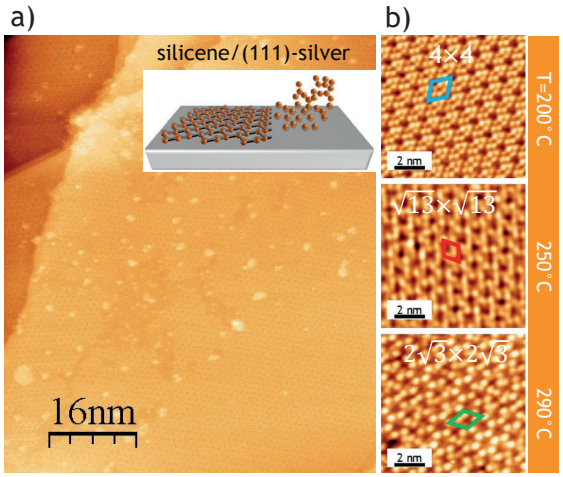

Figure 1 a) Large-scale STM topography of epitaxial silicene on Ag(111) (see growth scheme in sketch); b) Three structural motifs of silicene as a function of the growth temperature (see side bar).

heterostructure which discloses the possibility to pile-up diverse Xene layers in a fully Xene-based heterostructure scheme.
Not only the silicene-stannene heterostructure allows us to single out characteristic physical properties of silicene (like thermal conductivity and plasmonic edge) from any proximity effects from the substrates [7], but also it is the first step to develop an all-around encapsulation of the silicene. The second step consists of the sequential growth of a nanoscale Al_2O_3 capping layer at room temperature on the top silicene face [8]. Due to environmental degradation of silicene, all-around encapsulation is necessary to stabilize silicene out of the growth ambient and allows for the silicene transfer to other target substrates for further manipulation and technology exploitation. In the latter respect, under Raman spectrosocpy monitoring, we developed a delamination process flow surface starting from an epitaxial Ag/mica as host substrate for a silicene-stanene heterostructurte [9], and consisting of the mechanical removal of the substrate and the transfer to a target substrate. Eventually, the Ag layer can be chemically etched off, kept to ensure native electrodes, or reduced to provide a support layer in a flexible configuration. This process allowed to us to fabricate silicene field effect transistors with ambipolar behavior [10] and, more recently, to derive bendable silicene membranes with strain-sensitive response when integrated in a piezoresistor device [11].
Silicene membranes appears to be a prototypical platform to test relevant silicene features like piezoresistivity and thermoelectricity in atomically thin silicon under external solicitation, e.g. bending strain, external pressure, laser irradiation. The development of silicene by means of epitaxial methods and atomic control at the surface level is shown to be a viable path for Xene engineering towards the derivation of unique properties in carefully tailored configurations and the transfer into diverse device platforms (like transistors, piezoresistors, etc.). This approach can be universally extended to the whole class of the epitaxial Xenes towards a Xene-based science and technology.

Finacial support from EU ERC-CoG grant n. 772261 “XFab“ and from ERC-PoC 2021 grant n. 101069262 is gratefully acknowledged.

[1] “Xenes“ (1st ed.), Eds. A. Molle and C. Grazianetti, 2022 Woodhead Publishing, Elsevier (UK).
[2] A. Molle, et al., Nature Mater. 16, 163 (2017).
[3] P. Vogt, et al., Phys. Rev. Lett. 108, 155501 (2012).
[4] C. Grazianetti, A. Molle et al., Appl. Surf. Sci. 291, 109 (2014).
[5] S. Achilli, A. Molle, et al., Nanoscale 15, 11005 (2023).
[6] D. S. Dhunagan, A. Molle, et al., Adv. Funct. Mater. 31, 2102797 (2021).
[7] E. Bonaventura, A. Molle, et al., Nanoscale Horiz. 7, 924 (2022).
[8] D. S. Dhungana, C. Massetti, A. Molle, et al., Nanoscale Horiz. 8, 1428 (2023).
[9] C. Martella, A. Molle, et al., Adv. Funct. Mater. 30, 2004546 (2020).
[10] L. Tao, A. Molle, et al., Nature Nanotech. 10, 227 (2015).
[11] C. Martella, A. Molle, et al. Adv. Mater. 35, 2211419 (2023).

Two-dimensional atomic surfaces for defect-mediated resistive switching phenomenon

SungJin Yang, D. Akinwande

Electrical and Computer Engineering, and Texas Materials Institute
The University of Texas – Austin.
Texas, USA. 78758
deji@ece.utexas.edu

The advent of two-dimensional (2D) materials has ushered in a new era in the understanding of atomic defects and their physical consequences such as field-drived non-volatile resistance change, a phenomenon suitable for the contemporary paradign of brain-inspired or neuromorphic computing [1]. 2D materials and their high-speed low-energy prospects offer a transformative potential for information technology. These materials, often one atom thick, exhibit exceptional electrical, thermal, and mechanical properties that are markedly different from their bulk counterparts [2]. In the context of non-volatile resistive switching, 2D materials provide a unique platform due to their accessible atomic surface, quantum confinement effects, and the possibility of tailoring their electronic properties through physical and chemical modifications. This makes them ideal for use in memristors, a class of non-volatile memory devices, where they can facilitate high-density data storage with low power consumption [3]. Furthermore, in neuromorphic computing, which aims to mimic the neural structures and processing methods of the human brain, 2D materials enable the creation of devices that can efficiently emulate the functions of biological synapses and neurons. This is due to their ability to facilitate multiple resistance states and exhibit synaptic plasticity, a key requirement for learning and memory in artificial neural networks.

This work highlights the discovery of memory effect in 2D atomically-thin nanomaterials towards greater scientific understanding and advanced engineering applications. Non-volatile resistance change effect based on 2D materials are an application of defects and is a rapidly advancing field with rich physics that can be attributed to vacancies combined with metal adsorption in the monolayer limit in otherwise ordinary materials. Scanning tunneling microscopy (STM) and other advanced characterization tools have been employed to elucidate the underlying physical mechanisms of resistance change owing to defects in the atomic material [4]. In particular, this work will highlight our pioneering work on monolayer memory, also known as atomristors, that has expanded to over a dozen 2D sheets and can enable various applications including zero-power devices, non-volatile RF switches, and memristors for neuromorphic computing. These memory devices offer high-energy efficiency and fast switching that may benefit mobile systems, cloud computing and data centers towards reduced energy consumption worldwide.

The integration of 2D materials in neuromorphic systems promises significant advantages in terms of speed, energy efficiency, and miniaturization, potentially advancing AI systems by offering a closer approximation to the parallelism and adaptability of the human brain [3].

Acknowledgement

Support by the National Science Foundation (NSF) is gratefully acknowledged.

References

[1] R. Ge, et al., Advanced Materials 33 (7), 2007792 (2021).
[2] G. R. Bhimanapati, et al., ACS Nano (2015).
[3] S. Chen, et al., Nature Electronics (2020).
[4] S. M. Hus, et al., Nature Nanotechnology (2020).

Chemical principles for N-doped graphene nanostructures of different dimensionality

Shi-Xia Liu, Rémy Pawlak[1], Ulrich Aschauer[2], Laerte L. Patera[3], Silvio Decurtins, Jascha Repp[3], Pavel Jelinek[4], and Ernst Meyer[1]

Department of Chemistry, Biochemistry and Pharmaceutical Sciences, University of Bern, Switzerland (corresponding author: S.-X. Liu, e-mail: shi-xia.liu@unibe.ch)

[1] *Department of Physics, University of Basel, Switzerland*

[2] *Department of Chemistry and Physics of Materials, University of Salzburg, Jakob-Haringer-Straße 2A, 5020 Salzburg, Austria*

[3] *Institute of Experimental and Applied Physics, University of Regensburg, Germany; present address: Institut für Physikalische Chemie, Universität Innsbruck, Innrain 52c, Josef Möller Haus, 6020 Innsbruck, Austria*

[4] *Institute of Physics of Czech Academy of Sciences, Czech Republic*

Carbon-based functional nanomaterials, particularly graphene [1], have been highly attractive systems for technological applications in nanoelectronics, environmental science, energy storage, quantum information science, and biosensors [2]. To explore these potential applications, it is of prime importance to open up and control the bandgap in graphene nanomaterials [3]. On-surface self-assembly and chemical reactions have become an ideal platform not only for the access to carbon-based functional nanomaterials which are impossible to synthesize by wet chemistry, but also for fine-tuning the band gap, optical and electrical properties, and charge transport [4]. Due to intrinsic electronic properties of N-containing planar heterocycles, we have set ourselves the task of modulating band gap through dimensionality engineering by judicious chemical design and synthesis of nitrogenated polycyclic aromatic hydrocarbons (N-PAHs). As a consequence, a variety of tailored N-PAH precursors with different structural symmetry and functional groups have been prepared for the formation of a range of nanostructures, including molecular wires [5,6], triply fused porphyrin-graphene nanoribbon (GNR) hybrid [7], as well as 1D N-doped GNRs [8] and highly symmetric 2D *Kagome* nanographens [9] via surface-assisted C-C coupling reactions. We also successfully applied Scholl reaction for C-C bond formation via on-surface synthesis, which has the advantage that precursors do not need to be pre-functionalized [10, 11] in contrast to Ullmann coupling which occurs between halogen-functionalized building blocks. More importantly, it turns out that N-PAHs can self-assemble into nanostructures via

H-bonds [12,13] and/or halogen-halogen bonds [14], whereby different charge/spin states can be manipulated at the nanoscale [13,14].

This presentation will focus on our collaborative work on self-assembly and chemical reactions on various surfaces leading to the formation of N-doped graphene nanostructures by applying chemical principles. All of these atomically precise nanostructures can be directly visualized by scanning tunneling microscopy (STM) and noncontact atomic force microscopy (nc-AFM). The fine-tuned electronic properties by chemical modification are discussed.

Support by the SNF (projects CRSII5 213533, 200020_188445 and 200021_204053) is gratefully acknowledged.

[1] A. Geim, K. Novoselov, Nature Mater. 6, 183 (2007)

[2] Z. Li, L. Wang, Y. Li, Y. Feng and W. Feng, Compos. Sci. Technol. 179, 10 (2019)

[3] F. Schwierz, Nature Nanotech. 5, 487 (2010)

[4] O. Gröning, S. Wang, X. Yao, C. A. Pignedoli, G. Borin Barin, C. Daniels, A. Cupo, V. Meunier, X. Feng, A. Narita, K. Müllen, P. Ruffieux and R. Fasel, Nature 560, 209 (2018)

[5] R. Pawlak, J. G. Vilhena, P. D'Astolfo, X. Liu, G. Prampolini, T. Meier, T. Glatzel, J. A. Lemkul, R. Häner, S. Decurtins, A. Baratoff, R. Perez, S. X. Liu and E. Meyer, Nano. Lett. 20, 652 (2020)

[6] S. Karan, Y. Geng, S. Decurtins, S. X. Liu and J. Repp. Chem. Commun. 56, 7901 (2020)

[7] L. M. Mateo, Q. Sun, S. X. Liu, J. J. Bergkamp, K. Eimre, C. A. Pignedoli, P. Ruffieux, S. Decurtins, G. Bottari, R. Fasel and T. Torres, Angew. Chem. Int. Ed. 59, 1334 (2020)

[8] R. Pawlak, X. Liu, S. Ninova, P. D'Astolfo, C. Drechsel, S. Sangtarash, R. Häner, S. Decurtins, H. Sadeghi, C. J. Lambert, U. Aschauer, S. X. Liu and E. Meyer, J. Am. Chem. Soc. 142, 12568 (2020)

[9] R. Pawlak, X. Liu, S. Ninova, P. D'Astolfo, C. Drechsel, J. C. Liu, R. Häner, S. Decurtins, U. Aschauer, S. X. Liu and E. Meyer, Angew. Chem. Int. Ed. 60, 8370 (2021)

[10] N. Kocic, X. Liu, S. Chen, S. Decurtins, O. Krejci, P. Jelinek, J. Repp and S.-X. Liu, J. Am. Chem. Soc. 138, 5585 (2016)

[11] L. L. Patera, X. Liu, N. Mosso, S. Decurtins, S. X. Liu and J. Repp, Angew. Chem. Int. Ed. 56, 10786 (2017)

[12] X. Liu, A. Matej, T. Kratky, J. I. Mendieta-Moreno, S. Gunther, P. Mutombo, S. Decurtins, U. Aschauer, J. Repp, P. Jelinek, S. X. Liu and L. L. Patera, Angew. Chem. Int. Ed. 61, e202112798 (2022)

[13] N. Kocic, D. Blank, P. Abufager, N. Lorente, S. Decurtins, S. X. Liu and J. Repp, Nano Lett. 19, 2750 (2019)

[14] C. Li, C. Kaspar, P. Zhou, J.-C. Liu, O. Chahib, T. Glatzel, R. Häner, U. Aschauer, S. Decurtins, S.-X. Liu, M. Thoss, E. Meyer and R. Pawlak, Nat. Commun. 14, 5956 (2023).

On-surface synthesis and characterization of [19]-starphene

S. Salaverría[1], T. Wang[2], P. Angulo[3], J. Besteiro[4], L. Mateo[4], F. García[4], J. P. Calupitan[3], A. García-Fuente[5], J. Ferrer[5], D. Perez[4], M. Corso[3], D. Peña[4] and D. G. de Oteyza[1]

(corresponding author: D. G. de Oteyza, e-mail: d.g.oteyza@cinn.es)

[1] *Nanomaterials and Nanotechnology Research Center (CINN), CSIC-UNIOVI-PA, 33940 El Entrego, Spain*

[2] *Donostia International Physics Center, 20018 San Sebastián, Spain*

[3] *Centro de Fisica de Materiales (CFM-MPC), CSIC-UPV/EHU, 20018 San Sebastián, Spain*

[4] *CIQUS and Facultad de Química, Universidad de Santiago de Compostela, E-15782 Santiago de Compostela, Spain*

[5] *Departamento de Física, Universidad de Oviedo, 33007 Oviedo, Spain*

Starphenes are appealing compounds formed by symmetric trimerization of acenes. Large acenes themselves are readily very interesting molecules because of the open-shell character that they develop with increasing size. In starphenes, it is intriguing to know how the coupling between the three arms affects its electronic and magnetic properties, which may render the starphenes promising candidates for future organic optoelectronic applications. However, due to the low solubility and instability that large starphenes present, their synthesis has been challenging. To date, the largest starphene obtained is [16]-starphene, which basically comprises three pentacene arms [1]. Herein, we propose two new strategies using different molecules as precursors, whereby we obtain [19]-starphene by on-surface synthesis on Au(111) (Fig. 1a). Its characterization by scanning tunneling microscopy and spectroscopy (Fig. 1b,c) reveals a notably reduced HOMO-LUMO gap as compared to the previously studied (smaller) starphenes. Interestingly, the gap of starphenes is systematically lower than the gap of the acenes that form each of its arms (Fig. 1e), which supports that the arms are partically conjugated. In particular, the gap of [19]-starphene is not only lower than that of hexacene (the length of each arm), but lower than that of any reported acene, regardless of its size.

In order to expand the comparison to a larger range of sizes and to obtain a better understanding of these molecular systems, we have performed theoretical calculations (Fig.

1d). The calculations show remarkable resemblance to the experiments, with systematically lower HOMO-LUMO gap values for the (experimentally probed) starphenes and the value for [19]-starphene being lower than that of any calculated acene. However, for larger starphenes the gap increases and saturates to the same value as the gap of the acenes does. Modelling the DFT results with a simplified mean-field Hubbard model provides an intuitive description of the size dependence.

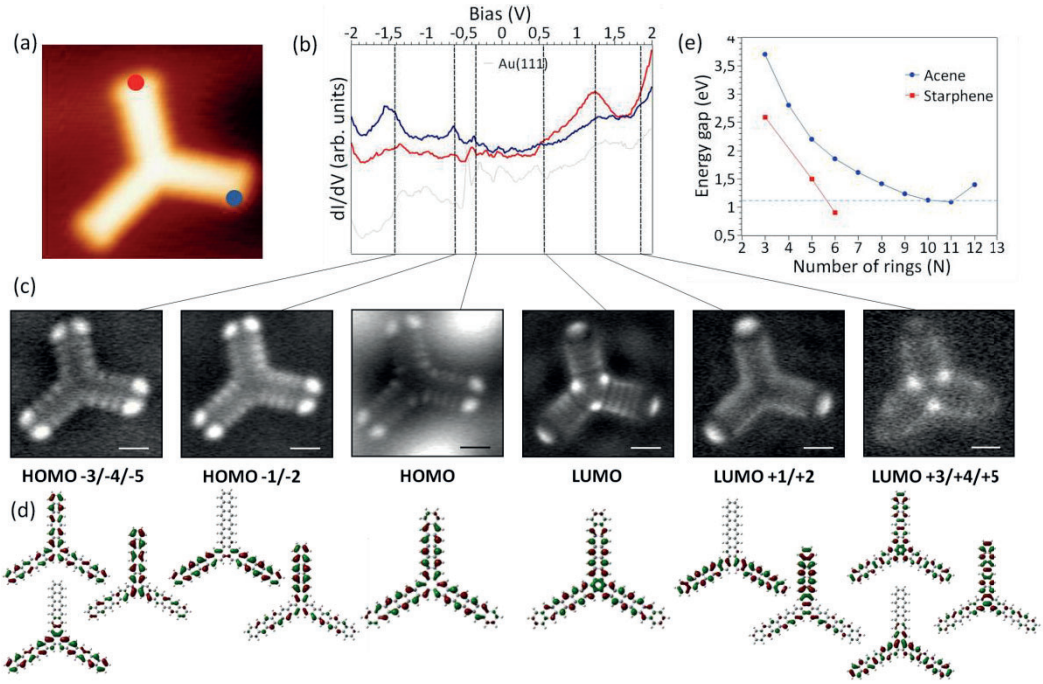

***Fig. 1**. a) STM image of [19]-starphene. b) Differential conductance point spectra acquired on the molecule at the positions marked in panel (a) and on the bare surface. c) Conductance maps acquired at -1.42 eV, -0.64 eV, -0.36 eV, 0.54 eV, 1.2 eV and 1.85 eV. d) Wavefunctions of the orbitals associated with each of the measured resonances and conduction maps in previous panels. e) HOMO-LUMO gap as determined by scanning tunneling spectroscopy for starphenes and acenes of varying size, For a better comparison, the starphene size is given by the number of rings on each of its arms, the currently analyzed [19]-starphene thus corresponding to N=6. The dashed horizontal line marks the smallest acene gap reported to date, observed on undecacene.*

Support by MCIN/AEI/10.13039/501100011033 (grant nos. PID2019-107338RB-C62, PID2019-107338RB-C63) and the European Union "NextGenerationEU"/PRTR (TED2021-132388B-C42, TED2021-132388B-C43), from MCIN/AEI/10.13039/501100011033/ERDF/EU (PID2022-140845OBC64), is gratefully acknowledged.

[1] J. Holec, B. Cogliati, J. Lawrence, A. Berdonces-Layunta, P. Herrero, Y. Nagata, M. Banasiewicz, B. Kozankiewicz, M. Corso, D. G. de Oteyza, A. Jancarik, A. Gourdon, A large starphene comprising pentacene branches, Angew. Chem. Int. Ed. **2021**, 60, 7752–7758

Covalent M-Porphyrin Networks: Synthesis, ORR/OER Performance and Stability

A. Vestergaard, J. V. Lauritsen

Interdisciplinary Nanoscience Center, Aarhus University, 8000 Aarhus, Denmark
(corresponding author: A. Vestergaard, e-mail: av@inano.au.dk)

Single-atom catalysts (SACs) have gained attention for the oxygen reduction/evolution reaction (ORR/OER) due to their high atom utilization and the ability to tune the state of the metal atom through various ligands [1]. The possibility of tuning reactivity also makes earth-abundant transition metals (Co, Ni, Fe, Mn) viable [2], potentially making them competitive with state-of-the-art Pt/C electrodes [3]. Metal-porphyrins stand out as promising candidates for SACs due to the well-defined coordination of the central metal atom by four nitrogen atoms (M-N_4). Therefore, they have been widely employed to form both metal-organic frameworks and covalent-organic frameworks [4]. However, detailed information regarding how these structures change chemically and structurally during operation remains limited.

Studying adsorbed porphyrins on surfaces allows for the utilization of techniques such as electrochemical scanning tunneling microscopy (EC-STM) and X-ray photoelectron spectroscopy (XPS). For example, EC-STM studies have explored the adsorption of species like O_2 and OH^- on the central Co atom in a Co-porphyrin [5,6]. Another study utilized STM to reveal the disordering (decomposition) during ORR (OER) of a Fe-coordinated Co-porphyrin [7].

Typically, surface science studies done on M-porphyrins involve adsorbed molecules interacting with each other through weak van der Waals forces [5,6]. We hypothesize that stability can be improved by covalently bonding these molecules to form an extended 2D network.

To create covalent M-porphyrin networks, we deposited a non-metalated porphyrin molecule (5,10,15,20-(tetra-4-bromophenyl)porphyrin) on an Au(111) support. Subsequently, metal atoms (Co, Ni, Fe, or a mix) were deposited using an e-beam, incorporating them into the porphyrin centers. Finally, the sample was annealed to facilitate an Ullmann coupling [8], resulting in the formation of C-C bonds. STM and XPS characterization revealed that the molecules formed a 2D network extending over the entire substrate, with the metal atoms in the center of the porphyrins.

To assess the activity and the stability of the M-porphyrin network, ORR, and OER were performed in our ultra-high vacuum (UHV) compatible EC cell [9]. The setup and the possibility to test different metals and metal combinations make it a versatile platform for identifying trends in reactivity between the different metals and potential synergistic effects

from mixing different metals. Preliminary findings indicate that covalent bonding leads to a slight enhancement in activity compared to a non-covalent sample.

After electrochemistry, the samples are brought back to the UHV environment to track changes caused by the electrochemical environment. Sweeping to ORR or OER potentials results in different states: after ORR the sample appears stable with an intact porphyrin network and the metal remaining in the M-N_4 coordination. OER, however, seemingly results in a degradation of the porphyrin network.

Support by the Fonds Danmarks Frie Forskningsfond is gratefully acknowledged.

[1] M. Humayun, M. Israr, A. Khan, M. Bououdina, Nano Energy 113 (2023) 108570

[2] R. Gutru, B. Vigolo, International Journal of Hydrogen Energy Volume 48, Issue 9 (2023)

[3] D. Yu, Y. Ma, F. Hu, C. Lin, L. Li, H. Chen, X. Han, S. Peng, Advanced Energy Materials (2021), 11, 2101242

[4] Z. Liang, H. Wang, H. Zheng, W. Zhang, R. Cao, Chem. Soc. Rev. (2021), 50, 2540

[5] Z. Cai, X. Wang, D. Wang, L. Wan, ChemElectroChem (2016), 3, 2048–2051

[6] X. Wang, Z. Cai, D. Wang, L. Wan, J. Am. Chem. Soc. (2019), 141, 7665−7669

[7] D. Hötger, M. Etzkorn, C. Morchutt, B. Wurster, J. Dreiser, S. Stepanow, D. Grumelli, R. Gutzler, K. Kern, Phys. Chem. Chem. Phys., (2019), 21, 2587-2594

[8] L. Grill, M. Dyer, L. Lafferentz, M. Persson, M. V. Peters, S. Hecht, Nature Nanotechnology vol. 2, p. 687–691 (2007)

[9] Z. Sun, J. V. Lauritsen, Rev. Sci. Instrum. 92, 094101 (2021)

Successive on-surface synthesis of fused anthracenyl-porphyrins

M. Baljozović[1], Joffrey Pijeat[2], Stéphane Campidelli[2], Karl-Heinz Ernst[1,3,4]

[1] *Molecular Surface Science Group, Empa - Swiss Federal Laboratories for Materials Science and Technology, 8600 Dübendorf, Switzerland*
(corresponding author: M. Baljozović, e-mail: milos.baljozovic@empa.ch)

[2] *Université Paris-Saclay, CEA, CNRS, NIMBE, LICSEN, 91191 Gif-sur-Yvette, France*

[3] *Department of Chemistry, University of Zurich, 8057 Zürich, Switzerland*

[4] *Nanosurf Laboratory, Institute of Physics, The Czech Academy of Sciences, 16200 Prague, Czech Republic*

On-surface chemistry has lately provided means for C-C bond creation that would otherwise hardly be accessible by conventional solution chemistry. It enables preparation of materials with peculiar properties such as bis-/tris-helicenes,[1,2] graphene nanoribbons,[3] graphene quantum dots[4–6] and carbon nanotubes[7]. By utilization of the bottom-up approach, these can be reliably and predictably created from smaller polycyclic aromatic hydrocarbons as precursors. At the same time, limited number of examples involving porphyrin-like precursors exist.[8–10] The latter are particularly interesting due to ability to host metals, providing another handle for tuning their electronic, transport and magnetic properties. Moreover, the synthesis of fused bis- and tetra-4,5-bis-(2,4,6-trimethylphenoxy)anthracen-9-yl porphyrins containing Ni(II) was reported by Anderson about 10 years ago and have shown astonishing shift of absorbance maxima by about 550 nm and 1000 nm for bis- and tetra-substituted molecules, respectively.[11,12] Nevertheless, the formation of π-extended porphyrins bearing unsubstituted anthracenyl moieties were so far never achieved.

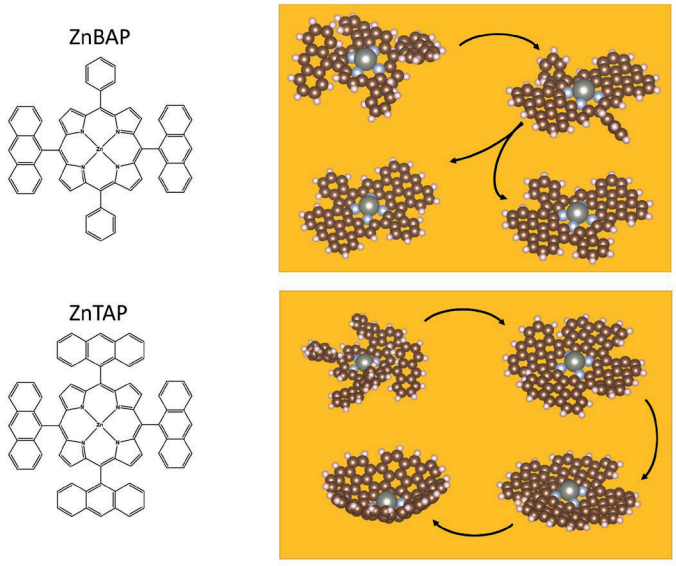

Figure 1. Molecular structures and schematics of anthracenyl-porphyrin (cyclo)dehydrogenation

In this contribution we demonstrate temperature controlled (cyclo)dehydrogenation of bis- and tetra-anthracenyl functionalized Zn-porphyrin molecules on Au(111) substrate. On-surface dehydrogenation is not limited only to the first dehydrogenation step involving fusion of anthracenyl units to the macrocycle, but can progress

further. The successive dehydrogenation with temperature elevation is leading to novel products that could be identified in our STM and ToF-SIMS study. Additionally, starting from tetra-anthracenyl porphyrins, bowl-shaped products are created at a very high surface coverage.

Support by the Swiss National Science Foundation and University Research Priority Program LightChEC is gratefully acknowledged.

[1] J. Li, K. Martin, N. Avarvari, C. Wäckerlin, K.-H. Ernst, *Chem. Commun.* **2018**, *54*, 7948–7951.
[2] A. Mairena, C. Wäckerlin, M. Wienke, K. Grenader, A. Terfort, K.-H. Ernst, *J. Am. Chem. Soc.* **2018**, *140*, 15186–15189.
[3] J. Cai, P. Ruffieux, R. Jaafar, M. Bieri, T. Braun, S. Blankenburg, M. Muoth, A. P. Seitsonen, M. Saleh, X. Feng, K. Müllen, R. Fasel, *Nature* **2010**, *466*, 470.
[4] R. Zuzak, J. Castro-Esteban, P. Brandimarte, M. Engelund, A. Cobas, P. Piątkowski, M. Kolmer, D. Pérez, E. Guitián, M. Szymonski, D. Sánchez-Portal, S. Godlewski, D. Peña, *Chem. Commun.* **2018**, *54*, 10256–10259.
[5] Z. Liu, S. Fu, X. Liu, A. Narita, P. Samorì, M. Bonn, H. I. Wang, *Advanced Science* **2022**, *9*, 2106055.
[6] J. Su, W. Fan, P. Mutombo, X. Peng, S. Song, M. Ondráček, P. Golub, J. Brabec, L. Veis, M. Telychko, P. Jelínek, J. Wu, J. Lu, *Nano Lett.* **2020**, *21*, 861–867.
[7] J. R. Sanchez-Valencia, T. Dienel, O. Gröning, I. Shorubalko, A. Mueller, M. Jansen, K. Amsharov, P. Ruffieux, R. Fasel, *Nature* **2014**, *512*, 61.
[8] L. M. Mateo, Q. Sun, S.-X. Liu, J. J. Bergkamp, K. Eimre, C. A. Pignedoli, P. Ruffieux, S. Decurtins, G. Bottari, R. Fasel, T. Torres, *Angew. Chem. Int. Ed.* **2020**, *59*, 1334–1339.
[9] Q. Sun, L. M. Mateo, R. Robles, N. Lorente, P. Ruffieux, G. Bottari, T. Torres, R. Fasel, *Angewandte Chemie International Edition* **2021**, *60*, 16208–16214.
[10] A. Wiengarten, K. Seufert, W. Auwärter, D. Ecija, K. Diller, F. Allegretti, F. Bischoff, S. Fischer, D. A. Duncan, A. C. Papageorgiou, F. Klappenberger, R. G. Acres, T. H. Ngo, J. V. Barth, *J. Am. Chem. Soc.* **2014**, *136*, 9346–9354.
[11] N. K. S. Davis, A. L. Thompson, H. L. Anderson, *J. Am. Chem. Soc.* **2011**, *133*, 30–31.
[12] N. K. S. Davis, A. L. Thompson, H. L. Anderson, *Org. Lett.* **2010**, *12*, 2124–2127.

Beyond dense packing: supramolecular interactions as a design element in self-assembled monolayers

Kirsty Munro[1], Michal Valásek[2], Andika Asyuda[3], Stephen Francis[1], Michael Zharnikov[3], Marcel Mayor[2,5], Manfred Buck[1]

[1]*EaStCHEM School of Chemistry, Univ. St Andrews, St Andrews, KY16 9ST, UK*
corresponding author: M. Buck, e-mail: mb45@st-andrews.ac.uk
[2]*Institute of Nanotechnology, Karlsruhe Inst. of Technology (KIT), 76021 Karlsruhe,Germany*
[3]*Angewandte Physikalische Chemie, Univ. Heidelberg, 69120 Heidelberg, Germany*
[5]*Department of Chemistry, Univ. Basel, 4056 Basel, Switzerland*

Self-assembly of molecular monolayers on surfaces comes in two flavours, supramolecular networks (SMNs) and self-assembled monolayers (SAMs, see Fig. 1). In the case of SMNs planar molecules lie flat on a surface and supramolecular interactions involving hydrogen or metal-organic coordination bonding in combination with molecular geometries are the structure determining factors [1,2]. In contrast, SAMs are characterised by a dense packing of upright standing molecules due to the molecule-substrate interaction as the main driving force for film formation. Both approaches have their advantages and limitations with SMNs, on the one hand, representing ultaprecise templates for hosting other species [3] but, on the other hand, being very limited in their functionalisation out of the surface plane. The situation is essentially inverted in SAMs where functionalisation orthogonal to the surface is easily possible but the control of lateral structures beyond a dense packing of molecules and, thus, control over intermolecular distances is very limited. So far, strategies to tackle this problem have relied on the use of a larger area base unit and a vertically oriented functional unit positioned at its center. Examples are the platform approach, where both units are combined in a single molecule [4], or the use of host-guest chemistry, where a macrocylic molecule defines the periodicity and the guest molecule determines the function [5].

Interestingly, another strategy which is based on supramolecular interactions between upright standing molecules, i.e., combines features characteristic of SMNs and SAMs, has been explored only very sporadically [6-8]. Here we report our recent investigation on SAM formation of BP-PCA, a biphenyl based aromatic pentacarboxylic acid (see Fig. 1) at the liquid/solid interface. Aiming for an open network SAM structure instead of layers with densely packed molecules, the molecule combines trimesic acid (TMA) and isophthalic acid (IPA). Containing two IPA structural motifs in opposing configuration this geometry allows for the formation of a layer where the aromatic rings of BP-PCA are twisted against each other, thus resulting in a structure which is determined by hydrogen bonding between the carboxylic acid groups as illustrated by the sketches on the right of Fig. 1. In such a configuration four out of the five COOH moieties are involved in the network formation

whereas the remaining one serves as anchor to the substrate. This means that both carboxylate and free carboxylic acid are present, and, therefore formation of the SAM is dependent on pH. If the pH is too high disordered layers form with more than one carboxy group per molecule interacting with the surface. If it is too low anchoring of the molecules is impeded.

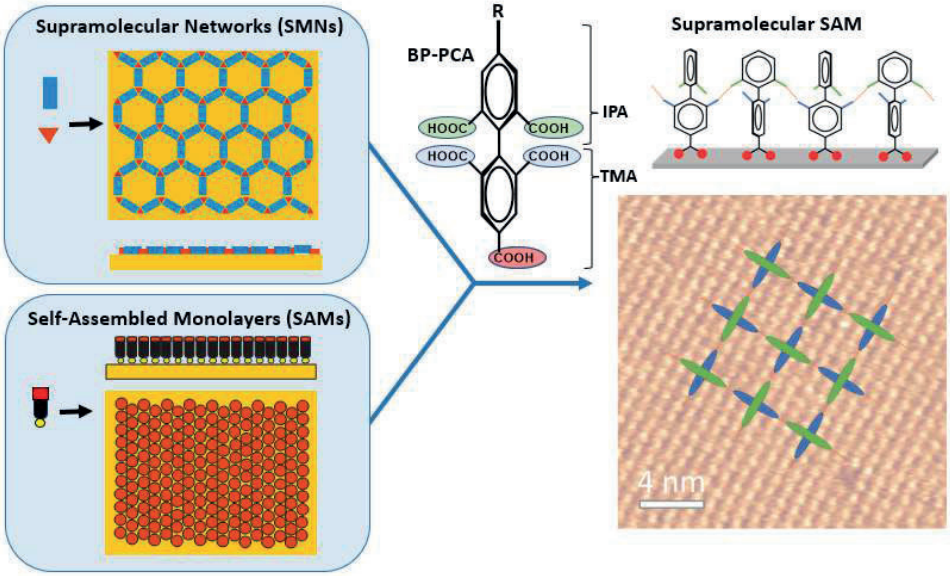

Fig. 1 In SMNs and SAMs (left) molecular orientation and layer structures are governed by different intermolecular and molecule-substrate interactions. BP-PCA, a combination of trimesic acid (TMA) and isophthalic acid (IPA), merges design elements of both types of molecular assemblies, which enables formation of a SAM with an open structure (right). The STM image shows a BP-PCA network SAM on a Au(111) surface modified by a bilayer of Ag.

(1) Écija, D.; Urgel, J. I.; Seitsonen, A. P.; Auwärter, W.; Barth, J. V. Acc. Chem. Res., *51*, 365 (2018)
(2) Goronzy, D. P.; Ebrahimi, M.; Rosei, F.; Arramel; Fang, Y.; De Feyter, S.; Tait, S. L.; Wang, C.; Beton, P. H.; Wee, A. T. S.; Weiss, P. S.; Perepichka, D. F. ACS Nano, *12*, 7445 (2018).
(3) Karamzadeh, B.; Eaton, T.; Munoz Torres, D.; Cebula, I.; Mayor, M.; Buck, M. Farad. Disc., *204*, 173 (2017).
(4) Jung, U.; Schütt, C.; Filinova, O.; Kubitschke, J.; Herges, R.; Magnussen, O. J. Phys. Chem. C, *116*, 25943 (2012).
(5) Escorihuela, E.; del Barrio, J.; Davidson, R. J.; Beeby, A.; Low, P. J.; Prez-Murano, F.; Cea, P.; Martin, S. Nanoscale, adv. Article, DOI: 10.1039/D3NR05122F (2023).
(6) Johnson, K. N.; Hurlock, M. J.; Zhang, Q.; Hipps, K. W.; Mazur, U. Langmuir, *35*, 5271 (2019).
(7) Ortiz de la Morena, R.; Asyuda, A.; Lu, H.; Aitchison, H.; Turner, K.; Francis, S. M.; Zharnikov, M.; Buck, M. Phys. Chem. Chem. Phys., *22*, 4205 (2020).
(8) Aitchison, H.; Lu, H.; Ortiz de la Morena, R.; Cebula, I.; Zharnikov, M.; Buck, M. . Phys. Chem. Chem. Phys. *20*, 2731 (2018).

Wednesday

The Dirty Surface Science of Niobium

V. Vonk[1], G.D.L. Semione[1,2], A. Zaidman[1,2], T.F. Keller[1,2], M. Wenscat[1], W. Hillert[2] A. Stierle[1,2]

(corresponding author: V. Vonk, e-mail: vedran.vonk@desy.de)

1 Centre for X-ray and Nanoscience), Deutsches Elektronen-Synchrotron (DESY), D-22607 Hamburg,

2 Physics Department, University of Hamburg, D-20355 Hamburg, Germany

Niobium is a type II superconductor with the highest critical transition temperature (T_c) of all pure metals. Owing to its favorable mechanical properties, it is the current material of choice for many superconducting applications. However, its superconducting properties are affected by the presence and precipitation of impurities in the near-surface region. This plays a huge role in the development and improvement of so-called superconducting radio-frequency cavities, which lie at the heart of modern accelerator facilities.

Over the past years, different annealing procedures have been discovered, which boost the SRF performance. However, a mechanistic understanding of the correlation between the performance and materials properties has not yet been established.

Here, an overview will be given of experimental studies [1-3], using surface science approaches, of the effect of annealing procedures in different environments. A variety of different samples, which have all been polished to near-atomic smoothness, have been used: UHV-annealed single crystals, large-grain polycrystals and fine-grain poly-crystals.

The most prominent feature consists of the dissolution of the native niobium oxide, a process starting around 430 K, and which results in an increasing concentration of interstitial oxygen in the metal lattice. These defects are believed to be detrimental to the superconductivity. Depending on the history of the sample, carbide precipitates are observed as well, especially near grain boundaries on polycrystalline samples. The heterogeneities of these effects can be resolved by SEM/EDX and by XRD using nanobeams (Fig 1.), for which as special measurement scheme has been developed.

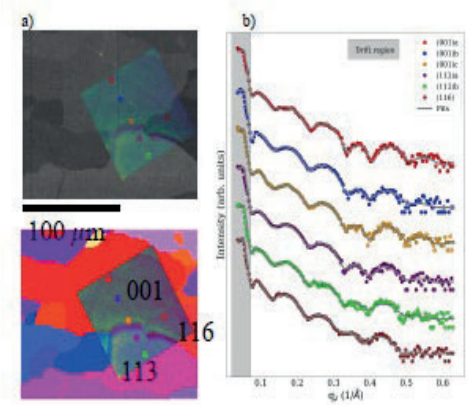

Fig. 1 a) SEM of a selected region (top) and the corresponding grain orientations (bottom). Overlain in a transparent color is the region mapped out by nanoXRR. The colored dots in a) indicate the positions where full XRR curves were taken. The results in b) show these XRR curves and fits (lines) using the same color coding.

[1] G. D. L. Semione, V. Vonk et al. Phys. Rev. Accelerators and Beams, 22, 10:103102, **2019**.

[2] M. Delheusy, A. Stierle et al 2008 Appl. Phys. Lett. 92 101911

[3] G. D. L. Semione, V. Vonk, M. Wenskat, A. Stierle et al. J. Phys: Cond. Mat. 33 (2021) 265001

Funded by BMBF project OPSCURES, Grant No. 05H18GURB1

How the support defines properties of 2D metal-organic frameworks: Fe-TCNQ on graphene vs. Au(111)

Z. Jakub, J. Planer, A. Shahsavar, P. Procházka, and J. Čechal

CEITEC – Central European Institute of Technology
Brno University of Technology, 61200 Brno, Czechia

(corresponding author: Z. Jakub, e-mail: zdenek.jakub@ceitec.vutbr.cz)

The functionality of 2D metal-organic frameworks (MOFs) crucially depends on the local environment of the embedded metal atoms. These atomic-scale details are best ascertained on MOFs supported on well-defined (metal) surfaces, but the interaction with the support often changes the system properties. This complicates the comparison of the atomically-defined models to the applied systems. We elucidate the extent of this effect by comparing an Fe-TCNQ 2D MOF on two weakly-interacting supports: graphene and Au(111). Using scanning tunneling microscopy, photoemission spectroscopy and density functional theory, we show that the Fe-TCNQ on graphene partially retains its intrinsic properties, as it is non-planar with iron in quasi-tetrahedral sites. In contrast, when synthesized on Au(111), a popular weakly-interacting support, the Fe-TCNQ structure is planarized by stronger van-der-Waals interaction.

The differences in physical and electronic structure result in distinct properties of the supported 2D MOFs. The d_{z^2} center position is shifted by 1.4 eV between Fe-sites on the two supports, which implies dramatically different adsorption and catalytic properties of these seemingly similar „single-atom catalyst“ sites. The implications of different physical structure of the Fe-sites are then experimentally studied using a TCNQ probe molecule, which chemically interacts with the Fe-TCNQ/graphene system, but only physisorbs on Fe-TCNQ/Au due to the lower accessibility of the the sunk-down Fe sites.

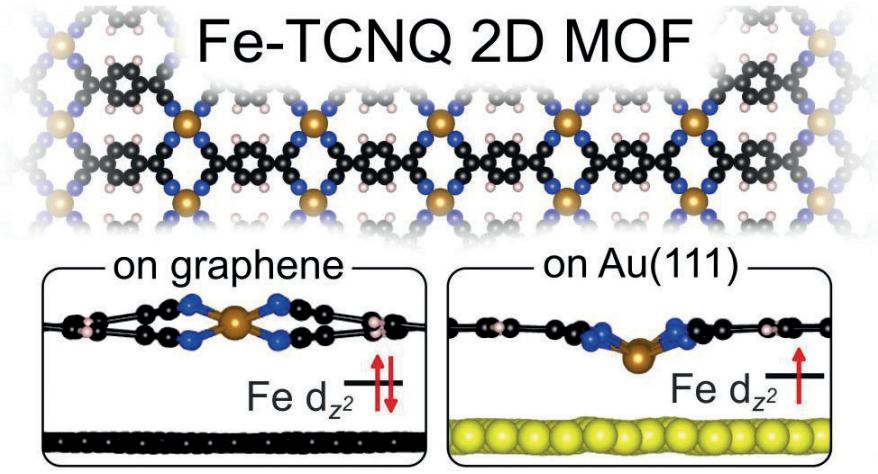

In summary, our results outline the limitations of common on-surface approaches using metal supports and show that the intrinsic MOF properties can be partially retained on graphene. We have previously demonstrated that graphene-supported metal-TCNQ systems are remarkably stable both thermally and chemically, thus we propose these as perfect models for research of single-atom catalysis.

We gratefully acknowledge funding from the European Union's Horizon 2020 research and innovation programme (MSCA grant agreement No. 101027667), from the European Social Fund (projects CZ.02.2.69/0.0/0.0/20_079/0017436 and CZ.02.01.01/00/22_010/0002552), from GAČR (grant number 22-05114S) and from MEYS CR (projects LM2018110 and e-INFRA CZ ID:90140).

References

[1] Z. Jakub et al., JACS, 2024 (accepted), DOI: 10.1021/jacs.3c13212

[2] Z. Jakub et al., Nanoscale, 2022,14, 9507-9515

Setup for Angle-Selective IRAS – Investigation of CO and D_2O on TiO_2(110)

David Rath, Jiri Pavelec, Moritz Eder, Ulrike Diebold, Michael Schmid, Gareth S. Parkinson

TU Wien, Institute of Applied Physics, Austria
(corresponding author: D. Rath, e-mail: david.rath@tuwien.ac.at)

Infrared (IR) spectroscopy is a versatile tool to identify molecular species and their structures based on their characteristic vibrational frequencies. It can be used in various environments, including ideal and operando conditions, making it a valuable tool for reaction monitoring in academic research as well as in industry. In contrast to other prominent techniques, such as X-ray photoelectron spectroscopy (XPS), IR spectroscopy is not restricted to low pressures. Hence, it is a powerful bridging technique for characterizing idealized systems in ultra-high vacuum (UHV) and applied conditions. IR spectroscopy can be performed in different ways; transmission spectroscopy is the most popular variant. However, studies of single crystals used in surface science require spectroscopy of the reflected light.

The identification of adsorbed species is crucial in investigating single-atom catalysts (SACs) [1], making Infrared Reflection Absorption Spectroscopy (IRAS) an ideal spectroscopic method due to its high surface sensitivity. IR light is detected after a single reflection on the sample surface using a Fourier transform infrared (FTIR) spectrometer to characterize adsorbates. However, measuring oxide surfaces is challenging due to their low reflectivity, the absence of the field-enhancement effect on metal surfaces and surface selection rules. The signal expected on oxide surfaces is typically one to two orders of magnitude lower than on metals. Therefore, applying SAC on metal oxides poses a great challenge due to the intrinsic problem of low sensitivity, further aggravated by a low density of adsorbates on the surface of an SAC. In this contribution, an IRAS design optimized for SACs on oxide substrates in UHV will be presented. The primary objective was to achieve exceptional sensitivity for low coverages of adsorbates on metal oxide surfaces. A novel approach was developed to perform incidence-angle-selective IRAS, which enhances peak heights and maximizes optical throughput while reducing noise levels.

To achieve reduced noise levels, a custom optics system ensures high throughput from the spectrometer (Bruker Vertex 80v) exit to the detector. To maintain throughput, a mirror with a short focal length concentrates the IR light onto a 3.5 mm circular adsorbate-covered area on the sample, created by a molecular beam [2]. The optical design includes four elliptical mirrors and one parabolic mirror for optimum performance, flexibility, and usability. Two of these mirrors are mounted on motorized kinematic mounts.
To optimize the peak height, it is necessary to assess the reflection properties of the sample with and without adsorbate. Calculations reveal that the differential reflectivity of non-metallic samples with adsorbed molecules varies significantly with the incidence angle and can even change sign, resulting in cancellation. Therefore, when measuring IRAS on oxides, it is crucial to carefully select the incidence angle range, as the optimum angle ranges vary for each material. Factors such as depolarization of the light, incidence angle spread, and illumination of areas not covered by adsorbates can affect the expected signals. Our IRAS system takes these factors into account by incorporating two apertures. One aperture controls the shape of the illumination spot on the sample to reduce the background signal, while a second aperture selects

the incidence angle range of the infrared radiation illuminating the sample in the range between 48° and 88°. This approach optimizes the light incidence angle range depending on the investigated material and the IR light polarization.

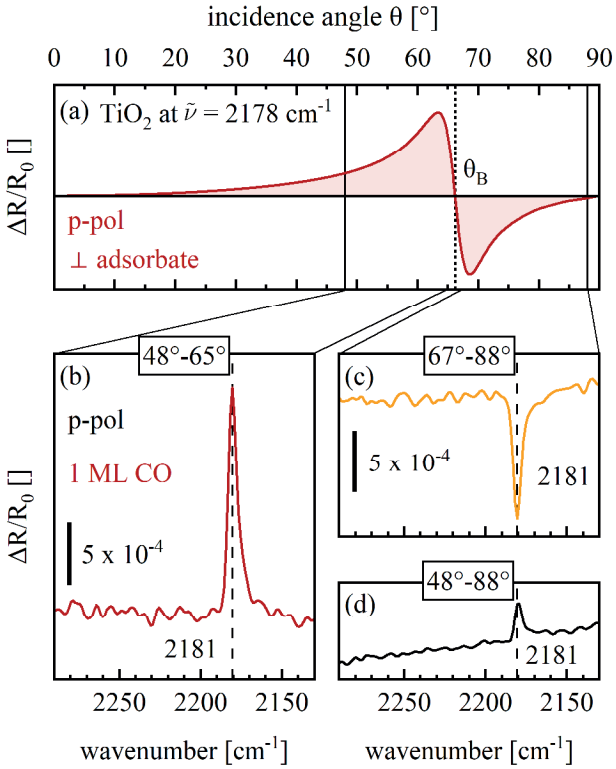

Figure 1. Calculated differential reflectivity and p-polarized raw spectra measured with different angular measurement configurations of the IRAS setup. (a) shows the simulated differential reflectivity $\Delta R/R_0$ for an adsorbate on TiO_2(110) surface. In (b), (c), and (d), spectra of 1 ML CO measured with different incidence angle ranges are visible. The spectra have all the same scale for comparability.

For verification of the setup, D_2O and CO absorbance measurements on a rutile TiO_2(110) surface were successfully executed; they agree with the established literature [3,4]. The full potential of the IRAS system is showcased by an evaluation of the signal-to-noise ratio as a function of the incidence angle range for one monolayer CO on TiO_2(110). Properly selecting the incidence angle range achieved a signal-to-noise ratio of ≈ 70 for 1 ML CO adsorbed on TiO_2 with only 150 seconds of measurement time. In addition, we measured sub-monolayer coverages of CO on TiO_2(110) decorated with Rh (≈ 0.05 ML) to show its potential in the investigation of SACs.

[1] G. S. Parkinson, Catal. Lett. **149**, 1137 (2019)

[2] J. Pavelec, et al., J. Chem. Phys. **146**, 014701 (2017)

[3] N. G. Petrik, et al., J. Phys. Chem. C. **126**, 12407 (2022)

[4] N. G. Petrik, and G. A. Kimmel, J. Phys. Chem. Lett. **3**, 3425 (2012)

Unveiling the Complexity of Single-Atom Catalysts on Rh-decorated TiO_2 (110) via Infrared Absorption Reflection Spectroscopy

Jiří Pavelec, Moritz Eder, David Rath, Chunlei Wang, Ulrike Diebold, Michael Schmid, Gareth S. Parkinson

Vienna University of Technology, Institute of Applied Physics, Austria
(corresponding author: Gareth S. Parkinson, e-mail: parkinson@iap.tuwien.ac.at)

Infrared Absorption Reflection Spectroscopy (IRAS) is a pivotal technique in catalysis research, effectively linking model catalysts on single crystals to those in powder form, and is a standard method in industrial applications. The study of low coverages of adsorbates on single-crystalline metal oxide supports, especially Single-Atom Catalysts (SACs), presents significant challenges, yet it offers a clear path to identifying IR signatures. In the SAC community, the gem-dicarbonyl IR signature is recognized as a proof of single atom sites [1]. However, our recent scanning probe study of CO on Rh-decorated Fe_3O_4(001) system suggests a more intricate scenario [2]. This contribution outlines a preparative study aimed at estabilishing a definitive link between the IR gem-dicarbonyl signature and various SAC model systems using a multi-technique surface science approach.

Employing a newly developed IRAS setup (explained on this conference in the contribution by David Rath), this research focuses on CO adsorption on a 0.05 ML Rh on TiO_2(110). Investigations of this system have been done predominantly on powder forms for the last 50 years, with sparse single-crystal studies primarily utilizing dissociative adsorption of $\{Rh(CO)_2Cl\}_2$ [3]. Building on our previous SPM/XPS study [4], where the stabilization of single atom Rh sites was achived by deposition at low temperatures (100K), we expose Rh-decorated TiO_2 (110) to CO and perform IRAS measurements.

After exposure to CO at 80K, we observed various signatures in the CO IR region, including those associated with the clean surface [5]. This suggests a complex adsorption behavior characterized by multiple CO coordination states. At this temperature, CO mobility appears to be limited. Annealing the system to 150K results in a distinct gem-dicarbonyl IR signature, which remains observable up to 300K. Upon increasing the temperature to 500K, we observe Rh clustering and CO desorption, as evidenced by shifts in IR peak positions, aligning with those seen in CO adsorbed on Rh metal surfaces [6]. Employing IRAS s-polarization measurements allowed us to determine the orientation of the gem-dicarbonyl, findings that are consistent with theoretical predictions [1] but in contrast with previous surface science studies utilizing dissociative adsorption of $\{Rh(CO)_2Cl\}_2$ [3]. Complementary Temperature-

Programmed Desorption (TPD) and X-ray Photoelectron Spectroscopy (XPS) measurements align with IRAS observations.

This study presents a comprehensive IRAS analysis of CO on Rh (0.05ML) decorated TiO_2(110), demonstrating the effectiveness of our IRAS setup for such investigations and its potential for synergistic use with SPM studies. Our findings offer reference points for IR signatures offering valuable insights into SACs.

[1] Y. Tang, C. Asokan, M. Xu, G. W. Graham, X. Pan, P. Christopher, J. Li, P. Sautet; Nat Commun.; 10 (1), (2019).

[2] Ch. Wang, P. Sombut, L. Puntscher, Z. Jakub, M. Meier, J. Pavelec, R. Bliem, M. Schmid, U. Diebold, C. Franchini, G. S. Parkinson, in submission; (2024).

[3] B. E. Hayden, A. King, M. A. Newton; Chemical Physics Letters; 269 (5); (1997).

[4] P. Sombut, L. Puntscher, M. Atzmueller , Z. Jakub, M. Reticcioli, M. Meier, G. S. Parkinson, C. Franchini; Top Catal. 65, (2022).

[5] N.G. Petrik, and G.A. Kimmel; J. Phys. Chem. Lett. 3 3425 (2012).

[6] M. M. Jansen, J. Gracia, J., B. E. Nieuwenhuys, J. W. Niemantsverdriet, Physical Chemistry Chemical Physics 11 (43), (2009).

www.hidenanalytical.com
info@hiden.co.uk

HIDEN ANALYTICAL

Instruments for Surface Analysis

Depth Profiling and Surface Imaging at the Nanoscale

Mass spectrometers for vacuum, gas, plasma and surface science

ToF-qSIMS

Investigate a full spectrum of materials, from alloys to pharmaceuticals, down to sub-ppm levels with the ToF-qSIMS.

Compact SIMS

Easily and quickly characterise nanoscale layer structures with 2D and 3D imaging plus mass spectral data using the Compact SIMS.

Hi5 SIMS

Simultaneously acquire positive and negative ions for complimentary data in a single shot using the Hi5 SIMS.

FIB-SIMS

Meet the analytical requirements of various depth profiling and nanoscale surface imaging applications using FIB-SIMS.

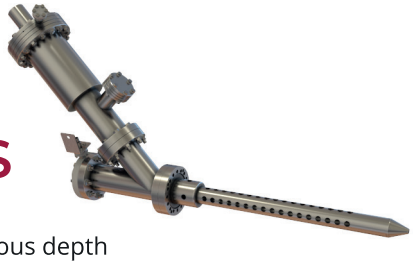

Postersession

The role of defects in the initial oxidation of Ru(0001) and their effect on surface chemistry

E. Perez Penco[1], S. van Vliet[1], J. Cottom[1], E. Olsson[1,2], and R. Bliem[1,2]

[1]*Advanced Research Center for Nanolithography, Science Park 106, 1098 XG Amsterdam, The Netherlands (corresponding author: R. Bliem, e-mail: r.bliem@arcnl.nl)*

[2]*Institute of Physics, University of Amsterdam, Science Park 904, 1098XH Amsterdam, The Netherlands*

The structure of a material is inextricably linked to its properties, including surface-focused ones such reactivity, selectivity, and stability in active environments. In addition to the structure of surfaces at application conditions, the predominant types of defects and their concentration are essential to the performance of materials in applications like catalysis, protective coatings, and micro-/nano-electronics. For oxide surfaces, oxygen vacancies have typically been considered the main defects of interest, since they are known to influence properties of functional oxides like TiO_2, MgO, or ZnO[1,2]. Recent studies combining experimental and computational methods, however, have unveiled the underestimated role of cation vacancies in selected systems[3,4].

Ruthenium and its surface oxides are an ideal model system to revisit with a focus on the role of defects because simple defect structures have not been sufficient to describe the initial oxidation of the metal's most stable surface, Ru(0001). The evolution of this surface in oxidizing environments is highly relevant since Ru oxides are excellent catalysts, for example for the oxygen evolution reaction. The close-packed Ru(0001) and the RuO_2(110) surfaces have thus been studied in detail and their structures are considered solved[5,6]. However, in the initial phase of oxidation, also disorder and nanostructuring have been reported[7], and experimental evidence regarding the transition from Ru(0001) layer to RuO_2(110) via the theoretically predicted O-Ru-O trilayer[8] has not been conclusive.

Here, we combine in situ X-ray photoelectron spectroscopy and density functional theory (DFT) to better understand thermal oxidation of Ru(0001) and provide new insight on the nature of the initial oxide, its growth, and the role of defects. At 280 to 480°C in 10^{-4} mbar O_2, the oxidation is observed to follow a two-step pathway, with fast growth up to thickness level of approximately 0.6 nm, followed by a plateau of constant thickness and finally a second regime of growth towards the saturation thickness of several nanometers. Upon exceeding 0.6 nm, the emergence of an electron energy loss satellite indicates the gradual transition to an electronically different phase, rutile RuO_2. This transition is accelerated by higher surface roughness and oxygen pressures, indicating a dependence of the rate-limiting step on defectivity and the chemical potential of oxygen. This observation is in excellent agreement with DFT results showing that the buildup of strain in the growing Ru oxide

trilayer leads to a tendency to introduce disorder and form Ru vacancies, facilitating further growth of the layer. We speculate that growth may require defects for diffusion to proceed, explaining the pressure- and roughness-dependent limitations of growth. The predicted defect-rich, disordered Ru oxide trilayer could further explain the difficulties to observe this intermediate oxide phase using surface-sensitive diffraction and imaging techniques.

The observed difference in the spectroscopic signature of the trilayer oxide and the stable bulk phase, rutile RuO_2, is a clear indicator for an electronic difference between the two oxides. This difference is reflected in the interaction of the two oxides with molecules in experiments on their reactivity and stability in gas environments. In situ exposure to SiH_4 (1% in Ar), for example, does not show any effect on rutile RuO_2/Ru(0001), but leads to the formation of a compound of Si, Ru, and O at the surface for the Ru oxide trilayer. Similarly, an atmosphere of water vapor (10^{-4} mbar) leaves rutile RuO_2 unaffected over a wide range of temperatures, whereas reduction and oxygen removal is observed for the Ru oxide trilayer at 180°C.

In summary, we propose that cation vacancies are essential in the formation and growth of the initial oxide layer on Ru(0001), explaining the kinetically hindered growth at low oxygen pressures and the observation of disordered layers in the literature. The different electronic and surface chemical properties of the Ru trilayer oxide motivate further study of its role in the application of Ru in catalysis, protective coatings, and micro-/nano-electronics.

This work has been carried out at the Advanced Research Center for Nanolithography, a public-private partnership of the University of Amsterdam, the Vrije Universiteit Amsterdam, the Dutch Research Council (NWO) and the semiconductor equipment manufacturer ASML.

[1] Diebold, U., Li, S. C., and Schmid, M. Oxide surface science. *Annu Rev Phys Chem* **61**, 129–148 (2010).

[2] Wöll, C. The chemistry and physics of zinc oxide surfaces. *Prog Surf Sci* **82**, 55–120 (2007).

[3] Bliem, R. *et al.* Subsurface cation vacancy stabilization of the magnetite (001) surface. *Science* **346**, 1215–1218 (2014).

[4] Zhang, J. *et al.* Cation vacancy stabilization of single-atomic-site $Pt_1/Ni(OH)_x$ catalyst for diboration of alkynes and alkenes. *Nat Commun* **9**, 1002 (2018).

[5] Over, H. *et al.* Atomic-scale structure and catalytic reactivity of the RuO_2(110) surface. *Science* **287**, 1474–1476 (2000).

[6] Reuter, K. and Scheffler, M. Composition, structure, and stability of RuO_2(110) as a function of oxygen pressure. *Phys Rev B* **65**, 035406 (2001).

[7] Goriachko, A. The Nanostructuring of Atomically Flat Ru (0001) upon Oxidation and Reduction. *Nanoscale Res Lett* **11**, 54 (2016).

[8] Reuter, K., Ganduglia-Pirovano, M.V., Stampfl, C., and Scheffler, M. Phys. Rev. B, 65, 165403 (2002).

Matrix dependence analysis enabling quantitative application of Low-Energy Ion Spectroscopy for wide bandgap semiconductor materials

C.Bocaniciu[1], C. Cupak[1], M. Ostermann[2], M. Kogler[2], L. Kalchgruber[1], S. Natemeyer[3], W.L. Sun[3], M. Nelhiebel[3] and M. Valtiner[1]

[1]*Applied Interface Physics Group, Institut für Angewandte Physik (IAP), Technische Universität Wien, E134 - 1040 Wien, Austria*

[2]*Center of Electrochemical Surface Technology (CEST), Viktor Kaplan-Strasse 2, 2700 Wiener Neustadt, Wien, Austria*

[3]*Infineon Technologies Austria, Siemensstrasse 2, 9500 Villach, Austria*

(Corresponding author: C. Bocaniciu, e-mail: bocaniciu@iap.tuwien.ac.at)

Semiconductors are a class of materials with electrical properties between conductors and insulators and have revolutionized modern technology. Their unique electronic behavior, rooted in quantum mechanics, enables precise control over the flow of electricity. This control forms the basis of semiconductor devices that power our electronically interconnected world.

At the heart of semiconductor physics lies the understanding of band theory which is explained by the state of the electrons on different energy levels [1]. The lower energetic levels are known as the valence band, while the higher energy level constitutes the conduction band. For semiconductors, the Fermi level is found between these two bands. Introducing specific chemical elements as dopants into semiconductors enables to tune the electronic properties, such as augmenting electron density, thereby bringing the Fermi level closer to the conduction band, or increasing hole concentration, thereby nearing the Fermi level to the valence band [2]. Electric conductivity elevates with the introduction of energy in the system by increasing the temperature, enabling electrons to traverse to higher energy levels within these bands.

Numerous chemical elements allow a favorable semiconducting band structure, including Silicon (Si), Germanium (Ge), and various binary compounds integrating elements from groups 13 and 15 in the periodic table, such as Gallium Nitride (GaN). GaN is characterized by a Wurtzite crystal structure and a known bandgap of 3.4 eV [3]. This material holds significant promise as a prime candidate for high-voltage transistors or RF electronics, attracting considerable research attention in recent years. The introduction of Aluminum (Al) into GaN enables the precise modulation of both its bandgap and electrical conductivity. However, the specific trapping mechanism within GaN involving Al — whether through substitution of Gallium or interstitial incorporation — remains undetermined. Moreover, differences between the stoichiometry in the bulk material and on its surface are expectable, as surface termination is may play a significant role. However, the properties of surfaces and interfaces are the key for semiconductor performance at present.

Our recent investigations employing low-energy ion scattering (LEIS) have been specifically directed towards establishment of quantitative analysis for semiconductor material surfaces, motivated to optimize device performance and production recipes. LEIS represents a pivotal surface analysis method capable of probing the composition and structural characteristics of materials at the very atomic surface level. Its methodology includes the irradiation of samples with monoenergetic noble gas ion beams, e.g., using He or Ne, and analyzing the backscattered ion energies. The energy spectrum usually includes characteristic element specific features, thus allowing qualitative insights into the surface elemental constituents. Also, elemental depth profiling can be conducted if Ar sputtering is used sequentially with LEIS. Complementing these qualitative aspects, quantitative information can be derived from the background-subtracted single-collision (SC) peak areas in the energy spectra. More specifically, the atomic abundance of a given element in a mixed sample can be determined by comparing the SC peak intensity of that element by the same signal observed from a pure reference material. This methodology enables the accurate determination of elemental concentrations on the examined material's surface.

However, conducting a quantitative analysis of a sample with LEIS necessitates to check first for potential presence of "matrix effects" within the sample. These "matrix effects", which relate to different ion neutralization properties between the sample of interest and a pure reference material, can emerge in samples which show different electronic binding structures. In fact, accurate determination of atomic percentages of elements within a sample relies heavily on the absence of "matrix effects" [4]. Therefore, recognition and mitigation of these effects are imperative for precise elemental quantification in our material analysis. As only limited number of literatures is existing for our materials of interest, investigation of "matrix effects" holds considerable significance.

In the presented work, the relevance of "matrix effects" is therefore tested by conducting multiple measurements using LEIS at various ion energies and ion species. The absence of "matrix effects" in the materials of interest is inferred if the relative abundance of elemental constituents remains constant as a function of different primary ion energies, following the argumentation by Brongersma et al. [4]. In this study, Ga, Al, and BN serve as reference materials against the semiconductor specimens — GaN and AlGaN — enabling a comprehensive analysis to determine the presence or absence of "matrix effects".

[1] Kittel, C. (2005). Introduction to Solid State Physics. John Wiley & Sons, Inc.

[2] Nave, R. (2021) "Doped Semiconductors". Oti Chukwunyere Christian Physics 102

[3] Levinshtein, M. E., Rumyantsev, S. L., & Shur, M. S. (2001). Properties of Advanced Semiconductor Materials: GaN, AIN, InN, BN, SiC, SiGe. John Wiley & Sons.

[4] Brongersma, H. H., Draxler, M., De Ridder, M., & Bauer, P. (2007). Surface composition analysis by low-energy ion scattering. Surface Science Reports, 62(3), 63-109.

Ion-specific and concentration-dependent adsorption on mica surfaces: A molecular dynamics study

A.T. Celebi, M. Olgiati, J. Dziadkowiec,[1] L.L.E. Mears, and M.Valtiner,

Institute of Applied Physics, Vienna University of Technology, Wiedner Hauptstrasse 8-10, A-1040, Vienna, Austria
(corresponding author: A.T.Celebi, e-mail: celebi@iap.tuwien.ac.at)

[1] *NJORD Centre, Department of Physics, University of Oslo, Oslo 0371, Norway*

Ion adsorption at solid-liquid interfaces and ion transport in confined spaces are central to many natural processes and practical applications in life and technology. For example, surface charge regulated membranes can enable high ion selectivity, and effective flow control for desalination and electrochemical energy storage systems [1]. Another physical process is clay swelling, a key phenomenon for oil and gas industry, is caused mainly due to the ion exchange of flowing fluid in rocks. Clay swelling significantly depends on the structure of the mineral and the composition of the aqueous environment [2]. For such applications, cation-specific effects and concentration-dependence is still little known. In this study, we carried out molecular dynamics (MD) simulations of aqueous electrolytes with various compositions confined between two negatively charged mica surfaces in order to explore processes such as ion adsorption, hydration and electric double layer (EDL) structuring, and ion transport at the solid-liquid interface.

Muscovite mica is a widely used representative mineral to study the adsorption and hydration at solid-liquid interfaces owing to its hexagonal crystal structure with the perfect cleavage and inherent negative charges [3]. Our simulation models consist of mica surfaces containing 8x4 unit cells in which surfaces are separated with a 6 nm slab thickness. As electrolyte, we use chloride solutions of different metals, namely Cs^{+}, Li^{+}, and Ca^{+2}, which represent monovalent and divalent metals. The number of salts is varied to obtain a wide range of ion concentrations. Additional cations are added in simulation system to balance the negative surface charge of mica surfaces [4]. A schematic configuration of our simulation model is shown in **Figure 1.**

We examine the variations in ion concentration, interfacial water density, molecular orientations, and ion mobility. Our simulation results show that Cs^{+} ions have the most prominent concentration peaks at the surface, indicating a stronger ion adsorption compared to Li^{+} and Ca^{+2} ions at the same ionic concentration. Interestingly, the number of Cs^{+} ions adsorbed at the surface exceeds the amount of net surface charge of mica. This refers to a phenomenon called as “charge overscreening”. As a result, the surface becomes positively charged, and the diffuse layer of EDL becomes co-ion dominated. However, this is not the

case for Li^+ and Ca^{+2} which they less strongly attach to the surface. Adsorbed Li^+ ions at the surface slightly undercharge the mica, while the net surface charge due to Ca^{+2} adsorption is the least among three different metals. Our simulations also show that almost all adsorbed Cs^+ ions occupy the center of hexagonal cavity of mica lattice, creating a diamond-shape pattern on the surface (See **Figure 1**). On the contrary, Li^+ and Ca^{+2} ions are located one of the binding oxygens of the mica next to the isomorphic substitution site. These structural arrangements are mainly attributed to the combined effects of the ion size, electron density and surface-ion interaction strength. We further observe that water densities of LiCl solution show more pronounced layering at the interface. Although there are less Li^+ ions at the surface compared to Cs^+, more water molecules come near to the surface from the center of the channel. Water molecules at the interface can pass through between adsorbed Li^+ layer and mica surface, strongly hydrating Li^+ ions whereas this is not possible for Cs^+. There are almost three times less water molecules available per Cs^+ ion at the surface. Accordingly, adsorbed Cs^+ ions are found to be more stagnant at the surface due to the weaker hydration while the adsorbing Li^+ ions are more mobile, allowing constant exchange of Li^+ ions from the channel center. These results further indicate that hydration is the driving force in the LiCl solution whereas the surface-ion interactions are the dominant force in CsCl solution.

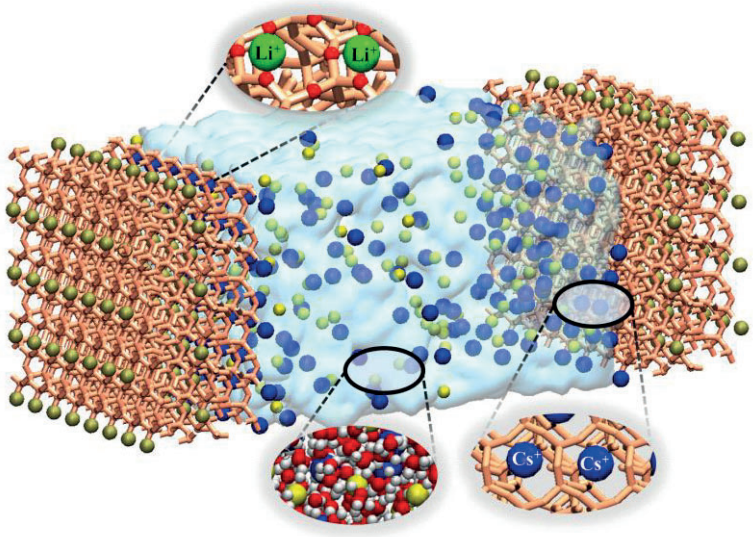

Figure 1. Schematic representation of the simulation model.

By assessing the competitive behavior of charged species at the surface, the ion adsorption coverage is quantified as a function of the bulk ion concentration. Our results show that Cs^+ coverage significantly increase with the increase of ion concentration while a linear but less prominent increase is obtained for Li^+ adsorption. On the other hand, increased ion concentration shows a negligible influence on the Ca^{+2} coverage. MD simulation results highlighting the ion adsorption as a function of type and concentration is critical to understand the interfacial thermodynamics directly from atomic force microscopy (AFM) imaging.

[1] U. Ramach, J. Lee, F. Altmann, M. Schussek, M. Olgiati, J. Dziadkowiec, L.L.E. Mears, A.T. Celebi, D. Lee, and M. Valtiner. Faraday Discuss. 246, 487-507 (2023).

[2] L.S. de Lara, V.A. Rigo, and C.R. Miranda. J. Phys. Chem. C, 121(37), 20266-20271 (2017).

[3] R. M. Pashley, J. Colloid Interface Sci. 83(2), 531-546 (1981).

[4] I.C. Bourg, S.S. Lee, P. Fenter, and C. Tournassat J. Phys. Chem. C, 121, 9402-9412 (2017).

The reconstructed $Al_2O_3(0001)$- $(\sqrt{31}\times\sqrt{31})\pm R9°$ Surface: An ideal case for non-contact AFM

Johanna Hütner, Andrea Conti, David Kugler, Florian Mittendorfer, Michael Schmid, Ulrike Diebold, and Jan Balajka

Institut für Allgemeine Physik, Technische Universität Wien, A-1040 Wien, Austria
(corresponding author: U. Diebold, e-mail: ulrike.diebold@.tuwien.ac.at)

Alumina is a ceramic material with an 8 eV band gap. It is also one of the most common support materials in heterogeneous catalysis. Thus, its surface structure has received considerable attention throughout the years, yet the highly insulating nature of the material has hampered the application of many surface science techniques.

Early results [1] on α-$Al_2O_3(0001)$ showed that the bulk-terminated (1×1) surface readily reconstructs and the $(\sqrt{31}\times\sqrt{31})\pm R9°$ structure is the most stable structure under reducing conditions. Based on SXRD measurements, a moiré-like overlayer of Al was postulated [2]. To apply surface science methods, ultrathin alumina layers on alloys such as NiAl(110) were established [3]. The structural details of the ultrathin film were resolved based on STM, DFT, and a healthy dose of intuition [4]; they differ considerably from those proposed for the surface of bulk alumina.

Reconstructed alumina single crystals have been an excellent test case for atomically-resolved AFM measurements [5, 6] and for testing the various models. Here we used nc-AFM with the qPlus sensor [7]. We modified the tip with a CuO_x termination as suggested in ref. [8], which allowed us to directly determine the lateral distribution of surface O and Al atoms. The $(\sqrt{31}\times\sqrt{31})\pm R9°$ surface shows building blocks that remind strongly of the ultrathin alumina film on NiAl(110) [4], see the Figure to the left. HRTEM images of a similar system, corundum $Fe_2O_3(0001)$ [9], show that only the top atomic layers differ from the unchanged bulk. Based on these observations and applying ML methods, we propose a structural model for $Al_2O_3(0001)$-$(\sqrt{31}\times\sqrt{31})\pm R9°$ with a very low surface energy. We also discuss the possible physical driving force, a general theme for non-polar surfaces.

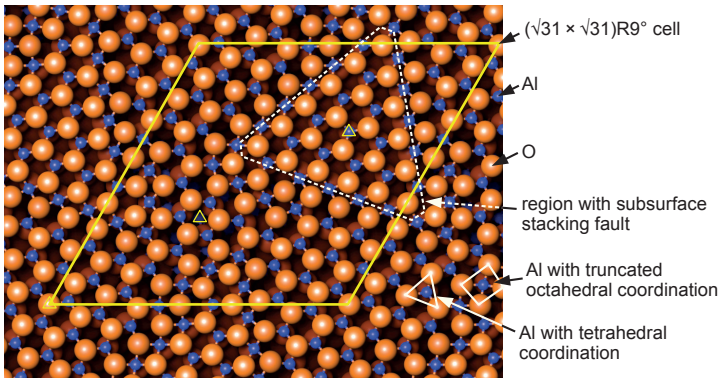

Funding from the European Research Council (ERC) under the European Union's Horizon 2020 research and innovation programme (grant agreement No. [883395], Advanced Research Grant 'WatFun') is gratefully acknowledged.

[1] T.M. French and G. Somorjai, *J. Phys. Chem*. **74**, 12 (1970).
[2] G. Renaud et al., *Phys. Rev. Lett*. **73**, 1825 (1994).
[3] R. Jaeger et al., *Surf. Science***, 259**, 235-252, (1991).
[4] G. Kresse et al., *Science* **308**, 1440 (2005).
[5] C. Barth and M. Reichling, *Nature*, **414** (6859), 54–57, (2001).
[6] J. V. Lauritsen et al., *Phys. Rev. Lett.* **103**, 076103 (2009).
[7] F.J. Giessibl, *Rev. Sci. Instrum*. **90**, 011101 (2019).
[8] B. Schulze Lammers et al., *Nanoscale* **13**, 13617 (2021).
[9] J. Redondo et al., *Adv. Mater. Interfaces* **10,** 230062 (2023).

Magnetism of single Tb atoms on MgO

J. Doležal[1], C. Soulard[1], S. Shan[1], J. Schwenk[1], S. Rusponi[1] and H. Brune[1]

[1]*Laboratory of Nanostructures at Surfaces (LNS), Institute of Physics (IPHYS), EPFL, Lausanne, Switzerland*

(corresponding author: J. Dolezal, e-mail: jiri.dolezal@epfl.ch)

Single rare-earth atoms adsorbed on surfaces represent a model system to study magnetism at atomic scale. For example, Ho on MgO exhibit long-lived magnetic quantum state with high thermal stability up to 35 K [1] making it a promising candidate for a single atom magnetic device thanks to its magnetic remanence [2]. In addition, long magnetic relaxation times are a prerequisite for the coherent control of magnetic states used in quantum information processing.

We use spin polarized STM with an out-of-plane magnetic field to study the stability and magnetic properties of the Tb species adsorbed to top oxygen and oxygen bridge sites of MgO/Ag(100) via two state switching time traces and scanning tunneling spectroscopy (STS). We found characteristic inelastic step in STS of Tb in the oxygen bridge position at ±23 mV only observable with a spin polarized tip. We attribute this to a spin pumping effect [3,4]. For the Tb on top oxygen with an out-of-plane easy axis of the magnetization, we recorded bias-induced switching of the atom magnetization probed by the change of the tunneling magnetoresistance. The piecewise liner fit of the switching rate (see Fig. 1) enabled us to determine three energy thresholds (72 ± 3, 123 ± 4 and 164 ± 4 meV) corresponding to the crystal field symmetry allowed spin transitions ($\Delta m_{J=+2}$, $\Delta m_{J=0}$ and $\Delta m_{J=+1}$). The observed field-dependent shift of the highest energy threshold for different ground state spin orientations is in agreement with the quantum chemical calculations and X-ray magnetic circular dichroism (XMCD) measurement [5] predicting the magnetic ground state with $J_z = \pm 6$. A remarkable spin contrast up to 25 pm has been observed with the spin polarized tips and can be explained by a large spin polarization of the Tb 6s5d shells [6]. We observe thermal stability of each spin state exceeding several tens of minutes up to 31 K in the out-of-plane magnetic field of 3 T.

Further studies will be devoted to probing the peculiar behavior of the magnetic lifetime as a function of the state initialization for a particular value of B_z field, which was previously observed in XMCD measurements.

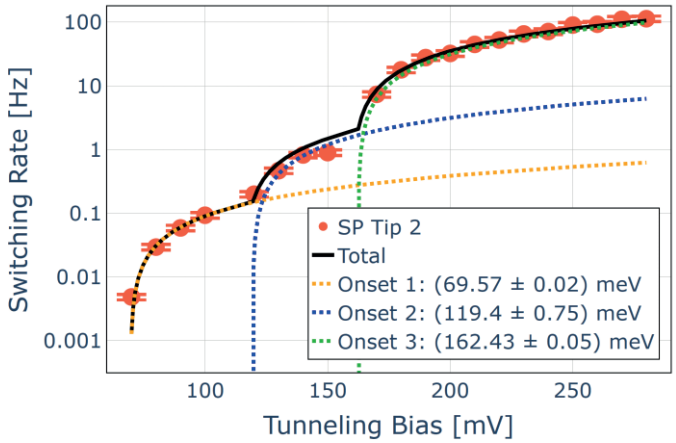

Fig.1: Switching rate of Tb_{top} (normalized to 1.5 nA tunneling current) as a function of the tunneling voltage, shown in a semi-log plot. The data are acquired at T = 0.4 K and B_z = 1.5 T.

Support from the SNSF AdG (TMAG-2_209266) is acknowledged.

[1] Natterer, F.D., Donati, F., Patthey, F. and Brune, H. Phys. Rev. Lett., **2018**, 121(2), 027201.
[2] Donati, F., Rusponi, S., Stepanow, S., Wäckerlin, C., Singha, A. *et al.* **2016,** Science, 352(6283), 318-321.
[3] Loth, S., Von Bergmann, K., Ternes, M., Otte, A.F., Lutz, C.P. *et al.*, **2010**, Nat. Phys., 6(5), 340-344.
[4] Baumann, S., Donati, F., Stepanow, S., Rusponi, S., Paul *et al.,* **2015,** Phys. Rev. Lett., 115(23), 237202.
[5] Persichetti, L., Stepanow S., Rusponi, S. Donati, F., Nistoret, C. *et al.,* Article in Preparation **2024**
[6] Pivetta, M., Patthey, F., Di Marco, I., Subramonian, A., Eriksson, O. *et al.,* **2020**. Phys. Rev. X, 10(3), 031054.

Laboratory studies on sputtering of structured tungsten model surfaces

M. Fellinger[1], C. Cupak[1], G. Alberti[2], D. Vavassori[2], L. Bana[2], D. Dellasega[2,3], M. Passoni[2,3], M. Pedroni[3], A. Uccello[3], E. Vassallo[3], R. Gonzalez-Arrabal[4] and F. Aumayr[1]

[1] *TU Wien, Institute of Applied Physics, Vienna, Austria*

(corresponding author: M. Fellinger, e-mail: fellinger@iap.tuwien.ac.at)

[2] *Politecnico di Milano, Department of Energy, Milan, Italy*

[3] *Istituto per la Scienza e Tecnologia dei Plasmi, Consiglio Nazionale delle Ricerche, Milan, Italy*

[4] *Universidad Politécnica de Madrid, Instituto de Fusión Nuclear "Guillermo Velarde" and Departamento de Ingeniería Energética, Madrid, Spain*

Using nuclear fusion as a source for efficient, save and reliable energy production is an ambition that has undergone large development in recent years and is steadily making progress [1]. However, several issues still limit the efficiency of current fusion machines. Additionally, the feasibility of ultimately upscaling research reactors to commercially usable facilities demands deeper insight into the long-term performance and the stability of such devices.

An important aspect, that is strongly coupled to lifetime predictions and performance estimates regarding fusion machines is the durability of plasma facing components in the reactor. Machine parts, directly facing the fusion plasma therefore demand thorough designing and materials need prior testing. In this sense, sputtering of such first wall materials resulting from bombardment with energetic particles is of major interest for nuclear fusion research [2].

Due to its high sputtering threshold energy, high melting point and low erosion yield, tungsten (W) is a promising first wall material candidate, making it generally interesting for detailed erosion studies. Dependencies of the sputtering yield on ion kinetic energy, ion incidence angle and mass ratio between target and projectile species are already well understood and described by theoretical models [3]. Additionally, simulation codes, often based on the binary collision approximation, can successfully describe sputtering processes [4, 5]. Recent developments have now also resulted in a code called SPRAY, capable of simulating sputtering of rough and structured surfaces [6].

In this work we aim to further validate the SPRAY code by experimentally determining sputtering yields of rough and structured surfaces. A high sensitivity quartz crystal microbalance (QCM) is combined with a low flux ion source and used to measure sputtering

yields of different model surfaces. To this end, the QCM will be employed both in a direct manner and in form of a catcher QCM that is placed in the vicinity of an irradiated target, collecting sputtered particles. This dual approach allows to probe the angular distribution of sputtered particles [7] as well as to measure direct yields as a function of, e.g., the ion incidence angle [8, 9].

It has been shown that Gaussian rough W surfaces can significantly reduce sputtering yields compared to flat targets [6]. Also, more regular types of structured W samples, such as nano-columns were found to have reduced yields, in good agreement with simulations [8, 9]. In this study, we focus now on W nano-pyramids and nano-columns. Emission characteristics as well as the long-term stability of such structures under Argon bombardment will be investigated.

Preliminary results further support proposed models [6] and furthermore illustrate, that additional factors, such as crystalline texture, can have a significant influence on the sputtering properties as well. We will present our current findings and hypothesis on the underlying physical effects at the conference.

This work has been carried out within the framework of the EUROfusion Consortium, funded by the European Union via the Euratom Research and Training Programme (Grant Agreement No 101052200 — EUROfusion). Views and opinions expressed are however those of the author(s) only and do not necessarily reflect those of the European Union or the European Commission. Neither the European Union nor the European Commission can be held responsible for them.

[1] E. Gibney, Nature 602 (2022) 371
[2] R. Behrisch, Nucl. Fusion. 12.6 (1972) 695
[3] P. Sigmund, Phys. Rev. Lett., 184 (1969) 383-416
[4] H. Hofsäss et al., Appl. Surf. Sci. 310 (2014) 134-141
[5] R. Arredondo et al., Nucl. Mater. Energy 18 (2019) 72-76
[6] C. Cupak et al., Appl. Surf. Sci. 570 (2021) 151204
[7] B. M. Berger et al., Nucl. Instrum. Methods Phys. Res. B 406 (2017) 533-537
[8] C. Cupak et al., Phys. Rev. Mat 7.6 (2023) 065406
[9] J. Brötzner et al., Nucl. Mater. Energy 37 (2023) 101507

Exploring the oxygen poisoning of the MoS_2 catalyst at Near-Ambient Pressures of H_2O

M. Hedevang, L. Mohrhusen, and J. V. Lauritsen

iNano Nanoscience Centre, Aarhus University, Aarhus, Denmark
(corresponding author: M. Hedevang, e-mail: mh@inano.au.dk)

A promising path for efficient bio-fuel production is pyrolysis, where biomass is heated in an O-free atmosphere. This process has a high liquid yield, but the product contains a large amount of unfavourable O-containing molecules, which cause the fuel to be unstable and corrosive [1]. O can be removed from the O-containing molecules through hydrodeoxygenation, where O is cleaved off by H_2 to create H_2O. MoS_2 is a promising catalyst for this reaction and has already been implemented in the industry for the similar hydrodesulfurization reaction. The main problem for MoS_2 is the relatively short life-time due to poisoning, mainly from O, N and coking [2]. The O containing molecule present in the largest amounts in the pyrolysis oil is H_2O, however, little is known about the interaction between H_2O and the MoS_2 catalyst on an atomic level. Thus, this study seeks to use surface sensitive techniques to understand the influence of H_2O on MoS_2.

To investigate the possible insertion of O into MoS_2 in the presence of H_2O, Scanning Tunneling Microscopy (STM) and X-ray Photoelectron Spectroscopy (XPS) were used to gain structural and chemical information, respectively. Both techniques were done both at Ultra High Vacuum (UHV) and at Near Ambient Pressure (NAP). Here a model system consisting of sub-monolayer MoS_2 on Au(111) was exposed to combinations of H_2O and H_2.

In the UHV-based studies MoS_2/Au(111) was first activated by exposing the system to 1e-4 mbar H_2 while heating the sample to a temperature of 650 K for 30 min. This is known to restructure the edge of the MoS_2 particles by removing one row of S-atoms and truncating the particle [3], as seen in Fig. 1a. This edge reduction is known to make the edges more reactive, and is also done in the industry [4]. The reduced MoS_2 denoted r-MoS_2, was subsequently subjected to a 1e-6 mbar H_2O atmosphere wherein the sample was heated to various temperatures. Using STM, depressions in the edge structure are observed after H_2O exposure, see Fig. 1b where the sample was heated to 573 K in the H_2O atmosphere. These depressions in the edge differ from larger MoS_2 islands, where the basal plane has similar depressions [5]. To gain chemical information the same experiment was done using synchrotron XPS (MatLine, ASTRID II, Aarhus). This experiment showed no O 1s signal and no change to the S 2p spectra. This is believed to be because the introduced chemical species observed by STM, were under the detection limit, highlighting the need for AP-XPS studies.

To investigate the chemical species inserted in the MoS_2 structure in the presence of H_2O, NAP-XPS was performed at the HIPPIE beamline at MAX IV Laboratories, Lund. Here, the

MoS_2/Au(111) model system was exposed to combinations of 0.25 mbar H_2O and 1 mbar H_2 at temperatures between RT and 600 K while doing in-situ measurements. These experiments showed the appearance of two different chemical species in the O 1s spectrum after H_2O exposure. This is in contrast to the UHV experiments, where only edge species were observed.

In addition to the NAP-XPS, STM was used to evaluate the structural changes of the MoS_2 islands after NAP exposures of H_2O and H_2 at elevated temperatures.

From these results we can propose a mechanism for the O-insertion into MoS_2 in the presence of mbar pressures of H_2O, which is associated with catalytic poisoning.

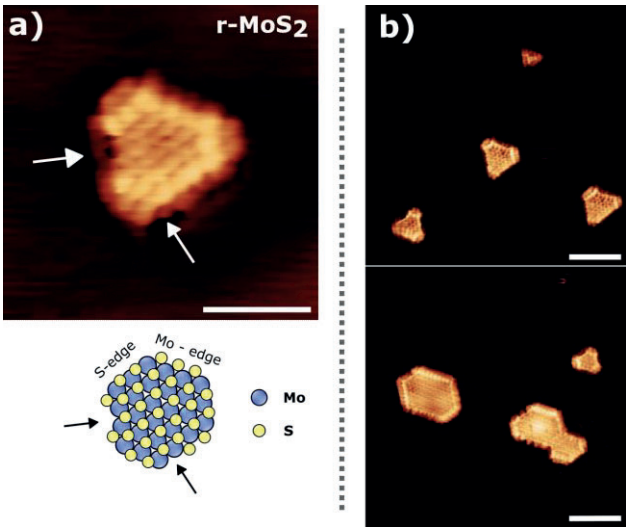

Figure 1 ***a)*** *STM image of a MoS_2/Au(111) island after exposure to 1e-4 mbar H_2 for 30 min at 650 K. A ball model shows the atomic composition of the restructured island. On both two arrows are inserted to show the position of S-vacancies.* ***b)*** *Two STM images showing a r-MoS_2/Au(111) model system after exposure to a 1e-6 mbar H_2O for 20 min at 573 K.*

Support by the Fonds Danmarks Frie Forskningsfond is gratefully acknowledged.

[1] L. Qu, X. Jiang, Z. Zhang, X. G. Zhang, G. Y. Song, H. L. Wang, Y. P. Yuan, and L. Y. Chang, Green Chemistry, 23(23), 9348-9376 (2021)

[2] P. M. Mortensen, J. D. Grunwaldt, P. A. Jensen, K. G. Knudsen, and A. D. Jensen, Applied Catalysis A 407(1-2), 1-19 (2011)

[3] S. S. Grønborg, N. Salazar, A. Bruix, J. Rodríguez-Fernández, S. D. Thomsen, B. Hammer and J. V. Lauritsen, Nature Communications, 9(1), 2211 (2018)

[4] M. T. H. Dabros, M. Z. Stummann, M. Høj, P. A. Jensen, J. D. Grunwaldt, J. Gabrielsen, P. M. Mortensen and A. D. Jensen, Progress in Energy and Combustion Science, 68, 268-309 (2018)

[5] S. S. Grønborg, K. Thorarinsdottir, L. Kyhl, J. Rodríguez-Fernández, C. E. Sanders, M. Bianchi, P. Hofmann, J. A. Miwa, S. Ulstrup and J. V. Lauritsen, 2D materials 6(4), 045013 (2019)

Photon, electron, ion and atom emission kinetics from the $Cl_2^{gas} + K^{solid}$ reaction.

Lars A. Hellberg*

Department of Physics, Chalmers University of Technology, S-412 96 Göteborg, Sweden
(corresponding author: Lars A. Hellberg, e-mail: lars.hellberg@chalmers.se)

The reaction between electronegative halogen molecules and electropositive alkali metal surfaces provides a model system for the study of charge transfer, dissociation dynamics and non-adiabatic energy dissipation in gas surface reactions. The emission of various particles stemming from the reaction process itself provides an unique insight into the reaction mechanisms. For the system under study here, $Cl_2^{gas} + K^{solid}$, simultaneous emission of photons, electrons, and electronically excited K atoms have previously been observed in our lab [1].

In an another study, we have measured how the exo-electron- and photon emission in the zero chlorine coverage limit depend on the normal incident velocities of Cl_2 molecules [2, 3]. In this work, however, we focus on the kinetics of the $Cl_2^{gas} + K^{solid}$ experiment, i.e., the time evolution of the measured quantities stated above, as well as the sticking coefficient and the work function change as functions of Cl_2 exposure. In particular, we provide data, which the lack of has caused some confusion as to the $Cl_2^{gas} + K^{solid}$ system, regarding the initial sticking coefficient and the content of the exo-current:

1. A counter-intuitive initial sticking coefficient of a few percent has previously been reported from our lab [1] and a sticking coefficient of about 0.5 for slow molecules has been reported from a group in Japan [4]. In this study we measure the initial sticking coefficient to be unity for all molecular velocities used in our experiments.

2. In an early study of the same chemical system, but under principally different experimental conditions, >99% of the emitted negative current was assigned to Cl^- and only a minute part to electrons [5]. In contrast, we find that more than ~98% of the negative current consists of electrons and the only other negative particle observed is Cl^-.

The results are discussed based on a combination of existing models for exo-electron- and photon emission in the zero coverage limit, [2,6,7] and a qualitative discussion of how successive accumulation of chlorine at the surface and the change of workfunction might influence the sticking and relevant charge transfer processes.

[1] D. Andersson, B. Kasemo, and L. Wallden, Surf. Sci. **152/153**, 576 (1985).
[2] L. Hellberg, J. Strömquist, B. Kasemo and B. Lundqvist, Phys. Rev. Lett. **74**, 4742 (1995).
[3] L. Hellberg, J. Campbell, and B. Kasemo, Surf. Sci. **502-503**, 399 (2002)
[4] S. Yoneda et al., Surf. Sci. **363**, 11 (1996).
[5] L. D. Trowbridge, D. R. Herschbach, J. Vac. Sci. Tech. **18**, 588 (1981).
[6] J. K. Nørskov, D. M. Newns, and B. I. Lundqvist, Surf. Sci. **80**, 179 (1979).
[7] J. Strömquist, L. Hellberg, B. Kasemo and B. Lundqvist, Surf. Sci. **352-354**, 435 (1996)

*This work was carried out in collaboration with the late professor Bengt Kasemo.

On-surface synthesis of radical 2D supramolecular assemblies and metal-organic frameworks

A. Sanchez Grande, F. Frezza, M. Kumar, A. Matěj, D. Soler, P. Jelínek

Institut of Physics oft he Czech Academy of Sciences, Prague, Czech Republic
(corresponding author: P. Jelinek, e-mail:jelinekp@fzu.cz)

In recent years, significant efforts have been focused on developing supramolecular radical chemistry, an interdisciplinary field combining supramolecular chemistry [1] and organic radicals [2]. The synergy between these two fields has important applications in different areas, such as host-guest systems, (photo)catalysis, or sensors. However, the high reactivity intrinsic to organic radical systems makes their synthesis and stabilization challenging, especially when the objective involves the formation of ordered 2D and 3D assemblies.

In this manuscript, we report the synthesis of a fluoradene-based molecule that spontaneously possesses an intrinsic unpaired electron, as demonstrated by scanning probe microscopy (SPM) techniques and theoretical calculations. Thanks to the design of the molecular precursor, with suitably located 7-azaindole groups, the molecules assemble into a Kagome phase, forming a high-quality and defect-free 2D hydrogen-bonded organic radical framework on the scale of hundreds of nanometers. The insights into the reaction mechanisms are unveiled by quantum mechanics/molecular mechanics (QM/MM) calculations, which reveal the fundamental catalytic role of single gold atoms in the reaction mechanism. Namely, our theoretical calculations show that the presence of single gold atoms not only reduces the activation barriers but also significantly reduces the radical character of the intermediate. This is due to the energetic stabilization of the intermediate, which enables the non-trivial synthesis of the radical fluorinated unit. This finding opens new directions in single-atom catalysis towards on-surface synthesis. Finally, we will discuss the possibility of using the radical SAM as a template for large-scale metal-organic frameworks.

[1] J.V. Barth, G. Costantini, K. Kern, Nature, 437, 671–679 (2005).

[2] B. Huang, et al. Chem. Sci. 12, 13648–13663. (2021).

Diffusion of polarons in transition metal oxides – how far must the polaron fly?

P. Kocán,[1] V. Gabriel,[1] M. Reticcioli,[2] J. Redondo,[1,3] M. Schmid,[3] D. Wrana,[1,4] U. Diebold,[3] C. Franchini[2,5] and M. Setvín[1,3]

[1]*Department of Surface and Plasma Science, Faculty of Mathematics and Physics Charles University, Prague, Czech Republic*

[2]*University of Vienna, Faculty of Physics, Center for Computational Materials Science, Vienna, Austria*

[3]*Institute of Applied Physics, TU Wien, 1040 Vienna, Austria*

[4]*Marian Smoluchowski Institute of Physics, Jagiellonian University, 30-348 Krakow, Poland*

[5]*Dipartimento di Fisica e Astronomia, Università di Bologna, 40127 Bologna, Italy.*

(corresponding author: P. Kocán, e-mail: pavel.kocan@mff.cuni.cz)

Excess charge in a polarizable material can be stabilized by deformation of the surrounding lattice, producing a quasiparticle called polaron [1]. Polarons play a key role in electrical conductivity [2] of many materials, such as transition metal oxides (TMO) studied here. The conductivity is crucial in technological applications like photo-induced water splitting, in which hematite α-Fe_2O_3, a representative TMO, is used as a catalyst [3].

We have reported previously [4] how polarons can be injected one-by-one into the surface of hematite at 4.7 K using the tip of the Q-plus sensor and how the same sensor can be used to monitor the spreading of the polaron cloud at elevated temperatures by measuring the local contact potential in the Kelvin probe microscopy regime.

We have developed a kinetic Monte Carlo (kMC) model considering electrostatic interactions among all injected polarons. Polaron hopping is based on Arrhenius statistics with an activation energy E_A and a frequency prefactor v_0, using either nearest-neighbor hops in a cubic lattice or longer hops without a fixed lattice. The results suggest that the short hops can succeed in fitting the experimental potentials only if extremely low values of the prefactors v_0 $\sim 10^5$ s^{-1} were used, compared to typical values $\sim 10^{13}$ s^{-1}.

Density functional theory (DFT) calculations suggest existence of a delocalized state of the extra charge introduced into hematite. We will discuss how the nonphysically low values of prefactors can be avoided in the kMC simulations when considering longer hops with the delocalized state as the transition state.

The discussion will be extended to more complex TMO materials, perovskites, where we succeeded in injecting polarons as well.

This work was supported by the Czech Science Foundation (GACR 20-21727X) and by MSMT CZ.02.01.01/00/22_008/0004572.

[1] C. Franchini, M. Reticcioli, M. Setvin, U. Diebold, Nat. Rev. Mater. 6, 560-586 (2021).

[2] K. M. Rosso, D. M. A. Smith, M. Dupuis, J. Chem. Phys. 118, 6455–6466 (2003).

[3] Li, C., Luo, Z., Wang, T. & Gong, J., Adv. Mater. 30, (2018).

[4] P. Kocán et al., Polaronic Diffusion in Doped Hematite – experiment vs. Kinetic Monte Carlo simulations, Symposium on Surface Science 2022, St. Christoph am Arlberg, Austria

Temperature-dependent reaction pathway selectivity and detection of a hidden carbon deposition channel in hydrocarbon oxidation

Ulrike Küst[1], Weijia Wang[2], Changda Wang[4], Jason F. Weaver[3], Helena Hagelin-Weaver[3], Andrey Shavorskiy[2], Johan Gustafson[1], Jan Knudsen[1,2]

[1] *Division of Synchrotron Radiation Research, Department of Physics, Lund University, Sweden*
(corresponding author: Ulrike Küst, e-mail: ulrike.kust@sljus.lu.se)

[2] *MAX IV Laboratory, Lund University, Sweden*
[3] *Department of Chemical Engineering, University of Florida, USA*
[4] *National Synchrotron Radiation Laboratory, University of Science and Technology of China*

Many reactions involve the possibility of forming deposits. As long as these accumulate on the surface, they are *detectable* with surface sensitive techniques that are usually employed to study heterogeneous catalysis. However, if the dissolution rate of the deposits into the bulk is faster than the deposition rate they become *hidden.* That might lead to the underestimation or even overlooking of reaction channels such as e.g. carbon deposition during hydrocarbon oxidation reactions which is problematic as carbon can have a significant influence on the catalytic activity [1,2].
Here, we will demonstrate how these previously undetectable deposition channels can be uncovered by means of time-resolved Ambient Pressure X-ray Photoelectron Spectroscopy

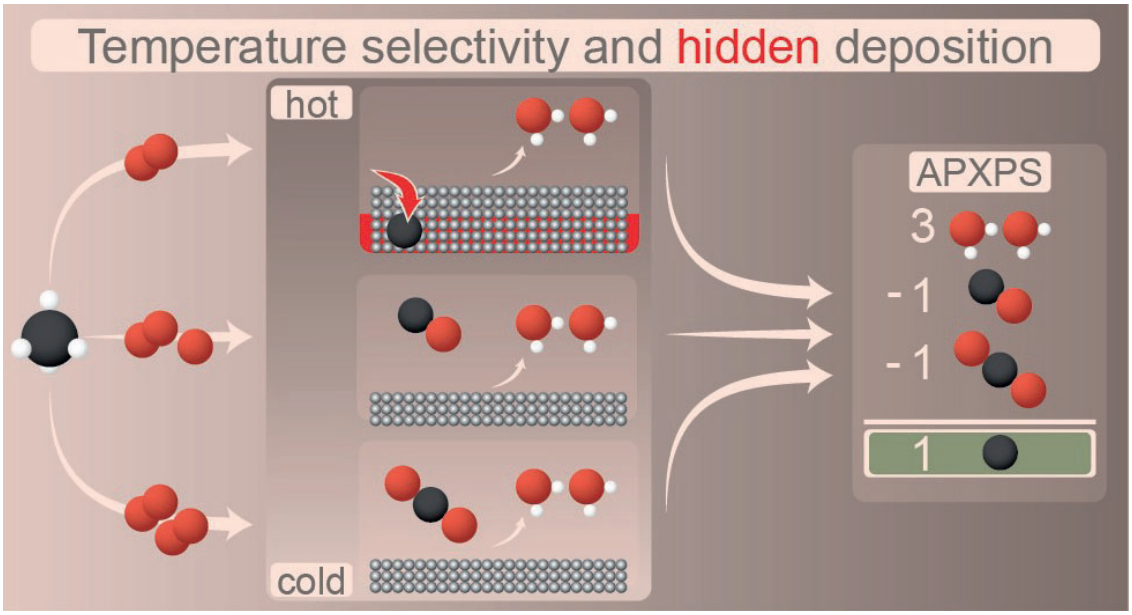

Figure 1: Schematic of the selected reaction pathway as function of temperature. The hidden carbon deposition can be made detectable by subtracting the CO and CO2 partial pressures from the H2O partial pressure measured in APXPS.

(APXPS) measurements of the gas phase in the near vicinity of the catalyst surface. As a case study, we discuss methane oxidation on a Pd catalyst in an oxygen-lean environment at a few millibar pressure. While ramping the temperature, we follow the time evolution of individual reaction pathways of methane oxidation, especially within the oxygen mass transfer limit.

The scientific take-home message is shown in Figure 1 in which the selected reaction pathway shifts toward reaction channels that consume less oxygen once the catalyst is heated. This is due an increased methane conversion, resulting in an oxygen mass transfer limited reaction. Here, CO is formed by partial combustion and carbon is deposited on the catalyst. Interestingly, however, carbon deposition can even be observed shortly before and after the oxygen mass transfer limit is reached. This means that carbon will form even if oxygen is still present in the vicinity of the catalyst. Carbon deposition could be uncovered in this study using the balance between the remaining reaction products.

As an outlook, I will discuss how temperature pulses and the ultra-sensitive detection of reactive components in a modulated catalytic reaction using Fourier Transformed APXPS [3] can be employed to study the exact time evolution of carbon deposition with respect to the other gaseous products and the surface composition.

We acknowledge MAX IV Laboratory for time on Beamline HIPPIE under Proposal 20211102. Research conducted at MAX IV, a Swedish national user facility, is supported by the Swedish Research council under contract 2018-07152, the Swedish Governmental Agency for Innovation Systems under contract 2018-04969, and Formas under contract 2019-02496. This work was supported by Swedish Research Council (J.K. and U.K. 2017-04840). J.W. acknowledges financial support provided by the Department of Energy, Office of Basic Energy Sciences, Catalysis Science Division through Grant DE-FG02-03ER15478 as well as the LINXS Institute of Advanced Neutron and X-ray Science.

[1] Yu *et al.*, Angewandte Chemie – Int. Ed. 36, 15294-15297 (2020)

[2] Gili *et al.*, ACS Catalysis 8, 8739–8750 (2018)

[3] Knudsen *et al.*, *Submitted.*

Advancing Single-Atom Catalysis: Development of an Apparatus for Reactions at Near-Ambient Pressure

A. Lagin, J. Filzmoser, J. Pavelec, U. Diebold, M. Schmid, and G. S. Parkinson

Institute of Applied Physics – Surface Science, Vienna University of Technology, 1040 Vienna, Austria
(corresponding author: A. Lagin, e-mail: lagin@iap.tuwien.ac.at)

Single-atom catalysts (SACs) have been a much-studied topic in surface physics in recent years. Due to their highly sensitive and selective properties, SACs offer a promising bridge between homogeneous and heterogeneous catalysis [1]. Nowadays, model systems consisting of metal atoms adsorbed on single-crystal metal oxide surfaces are typically prepared and studied in ultra-high vacuum (UHV) [2]. A step towards the successful implementation of SACs in the industrial field is the investigation of model catalytic systems under conditions closer to reality, i.e., at elevated temperatures and pressure of reactants [3].

This work aims to develop a UHV-compatible reaction cell, allowing the sample exposure to reactive gases at about 1 mbar pressure and 300°C. Utilizing inert materials and a previously tested sealing system that doesn't require O-rings will confine the reactive area exclusively to above the single-crystal sample surface. The conceptual solution also implements an “in-situ irradiation path”, which allows us to perform photo-induced reactions or to examine the sample surface with infrared spectroscopy during the catalytic process. The exhaust gas composition from the reaction cell is analyzed quantitatively by mass spectroscopy. Due to the low number of active sites on the SAC model system, the measurement of turnover frequencies presents a significant challenge. Therefore, we investigate methods to improve the sensitivity of mass spectroscopy.

The newly designed reaction cell will be situated in a UHV environment. It allows us to use standard preparation procedures for SACs and experimental methods such as X-ray photoemission spectroscopy (XPS) or scanning tunneling microscopy (STM) before and after exposing the sample to elevated gas pressures and temperatures. By combining these techniques, we expect to gain a better insight into the behavior of SAC under more realistic conditions.

[1] G. S. Parkinson, Catal. Lett. 149, 1137 (2019).

[2] L. Caulfield, E. Sauter, H. Idriss, Y. Wang, and C. Wöll, J. Phys. Chem. C 127, 14023 (2023).

[3] J. N. Riedel, M. D. Rötzer, M. Jørgensen, U. G. Vej-Hansen, T. Pedersen, B. Sebõk, F. F. Schweinberger, P. C. K. Vesborg, O. Hansen, J. Schiøtz, U. Heiz, and I. Chorkendorff, Catal. Sci. Technol. 6, 6893 (2016).

Model for Nanopore Formation in Two-Dimensional Materials by Impact of Highly Charged Ions

A. Sagar Grossek[1,2], A. Niggas[1], R. A. Wilhelm[1], F. Aumayr[1], and C. Lemell[2]

[1] *Institute of Applied Physics, TU Wien, A-1040 Vienna, Austria*
[2] *Institute for Theoretical Physics, TU Wien, A-1040 Vienna, Austria*
(corresponding author: C. Lemell, e-mail: christoph.lemell@tuwien.ac.at)

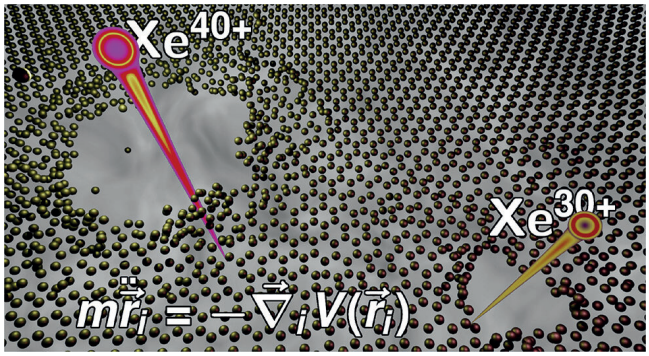

We investigate the response of 2-dimensional structures to the transmission of highly charged ions (HCIs) from the first electron transfer from the target to the projectiles locally charging up the impact area to the emission of excess electrons and target atoms leaving behind nanopores in the 2d-material thereby changing target properties. Aim of our studies is the control of nanopore formation which may lead to technical applications like, e.g., water purification or gas filtering.

It has been found that hole formation depends on both target properties, in particular its electron mobility, as well as the charge state of the incoming projectile, i.e., the potential energy carried into the collision [1]. Experiments have been conducted with multiple targets ranging from conducting single-layer graphene (SLG) to MoS_2 with an electron mobility three orders of magnitude smaller. While the high electron mobility in SLG enables fast reneutralization of the electron-depleted impact area thus ensuring long-time stability of the target, MoS_2 may disintegrate when excited by an HCI due to the formation of a long-lasting charge patch initiating Coulomb-driven disintegration of the target layer. It was found that a minimum charge state Q_{in} of the projectile was required in order to produce nanopores [2].

To investigate the hypothesis of Coulomb-driven hole formation, we have recently set up a simulation modeling all three aspects of the process, the electron transfer to the projectile, charge transport in the target, and a molecular-dynamics simulation for the motion of atoms in the 2d-structure in the presence of Coulomb forces [3].

Based on the charge mobility of 2D materials, this model is able to reproduce the dependence of the pore diameter on the initial charge state of the impinging projectile or the reduction of the number of electrons extracted from materials with small charge mobility. Only for single-layer graphene, a material with high mobility, pore formation was not observed irrespective of the incident charge Q_{in}. For other materials characterized by their conductivity we find a

threshold charge for pore formation that approximately depends on the square root of the charge mobility.

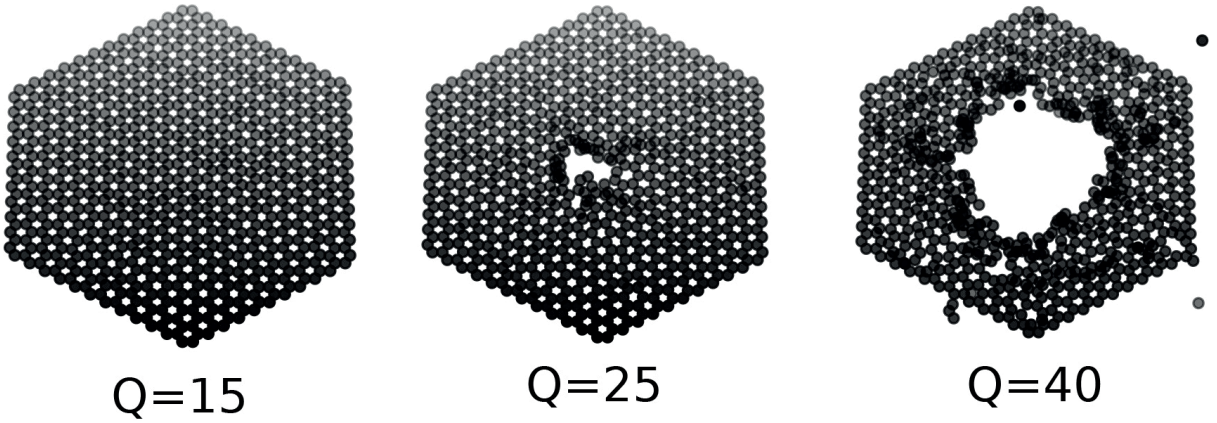

Fig. 1: Dependence of hole diameter on the charge state of the incident ion. For materials with a conductivity larger than that of graphene a threshold behavior has been observed in the simulation which qualitatively reproduces the results of experiments performed so far.$

The stability of a target material irradiated by HCIs can be represented in phase diagram as a function of the initial charge state of the projectile and the relevant material parameter of the 2D structure, its charge mobility. Based on comparisons of our simulation results with experimental data we expect that our predictions should properly capture the qualitative dependences of pore formation in HCI–2D layer interactions.

We acknowledge support from Austrian Science Fund FWF under project Nos. Y1174-N36, I4914-N, and P36264-N. The computational results presented have been achieved using the Vienna Scientific Cluster (VSC); technical support by the VSC team is highly appreciated.$

[1] J. Schwestka, H. Inani, M. Tripathi, A. Niggas, N. McEvoy, F. Libisch, F. Aumayr, J. Kotakoski, and R.A. Wilhelm, ACS Nano 14, 10536 (2020).

[2] R. Kozubek, M. Tripathi, M. Ghorbani-Asl, S. Kretschmer, L. Madauß, E. Pollmann, M. O'Brien, N. McEvoy, U. Ludacka, T. Susi, G. S. Duesberg, R. A. Wilhelm, A. V. Krasheninnikov, J. Kotakoski, and M. Schleberger, J. Phys .Chem .Lett. **10**, 904 (2019).

[3] A. Sagar Grossek, A. Niggas, R.A. Wilhelm, F. Aumayr, and C. Lemell, Nano Lett. 22, 9676 (2022).

Extended support structure dictates the reactivity of model single-atom catalysts for dissociative oxygen adsorption

F. J. Lewis, A. Rafsanjani-Abbasi, M. Meier, M. Schmid, U. Diebold, G. S. Parkinson

Institut für Allgemeine Physik, Technische Universität Wien, A-1040 Wien, Austria
(corresponding author: F. J. Lewis, e-mail: lewis@iap.tuwien.ac.at)

A goal of single atom catalysis (SAC) is to find a support that stabilizes single metal adatoms in geometries that make them catalytically active. For this to be possible, the adatoms must be able to change their coordination state by forming and breaking bonds. Iron oxides are popular supports used in SAC because of their low cost, chemical stability, and non-toxicity.[1] Given its ubiquity in catalysis, platinum is an attractive metal to be used in SAC.

I will discuss the similarities and differences between Pt adatoms on hematite, α-$Fe_2O_3(1\bar{1}02)$-(1×1), and magnetite, $Fe_3O_4(001)$. Scanning tunneling microscopy (STM), x-ray photoelectron spectroscopy (XPS), and density functional theory (DFT) were used to characterize these surfaces and how Pt atoms bind to them. In both cases, Pt is 2-fold coordinated to lattice oxygen atoms, but the reactivity differs. Interestingly, we find that the second coordination sphere plays an important role defining the reactivity to molecular oxygen.

Support from the European Research Council (ERC) under the European Union's Horizon 2020 research and innovation program (grant agreement No. [864628], Consolidator Research Grant "E-SAC").

[1] Kraushofer, F., *Single Atom Catalysis: Insights from Model Systems,* Chemical Reviews, 2022. 122, 18, 14911–14939.
[2] Parkinson, G.S., *Iron oxide surfaces.* Surface Science Reports, 2016. **71**(1): p. 272-365.

Atomic-scale imaging of K-feldspar surfaces and their interaction with water

L. Lezuo, A. Conti, R. Abart,[1] F. Mittendorfer, M. Schmid, U. Diebold and G. Franceschi

Institute of Applied Physics, TU Wien, Wiedner Hauptstrasse 8-10/E134, 1040 Wien, Austria
(corresponding author: L. Lezuo, e-mail: lezuo@iap.tuwien.ac.at)

[1] *Department of Lithospheric Research, Universität Wien, 1090 Wien, Austria*

Feldspars are common minerals in the Earth's crust and play a crucial role as ice nucleators in atmospheric processes [1]. Understanding the interaction of different feldspars with water is essential for various scientific fields, including atmospheric chemistry and climate science [2].

Feldspars are tectosilicates whose crystal structure is formed by a network of oxygen-sharing SiO_4 and AlO_4 tetrahedra, which hosts additional cations (K, Na, Ca) in large cavities formed by the tetrahedral network. Depending on the ordering of the Al and Si ions in the tetrahedral network, different structure variants with the same nominal composition exist. For K-feldspars ($KAlSi_3O_8$), three polymorphs are discerned: microcline, orthoclase, and sanidine [3]: Microcline is the stable low-temperature polymorph forming upon slow cooling or hydrothermal re-crystallization. It has triclinic symmetry with the Al ions occupying only one specific out of four non-equivalent tetrahedral sites. Orthoclase and sanidine are formed when the material is cooled quicker, so less ordered crystal structures are formed. There, the Al-atoms are homogeneously distributed over two (orthoclase) or all four (sanidine) non-equivalent tetrahedral sites.

Notably, K-feldspars present in airborne mineral dust are highly active ice nucleators. The three K-feldspar polymorphs have different ice nucleation activities, with microcline being the most active [4]. To date, a conclusive explanation of the mechanism leading to the high ice nucleation activity of microcline, and in general, of the atomic-scale mechanism underlying ice nucleation, is still missing [5]. Different mechanisms have been proposed, including the action of active sites [6], step edges exposing high energy surfaces [7], chemical alterations [8], molecules and biological substances adsorbing on the surface [9], and the availability of surface OH groups [10].

In our previous work [11], we have explored the role of surface chemistry by investigating the binding of water on the cleaved microcline (001) surface. We have observed that this system exposes an ordered lattice of silanol (Si-OH) and aluminol (Al-OH) groups correlated to the atoms occupying the underlying tetrahedral sites. The acidity of these hydroxyl groups strongly influences the adsorption of water molecules and impacts their configuration on this surface, pointing to the potentially important role of surface chemistry for facilitating ice nucleation.

Here, we expand our studies beyond microcline by investigating how the order of Al and Si atoms changes atomic arrangement of the cleaved surface and possibly influences water adsorption at low temperatures. Specimens of gem-quality alkali feldspar were cleaved in ultra-high vacuum and analyzed with non-contact atomic force microscopy (AFM) and X-ray photoelectron spectroscopy (XPS). This provides us direct atomic insight into the ordering of the tetrahedral framework, which is otherwise only possible via averaging techniques such as X-ray diffraction [3] and nuclear magnetic resonance [12]. Additionally, we study the onset of ice nucleation by introducing H_2O vapor at low temperatures on the hydroxylated surfaces and observe how the different arrangements of surface silanol and aluminol groups affect the binding of water at low temperatures. Ab-initio density functional theory calculations in tandem with AFM simulations employing the Probe Particle Model [13] help us interpret our results.

Support from the European Research Council (ERC) under the European Union's Horizon 2020 research and innovation programme (grant agreement No. 883395, Advanced Research Grant 'WatFun') is gratefully acknowledged. The computational results have been achieved using the Vienna Scientific Cluster (VSC).

[1] A. Kumar, et al., Atmos. Chem. Phys. 18, 7057 (2018).
[2] B. J. Murray and X. Liu, in Aerosols and Climate, ed. K. S. Carslaw, Elsevier 2022, pp. 619–649, (doi: 10.1016/B978-0-12-819766-0.00014-6)
[3] J. D. C. McC., *J. V. Smith,* Geol. Mag. 114, 69 (1977).
[4] A. D. Harrison, et al., Atmos. Chem. Phys. 16, 10927 (2016).
[5] A. Soni and G. N. Patey, J. Chem. Phys. 150, 214501 (2019)
[6] M. A. Holden, et al., Sci. Adv. 5, eaav4316 (2019)
[7] A. Kiselev, et al., Science (1979) 355, 367 (2016).
[8] S. Augustin-Bauditz, et al., Geophys. Res. Lett. 41, 7375 (2014).
[9] F. Conen, et al., Atmos. Chem. Phys. 11, 9643 (2011).
[10] M. A. Freedman, J. Phys. Chem. Lett. 6, 3850 (2015).
[11] G. Franceschi, et al., J. Phys. Chem. Lett. 15, 15-22 (2024), (doi: 10.1021/acs.jpclett.3c03235).
[12] Y. Xiao, et al., Mineral. Mag. 59, 47 (1995).
[13] P. Hapala, et al., Phys. Rev. B 90, 085421 (2014).

Understanding interaction forces at silicon wafer interfaces to optimize nanoscale cleaning processes.

Daniela Miano[1], Pierluigi Bilotto[2], Bernhard Loidl[3], Shane Garvey[3], Markus Valtiner[1,2]

(corresponding author: D.Miano, e-mail: daniela.miano@cest.at)

[1] CEST Center for Electrochemical Surface Technology, 2700, Wiener Neustadt
[2] Vienna University of Technology, Institute of Applied Physics, 1040, Vienna,
[3] LAM Research AG, 9500, Villach

The increasing demand for efficient electronics affects semiconductor industry. The recent global crisis and experienced shortage of materials have highlighted the need for Europe to invest more in semiconductor industry, which brought to major economical actions such as the recent Chips act. One of the strategies to reduce the amount of material in use is miniaturization of electronic elements down to the nanoscale. There, the presence of particles with a diameter in the nanometre range becomes a major issue as they might alter the correct functioning of the miniaturized electronic units. Therefore, it is crucial to establish innovative cleaning protocols able to remove particles of nanometre sizes from silicon wafers.

In CleanWaferPro we focus on the formation of surface nanobubbles to facilitate the detachment of nanoparticles from wafers. In literature this proof of concept has been demonstrated, but the underlying physical and chemical principles driving the surface nanobubble/particle/wafer/solvent interface has not been elucidated yet [1,2,3].

Our strategy is to breakdown the complexity of the interactions at the nanoscale while developing a dedicated atomic force microscope (AFM) setup where all the parameters participating in the cleaning process can be tuned.

We utilize thiol functionalization to define model systems and mimic the different interaction forces, explaining according to the DLVO theory, and that might take place onto a wafer surface during its industrial cleaning process.

In parallel we also cover with different size nanoparticles our surfaces, that should reproduce the possible impurity of a real Si surface, we study if it is possible to use the solvent exchange for remove these objects and we try to understand how to implement the cleaning process protocol.

In this presentation, I will discuss our current experimental set-up, some imaging of surface nanobubbles, adhesion maps obtained with an AFM for different model systems studied in air, water, ethanol, and isopropanol and some preliminary study about the removing particle process.

The final goal is to clarify the fundamental science at the liquid-solid-gas interface and behind the nanobubble-particle-wafer interaction in order to propose a protocol that could be applied by the industries working on wafer cleaning processes.

The COMET Centre CEST is funded within the framework of COMET - Competence Centers for Excellent Technologies byBMK, BMDW as well as Land Niederösterreich and Oberösterreich. The COMET programme is managed by FFG.

LAM Research is an American cooperation that is the world market leader in the design, making and service of semi-conductor processing equipment. In Villach, Austria LAM research operates a large-scale research and development activity for spin-etching and surface treatment of semiconductor wafers.

[1] Yang, S., & Duisterwinkel, A. (2011). Removal of Nanoparticles from Plain and Patterned Surfaces Using Nanobubbles. Langmuir, 27(18), 11430– 11435. doi:10.1021/la2010776;

[2] Physical Properties of Nanobubbles on Hydrophobic Surfaces in Water and Aqueous Solutions. Langmuir, 22(11), 5025–5035. doi:10.1021/la0601814 ;

[3] Characterization of Nanobubbles on Hydrophobic Surfaces Langmuir, Vol. 23, No. 13, 2007 7077.

The intrinsic short-range ordering of K^+ ions on cleaved muscovite mica

F. Mittendorfer, G. Franceschi, P. Kocán[1], A. Conti, S. Brandstetter, J. Balajka, I. Sokolović, M. Valtiner, M. Schmid, M. Setvin[1], and U. Diebold

Institute of Applied Physics, Technische Universität Wien, A-1040 Wien, Austria
(corresponding author: F. Mittendorfer, e-mail: Florian.Mittendorfer@tuwien.ac.at)

[1] *Department of Surface and Plasma Science, Charles University, Prague, Czech Republic*

Muscovite, a common layered mica silicate, can be easily cleaved into atomically flat surfaces. The ease of preparation combined with a low chemical activity has led to a widespread use as substrate material for decades. Nevertheless, the atomistic details of the surface structure are still under debate [1].

With a formal composition of $KAl_2(Si_3Al)O_{10}(OH)_2$, muscovite contains a central octahedral AlO_6 layer between two tetrahedral sheets with mixed SiO_4 and AlO_4 building blocks forming a hexagonal structure. The resulting silicate sheets are separated by layers of K^+ ions, facilitating the cleavage of the material. After splitting the crystal, only half the number of the K^+ ions are present on each surface. In a recent combined experimental and theoretical study [2], we have investigated the distribution of the K^+ ions using non-contact atomic force microscopy (AFM), density functional theory (DFT) calculations and Monte-Carlo (MC) simulations.

The atomically resolved AFM images of the mica surface in ultra-high vacuum (UHV) clearly show that the K^+ ions occupy sites in a hexagonal lattice. Yet they only display short-range ordering, leading to the formation of short alternating rows in the low-indexed directions. In addition, a high density of kinks and intersections are observed. The DFT calculations using the Vienna ab-initio simulation package (VASP)[3] and the r^2SCAN meta-GGA xc-functional [4] confirm that local configurations including kinks yield similar energies as the straight rows, suggesting a coexistence of the patterns. In addition, the calculations show a pronounced influence of the Al distribution in the subsurface layer, as the configurations with K^+ ions in rings containing 2 Al ions are ~0.2 eV more stable compared to rings with a single Al ion. Furthermore, the calculated moderate DFT K^+ hopping barriers of ~0.7–1 eV indicate that some diffusion can take place at room temperature. The strong correlation between the distribution of the K^+ ions and the subsurface Al ions is also confirmed by the MC simulations.

Funding from the European Research Council (ERC) under the European Union's Horizon 2020 research and innovation program (grant agreement No 883395, Advanced Research Grant 'WatFun') is gratefully acknowledged. The Vienna Scientific Cluster (VSC) is acknowledged for providing CPU time.

[1] H.K. Christensen and N.H. Thomson, Surf. Sci. Rep. 71, 367 (2016)

[2] G. Franceschi, P. Kocan, A. Conti *et al*., Nature Communications 14, 208 (2023)

[3] G. Kresse and J. Hafner, Phys. Rev. B. 47, 558 (1993)

[4] J.W. Furness, A.D. Kaplan, J. Ning *et al*, J. Phys. Chem. Lett. 11, 8208 (2020)

Au(111) Oxidation Imaged in Oxygen Free Alkaline Media with Electrochemical Scanning Tunneling Microscopy

Toni Moser[1], Christoph Griesser[1], Andreas Oss[1], Julia Kunze-Liebhäuser[1],

[1]*University of Innsbruck, Innrain 52c, 6020 Innsbruck, Austria*
(corresponding author: Toni Moser, email: toni.moser@uibk.ac.at)

For a long time, gold (Au) was considered too noble for catalytic materials applications and therefore overlooked as a catalyst but explored in alloys or bimetallic configurations for enhanced chemical stability. A significant revelation occurred when Au emerged as an efficient pure metal catalyst in alkaline media for carbon monoxide (CO) oxidation [1]. Ever since, Au has been in the focal point of electrochemical research due to its noble character and its ideal properties as a model system in fundamental research. The electrochemical oxidation of Au(111) is also widely studied, but the complete comprehension of the oxidation process remains incomplete. Although several studies have investigated the surface during and after oxidation using electrochemical scanning tunneling microscopy (EC-STM) in acidic media [2,3,4], there has been a lack of investigations in alkaline electrolytes. This is surprising considering that CO oxidation on Au(111) is strongly enhanced under alkaline conditions and has been extensively studied by classical electrochemical methods [5,6], due to its significance in low-temperature fuel cells, where CO is considered a key intermediate. These mechanistic studies always assume the flat Au(111) surfaces to prevail even under CO oxidation conditions, which has not been investigated with STM to date. This assumption is however fairly questionable, because in the case of Cu(111), the CO oxidation is accompanied by a pronounced and quasi-reversible surface reconstruction and ejection of Cu clusters onto the surface [7]. Surface X-ray scattering (SXS) studies on Au single crystals [8] give first insights into the surface structure with and without CO, in-depth microscopy studies to image the surface directly under reaction conditions are however still missing.

In this study, we want to give an overview of the Au(111) structure/morphology evolution in alkaline media investigated by EC-STM, focusing on its oxidation and reduction. All experiments were conducted inside an argon-filled glovebox to ensure a truly oxygen-free environment, which is difficult to achieve in other set-ups. We show the herringbone reconstructed surface (Fig. 1A) and its evolution during early and later stages of oxide formation (Fig. 2C) and reduction. Similar observations were made as in acidic media [3], where it was shown that the surface morphology is dependent on whether the reduction occurs during a potential sweep or step. The roughened surface smoothens during oxide reduction, while (vacancy) islands remain. In alkaline media, however, far fewer islands are observed after potential jumps when compared to acidic electrolyte, and most of them disappear quickly with time. Repeated oxidation and reduction cycles do not result in an increased surface roughening,

while large terraces with monoatomic vacancy islands are recovered. In general, it can be observed that surface flattens/"heals" quickly after oxidation compared acidic conditions.

To ultimately investigate possible CO oxidation pathways [5,6], the surface morphology and structure of Au(111) were imaged during CO oxidation, where the herringbone reconstruction can be observed under reaction conditions. These findings agree well with the previous structure investigations (SXS) [8] and give another valuable insight into this model catalyst system.

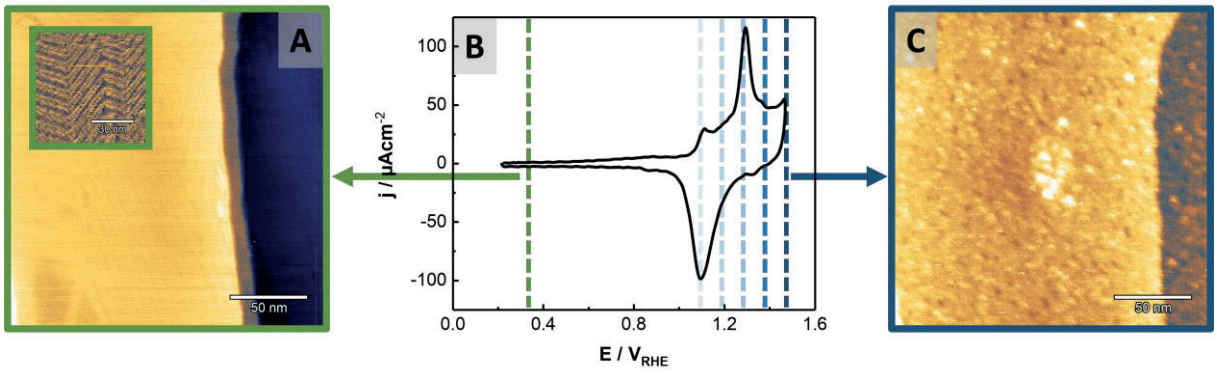

Figure 1. (A) Pristine Au(111) surface at E=0.35 V_{RHE} in alkaline solution. Inset shows the herringbone reconstruction, (B) Cyclic voltammogram recorded inside the EC-STM cell. The light blue line at E=1.1 V_{RHE} marks the lifting of the herringbone reconstruction and the onset of the oxidation. (C) Oxidized surface at E=1.5 V_{RHE}.

We would like to thank the Fonds zur Förderung der Wissenschaftlichen Forschung for the financial support.

[1] J. L. Roberts Jr & D. T. Sawyer, *Electrochimica Acta, 1965*, *10*(10), 989-1000.

[2] H. Honbo, S. Sugawara & K. Itaya, Analytical chemistry, 1990, 62(22), 2424-2429.

[3] M. A. Schneeweiss, D. M. Kolb, D. Liu & D. Mandler, Canadian journal of chemistry, 1997, 75(11), 1703-1709.

[4] C. Stumm, S. Grau, F. D. Speck, F. Hilpert, V. Briega-Martos, K. Mayrhofer, ... & J. Libuda, The Journal of Physical Chemistry C,2021, 125(41), 22698-22704.

[5] P. Rodríguez, A. A. Koverga, & M. T. Koper, Angewandte Chemie, 2010, 122(7), 1263-1265.

[6] P. Rodríguez & M. T. Koper, Physical Chemistry Chemical Physics, 2014, 16(27), 13583-13594.

[7] A. Auer, M. Andersen, E. M. Wernig, N. G. Hörmann, N. Buller, K. Reuter, & J. Kunze-Liebhäuser, Nature Catalysis, 2020, 3(10), 797-803.

[8] M. E. Gallagher, B. B. Blizanac, C. A. Lucas, P. N. Ross & N.M. Marković, Surface science, 2005, 582(1-3), 215-226.

Ferromagnetism in a Monolayer 2D Metal-Organic Framework

Egzona Isufi Neziri[1,2], Celine Hensky[4,5], Aleksandra Cebrat[1,2], Manfred Parschau[1], Karl-Heinz Ernst[1,2,3], Christian Wäckerlin[4, 5]

[1] *Empa, Swiss Federal Laboratories for Materials Science and Technology, 8600 Dübendorf, Switzerland*
(corresponding author: E. Isufi Neziri, e-mail: egzona.neziri@empa.ch)

[2] *University of Zürich, 8006 Zürich, Switzerland*

[3] *Nanosurf Laboratory, Institute of Physics, The Czech Academy of Sciences, 16200, Prague, Czech Republic*
[4] *Paul Scherrer Institute, 5232 Villigen, Switzerland*

[5] *EPFL, 1015 Lausanne, Switzerland*

Ising's work in 1924 marks the earliest research of magnetic properties in a low-dimensional system. The Mermin-Wagner theorem establishes that in systems governed by the isotropic Heisenberg model with short-range interactions in dimensions $d \leq 2$, continuous symmetries cannot break spontaneously at finite temperatures.[1] This theorem explains the challenge of obtaining long-range magnetic order in two-dimensional (2D) systems. However, the presence of a significant magnetic anisotropy can counteract random spin reorientations caused by thermal fluctuations, therefore offering a potential opportunity to observe magnetic behavior in 2D. In this work, we show the existence of ferromagnetic coupling on a 2D-MOF consisting of Ni atom centers and tetracyanoethylene (TCNE) molecules on Au(111) surface. Analysis of scanning tunneling microscopy (STM), x-ray absorption spectroscopy (XAS) and x-ray magnetic circular dichroism (XMCD) measurements reveals a strong out-of-plane magnetic anisotropy and a square like hysteresis loop with a coercive field of ~ 1 T.

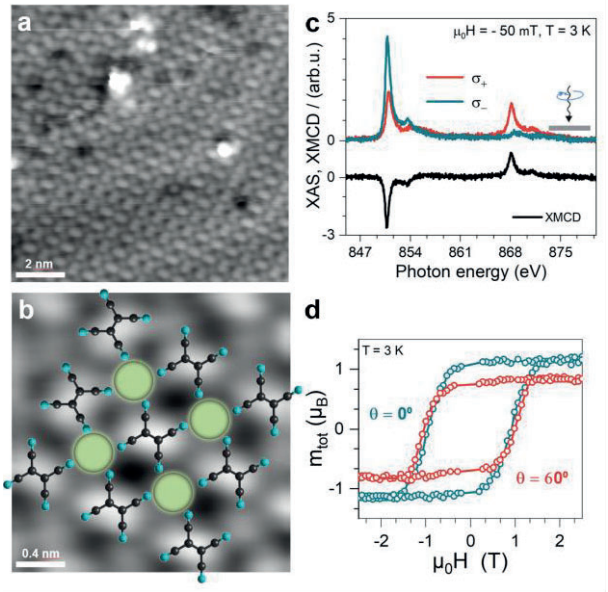

Figure 1. (a) STM atomic structure of 2D Ni-TCNE network on Au(111). (b) Overlaid model of the MOF structure (green, blue and black spheres represent Ni, N and C atoms, respectively). (c) Ni XAS, XMCD spectra after field ramp from 6.8 T to -0.05 T, remaining magnetization is evidenced by the presence of XMCD. (d) Hysteresis loop obtained at 3K in normal and grazing incidence.

[1] Mermin, N. D.; Wagner, H. Absence of Ferromagnetism or Antiferromagnetism in One- or Two Dimensional Isotropic Heisenberg Models. *Phys. Rev. Lett.* **1966**, *17* (22), 1133–1136. https://doi.org/10.1103/PhysRevLett.17.1133.

On the low-energy secondary electron emission from surfaces

A. Niggas[1], D. Thima[1], M. Werl[1], J. Buck[2,3], F. Simperl[1], F. Blödorn[1], K. Rossnagel[2,3], W.S.M. Werner[1], F. Aumayr[1], R.A. Wilhelm[1]

[1] *TU Wien, Institute of Applied Physics, 1040 Vienna, Austria*
[2] *Ruprecht Hänsel Laboratory, Deutsches Elektronen-Synchrotron DESY, 22607 Hamburg, Germany*
[3] *Institut für Experimentelle und Angewandte Physik, Christian-Albrechts-Universität zu Kiel, 24098 Kiel, Germany*

(corresponding author: A. Niggas, e-mail: anna@iap.tuwien.ac.at)

Particle-induced electron emission from surfaces is an important process not only for material analysis techniques but also for many plasma applications [1]. Several studies in the past concerning ion-induced electron emission focused mainly on high-energetic electrons from, e.g., Auger-Meitner processes, which, however, only make up a minority of the total electron yield. The high-intensity but low-energy tail (<20eV) of secondary electrons was often not discussed, inter alia, because of the technical challenges when studying low-energy electrons.

The broad energy landscape of emitted electrons stems from a variety of different mechanisms driving their emission, like kinetic emission through momentum transfer or plasmon excitations and subsequent decay [2]. If ions are involved (possibly even in high charge states), additional potential emission processes from the deexcitation cascade of the projectile contribute to the electron emission. Bercx *et al.* [1] further showed that the energy distribution depends strongly on target-projectile combinations.

Using freestanding monolayer graphene as a model system, we recently studied the electron emission from a surface-only material induced by highly charged Xe ions in a coincidence spectrometer [3], which allows us to omit any contamination and multiplication effects from sub-surface layers [4]. Therewith, we were able to show that the total yield of electrons is dominated by the surface of the material, i.e., we find a high yield of up to 100 emitted electrons from this single layer of material [5]. Further, we found that the electron energy spectrum has a bimodal structure [6], which indeed seems to represent the combination of kinetic and potential emission.

To further unravel these processes, we decouple these effects to study them separately: On the one hand, the ASPHERE III ARPES setup at DESY is used to perform angle-resolved ion-induced electron emission spectroscopy (ARIIEES) for singly charged as well as highly charged ions. On the other hand, to get a better understanding of correlation effects leading to electron emission by plasmon decay, we studied (quasi-freestanding) single- and bilayer graphene grown on SiC in a (e,2e) electron coincidence spectrometer [7]. There, electrons are used instead of ions as projectiles and two emitted electrons are detected in coincidence. This

way, the energy loss of the primary electron (e.g., due to plasmon excitation) can be correlated with low-energy secondary electrons stemming from the plasmon decay.

In this contribution, I will give an overview of our recent progress in understanding secondary electron emission from the carbon-based 2D materials single- and bilayer graphene as well as their 3D counterpart highly oriented pyrolytic graphite (HOPG) from the three techniques briefly described above: highly charged ion spectroscopy for total yields and energy distributions, ARIIEES and (e,2e) spectroscopy.

Support by the Austrian Science Fund (FWF) through projects 10.55776/Y1174, 10.55776/I4914, and 10.55776/P36264is gratefully acknowledged.

[1] M. Bercx *et al. Contrib. Plasma Phys*. e202300054 (2023)

[2] H. Winter. In: Slow Heavy-Particle Induced Electron Emission from Solid Surfaces. Springer Tracts in Modern Physics **225**. Springer, Berlin, Heidelberg (2007)

[3] J. Schwestka *et al.* Rev. Sci. Instrum. **89** 085101 (2018)

[4] A. Niggas et al. *Proc. SPIE* **12131** Nanophotonics IX, 121310H (2022)

[5] J. Schwestka *et al. J. Phys. Chem. Lett.* **10** 4805 (2019)

[6] A. Niggas *et al. Phys. Rev. Lett.* **129** 086802 (2022)

[7] W.S.M. Werner *et al. Phys. Rev. Lett.* **125** 196603 (2020)

The double-functionalized STM probe reveals the interference of Bogoliubov quasiparticles around magnetic Fe atoms on the superconducting Nb(110) surface

Artem Odobesko,[1] Raffael L. Klees,[2] Felix Friedrich,[1] Ewelina M. Hankiewicz,[2] and Matthias Bode[1]

[1]*Physikalisches Institut, Experimentelle Physik II, Julius-Maximilians-Universität Würzburg, Würzburg, Germany*

(corresponding author: A. Odobesko, e-mail: artem.odobesko@uni-wuerzburg.de)

[2]*Institut für Theoretische Physik und Astrophysik Julius-Maximilians-Universität Würzburg, Würzburg, Germany*

The invention of the scanning tunneling microscope has revolutionized our understanding of materials and their properties. This progress was made possible by the capability of correlating topographic data of the sample structure obtained by constant-current or constant- height scanning tunneling microscopy (STM) with the data obtained by scanning tunneling spectroscopy (STS). However, when performed with normal metal tips, these methods have their specific limitations, which can be overcome by purposive functionalization. The spatial resolution of topographic STM measurements can be enhanced by attaching a CO-molecule to the apex of the STM tip, and a superconducting probe boosts the energy resolution in STS beyond the thermal broadening limit.

Remarkably, enhancing probe functionalization methods can yield further advancements. In this work we employ a combination of a superconducting probe and CO molecule, creating a double-functionalized CO-SC-probe. Leveraging simultaneously improved spectroscopic and spatial resolution, we explore previously inaccessible details in the local density of states (LDOS) around magnetic Fe atoms on a superconducting Nb(110) surface [1]. We are able to detect the interference patterns in spatially resolved differential conductance maps that correspond to hybridized YSR states of the Fe dimer with even and odd spatial symmetry. We demonstrate the simultaneous enhancement of the spatial and the energy resolution by comparing data obtained on the Fe dimer using the same superconducting probe tip before and after additional functionalization with a CO molecule. Only when the double-functionalized CO-SC probe is used, do the characteristic features in the interference maps appear, which carry information about the anysotropy of the Fermi surface of the Nb(110) substrate [2].

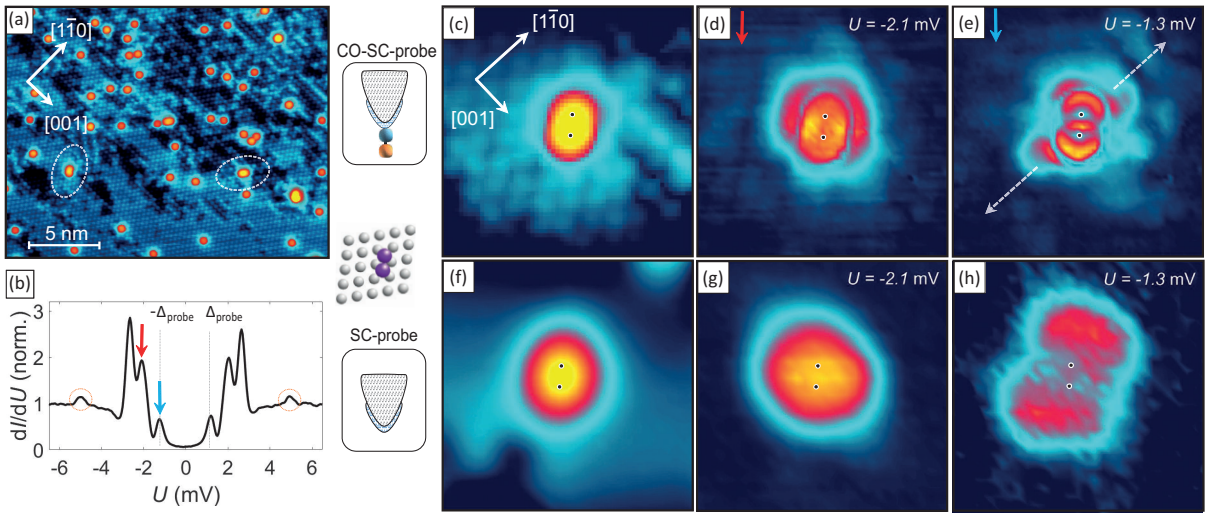

Fig. 1. (a) STM topography of Fe atoms (bright protrusions) deposited on Nb(110) taken with a CO-SC probe; (b) Differential tunneling conductance spectrum taken with the CO-SC probe on top of Fe dimer; (c-e) Data simyltaneosly obtained with a double-functionalized CO-SC-probe: topographic image of Fe dimer (c), spatial dI/dU maps taken at the tunneling bias corresponding to the high-energy YSR state with even symmetry (d), and at the tunneling bias corresponding to the low-energy YSR state with odd-symmetry (e); (f-h) Same data as in (c-e) taken with a single-functionalized SC-probe without a CO-molecule attached.

[1] F. Friedrich et al., Phys. Rev. B 103 235437 (2021)
[2] A. Odobesko et al., arXiv:2303.02406 (2023)

Towards lightwave driven magnetic field scanning tunneling microscopy

A. Rank, V. Ruckerbauer, C. Meineke, R. Huber, J. Repp

Department of Physics, University of Regensburg, Regensburg, Germany
(corresponding author: Andreas Rank, e-mail: Andreas.Rank@physik.uni-regensburg.de)

Lightwave driven scanning tunneling microscopy (LW-STM) is based on the key idea to directly steer electron tunneling in an STM by ultrashort light pulses. When focusing laser pulses in the terahertz (THz) regime directly onto the tunneling junction their electric-field transient translates into an ultrafast AC bias potential between tip and sample, allowing to steer femtosecond tunneling processes. This technique therefore adds femtosecond temporal resolution to STM without losing the existing atomic-scale spatial resolution [1].

In the past, this technique was used to study the motion of single molecules on its intrinsic timescales. In pump-probe schemes, pentacene molecules adsorbed on a thin insulating layer were excited via a THz pump-pulse to a molecular vibration which is read out by a second probe-pulse [2]. In a similar scheme, the motion of a molecular switch an adsorbed magnesium phtalocyanine (MgPC) was investigated. It was shown that by means of LW-STM femtosecond forces could be exerted localized to atomic scale beneath the tip [3].

Combining the development of the LW-STM with a tunable magnetic field would allow to follow spin dynamics – spin precession, for example – in molecules and other atomistic structures with single- electron sensitivity. To this end we develop a novel LW-STM including an external magnetic field to resolve single-spin dynamics with atomic spatial and ultrafast temporal resolution. In this contribution, we will discuss the instrumental challenges like the design of the cryostat. A split-coil magnet, providing a field of up to three tesla, needs to be installed, while it is required to couple in the THz laser pulses with large numerical aperture. Further, we will address the issue of how to couple in the laser pulses into the tunneling junction. To this end, a new STM head design was developed. For most flexible positioning of the laser focus, the tip and the sample have combined six degrees of freedom of motion. To accomplish these many degrees the head combines design principles of a Pan and a beetle type STM.

Support by the ERC Synergy Grant MolDAM (951519) and DFG CRC 1277 is gratefully acknowledged.

[1] T.L.Cocker, V. Jelic, M. Gupta, S. Molesky, J. Burgess, G. Reyes, L. Titova, y. Tsui, M. Freeman and F. Hegmann, Nature Photonics 7, 620-625 (2013)

[2] T. L. Cocker, D Peller, P. Yu, J. Repp and R. Huber, Nature 539, 263-267 (2016)

[3] D. Peller, L. Kastner, T. Buchner, C. Roelcke, F. Albrecht, N. Moll, R. Huber and J. Repp, Nature 585, 58-62 (2020)

Electronic states and collective electronic excitations in sub-atomic-thick slots

V. M. Silkin[1,2,3], U. Muniain[1], R. Esteban[1,4], I. V. Silkin[5], J. J. Baumberg[6], and J. Aizpurua[1,3,4]

[1] *Donostia International Physics Center, 20018 San Sebastian, Spain*
(corresponding author: V. M. Silkin, e-mail: waxslavas@ehu.es)

[2] *Departamento de Polímeros y Materiales Avanzados: Física, Química y Tecnología,, Facultad de Ciencias Químicas, Universidad del País Vasco UPV/EHU, 20080 San Sebastián, Spain*

[3] *IKERBASQUE, Basque Foundation for Science, 48009, Bilbao, Spain*

[4] *Centro de Física de Materiales, Centro Mixto CSIC-UPV/EHU, 20018 San Sebastian, Spain*

[5] *Tomsk State University, 634050 Tomsk, Russia*
[6] *Nanophotonic Centre, Cavendish laboratory, University of Cambridge, Cambridge CB3 0HE, United Kingdom*

Atomically flat surfaces can be realized in many metallic nanostructures. A prototypical example is the (111) face of coinage metals. Such surfaces support, in addition to the bulk-trancated electronic states, so-called Shokley surface states [1] with energy dispersion crossing the Fermi level, E_F . Thus, the electronic structure at E_F is characterized by two types (bulk- and surface-like ones) of carriers with the different Fermi velocities. As a result, in addition to the conventional surface plasmon [2], a well-defined surface mode with a sound-like dispersion can appear [3]. An usual way to create a quantum metallic state with strong localization at the surface is deposition of the adlayers. On the other hand, sometimes in nanostructures a top monolayer can be lifted to some extent. For instance, due to random atomic movements such delamination was observed on the edge of Au nanoparticles [4].

In this work we demonstrate that shifting up of the top atomic layer on the Au(111) surface can lead to appearance of the two-dimensional occupied electronic states spatially separated from the Au(111) electronic states. We perform first principles calculations of the electronic structure and the response function of the Au(111) surfaces with a gap between the top and the next atomic layers varying from 0 to 2.5 Å. A slab consisting of 21 atomic layer of Au(111) in a superlattice geometry was employed. The band structure was obtained with the use of a norm-concerving pseudopotential.

We found that when the top monolayer lifts by about 2 Å from its ground-state position, a new mode is formed in the resulting subatom-thick slot. We explain the appearance of such a mode by separation of the valence charge density of the detached monolayer from the

underlaying bulk sustem at distances exceeding ~1.5 Å [5]. The induced charge distribution related to the excitation of this mode results in a tightly confined optical field in the slot. The slot plasmons are characterised by slow propagation velocity and can survives for up to a few periods. They occurs for extremely large values of in-plane momenta with energies spanning the infra-red range. We speculate that the found subatomic slot modes might manifest in a variety of unexplained phenomena, like transient signals related to surface defects in the high-speed dark-field and surface-enhanced Raman spectroscopies [6-8].

Support by MCIN/AEI/10.13039/501100011033 through projects PIB2019-105488GB-I00, PID2022-139230NB-I00, and PID2022-139579NB-I00, and "ERDF A way of making Europe" through Project Ref. No. IT 1526-22, by the Ministry of Education and Science of the Russian Federation within State Task No. FSWM-2020-0033, and by the EPSRC (Cambridge NanoDTC EP/L015978/1, EP/L027151/1, EP/S022953/1, EP/X037770/1).

[1] S. G. Davidson and M. Stęślicka, *Basic Theory of Surface States*; Oxford University Press: Oxford, UK, 1992

[2] R. H. Ritchie, Phys. Rev. 106, 874 (1957)

[3] V. M. Silkin, A. García-Lekue, J. M. Pitarke, E. V. Chulkov, E. Zaremba, and P. M. Echenique, Europhys. Lett. 66, 260 (2004)

[4] B. Song, J. Jansen, F. D. Tichelaar, H. W. Zandbergen, G. Gajewski, C. W. Pao, D. J. Srolovitz, Surf. Sci. 608, 154 (2013)

[4] K. Pohl, B. Diaconescu, G. Vercelli, L. Vattuone, V. M. Silkin, E. V. Chulkov, P. M. Echenique, and M. Rocca, EPL 90, 57006 (2010).

[5] J. J. Baumberg, R. Esteban, Shu Hu, U. Munian, I. V. Silkin, J. Aizpurua, V. M. Silkin, Nano Lett. 23, 10696 (2023)

[6] N. C. Lundquist, C. D. L. de Albuquerque, R. G. Sobral-Filho, I. Paci, and A. G. Brolo, Nat. Nanothecnol. 14, 981 (2019)

[7] C. Carnegie et al., Nat. Commun. 11, 682 (2020)

[8] W. Chen et al., Nat. Commun. 12, 2731 (2021)

Towards mid-Infrared Lightwave Scanning Tunneling Microscopy

R. Spachtholz, T. Buchner, A. Rank, L. Kastner, R. Huber and J. Repp

Department of Physics, University of Regensburg, Regensburg, 93040, Germany
(Corresponding author: R. Spachtholz, e-mail: Raffael.spachtholz@ur.de)

Scanning tunneling microscopy (STM) has revolutionized the field of surface science, enabling the visualization and the manipulation of matter at the scale of single atoms and molecules. However, STM is a very slow technique. This implies that conventional STM provides mostly static information, whereas phenomena occurring on fast time scales are out of reach. Incorporating sub-picosecond temporal resolution into STM has been achieved through the development of lightwave STM [1], as reviewed in the following.

The implementation of a pump-probe scheme for the bias voltage represents a milestone in implementing temporal resolution in STM [2]. In this seminal work it was shown to enable nanosecond resolution [2], and spin relaxation was investigated by monitoring the tunneling current as a function of delay time between the pump and the probe pulses.

However, many atomic-scale phenomena, like charge-carried and phonon dynamics, occur on sub-picosecond timescales – orders of magnitude faster than any signals in conventional electronics. Hence, to reach the sub-picosecond timescale, being relevant for many physical phenomena, requires a fundamentally different approach. Following the concept of lightwave electronics, instead of using voltage pulses for the bias modulation, ultrashort phase-stable laser pulses in the THz regime are coupled into the tip-sample junction. These pulses act as an ultrashort bias transient in analogy to the electronic pump-probe scheme mentioned above. However, thanks to the novel approach, this technique permits steering the tunneling of single electrons on a femtosecond timescale, opening the pathway to tracking ultrafast molecular motion [3] and sub-cycle atomic-scale force control [4].

These achievements spurred us to develop a next-generation lightwave STM, which will be presented. The newly designed microscope, operating at liquid helium temperatures and under ultra-high vacuum conditions, has a movable parabolic mirror in close proximity to the tip-sample junction providing a large numerical aperture and covering a huge solid angle ($\Omega \approx \pi$). Numerous piezo movers allow in-situ focusing of the laser to the tip-sample junction, even without losing the focus during sample exchange. By utilizing an advanced laser source that delivers sub-cycle mid-infrared laser pulses, we aim to attain sub-20-fs time scales. Furthermore, the laser source has a broad spectrum of pump pulses in the visible spectrum which enables a variety of systems to be excited. This new laser source should allow for addressing various dynamics like intra molecular vibrations, observing the propagation of

charge carriers in nanostructures or molecules, conformational changes of molecules or even chemical reactions.

Funding from the ERC Synergy Grant MolDAM (no. 951519) and the Deutsche Forschungsgemeinschaft (DFG, German Research Foundation) through INST 89/414-1 and RE2669/8 is gratefully acknowledged.

[1] T. L. Cocker, et al., Nature Photonics 7, 620-625 (2013)
[2] S. Loth, M., et al., Science 329, 1628-1630 (2010)
[3] T. L. Cocker, et al., Nature 539, 263-267 (2016)
[4] D. Peller, et al., Nature 585, 58-62 (2020)

Thursday

Enantioselective adsorption on ferromagnetic surfaces

M. R. Safari, F. Matthes, Ni. Atodiresei C. M. Schneider, D. E. Bürgler and K.-H. Ernst[1,2,3]

Peter Grünberg Institute, Forschungszentrum Jülich, 52425, Jülich, Germany

[1] *Empa, Swiss Federal Laboratories for Materials Science and Technology, 8600, Dübendorf, Switzerland*

[2] *Department of Chemistry, University of Zurich, 8057, Zürich, Switzerland*

[3] *Nanosurf Laboratory, Institute of Physics, The Czech Academy of Sciences, 16200, Prague, Czech Republic*

(corresponding author: K.-H. Ernst, e-mail: karl-heinz.ernst@empa.ch)

From the inception of molecular theory, the interplay between chirality and magnetism has been a source of fascination for scientists. The question of whether enantiospecific adsorption of chiral molecules takes place on magnetic surfaces still lingers. Enantiomer discrimination was initially postulated to result from the absolute handedness of molecules and their exchange interaction with the substrate's magnetization. Nevertheless, a comprehensive understanding of CISS, along with a suitable theoretical framework, remains elusive.

In this study, we present findings regarding the enantiospecific adsorption of heptahelicene ($C_{30}H_{18}$, [7]H), a chiral helical polyaromatic molecule, on ferromagnetic single-crystal cobalt surfaces in ultrahigh vacuum using spin- polarized scanning tunneling microscopy (SP-STM). Immobilization of molecules in the chemisorbed state suggest that enantiospecificity is a consequence of spin-dependent van der Waals (vdW) interactions in a physisorbed precursor state. Notably, lateral enantioselection occurs on domains with opposite out-of-plane magnetization initially in a transient physisorbed precursor state before progressing to chemisorption.

Bilayer Co nanoislands are formed on a Cu(111) single-crystal surface through the deposition of metallic cobalt [9, 10]. These islands are recognized for their out-of-plane magnetization. To determine the magnetization orientations of these islands, spin-polarized scanning tunneling microscopy and spectroscopy (SP-STM/STS) are employed. Specifically, the tungsten tip of the STM is coated with Co before imaging. A contrast in differential conductance (dI/dV) emerges due to the varying spin-polarized tunneling probabilities between the oppositely magnetized Co nanoislands and the magnetic STM tip, as illustrated in Figures 1A-C. Since the absolute magnetization direction of the STM tip remains unknown, it is possible to assign only

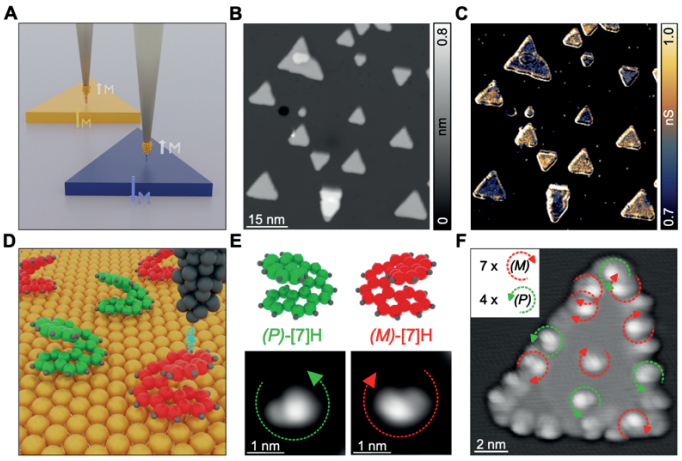

Figure 1. Principles of spin-polarized and enantio-resolved STM. (**A**) Sketch of two oppositely out-of-plane magnetized Co nanoislands probed with a magnetic Co- functionalized STM tip. (**B**) Constant-current topo-graphic STM image of Co nanoislands on Cu(111). (**C**) dI/dV map at Vbias = −600 mV measured with a magnetic Co-functionalized STM tip simultaneously with the topographic image in (**B**). (**D**) Sketch of STM imaging of single molecules. (**E**) Ball-and- stick model of [7]H enantiomers and assignment of their absolute handedness from topographic STM contrast. Counter-clockwise increase of brightness denotes a *(P)*-enantiomer (left), while clockwise increase of brightness denotes an *(M)*-enantiomer (right). (**F**) Example for 'chirality counting' of [7]H molecules on a single Co nanoisland. Indicated by circular arrows, 4 *(P)*- and 7 *(M)*-enantiomers are identified.

a relative distinction of a higher or lower dI/dV signal in relation to the direction of the island's magnetization, M.

Sub-monolayer quantities of racemic heptahelicene $C_{30}H_{18}$ molecules ([7]H) are adsorbed on these ferromagnetic islands. To ascertain the handedness of each adsorbate, STM examination is carried out, as depicted in Figure 1D. The orientation of the [7]H molecules during adsorption positions their proximal phenanthrene group parallel to the surface, resulting in their helical axis being perpendicular to the surface. Consequently, the absolute handedness is distinctly discernible based on a clockwise or counter-clockwise change in apparent height in constant-current STM images, as illustrated in Figure 1E. Following the determination of the absolute handed-ness on each island, the ratio of left- handed to right-handed molecules adsorbed on it is calculated (Figure 1F). In principle, the adsorption of [7]H occurs in four possible combinations of substrate magnetization direction (c or M=↓) and enantiomer handedness [*(P)* or *(M)*]. Enantiospecific adsorption of [7]H molecules on Co islands is evidenced by directly counting the occurrence of the four combinations in topographic STM images measured on Co nanoisland with magnetization directions determined from spin-polarized differential conductance maps. A statistical analysis encompassing over 740 molecules on 110 islands unveiled a significant disparity in the handedness of adsorbed [7]H molecules concerning the direction of the substrate's out-of-plane magnetization. If the ratio $\mathbf{r} = [(P)/\mathrm{M}\uparrow + (M)/\mathrm{M}\downarrow]/\,[(P)/\mathrm{M}\downarrow + (M)/\mathrm{M}\uparrow]$ deviates from 1, enantiospecific adsorption is present. Our statistical analysis, conducted within the framework of a trinomial distribution, reveals that for the combined datasets, the magneto-enantiospecific ratio is $\mathbf{r} = 0.68 \pm 0.06$. In other words, **r** deviates from 1 by about five standard deviations. This signifies that the adsorption of [7]H enantiomers on a ferromagnetic Co(111) island is notably influenced by both the molecular handedness and the substrate magnetization [1].

[1] M. R. Safari, F. Matthes, V. Caciuc, N. Atodiresei, C. M. Schneider, K.-H. Ernst, D. Bürgler, *Advanced Materials (accepted)*

Calculating core-level binding energies for small molecules on magnetite (111)

Pauline Schütt[1,2,3], Wernfried Mayr-Schmölzer[1], Heshamt Noei[2], Andreas Stierle[2,3], and Gregor B. Vonbun-Feldbauer[1]

[1]*Institute of Advanced Ceramics, Hamburg University of Technology, 21073 Hamburg, Germany*

(corresponding author: G. Vonbun-Feldbauer, e-mail: gregor.feldbauer@tuhh.de)

[2] *Deutsches Elektron-Synchrotron (DESY), Notkestraße 85, 22607 Hamburg, Germany*

[3] *Department Physik, Universität Hamburg, Jungiusstr. 11, 20148 Hamburg, Germany*

Magnetite (Fe_3O_4) is a highly interesting material because of its intriguing properties and potential applications in diverse fields, including heterogeneous catalysis [1], medicine [2], and hierarchical materials systems [3]. In the Fischer-Tropsch synthesis, magnetite can be used as a catalyst and magnetite nanoparticles can be employed in medical applications, for water decontamination [4] or as basis of hybrid materials. Nanoparticles functionalized with organic ligands can be assembled into supercrystalline nanocomposites [5]. Crosslinking between the linker molecules allows to achieve exceptional mechanical properties. Chemical reactions between adsorbed molecules are particularly important for catalysis and the creation of hybrid materials [6], but mechanistic understanding is often limited, hindering the optimization of the processes involved. The identification of reaction products and intermediates is helpful to gain detailed insights. Experimentally, X-ray photoelectron spectroscopy (XPS) is often used for this purpose. However, unambiguous identification of the species present is however often difficult because of overlapping peaks and peak shifts depending on the chemical environment. Computational predictions of core-level electron binding energies can help in the identification and to rationalize binding energy shifts.

Here, chemical species of particular relevance to Fischer-Tropsch synthesis are investigated. Various small organic and inorganic carbon compounds adsorbed on a magnetite (111) surface are studied using Density Functional Theory (DFT). The 1s binding energies are calculated for carbon and oxygen atoms in adsorbates including methane, ethanol, carbonate, formic acid, ether, and inorganic carbon species as well as for magnetite oxygen atoms. All DFT calculations were performed using the Vienna Ab initio Simulations (VASP) package. The exchange correlation (XC) functional PBE was used. The strong correlation of the Fe d-electrons was accounted for by adding an on-site Coulomb potential using an effective Hubbard parameter of U_{eff} = 4.0 eV. After geometry optimization of the studied systems and

stability analysis for selected molecules using ab initio thermodynamics, the core level binding energies of the oxygen and carbon atoms are calculated using different approximations within the DFT. These are the initial state, the final state and the Slater-Janak approach. Comparison of the results of the three methods with each other and with experiments at UHV and operando conditions shows their applicability and limitations. The initial-state approach does not give binding energies and energy shifts in good agreement with experiments, but general trends can be observed. The final-state approach works well for 1s oxygen binding energies but not for C 1s binding energies. The Slater-Janak approach performs similarly to the final-state method for O 1s, but gives better results for C 1s. The calculated binding energies are rationalized using charge and bond arguments. Different species in the experimental data are identified or excluded. This provides insight into the mechanism of the Fischer-Tropsch synthesis.

Supported by the Deutsche Forschungsgemeinschaft (DFG), Projektnummer 192346071 - SFB 986 “M3”.

[1] Baeza *et al*., ChemCatChem 8, 49 (2016).
[2] Dilnawaz *et al*., Biomaterials 31, 3694 (2010).
[3] Dreyer *et al.*, Nature Mater 15, 522 (2016).
[4] Park *et al.*, Nat. Sustain. 3, 129 (2020).
[5] Giuntini *et al.*, Nano Lett. 21, 2891 (2021).
[6] Plunkett *et al.*, ACS Nano 16, 11692 (2022).

Laboratory based NAP-XPS for probing the electrified solid-liquid interface

Christoph Griesser, Toni Moser, Daniel Winkler, Matthias Leitner, Sergio Diaz-Coello and Julia Kunze-Liebhäuser

Institute of Physical Chemistry, University of Innsbruck, Innrain 52c, Innsbruck, 6020, Austria
(corresponding author: J. Kunze-Liebhäuser, e-mail: Julia.kunze@uibk.ac.at)

A profound understanding of the solid/liquid interface is central in electrochemistry and electrocatalysis, as the interfacial properties determine the electro-reactivity of the system. Specifically, in electrochemical energy conversion processes, the surface and interface chemistry determine the selectivity, efficiency and activity of a given catalyst, and its fundamental understanding is pivotal to further advance energy conversion technologies. Although there are several methods to characterize the surface structure under *operando* conditions, the surface chemistry (i.e. oxidation state) is still often evaluated by *ex-situ* X-ray photoelectron spectroscopy (XPS). However, the surface and interface properties can drastically change under operating conditions[1], which makes *in situ* XPS experiments vital for a deeper fundamental understanding of electrocatalytic processes, in general.

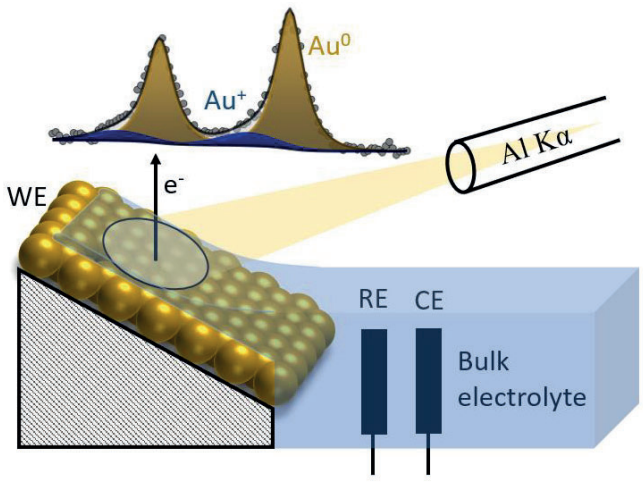

Figure 1: Scheme of the *in-situ* approach utilized for the electrochemical EC NAP-XPS experiments.[2]

Here, we demonstrate the power of near ambient pressure (NAP) XPS as laboratory technique to track the electrified solid/liquid interface of an electrode under reaction conditions.

Furthermore, we discuss the potential drop at this interface by following the potential dependent binding energy position of the O 1s spectra. With our approach, we shed light on the experimental options of laboratory based electrochemical (EC) NAP-XPS, with focus on probing the solid/liquid interface under potential control and reaction conditions.

This presentation is based on three distinct studies.

The first proof-of-principle experiment focuses on the oxidation of polycrystalline gold (Au), one of the best-studied materials in electrochemistry. The findings reveal a stepwise Au oxidation, initially forming a one-dimensional Au^{+} oxide, followed by the development of a three-dimensional Au^{3+} oxide upon entering the oxygen evolution regime. The findings are perfectly in line with electrochemical scanning tunneling microscopy (STM) results that will be separately presented at this conference.

The second example sheds light on the interface chemistry during the CO electro-reduction on $Co(OH)_2$-modified Cu(111). Notably, a departure from the 1 eV/V binding energy shift of the O 1s core level, associated with the electrolyte was observed, coinciding with the onset of the CO reduction reaction – a behavior not discussed previously.

The third study reveals the *in-situ* surface chemistry evolution of tungsten carbide (WC) powders during the hydrogen evolution reaction (HER). WC is known for its platinum-like properties but prone to passivation upon air or electrolyte exposure. It is found that the unpreventable surface passivation layer on WC dissolves into the electrolyte under HER conditions, releasing the bare WC surface. This explains the typically measured high electrocatalytic activity of this compound material.

In conclusion, the data accessible with EC NAP-XPS can provide profound chemical understanding of the electrode/electrolyte interface that exceeds our current knowledge and is not or hardly accessible with other methods. This enables fundamental contribution to bottom-up electrocatalyst development, which is an essential step towards the realization of energy conversion and storage technologies.

We would like to thank for the financial support by the Fonds zur Förderung der Wissenschaftlichen Forschung.

References:

[1] A. Auer, M. Andersen, E.-M. Wernig, N. G. Hörmann, N. Buller, K. Reuter, J. Kunze-Liebhäuser, Nature Catal. 3 (2020) 797.

[2] C. Griesser, D. Winkler, T. Moser, L. Haug, M. Thaler, E. Portenkirchner, B. Klötzer, S. Diaz-Coello, E. Pastor, J. Kunze-Liebhäuser, Electrochemical Science Adv. (2023) e2300007.

The Oxygen Evolution Reaction Drives Passivity Breakdown of Ni-Cr-Mo alloys

A. Larsson[1], A. Grespi[1], G. Abbondanza[1], J. Eidhagen[2,3], D. Gajdek[4], K. Simonov[5], X. Yue[2], U. Lienert[6], Z. Hegedüs[6], M. Scardamaglia[7], A. Shavorskiy[7], L. R. Merte[4], J. Pan[2], and E. Lundgren[1]

[1]Lund University, Division of Synchrotron Radiation Research, Lund, Sweden

(corresponding author: A. Larsson, e-mail: alfred.larsson@sljus.lu.se)

[2]KTH Royal Institute of Technology, Division of Surface and Corrosion Science, Stockholm, Sweden

[3]Alleima (former Sandvik Materials Technology), Sandviken, Sweden

[4]Malmö University, Materials Science and Applied Mathematics, Malmö, Sweden

[5]Swerim AB, Department of Materials and Process Development, Kista, Sweden

[6]DESY Photon Science, Hamburg, Germany

[7]MAX IV Laboratory, Lund, Sweden

Corrosion protection, enabling the widespread use of metallic materials in society, is governed by thin, spontaneously forming oxide films that make the metals passive even in aggressive environments. Corrosion results in costs of 4% of each nation's GDP annually [1], and the production of metals is responsible for 40 % of industrial greenhouse gas emissions and 10 % of global energy consumption [2].

Ni-Cr-Mo alloys are known for their excellent mechanical properties and corrosion resistance and are used in many demanding industrial environments. Standard electrochemical techniques for studying the passivity breakdown of other alloys may not be applicable to Ni-Cr-Mo alloys because the measured electrochemical current is not only due to corrosion reactions [3]. Ni and Mo are good catalysts for the Oxygen Evolution Reaction (OER) [4], which adds another dimension of complexity to the material system since OER is known to be coupled with dissolution and degradation in other material systems such as IrO_2 and RuO_2 [5].

Our current understanding of the structure and chemistry of these passive films is largely based on *ex situ* surface analysis using X-ray Photoelectron Spectroscopy (XPS) [6] and Scanning Tunneling Microscopy [7]. These electron-based techniques have traditionally been limited to UHV, an environment far from the real electrochemical solid/liquid interface. To observe corrosion initiation and progression and obtain a fundamental understanding of corrosion mechanisms, there is a need for techniques that can combine *in situ* capabilities with detailed chemical and structural information from the surface region.

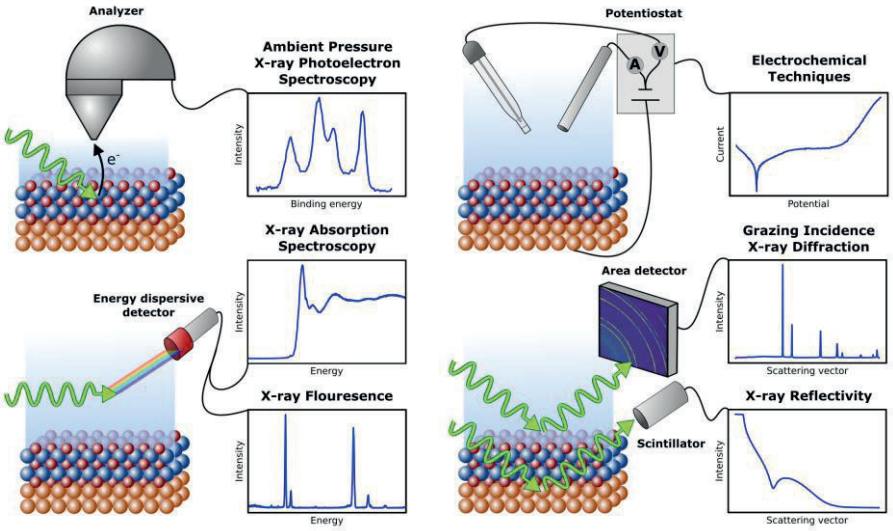

Fig. 1: Schematic illustration of experimental techniques used.

Here, we present comprehensive results from a recently published study [8] combining several synchrotron-based techniques to study the surface region of a Ni-Cr-Mo alloy in NaCl solutions *in situ* during electrochemical polarization, as shown in Fig 1. X-ray Reflectivity (XRR) and Ambient Pressure XPS were used to investigate the thickness and chemistry of the passive film. Grazing Incidence X-ray Diffraction (GI-XRD) was used to determine the change in the metal lattice underneath the passive film. X-ray Fluorescence (XRF) was used to quantify the dissolution of alloying elements. X-ray Absorption Near Edge Structure (XANES) was used to study the chemical state of the dissolved species in the electrolyte. Combining these techniques allowed us to study the corrosion process, detect the passivity breakdown *in situ,* and correlate it to the onset of OER.

1. Koch, G., *1 - Cost of corrosion*, in *Trends in Oil and Gas Corrosion Research and Technologies*, A.M. El-Sherik, Editor. 2017, Woodhead Publishing: Boston. p. 3-30.
2. Raabe, D., *The Materials Science behind Sustainable Metals and Alloys.* Chemical Reviews, 2023. **123**(5): p. 2436-2608.
3. Bettini, E., C. Leygraf, and J. Pan, *Nature of Current Increase for a CoCrMo Alloy: "transpassive" Dissolution vs. Water Oxidation.* International Journal of Electrochemical Science, 2013. **8**: p. 11791-11804.
4. Liao, H., X. Zhang, S. Niu, P. Tan, K. Chen, Y. Liu, G. Wang, M. Liu, and J. Pan, *Dynamic dissolution and re-adsorption of molybdate ion in iron incorporated nickel-molybdenum oxyhydroxide for promoting oxygen evolution reaction.* Applied Catalysis B: Environmental, 2022. **307**: p. 121150.
5. Lončar, A., D. Escalera-López, S. Cherevko, and N. Hodnik, *Inter-relationships between Oxygen Evolution and Iridium Dissolution Mechanisms.* Angewandte Chemie International Edition, 2022. **61**(14): p. e202114437.
6. Strehblow, H. and P. Marcus, *X-ray photoelectron spectroscopy in corrosion research.* CORROSION TECHNOLOGY-NEW YORK AND BASEL-, 2006. **22**: p. 1.
7. Maurice, V. and P. Marcus, *Progress in corrosion science at atomic and nanometric scales.* Progress in Materials Science, 2018. **95**: p. 132-171.
8. Larsson, A., A. Grespi, G. Abbondanza, J. Eidhagen, D. Gajdek, K. Simonov, X. Yue, U. Lienert, Z. Hegedüs, A. Jeromin, et al., *The Oxygen Evolution Reaction Drives Passivity Breakdown for Ni-Cr-Mo Alloys.* Advanced Materials, 2023. **n/a**(n/a): p. 2304621.

Tuning the magnetic properties of Co-Ni bimetallic nanoparticles and turning them into $NiCo_2O_4$

P. Ternero, M. Sedrpooshan[1], D. Wahlqvist[2], B.O. Meuller, M. Ek[2], J. Hübner[2], R. Westerström[1], M.E. Messing[1]

Solid State Physics & NanoLund, Lund University, Box 118, 221 00 Lund, Sweden
(corresponding author: M E Messing, e-mail: maria.messing@ftf.lth.se)

[1] *Synchrotron Radiation Research & NanoLund, Lund University, Box 118, 221 00 Lund, Sweden*

[2] *Center for Analysis and Synthesis & NanoLund, Lund University, Box 118, 221 00 Lund, Sweden*

Metal and metal oxide nanoparticles hold promise for various applications, such as in magnetism and energy storage [1]. This study focuses on the template-free generation of NiCo nanoparticles and nano chains with tunable magnetic properties and their transformation into $NiCo_2O_4$, a material known for its electrochemical supercapacitor potential [2]. Synthesizing $NiCo_2O_4$ remains challenging, with its performance reliant on the preparation method [3].

The research introduces a novel approach: generating NiCo nanoparticles via spark ablation, a method involving material vaporization and condensation into nanoparticles through a plasma channel between electrodes [4]. This technique offers scalability, cost-effectiveness, and minimal environmental impact, aligning with current sustainability goals.

Using $NiCo_2$ alloy electrodes, the study demonstrates elemental composition tuning, from metallic NiCo alloy particles to fully oxidized NiCo particles, achieved by manipulating carrier gas types. The introduction of hydrogen into nitrogen creates a reducing environment while replacing nitrogen with air generates a fully oxidative atmosphere, resulting in nanoparticles with very different magnetic properties [5, 6, 7] (Figure 1).

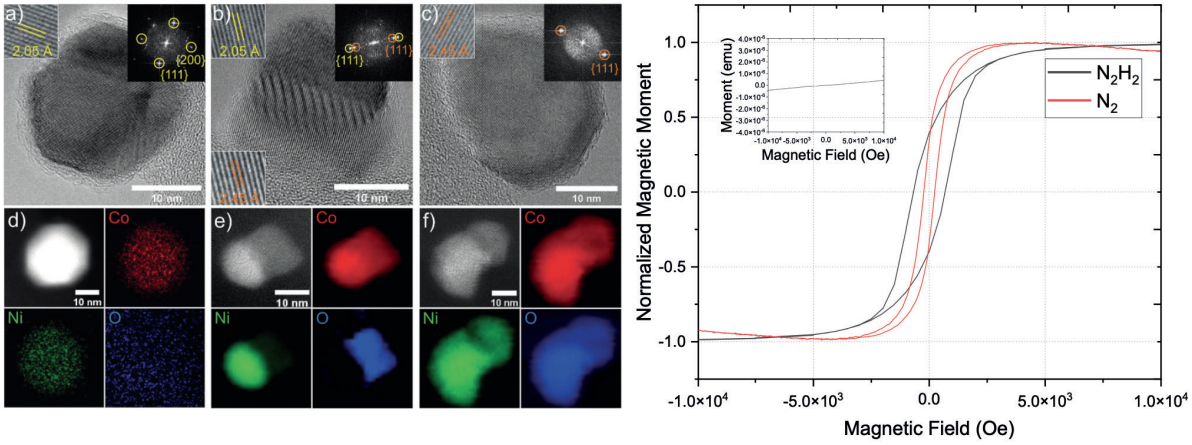

Figure 1: (left) High-resolution TEM micrographs and scanning TEM-EDS mappings of particles generated with a,d) N2/H2, b,e) N2, and c,f) air, respectively. **(right)** SQUID measurements of the magnetic field as a function of the magnetic moment for samples produced with N2/H2 (black), N2 (red), and air (inset).

To transform NiCo particles into $NiCo_2O_4$, a critical thermal treatment oxidation step is employed, either in an air-introduced oven or within an environmental transmission electron microscope (ETEM). ETEM allows in-situ observation of the oxidation process, elucidating surface-initiated oxidation and structural transformations.

Ex-situ TEM and XRD analyses reveal slight compositional differences in formed $NiCo_2O_4$ based on the controlled oxidation state during spark ablation. Additionally, ETEM experiments provide insights into the oxidation dynamics, showcasing structural changes validated by lattice spacing alterations (Figure 2).

The presentation aims to offer a comprehensive understanding of the synthesis and oxidation dynamics shaping $NiCo_2O_4$ nanoparticle characteristics, combining findings from XRD, ex-situ TEM, and in-situ ETEM experiments, advancing the knowledge of tailored nanoparticle synthesis for magnetic and energy storage applications.

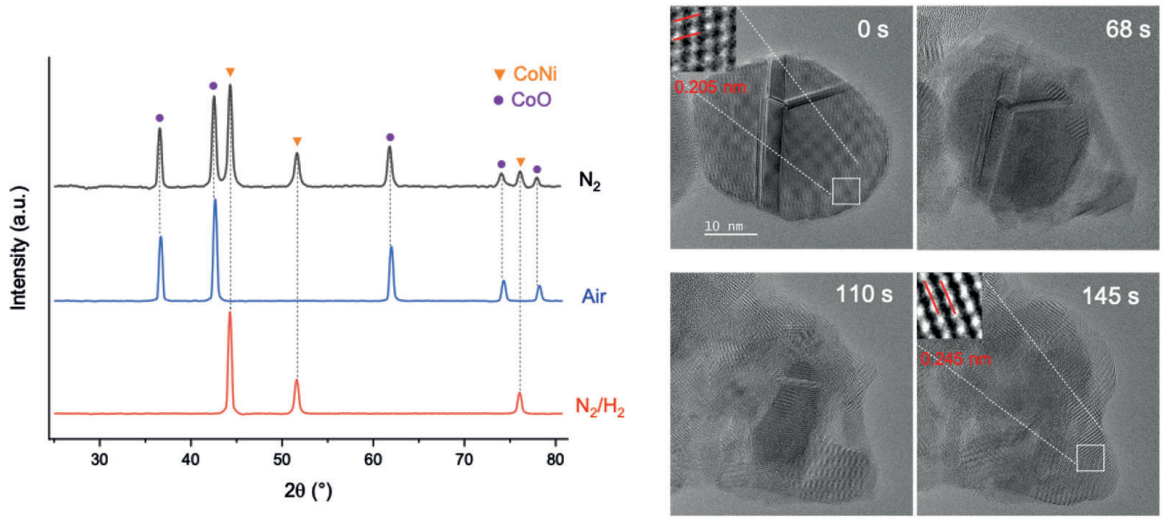

Figure 2: (left) XRD measurements of pristine NiCo nanoparticles generated with N_2, air, and N_2/H2. **(right)** In situ oxidation of a NiCo nanoparticle produced by N_2/H_2 into $NiCo_2O_4$.

This research received funding from the European Union's H2020 MSCA (Grant No. 945378) (GenerationNano), the Swedish Research Council (Grant No. 2019-04970), the Swedish Foundation for Strategic Research (Grant No. FFL18-0282), the Swedish Energy Agency (Grant No. 50689-1), and NanoLund.

[1] Y. Zhang, L. Li, H. Su, W. Huang et al., J. Mater. Chem A. 3, 43 (2015)
[2] G. Zhang and X. W. Lou, Adv. Mater. 25, 976 (2013)
[3] S. Liu, L. Hu, X. Xu, A. A. Al-Ghamdi et al., Small 11, 4267 (2015)
[4] R. T. Hallberg, L. Ludvigsson, C. Preger, B. O. Meuller et al., Aer. Sci. Technol. 52, 347 (2018)
[5] P. Ternero, M. Sedrpooshan, D. Wahlqvist et al., J. Aer. Sci. 170, 106146 (2023)
[6] C. Bulbucan, P. Ternero, C. Preger, et al., J. Magn. Magn. Mater., 570, 170359 (2023)
[7] M. Sedrpooshan, C. Bulbucan, P. Ternero, et al., Nanoscale, 15, 18500 (2023)

Bulk photovoltaic effect in nanotubes and layered Weyl semimetals

A. Puente-Uriona[1], J. Krishna[2], P. Garcia-Goiricelaya, J. Sivianes[1], and J. Ibañez-Azpiroz[1,3,4]

(corresponding author: J. Ibañez-Azpiroz, e-mail: julen.ibanez@ehu.eus)

1 Centro de Física de Materiales, Universidad del País Vasco (UPV/EHU), 20018 San Sebastián, Spain

2 Max Born Institute, Berlin, Germany

3 Ikerbasque Foundation, 48013 Bilbao, Spain

4 Donostia International Physics Center (DIPC), 20018 Donostia-San Sebastián, Spain

The bulk photovoltaic effect (BPE) is the nonlinear optical effect that relates the generation of a dc photocurrent to light absorption in a homogeneous material [1]. The BPE finds its origin in the imbalance of carrier motion along different directions of the Brillouin zone [2], and at variance with the standard photovoltaic effect attained in p-n junctions, this one is not tied to the band gap of the material and giving rise to large measured photovoltages [3]. While traditionally the BPE has been predominantly studied in bulk ferroelectrics such as BaTiO3, the progress in materials synthesis undergone in the past years has allowed measuring the BPE in new structures like nanotubes, distorted semiconductors, or Weyl semimetals.

In this contribution, we discuss the properties of the BPE combining the predictions of our theoretical calculations with available optical measurements. In first place, we consider a WS_2 nanotube upon light irradiation and study the relation between internal structure, radious and the photoconductivity of a single-wall nanotube [4]. We then perform a comparative analysis with the results calculated on a flat monolayer and discuss the similarities and differences of the optical properties in both structures. We finally estimate the total dc photocurrent of a multi-wall nanotube typically employed in experiment and discuss our results and the role of the BPE in the context of recent measurements [5].

In the second part, we consider the type-II Weyl semimetal $TaIrTe_4$, a layered material that exhibits an accute nonlinear optical absorption [6]. At variance with most bulk photovoltaics, the BPE in this material appears to originate from *third-order* electric field effects, given that the usually predominant quadratic contribution is forbidden by symmetry. We study the implications of this case by assessing the impact of several third-order contributions, and propose the effect known as the *jerk current* as the most likely candidate to explain the experimental optical absorption [7]. We also discuss the role of the Weyl points and their topology in nonlinear current generation [8].

Funding provided by the European Union's Horizon 2020 research and innovation programme under the European Research Council (ERC) grant agreement No 946629.

[1] R. von Baltz and W. Kraut, Phys. Rev. B 23, 5590 (1981)

[2] J. E. Sipe and A. I. Shkrebtii, Phys. Rev. B 61 , 5337 (2000)

[3] J. E. Spanier, V. M. Fridkin, A. M. Rappe, A. R. Akbashev, A. Polemi, Y. Qi, Z. Gu, S. M. Young, C. J. Hawley, D. Imbrenda, G. Xiao, A. L. Bennett-Jackson, and C. L. Johnson, Nature Photonics, 10, 9, 611–616, (2016)

[4] J. Krishna, P. Garcia-Goiricelaya, F. de Juan, and J. Ibañez-Azpiroz, Phys. Rev. B 108, 165418 (2023)

[5] Y. J. Zhang, T. Ideue, M. Onga, F. Qin, R. Suzuki, A. Zak, R. Tenne, J. H. Smet, and Y. Iwasa, Nature, 570, 7761, 349 (2019)

[6] J. Ma, Q. Gu, Y. Liu, J. Lai, P. Yu, X. Zhuo, Z. Liu, J.-H. Chen, J. Feng, and D. Sun, Nat. Mater. 18, 476 (2019).

[7] A. R. Puente-Uriona, S. S. Tsirkin, I. Souza and J. Ibañez-Azpiroz, Phys. Rev. B 107, 205204 (2023)

[8] J. Sivianes and J. Ibañez-Azpiroz, Phys. Rev. B 108, 155419 (2023)

Experimental determination of forces on adatoms in external fields

F. Leroy, A. El Barraj, F. Cheynis, P. Müller, S. Curiotto.

Aix Marseille University, CNRS, CINaM, Marseille, France
(corresponding author: F. Leroy, e-mail: frederic.leroy.3@univ-amu.fr)

Adatom diffusion plays a key role in surface physics and crystal growth [1,2]. Strong external fields are known to create biased adatom migration that may give birth to undesirable effects or may be used as a control parameter to, for instance, tune atomic transport and/or nanostructure motion on surfaces [3,4].

The action of external fields due to a gradient of electrical potential or a thermal gradient are respectively known as electromigration and thermomigration. In she standard treatment of irreversible thermodynamics, the adatom mass flow reads: $J = (Dc/k_B T)F$ where D is the surface diffusion constant, c the adatom concentration, k_B the Boltzmann constant, T the temperature and F an effective force acting on the adatoms. For electromigration [5,6] this force reads $F^{el.} = Z^* E$ where E is the electrical field and Z^* an effective charge that can itself be decomposed into electrostatic and wind contributions (see Fig. 1). For thermomigration [7,8] $F^{th.} = -Q^* \nabla T/T$ where ∇T is the thermal gradient and Q^* an effective quantity named the atomic heat of transport (see Fig. 2). The measurement of the effective quantities Z^* and Q^* is a genuine experimental challenge. These quantities are thus generally obtained indirectly and with a high degree of uncertainty (sometimes several order of magnitude).

In this paper we propose two methods of measurement based on *in-operando* Low Energy Electron Microscopy experiments.

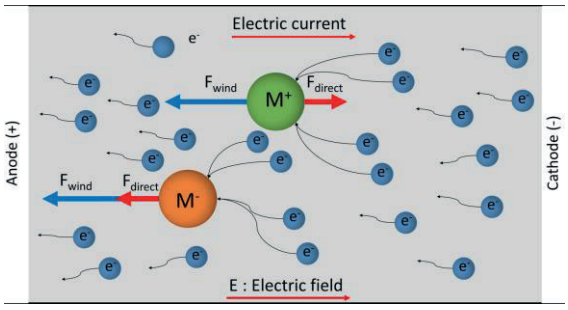

Figure 1 : Electromigration process

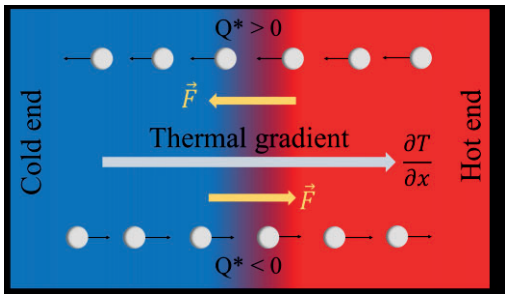

Figure 2 : Thermomigration process

For electromigration [9], we study the evolution versus time of a 2D gas phase of Au deposited on Ge(111) submitted to an electrical field $E = 150V/\text{m}$. From a careful examination of the concentration $c(x)$ of an adatom gas spatially retained by a strong Ehrlich-Schwoebel barrier at a downhill step edge (see Fig. 3), we show that it is possible to **directly** extract the value of the effective charge Z^*. In the case under study we find $Z^*/e = -82 \pm 15$ where e is the electron charge.

For thermomigration [10], we measure the drift velocity, induced by a thermal gradient of 10^4 K/m, of 2D supercooled advacancy islands on a Si(111) 7x7 surface (see Fig. 4). We find that Si adatom migration is biased in the direction opposite to the thermal gradient and are able to extract the heat of transport of Si adatoms: $Q^* = 1.2 \pm 0.4$ eV. A simple modeling enables us to attribute Q^* to combined effects of adatom creation at step edges and adatom diffusion on atomically flat terraces.

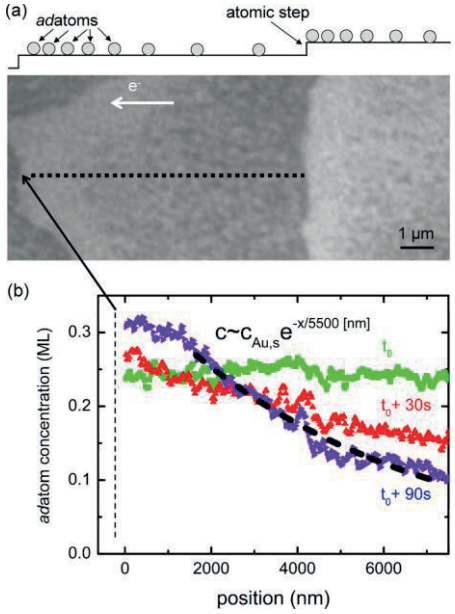

Figure 3: LEEM image of a 2D gas of adatoms and coverage profiles versus time of Au adatoms along the dashed line.

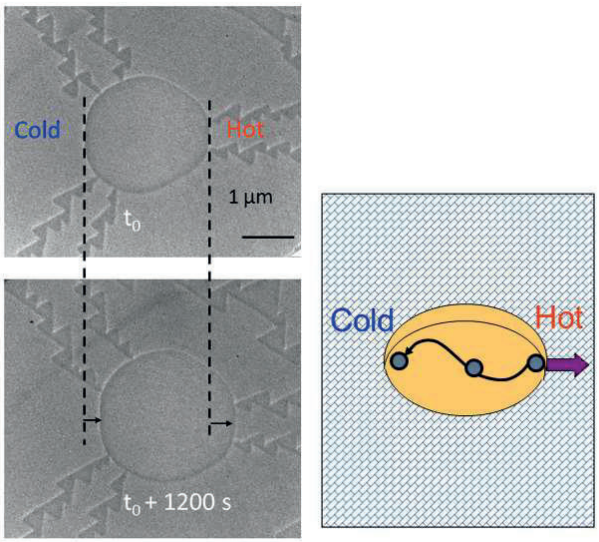

Figure 4: Thermomigration of a supercooled advacancy islands on a Si(111) 7x7 surface and the atomic mechanism at work.

Supported by the ANR grants Hololeem and Thermotweets

[1] A.G. Nauvets, Y.S Vedula, Surface Science Reports 4, 365 (1985)
[2] H. Yasunaga, A. Natori, Surface Science Reports 15, 205 (1992)
[3] S. Curiotto, P. Müller, A. El Barraj, F. Cheynis, O. Pierre-Louis, Appl. Surf. Sci. 469, 463 (2019)
[4] S. Curiotto, F. Cheynis, P. Müller, F. Leroy, ACS Applied nanomaterials 3, 1118 (2020)
[5] H.-C. Jeong, E.D. Williams, Surface Science Reports 34, 171 (1999)
[6] P. Ho, T. Kwok, Rep. Prog. Phys. 52, 301 (1989)
[7] R. Oriani, J. Phys. Chem. Solid 30, 339 (1969)
[8] A. Roux, N. Combe, Phys. Rev. B 108, 115410 (2023)
[9] F. Leroy, A. El. Barraj, F. Cheynis, P. Müller, S. Curiotto, Phys. Rev. B 106, 115402 (2022)
[10] F. Leroy, A. El. Barraj, F. Cheynis, P. Müler, S. Curiotto, Phys. Rev. Lett. 131, 116202 (2023)

Comeback of JT-Cooling for Low Temperature SPM: the new USM1200-JT

T.Berghaus[1], A.Bettac[1], R.Shibuya[2], J.Kasai[2], T.Koyama[2], M.Yokota[2], and Y.Miyatake[2]

[1] nanoscore gmbh, Maisebachstr. 3, 61479 Glashütten, Germany
(corresponding author: T. Berghaus, e-mail: t.berghaus@nanoscore.de)

[2] UNISOKU Co., Ltd. Hirakata, Osaka 573-0131, Japan

Joule Thomson (JT) cooling [1] has become broadly popular in Low Temperature Scanning Probe Microsopy (LT-SPM) initially when SPECS introduced their JT-STM [2] as a commercial product to the market. The design was based on a development by Wulfhekel et al. [3] and licensed by KIT [4]. Over the years the product turned out to be highly complex and increasingly costly, and the commercial offering decreased significantly.

Now UNISOKU has launched the new USM1200-JT. Based on the LHe/LN2 bath cryostat with very long hold time of the USM1200 [5], an entirely new JT-cooling stage has been added. The JT-cooler is implemented as a closed loop circuit with zero gas consumption. The base temperature approaches 1.1K under operation with ^{4}He gas.

USM1200-JT
operated with ^{4}He

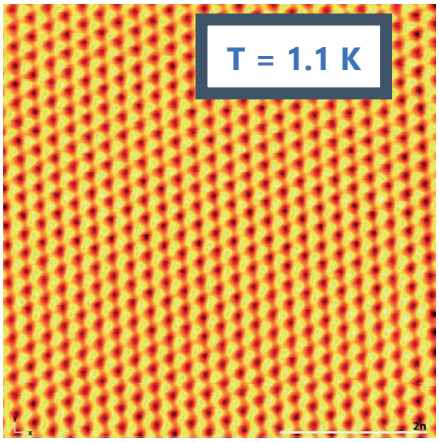

HOPG topography at T=1.1K

USM1200-JT
operated with ^{3}He

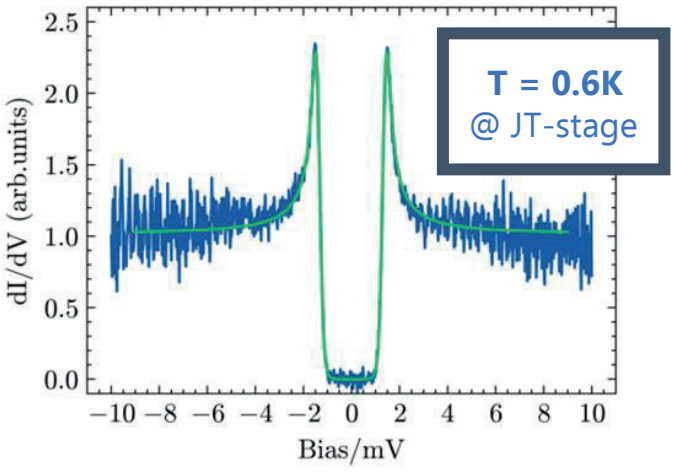

measured SC gap Spectrum of Pb (blue) fit (green) reveals an effective T=0.9K

The closed loop design of the JT-stage facilitates operation with ^{3}He gas out of the box. Operated with ^{3}He gas a base temperature of 0.6K is achieved at the JT-stage. With further improvement of the RF filter configuration we expect an effective electron temperature of the sample of ~750mK.

The USM1200-JT is available with traditional UNISOKU sample holders or with flag-style sample plates. The latter version with the wide spread sample holder format ensures compatibility with common XPS and sample preparation system. Last but not least it is available with a superconducting magnet providing up to 3Tesla magnetic field perpendicular to the sample plane.

[1] J. P. Joule, W. Thomson: On the thermal effects experienced by air in rushing through small apertures, Philosophical Magazine, Series 4, Volume 4, Issue 284, Seiten 481-492 (1852)

[2] SPECS Surface Nano Analysis GmbH, Voltastrasse 5, 13355 Berlin / Germany https://www.specs-group.com/nc/specsgroup/knowledge/methods/detail/spm-stm-afm/ and SPECS brochure "JT-STM Joule-Thomson Scanning Tunneling Microscope", 2010

[3] L. Zhang, T. Miyamachi, T. Tomanić; R. Dehm, W. Wulfhekel, Rev. Sci. Instrum. 82, 103702 (2011) https://doi.org/10.1063/1.3646468

[4] Karlsruher Institut für Technologie, www.kit edu

[5] https://nanoscore.de/products/uhv-spm-systems/usm-1200/

Enriching Photoelectron Spectroscopy Instrumentation: New Developments in NAP-XPS Analysis

Francesca Mirabella, Paul Dietrich, Andreas Thissen

SPECS Surface Nano Analysis GmbH, Berlin, Germany
(corresponding author: F. Mirabella, e-mail: Francesca.Mirabella@specs.com)

NAP-XPS has broadened the applicability of the XPS method to include studies of liquids, solid-liquid interfaces, gas-solid interfaces, gas-liquid interfaces, and more. Alongside innovations in "active" components such as excitation sources and electron analyzers, significant progress has been achieved in sample environments, sample handling, system setup, automation, combination with other techniques, and data quantification.

In this presentation, we explore the evolution of NAP-XPS instrumentation over the last five decades, from its inception to its current status as a laboratory- and synchrotron-based method. We also delve into the exciting possibilities EnviroMETROS brings to the forefront. By exploring the current equipment and its challenges, we open the door to upcoming improvements that will make NAP-XPS more accessible to routine analysis in both fundamental and applied science.

Join us in this exploration of cutting-edge instrumentation, where we bridge the past and the future of Photoelectron Spectroscopy, propelling the field towards new frontiers of analytical possibilities.

Computationally efficient model for the transport of multi-component electrolytes in chemically active nano-tubes

F. Altmann, A.T. Celebi, and M.Valtiner,

Institute of Applied Physics, Vienna University of Technology, Wiedner Hauptstrasse 8-10, A-1040, Vienna, Austria

(corresponding author: F. Altmann, e-mail: altmannf@iap.tuwien.ac.at)

Modelling the transport of multi-component electrolytes through chemically active nano-tubes is of great interest for many technological applications, *e.g.* for electrochemical energy storage and semi-conductor manufacturing. Performing (dynamic) simulations of such systems is computationally expensive due to the underlying non-linear multi-physics of diffusion and electro-migration transport together with concentration dependent chemical reactions in the electrolyte and at the solid-liquid interface (tube wall surface reactions). The latter are responsible for inducing net charges at the tube wall that lead to the formation of an electric double layer (EDL) in the radial direction of the tube. Usually, such systems are modelled within a full 2D Poisson-Nernst-Planck equation framework that considers concentration and electric potential gradients in both the axial and radial direction.

In many technological applications the tube length L is much larger than the tube radius ($L >> R$), which would usually suggest a simple 1D treatment for the mass transport in the axial direction. However, due to the inherent EDL structure such an approach is only valid for extremely weak electrolytes in which Debye length is much larger than the tube radius ($\lambda_D >> R$), such that the electric potential can be assumed constant in the radial direction.

We present here a modelling framework which allows to capture the EDL structure in a quasi-1D manner, circumventing a full 2D simulation by combining numerical modelling with analytical solution of the Poisson-Boltzmann equation in the weak electrolyte limit ($\lambda_D > R$) [1]. The coupled governing equations are then linearised in time [2], avoiding computationally expensive Newton iterations at each time-step during dynamic simulations. Spatial discretization based on a Chebyshev collocation method [3] in combination with variable time stepping that depends on the transient behaviour of the simulation [4] further assures extremely efficient computation.

The presented modelling framework is further applied to the technologically relevant wet-cleaning process of silica nano-tubes in semiconductor manufacturing. This intricate process involves a variety of different species that undergo chemical reactions in the liquid electrolyte and at the liquid-silica interface. We find that the surface chemistry of silanol deprotonation drastically influences the ionic concentration in the tube, directly influencing the cleaning efficiency. Surprisingly, it is not the mass transport hindrance of sub 10 nm tubes that lead to

decreased cleaning rates, but the tube wall surface chemistry and resulting EDL formation. Molecular dynamics simulations further substantiate our findings.

Our model is aimed to provide a simple, analytically tractable, and computationally efficient framework for the simulation of dynamic and steady-state transport of electrolytes in nano-tubes, applicable to many technological areas. We were able to successfully apply the model to the wet-cleaning process of semiconductor nano-structures. In the future, we want to use this model to study ion exchange dynamics in multi-component electrolytes and incorporate also steric and hydration effects to complement our previous studies [5].

[1] Herrero and Joly, Poisson-Boltzmann formulary (2022)

[2] T. W. H. Sheu and R.K. Lin, Int. J. Num. Methods Fluids 44, 297 (2003)

[3] L. Trefethen, Spectral Methods in MATLAB (2000)

[4] D. Murschenhofer, D. Kuzdas, S. Braun, and S. Jakubek. Energy Conv. Manag. 162, 159 (2018)

[5] U. Ramach, J. Lee, F. Altmann, M. Schussek, M. Olgiati, J. Dziadkowiec, L.L.E. Mears, A.T. Celebi, D. Lee, and M. Valtiner. Faraday Discuss. 246, 487-507 (2023).

Sputtering yields of lunar soils under solar wind ion impact

J. Brötzner, H. Biber, N. Jäggi[1], A. Nenning[2], L. Fuchs, P.S. Szabo[3], A. Galli[4], P. Wurz[4] and F. Aumayr

Institut of Applied Physics, TU Wien, 1040 Vienna, Austria
(corresponding author: J. Brötzner, e-mail: broetzner@iap.tuwien.ac.at)

[1] *Department of Material Science and Engineering, University of Virginia, Charlottesville, VA 22904, USA*

[2] *Institute of Chemical Technologies and Analytics, TU Wien, 1060 Vienna, Austria*

[3] *Space Sciences Laboratory, University of California,Berkely, CA 94720, USA*

[4] *Space Research and Planetary Sciences, Physics Institute, University of Bern, 3012 Bern, Switzerland*

The Sun is the source of a multitude of processes that affect the surfaces of rocky objects and planets in the solar system. Besides thermal and electromagnetic irradiation, the solar wind is a plasma stream of mostly H^+ and He^{2+} ions that predominantly interact with objects lacking a protective atmosphere or magnetic field. The impacts of these ions lead to surface sputtering, the liberation of material on a mostly atomic level, and thus contributes to the formation of a tenuous gas envelope called exosphere [1]. The exosphere's properties are tightly linked to both the surface properties and the release mechanism. The exosphere therefore provides an opportunity to study the relevant object without the need for a lander, either by optical spectroscopy from or by mass spectroscopy during flybys or in orbit. The former has been achieved, e.g., for Mercury by the MESSENGER mission [2] while more recently, ESA's BepiColombo mission to Mercury and NASA's Artemis program for exploration of the Moon are expected to perform new in-situ studies soon.

In all cases, laboratory data are necessary as a benchmark for models of exosphere formation and to draw valid conclusions from available spacecraft data to better understand how the solar wind ions interact with planetary surfaces. Especially for the Moon, the degree of surface erosion due to ion sputtering has been of interest for decades [3]. However, most attempts of experimental quantification have struggled to use relevant materials analogous to the expected lunar surface mineralogy and petrology. Only recently, investigations with representative samples were published [4–6].

In this study, we present measurements on the sputtering yields of lunar soils using samples that were returned during the Apollo 16 mission (sample number 68501) by means of a quartz crystal microbalance (QCM) method in two configurations. Firstly, a thin vitreous layer of this lunar material was grown on a quartz resonator using pulsed laser deposition. Because of the relation between QCM mass and resonance frequency [7], we can quantify the mass depletion due to sputtering as a result of H and He ion irradiation. Secondly, we placed another QCM, the catcher QCM, in the experimentation chamber, facing the irradiated sample. The catcher QCM is rotatable and collects the ejecta, allowing us to probe the angular distribution of the sputtered particles.

Moreover, we repeated these measurements with pellets pressed from lunar regolith and otherwise prepared analogously to the description in [8]. These pellets represent the lunar surface more realistically because they retain their original grains and preserve their roughness. However, sputtering yield determination is no more available via the direct QCM method. Therefore, we compared the angular emission profiles of the ejecta measured with the catcher QCM to the reference measurements with thin film targets and inferred the sputtering yield indirectly.

Using this setup, we were able to quantify the sputtering yields of lunar soils for solar wind bombardment under different angles of incidence with unprecedented accuracy. We will present our experimental findings along with the simulation approaches used to model these results, providing insights into the sputtering of the surfaces of the Moon and other celestial bodies.

[1] B. Hapke, *J. Geophys. Res. Planets* **106** (2001) 10039–10073, doi:10.1029/2000JE001338.

[2] R.J. Vervack, W.E. McClintock, R.M. Killen, A.L. Sprague, et al., *Science* **329** (2010) 672–675, doi:10.1126/science.1188572.

[3] G.K. Wehner, C. Kenknight, D.L. Rosenberg, *Planet. Space Sci.* **11** (1963) 885–895, doi:10.1016/0032-0633(63)90120-X.

[4] P.S. Szabo, R. Chiba, H. Biber, R. Stadlmayr, et al., *Icarus* **314** (2018) 98–105, doi:10.1016/j.icarus.2018.05.028.

[5] H. Biber, P.S. Szabo, N. Jäggi, M. Wallner, et al., *Nucl. Instrum. Methods. Phys. Res. B* **480** (2020) 10–15, doi:10.1016/j.nimb.2020.07.021.

[6] H. Biber, J. Brötzner, N. Jäggi, P.S. Szabo, et al., *Planet. Sci. J.* **3** (2022) 271, doi:10.3847/PSJ/aca402.

[7] G. Sauerbrey, *Z. Physik* **155** (1959) 206–222, doi:10.1007/BF01337937.

[8] N. Jäggi, A. Galli, P. Wurz, H. Biber, et al., *Icarus* **365** (2021) 114492, doi:10.1016/j.icarus.2021.114492.

Using High Sensitivity – Low Energy Ion Scattering Spectroscopy (HS-LEIS) to unravel the complex nature of multi principal element alloys.

Matthias Kogler[1,2], Christian M. Pichler[1,2], Markus Valtiner[1,2]

[1]*Centre for Electrochemistry and Surface Technology GmbH, Wr. Neustadt/Austria*

[2]*Vienna University of Technology, Vienna/Austria*

(corresponding author: M. Kogler, e-mail: kogler@iap.tuwien.ac.at)

Complex metallic materials such as Multi-Principal Alloys (MPEAs) and High Entropy Alloys (HEAs) have emerged as a promising class of materials given their unique inherent characteristics. First mentioned by Cantor [1] and Yeh [2], the Cantor alloy (CrMnFeCoNi) and associated subsystems are among the best-known representatives. Excellent mechanical, thermal, and corrosion properties allow for a broad spectrum of applications. However, due to the multi-element nature of these alloys, characterization of the composition and microstructure, and subsequent linking to material behavior, proves to be a challenging task.

Especially with regard to corrosion-protective passivation films, the complex correlations with the corrosion behaviour are fully unclear to date, and require an in-depth atomic level characterisation and rationalisation. Since the thickness of such oxides lies in the region of 1-5 nm, the precise layer by layer structure of these passive films is particularly demanding to assess.

Conventional advanced surface techniques, such as XPS (X-ray photoelectron spectroscopy) or AES (Auger electron spectroscopy), are employed to address this analytical question, providing valuable information about the outer few nanometres of the material. However, due to analysis penetration depths of several nanometres, they cannot achieve atomic layer resolution. To fully understand and quantify the passivation layer structure, such an atomic layer resolution of the surface region is necessary, due to the complexity of the alloys.

In order to obtain an exact understanding of the atomistic mechanism at the monoatomic layer level, High-Sensitivity - Low Energy Ion Scattering Spectroscopy (HS-LEIS), was applied. This technique is based on the scattering of low-energy noble gas ions on the material surface. Due to the low energies of the primary ions – typically 1-8 keV, there is a high probability of neutralization upon interaction with the surface. Since only charged particles are registered by the detector, only those ions scattered at the outermost atomic layer have sufficiently short interaction times to avoid neutralization. [3] By exploiting this principle, the required monolayer resolution to study the passivation layers of such complex multi-component alloys can be provided.

In this work, the quinary Cantor alloy and different subsystems were investigated with LEIS. The unique surface sensitivity combined with the implementation of novel in-situ treatment methods enabled the real-time study of oxide layer growth, as well as the analysis of temperature-dependent changes in the elemental surface composition. Due to the high resolution achieved by static and dynamic sputter depth profile modes, we could determine the exact composition of the HEA passivation layer with resolution on atomic monolayer scale.

The findings provide the potential to significantly advance the current understanding of the passivation behaviour of MPEAs and HEAs, and the development of novel metallic materials with superior properties. Valuable insights for understanding the material characteristics for those highly advanced materials could thereby be generated.

For the LEIS instrument, the funding from the state of Lower Austria and the European Regional Development Fund under grant number WST3-F-542638/004-2021 is gratefully acknowledged. Financial support of “Gesellschaft fuer Forschungsfoerderung NOE” (FTI21 - Dissertationen) and the FFG COMET funding scheme (Competence Centers for Excellent Technologies by BMVIT, BMDW as well as the Province of Lower Austria and Upper Austria) is gratefully acknowledged.

[1] B. Cantor, I.T.H. Chang, P. Knight, A.J.B. Vincent, Materials Science and Engineering: A, 375-377 (2004) 213-218.

[2] J.W. Yeh, S.K. Chen, S.J. Lin, J.Y. Gan, T.S. Chin, T.T. Shun, C.H. Tsau, S.Y. Chang, Advanced Engineering Materials, 6 (2004) 299-303.

[3] C.V. Cushman, P. Brüner, J. Zakel, G.H. Major, B.M. Lunt, N.J. Smith, T. Grehl, M.R. Linford, Anal. Methods, 8 (2016) 3419-3439.

Friday

Structure of copper oxide films solved by noncontact AFM and machine-learning methods

D. Wrana,[1] J. Redondo,[1] F. Brix,[2] S. Auras,[3] E. Ortega,[3] M. Setvin,[1] and B. Hammer[2]

(corresponding author: M. Setvin, e-mail: martin.setvin@mff.cuni.cz)

[1] *Department of Surface and Plasma Science, Faculty of Mathematics and Physics Charles University, Prague, Czech Republic*

[2] *Center for Interstellar Catalysis, Department of Physics and Astronomy, Aarhus University, DK-8000 Aarhus C, Denmark*

[3] *Centro de Física de Materiales CSIC-UPV/EHU-Materials Physics Center, 20018 San Sebastian*

Resolving the arrangement of atoms at surfaces is one of the main tasks of surface science. The surface atomic structure translates into chemical, catalytic and electronic properties of materials, yet its understanding is a nontrivial task. Oxidation of metallic copper is a complex process that is not well understood at the atomic level and therefore represents a long-standing challenge in surface science. The importance of copper oxides recently grows mainly due to their good performance in catalysis of small organic molecules [1].

The atomic structure of such a challenging system can be effectively resolved by a combination of novel experimental and theoretical techniques. Here, combined STM/AFM (scanning tunnelling microscopy and noncontact atomic force microscopy) provides atomically resolved information about the positions of surface oxygen and copper atoms and XPS (x-ray photoelectron spectroscopy) is used to characterize the chemical state of the involved atoms. The atomic structure is resolved by the GOFEE method [2] that is based on a combination of DFT and machine learning.

Here, Cu (111) surfaces were oxidized at various partial O_2 pressures ranging from 10^{-8} to 10^{-3} mbar and temperatures ranging from room temperature to 600 °C. This leads to the development of a variety of copper oxide phases. Oxidation at room temperature results in the formation of an oxide film with Cu_3O_2 stoichiometry that is amorphous but has well-defined rules for atomic arrangement. Oxidation at elevated temperatures can result in a myriad of structures, where the most famous one is called the “29” reconstruction [3]. We show that all these reconstructions have similar building blocks and resolve the “29” reconstruction as a showcase.

This work was supported by the Czech Science Foundation (GACR 20-21727X), and by MSMT CZ.02.01.01/00/22_008/0004572.

[1] S. Nitopi *et al.,* Chem. Rev. **119**, 7610 (2019)

[2] M. K. Bisbo, B. Hammer, Phys. Rev. Lett. **124**, 086102 (2020)

[3] A. J. Therrien *et al*., J. Phys. Chem. C **120**, 10879 (2016)

Atomic layer deposition of 2D semiconductors on atomically defined oxide surfaces: Insights from surface science

J. Libuda

Interface Research and Catalysis, ECRC,
Friedrich-Alexander-Universität Erlangen-Nürnberg, 91058 Erlangen, Germany
(corresponding author: J. Libuda, e-mail: joerg.libuda@fau.de)

Two-dimensional (2D) semiconductors, in particular transition-metal dichalcogenides (TMDCs), have attracted a lot of interest due to their unusual electrical and optical properties. Besides MoS_2, which has been studied the most, HfS_2 is a particularly interesting compound which has been reported to show higher mobility and a well-suited band gap. In order to build electronic devices based on TMDCs, controlled deposition of well-defined films and nanostructures is a key prerequisite. Here, innovative deposition methods such as atomic layer deposition (ALD) open completely new possibilities. ALD is based on self-terminating reactions of two precursors supplied suppled from the gas or liquid phase. ALD is superior to molecular beam epitaxy or chemical vapor deposition, as the method provides better control of thickness and conformality and can be applied even to highly corrugated surfaces. However, control over the nucleation process is essential to achieve continuous, defect-poor, and pinhole-free films.

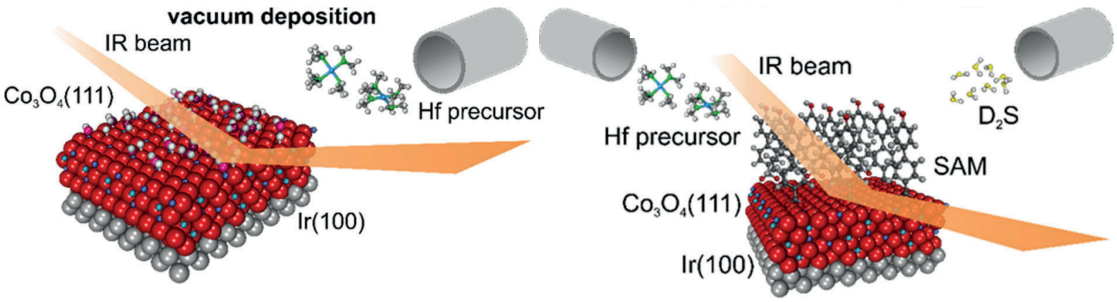

***Fig. 1: In-situ IR spectroscopy during ALD of HfS_2 in UHV**; left: growth on an atomically defined $Co_3O_4(111)$ surface; right: Growth on a functionalized SAM anchored to an atomically defined $Co_3O_4(111)$ surface.*

In this work, we investigated ALD of HfS_2 on an atomically defined $Co_3O_4(111)$ film under ultrahigh-vacuum (UHV) conditions. The nucleation and growth steps were monitored in-situ by time-resolved and temperature-controlled infrared reflection absorption spectroscopy (IRAS).[1,2] HfS_2 was grown by sequential dosing of tetrakis-(dimethylamido)-hafnium (TDMAH) and D_2S onto the surface exposing well-defined OD groups and partially dissociated OD/D2O aggregates.

We found that the initial half-cycle of the ALD process comprises of several regimes.[2] Initially, TDMAH loses all ligands due to a reaction with mobile OD/D_2O species on the surface. With increasing exposure to TDMAH, the stoichiometry of the growth nuclei changes.

We observe the formation of partially hydrolyzed $Hf(NMe_2)_n(O)_x(OD)_m$ species and the consumption of OD/D_2O aggregates. In the final growth step, the partially hydrolyzed $Hf(NMe_2)_n(O)_x(OD)_m$ species react with TDMAH until all OD groups are consumed.
To better control the nucleation process, we investigated ALD of HfS_2 on both functionalized and non-functionalized self-assembled monolayers (SAMs) grown on $Co_3O_4(111)$.[3] In particular, we compared the growth on the hydrocarbon-terminated biphenyl-4-carboxylic acid (BP4CA) SAM to the OH-terminated 4′-hydroxy-4-biphenylcarboxylic acid (4HBP4CA) SAM.[3] We observed that the deposition of HfS_2 can be efficiently controlled by the surface termination of the SAM. Nucleation of HfS_2 is suppressed on the BP4CA SAM up to temperatures of 400 K. The initial nucleation process on the 4HBP4CA SAM again comprises of several growth regimes with the stoichiometry of the $Hf(NMe_2)_nOR_m$ nuclei changing during the first ALD half cycle. Moreover, the Hf-containing nuclei affect the structure of the underlying SAM.

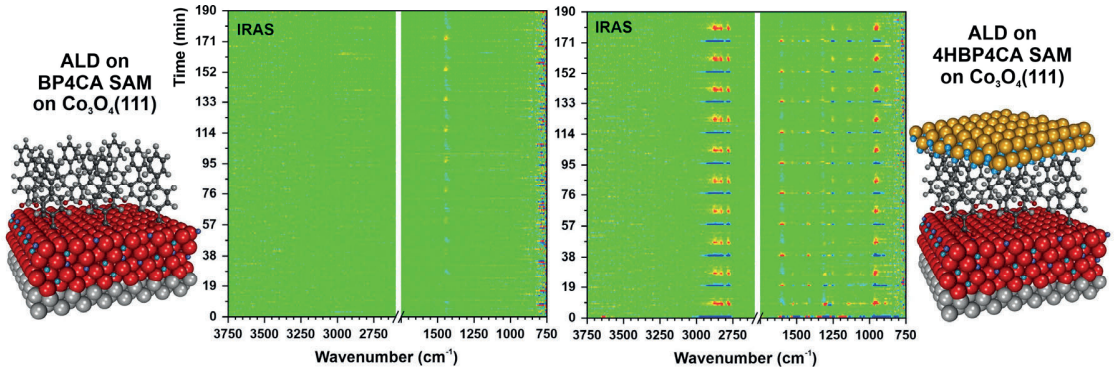

***Fig. 1: In-situ IR spectra recorded during ALD of HfS_2 in UHV**; left: suppressed deposition on a hydrocarbon-terminated SAM (BP4CA) on $Co_3O_4(111)$ surface; right: Growth on a COOH-functionalized SAM (4HBP4CA) on $Co_3O_4(111)$.*

Our findings demonstrate that the initial nucleation step of the ALD procedure is a very complex process in which it is essential to control not only the classical growth parameters such as temperature and flux, but also the nature and the mobility of the OD/D_2O aggregates on the surface. Finally, we give an outlook on our recent studies aimed at transferring the ALD method to liquid-phase reactions (solution ALD) and developing methods for monitoring the deposition processes by in situ IR spectroscopy.[4]

This work was supported by the FAU Competence Center Engineering of Advanced Materials at the Friedrich-Alexander-Universität Erlangen-Nürnberg and by the Deutsche Forschungsgemeinschaft (DFG, German Research Foundation) via FOR 1878 (project 214951840).

[1] Y. Cao, et int., D. M. Guldi, A. Görling, J. Maultzsch, T. Unruh, E. Spiecker, M. Halik, J. Libuda, J. Bachmann Adv. Mater. Interfaces, 7, 2001493 (2020)
[2] G. Fickenscher, L. Fromm, A. Görling, J. Libuda "Atomic Layer Deposition of HfS2 on Oxide Interfaces: A Model Study on the Initial Nucleation Processes" J. Phys. Chem. C 126, 21596 (2022)
[3] G. Fickenscher, J. Steffen, A. Görling, J. Libuda, J. Phys. Chem. C, accepted (2023)
[4] F. Hilpert, P.C. Liao, E. Franz, V. M. Koch, L. Fromm, E. Topraksal, A. Görling, A.S. Smith, M.K.S. Barr, J. Bachmann, O. Brummel, J. Libuda, J., ACS Appl. Mater. Interfaces 15, 19536 (2023)

C_{60} layers on epitaxial $CsPbBr_3$ films on Au(100)

M. Alexander Schneider, Hannah Loh, Andreas Raabgrund

Solid State Physics, FAU Erlangen-Nürnberg, 91058 Erlangen, Germany
(corresponding author: M.A. Schneider, e-mail: alexander.schneider@fau.de)

While the efficiency of $CsPbBr_3$ all-inorganic perovskite solar cells lags behind that of its hybrid counterparts (where Cs is replaced by an organic molecule), it is nevertheless a promising all-inorganic light-absorbing material due to its superior stability at operation conditions. In such solar cells charge carriers have to be separated at the interface to e.g. organic electron or hole transport layers. To better understand the interfaces between the materials, we have grown epitaxial films of $CsPbBr_3$ on Au(100) in ultra-high vacuum and subsequently added C_{60} which is known to act as an electron transport layer.

In this contribution we will introduce epitaxial system $CsPbBr_3$ on Au(100) as a suitable platform to carry out investigations by STM at 80 K. When CsBr and $PbBr_2$ are (co-)deposited onto Au(100) and annealed up to 150°C, continuous perovskite $CsPbBr_3$(001) films of homogeneous thicknesses in (2 x 2) substrate registry can be produced with grain sizes exceeding the micrometre range [1]. When their thickness exceeds 4 monolayers (ML), the films exhibit a complex surface topology exhibiting a $(2\sqrt{2} \times \sqrt{2})R45°$ and a (2×2) surface reconstruction w.r.t. the perovskite (1×1) cell coexisting at temperatures below ≈ 120 K (Fig1 (a),(b)). Both reconstructions have also been reported when growing the material on Au(111) [2], however, the epitaxy is much better on Au(100) allowing a more detailed analysis.

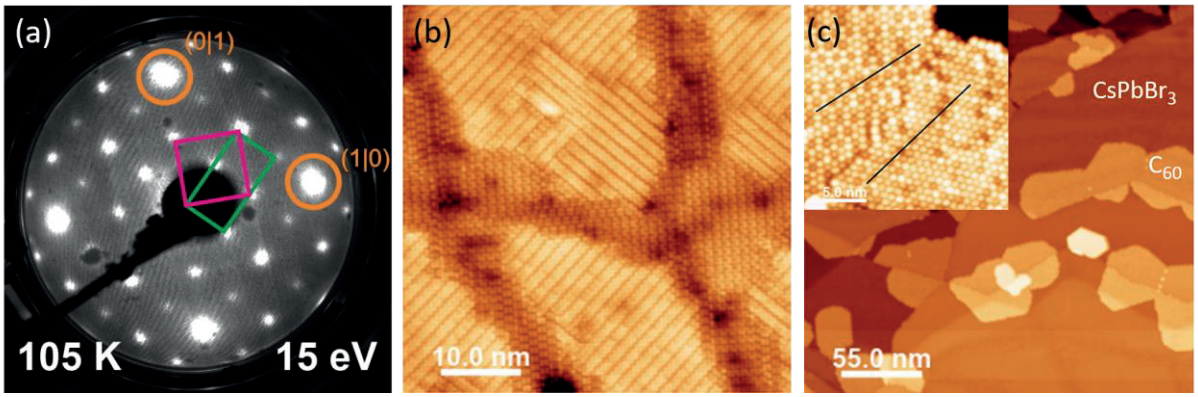

Fig. 1. (a) LEED pattern and (b) STM scan at 80 K of a 5 ML thick $CsPbBr_3$ film on Au(100). The beam indices in (a) refer to the unreconstructed $CsPbBr_3$ (001) unit cell. (c) shows the surface with sub-monolayer amounts of C_{60} deposited. In the inset the two dominant molecular arrangements are depicted that are slightly rotated with respect to each other.

Particularly, the topology of the perovskite thin films can be tuned by changing their CsBr / $PbBr_2$ ratio. This influences the relative abundance of the two surface reconstructions and the workfunction measured by ultra-violet photoemission spectroscopy [1]. While there are indications that the terminations of the films may be tuned from CsBr-like to $PbBr_2$-like by changing the ratio of CsBr / $PbBr_2$ during growth an alternative explanation could be the stabilisation of the $(2\sqrt{2} \times \sqrt{2})$ surface reconstruction by defects that are healed when a "$PbBr_2$-rich" film is prepared which shows a (2×2) reconstruction only. The current state of this will be discussed.

When depositing submonolayer amounts of C_{60} on the films at room temperature we find single-layer-high molecular islands. The molecules are ordered in a hexagonal pattern with nearest-neighbor distance of 1 nm. After post-annealing to 150 °C the molecular layers rearrange to become multi-layer high islands. These observations are interpreted as a consequence of a dominant molecule-molecule and a relatively low molecule-substrate interaction. STS shows that the LUMO resides below and the LUMO+1 above the conduction band minimum.

[1] J. Rieger, T. Kisslinger, A. Raabgrund, J. Hauner, D. Niesner, M.A. Schneider, Th. Fauster, Phys. Rev. Materials **7**, 035403 (2023)

[2] J. Hieulle, S. Luo, D.-Y. Son, A. Jamshaid, C. Stecker, Z. Liu, G. Na, D. Yang, R. Ohmann, L. K. Ono, L. Zhang, Y. Qi, J. Phys. Chem. Lett., **11**, 818 (2020)

Spatially resolved surface X-ray diffraction on polycrystalline surfaces

H. Sjö[1] A. Shabalin[2], U. Lienert[2], J. Hektor[3], A. Schaefer[4],
P.-A. Carlsson[4], J. Gustafson[1]

[1] *Lund University, Division of Synchrotron Radiation Research, Lund, Sweden*

[2] *Deutsches Elektronen-Synchrotron DESY, Hamburg, Germany*

[3] *Department of Materials Science and Applied Mathematics, Malmö University, Malmö, Sweden*

[4] *Department of Chemistry and Chemical Engineering, Chalmers University of Technology, Göteborg, Sweden*

(corresponding author: H. Sjö, e-mail: hanna.sjo@sljus.lu.se)

Polycrystalline surfaces are of interest when studying, for example, catalytic reactions since they are more realistic model catalysts than single crystals and allow us to measure more than one surface orientation at once. There are tools, such as electron backscattering diffraction[1] and photoemission electron microscopy[2], that can be used to study polycrystalline surfaces, but these are limited to vacuum environments. Surface X-ray diffraction (SXRD) can measure long-range atomic structures down to sub-Ångström resolution, even in high-pressure or liquid environments. SXRD is, however, currently limited to simple samples, such as single crystals, since the long beam footprint, stemming from the grazing incidence angle, will give signal from large parts of the sample. We use the high intensity in small X-ray beams, available at modern synchrotrons, to develop spatially resolved SXRD to complement the operando surface science toolbox. This is part of a project that aims to create a tool for full maps using CTRs and superstructure rods, providing spatially resolved maps of surface structures through the so-called tomographic surface X-ray diffraction (TSXRD). In this presentation, we will give an update on the progress with examples of methane oxidation over polycrystalline Pd.

The first step in the methodology development is a method for grain mapping polycrystalline surfaces using an SXRD setup. For this, we use the near-surface Bragg reflections together with tools from 3D-XRD[3,4], adapted to a surface diffraction setup. With a wide beam and a fast analysis, this provides the orientation and center of mass position of the different grains. With more thorough measurements and analysis, spatially resolved maps are achieved (see Figure 1a). Knowing the grain positions allows us to perform SXRD scans, rotating the sample around its surface normal, with specific grains at the center of rotation. This enables us to follow the surface diffraction from the selected grains.

Figure 1b-d shows preliminary results from polycrystalline Pd during methane oxidation. A selection of grains were scanned while the temperature was increased slowly in a mixture of 1 mbar O_2 and 0.05 mbar CH_4. By following the shape of the CTRs, we can follow how the initial structure changes. Here, we look at the intensity summed along a CTR, relative to the initial intensity, and find that the change varies between different grains. For example, the CTR belonging to grain 4 drops more than that of grain 1, compared to the metallic surface. Furthermore, the oxide signal is stronger for grain 4.

In conclusion, mapping surfaces using x-ray diffraction allows us to find the grain structure, even under operando conditions. The method of scanning grains can, similar to a classic SXRD measurement, provide information about surface structure and surface changes, as shown here for polycrystalline Pd. These are the first steps in developing TSXRD, where, as a complement to single scans of grains, maps of the whole sample can be created for an even deeper understanding of the polycrystalline sample as a catalyst.

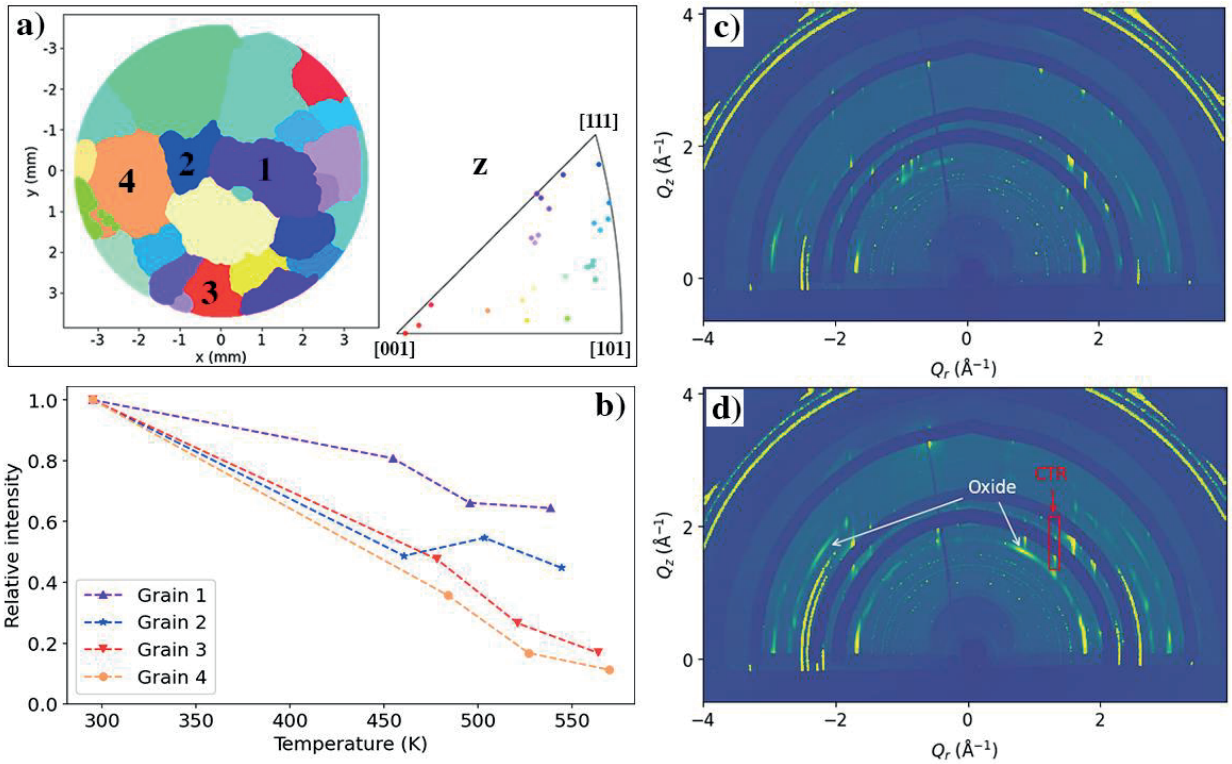

Figure 1: a) The inverse pole figure map of the polycrystalline Pd sample from grazing incidence XRD. The numbers mark the grains used in b). **b)** The summed intensity, relative to the summed intensity before heating, of a CTR of the grains in a) plotted against the temperatures when the scan started. **c)** The SXRD result at 538 K for grain 1. An oxide signal is visible. **d)** The SXRD result at 544 K for grain 4. A strong oxide signal is visible. Examples of oxide and the CTR used for this grain are marked.

[1] A.-F. Gourgues-Lorenzon, Journal of Microscopy, 233, 460-473 (2009)
[2] P. Winkler, J. Zeininger, Y. Suchorski, M. Stöger-Pollach, P. Zeller, M. Amati, L. Gregoratti & G. Rupprechter, Nature Communications volume 12, (2021)
[3] S. Schmidt, Journal of Applied Crystallography, 47, 276-284 (2014)
[4] E. M. Lauridsen, Journal of Applied Crystallography, 34, 744-750 (2001)

Strong coupling between surface excitations observed by STEM - EELS

P. Gallina[1], M. Kvapil[1,2], A. Konečná[1,2], O. Bitton[3], J. Liška[1,2], L. Houben[3], V. Křápek[1,2], R. Kalousek[1,2], G. Haran[4], J. C. Idrobo[5], and T. Šikola[1,2]

[1] *CEITEC BUT, Brno University of Technology, 612 00 Brno, Czech Republic*
(corresponding author: T. Šikola, e-mail: sikola@fme.vutbr.cz)

[2] *Institute of Physical Engineering, Brno University of Technology, 61669 Brno, Czech Republic*

[3] *Chemical Research Support Department, Weizmann Institute of Science, Rehovot, Israel¨*

[4] *Department of Chemical and Biological Physics, Weizmann Institute of Science, Rehovot, Israel*

[5] *Center for Nanophase Materials Sciences, Oak Ridge National Laboratory, Oak Ridge, Tennessee, USA*

In the recent years, strong coupling between different types of surface excitations, for instance surface plasmon polaritons with excitons or phonon polaritons, has become a subject of a growing interest. It has been caused by both the fundamental and application research reasons covering new quantum nano-optics effects, electromagnetically induced transparency (EMT), chemical dynamics and reactivity, and other novel issues. Such an interesting physical phenomenon associated with the Rabi splitting and creation of new hybrid modes has been mostly studied by conventional reflection/transmission optical spectroscopic methods. However, using these techniques not all modes can be generated and observed. Therefore, there are attempts to study these coupling effects by application of electron beams capable of generating sub-radiant dark modes and being suitable for their detection by electron energy loss spectroscopy (EELS). To do it both at sufficient spatial (< 10 nm) and energy ($\leq 10^0$ eV) resolutions, STEM-EELS systems with monochromatized probe electron beams have to be used.

In the presentation, basic principles of STEM-EELS physics and technique will be explained and relevant examples shown.

First, strong coupling between localized surface plasmons (LSPs) and excitons in the visible optical range will be presented. It will be demonstrated that a dark mode of an individual plasmonic bowtie antennas can interact with a small number of quantum emitters, as evidenced by Rabi-split spectra [1].

Second, strong coupling effects between LSPs and vibration modes of SiO_2 membranes will be discussed. As the frequencies of these modes fall into the mid-IR regions, such

experiments represent a challenging experimental task. Therefore, a state-of-the art STEM-EELS system providing energy resolution below 10 meV (Nion) located in the Oak Ridge National Laboratory was used. More specifically, the study covers an electromagnetic coupling between MIR phonon polaritons (PhPs) in a silicon dioxide membrane and low-energy LSP modes formed by the confinement of plasmon polaritons in micrometer-long gold antennas. It will be shown that by precisely positioning the electron beam, the coupling between the polaritonic excitations can selectively trigger either uncoupled PhPs or coupled LSPs/PhPs [2]. Further, the results on comparative optical spectroscopy experiments showing that far-field IR spectra can be substantially different from the EEL spectra will be presented as well.

We acknowledge support from the EU H2020 project 810626 – SINNCE, Czech Science Foundation (Grant No. 20-28573S), and MEYS - Czech Republic (CzechNanoLab Research Infrastructure - LM2018110). EELS measurements were supported by the Center for Nanophase Materials Sciences (CNMS), which is a U.S. Department of Energy, Office of Science User Facility.

[1] O. Bitton et al, Nat. Commun. 11, 487 (2020).
[2] P. Gallina et al., Phys. Rev. Appl. 19, 024042 (2023).

Probing the molecular conformation *via* photoemission orbital tomography.

David Maximilian Janas,[1] Andreas Windischbacher,[2] Mira Sophie Arndt,[1] Peter Puschnig,[2] Mirko Cinchetti,[1] Giovanni Zamborlini[1,2]

[1] *TU Dortmund University, Department of Physics, 44227 Dortmund, Germany*
[2] *Karl-Franzens-Universit¨at Graz, Institut für Physik, NAWI Graz, 8010 Graz, Austria*
(corresponding author: G. Zamborlini, e-mail: giovanni.zamborlini@uni-graz.at)

Tetrapyrrolic compounds, such as porphyrins and phthalocyanines, have raised a lot of attention due to their remarkable chemical stability and outstanding tunability. [1] Their chemical and physical properties can be controlled on-demand either by attaching different peripheral substituents to their tetrapyrrolic unit, or *via* the incorporation of different transition metal ions in their center. On proper surface templates, porphyrins can be confined in two-dimensional (2D) arrays, where the chemical state and the adsorption properties of each molecule are well-defined and homogeneous. This opens the possibility of utilizing them in a variety of electronic and spintronic devices and exploiting them as single-atom catalysts.

In this regard, the macrocycle conformation is one of the keys to control the chemical and physical properties of the molecule, as it can strongly affect in the electronic structure, altering not only the optical properties [2] but affecting also the capability of the metal center of anchoring ligands, which would be the first step for a catalytic reaction. For example, it has been demonstrated that the macrocycle saddling (*i.e.* tilting of the macrocyclic pyrrole rings) can promote the coordination of CO in a *cis*- or *trans*-configuration either to the pyrrole groups or the metal center, respectively, while the ligation does not occur for a completely planar macrocycle. [3] Therefore, understanding those properties is pivotal for the design and implementation of organic-based devices.

So far, the molecular conformation was often probed by X-Ray Absorption Spectroscopy (XAS) and ultraviolet photoemission spectroscopy (UPS) was used to access the molecular electronic structure. While the former requires tunable X-ray radiation and thus can only be performed at synchrotron facilities, the latter suffers from the energy overlap of broad molecular states, that complicates the determination of the orbital origin for each peak, which is vital for a deeper understanding of the substrate-molecule interaction, as well as intermolecular interactions for multilayer films.

However, with specific assumptions about the photoemission transition matrix element, it is possible to compare the angular (momentum) distribution of the photoemitted electrons to the modulus square of the Fourier transform $|FT|^2$ of a specific molecular orbital, which can be calculated by means of density functional theory (DFT). This approach is called photoemission orbital tomography (POT), [4] which has proven to be a valuable tool for accessing both the electronic structure and the molecular adsorption geometry. [5]

By means of POT supported by density functional theory calculations (DFT), we investigate the electronic and geometrical structure of two metallated tetraphenyl porphyrins (MTPPs),

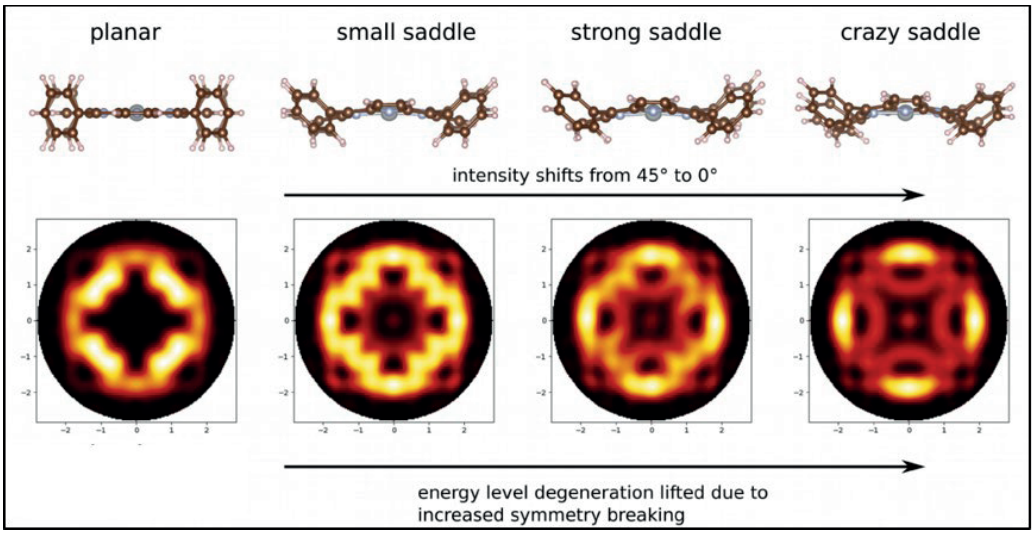

Figure 1. Simulated POT data of the NiTPP HOMO as a function of the macrocycle saddling, from a planar (left) to an extremely saddled configuration (right).

namely ZnTPP and NiTPP, adsorbed on the oxygen-passivated Fe(100)-p(1x1)O surface. [6] Both molecules weakly interact with the surface as no charge transfer is observed. In the case of ZnTPP our data correspond to those of moderately distorted molecules, while NiTPP exhibits a severe saddle-shape deformation. In fact, the photoelectron intensity distribution of the molecular orbitals strongly depends on the geometrical conformation of the macrocycle. The macrocycle saddling induces significant changes in the simulated momentum maps (See Figure 1). Therefore, by comparing the simulated and experimental data, it is possible to quantify with extreme precision the saddling degree of the molecular backbone, while at the same time we can access its electronic structure.

From additional experiments on NiTPP multilayer films, we conclude that this distortion is a consequence of the interaction with the substrate, as the NiTPP macrocycle of the second layer turns out to be flat. We further find that distortions in the MTPP macrocycle are accompanied by an increasing energy gap between the highest occupied molecular orbitals (HOMO and HOMO-1). Our results demonstrate that photoemission orbital tomography can simultaneously probe the energy level alignment, the azimuthal orientation, and the adsorption geometry of complex aromatic molecules even in the multilayer regime.

[1] J. M. Gottfried, Surf. Sci. Rep. **70**, 259 (2015).
[2] R. E. Haddad, S. Gazeau, J. Pécaut, J.-C. Marchon, C. J. Medforth, and J. A. Shelnutt, J. Am. Chem. Soc. **125**, 1253 (2003).
[3] P. Knecht, J. Reichert, P. S. Deimel, P. Feulner, F. Haag, F. Allegretti, M. Garnica, M. Schwarz, W. Auw, P. T. P. Ryan, T. Lee, D. A. Duncan, A. P. Seitsonen, J. V Barth, and A. C. Papageorgiou, Angew. Chem. Int. Ed. **60**, 16561 (2021).
[4] P. Puschnig, S. Berkebile, A. J. Fleming, G. Koller, K. Emtsev, T. Seyller, J. D. Riley, C. Ambrosch-Draxl, F. P. Netzer, and M. G. Ramsey, Science (80-.). **326**, 702 (2009).
[5] P. Hurdax, C. S. Kern, T. G. Boné, A. Haags, M. Hollerer, L. Egger, X. Yang, H. Kirschner, A. Gottwald, M. Richter, F. C. Bocquet, S. Soubatch, G. Koller, F. S. Tautz, M. Sterrer, P. Puschnig, and M. G. Ramsey, ACS Nano **16**, 17435 (2022).
[6] D. M. Janas, A. Windischbacher, M. S. Arndt, M. Gutnikov, L. Sternemann, D. Gutnikov, T. Willershausen, J. E. Nitschke, K. Schiller, D. Baranowski, V. Feyer, I. Cojocariu, K. Dave, P. Puschnig, M. Stupar, S. Ponzoni, M. Cinchetti, and G. Zamborlini, Inorganica Chim. Acta **557**, 121705 (2023).

Angle-resolved photoemission mapping of hybrid states characteristic of metal-organic nanostructures

D. Baranowski[1], M. Thaler[2], D. Brandstetter[3], A. Windischbacher[3], I. Cojocariu[1,4,5], S. Mearini[1], V. Chesnyak[5,6], L. Schio[6], L. Floreano[6], C. Gutiérrez Bolaños[7,8,9], P. Puschnig[3], L. L. Patera[2], V. Feyer[1,10] and C. M. Schneider[1,10,11]

[1] *Peter Grünberg Institute (PGI-6), Jülich Research Center, 52428 Jülich, Germany (corresponding author: D. Baranowski, e-mail: d.baranowski@fz-juelich.de)*

[2] *Institute of Physical Chemistry, University of Innsbruck, 6020 Innsbruck, Austria*

[3] *Institute of Physics, University of Graz, 8010 Graz, Austria*

[4] *Elettra-Sincrotrone, S.C.p.A, S.S 14 - km 163.5, 34149 Trieste, Italy*

[5] *Dipartimento di Fisica, Università degli Studi di Trieste, Via A. Valerio 2, 34127 Trieste, Italy*

[6] *TASC Laboratory, CNR-IOM, 34149 Trieste, Italy*

[7] *CNR-ICMATE and INSTM, 35131 Padova, Italy*

[8] *Structure and Mechanics of Advanced Materials, Paul Scherrer Institute, 5232 Villigen, Switzerland*

[9] *Institute of Materials, Ecole Polytechnique Federale Lausanne, 1015 Lausanne, Switzerland*

[10] *Faculty of Physics and Center for Nanointegration Duisburg-Essen (CENIDE), University of Duisburg-Essen, 47048 Duisburg, Germany*

[11] *Department of Physics and Astronomy, UC Davis, CA 95616 Davis, USA*

Supramolecular self-assembly at the solid-vacuum interface allows precise control over the fabrication of metal-organic structures via coordination bonds between organic linkers and transition metal cores [1]. Single layers of extended metal-organic frameworks, tunable by the interaction with the supporting surface, become experimentally accessible with highest precision. This is crucial for both a fundamental understanding of their properties and the design of miniaturized devices [2]. A deep understanding of the interaction between the transition metal core's 3*d* orbitals and ligand π orbitals is critical in this context. This interaction defines the delocalization effects, contributing to exciting functionalities like high electrical conductivity [3] and magnetic coupling between transition metal cores [4]. Angle-

resolved photoemission spectroscopy appears as the ideal tool for the characterization of the frontier electronic properties of metal-organic structures. Low intensities, radiation damage, averaging out of different symmetry-equivalent domains, the experimental availability of only higher order Brillouin zones at high $k_{\parallel}$ values as well as the superposition of the states of the metal-organic framework with the ones of their supporting surface make their characterization quite challenging [5].

For organic molecules adsorbed on surfaces the same challenges apply. When collecting the photoelectron hemisphere up to large $k_{\parallel}$ values around 2 A^{-1}, the photoelectron distribution patterns characteristic of molecular overlayers become quite evident and distinct from the features of the surface underneath. Then, a protocol that allows to correlate their characteristic photoelectron distribution patterns in *k*-space to their real-space molecular orbitals based on a plane-wave photoemission final state can be applied. This protocol is known as photoemission orbital tomography [6], and, its applicability to metal-organic nanostructures would be desirable as a direct probe of their frontier electronic properties. Indeed, we demonstrate this is the case based on the Ni 3*d*-based states characteristic of different metal-organic phases, which are constituted by Ni cores and the organic ligand 1,2,4,5-tetracyanobenzene (TCNB). Depending on the amount of Ni a pristine TCNB layer on Au(111) was exposed to [7], isolated metal-organic $Ni(TCNB)_4$ complexes are transformed into the extended two-dimensional metal-organic $Ni(TCNB)_2$ framework. Thereby, the Ni 3*d*-based molecular orbitals characteristic of the isolated $Ni(TCNB)_4$ units evolve into energy-dispersive states characteristic of the extended $Ni(TCNB)_2$ structure. Furthermore, we show how the metal-organic framework can be tuned via charge transfer when grown on the more reactive Ag(100) surface. Thereby, we address the fact how the photoelectron distribution patterns are further influenced due to different amounts of symmetry-equivalent domains when compared to Au(111).

We acknowledge Elettra Sincrotrone Trieste for providing access to its synchrotron radiation facilities.

[1] J. Barth, et al., Nature 437, 671–679 (2005).
[2] J. Lui, et al., J Phys Chem Lett 13, 1356–1365 (2022).
[3] X. Huang, et al., Nat Commun 6, 7408 (2015).
[4] R. Dong, et al., Nat Commun 9, 2637 (2018).
[5] F. Frezza, et al., Nanoscale 15, 2285–2291 (2023).
[6] P. Puschnig, et al., Science 326, 702-706 (2009).
[7] S. Kezilebieke, et al., Nano Research 7, 888-897 (2014).

Single particle catalysis: Lanthanum effect on a Rh nanotip in hydrogen oxidation

Maximilian Raab, Johannes Zeininger, Yuri Suchorski, Alexander Genest, Carla Weigl, Günther Rupprechter

Institute of Materials Chemistry, TU Wien, Getreidemarkt 9/BC, 1060 Vienna, Austria
(corresponding author: guenther.rupprechter@tuwien.ac.at)

Operando spectroscopy of catalytic reactions has been very successful in mechanistic studies [1]. However, as spectroscopy typically examines large areas/volumes, this averaging "smoothens out" local variations that may be critical to understand how a reaction proceeds. Furthermore, dynamics in catalyst structure, composition and adsorbate coverage may also go unnoticed by averaged spectral data.
A straightforward way overcoming these limitations is to use correlative surface microsopy [2,3] to directly "watch" ongoing catalytic reactions both at the mesoscale and nanoscale: the very same catalyst locations are imaged by different microscopic techniques under identical conditions, preferentially in a single apparatus.

Along these lines, field ion microscopy (FIM) enables to determine the atomic surface structure and shape of a single metal nanoparticle, while field emission microscopy (FEM) can be applied to the very same nanoparticle for real-time *in situ* imaging of an ongoing catalytic reaction (Fig. 1) [4]. Note that both methods not only image the catalyst, but also the locally-resolved adsorbed reactants, so that active and inactive states can be discerned (kinetics by imaging [5]), active regions identified and mechanisms elucidated (active/bright vs. inactive/dark; see. e.g. videos in the SI of [4]).

This revealed a wealth of information, providing detailed insight on various phenomena: (i) transition from the inactive to the active state via chemical waves, how reaction fronts spread on different terminations, and the coexistence of regions with different activity, (ii) the mechanism of oscillatory reactions, (iii) whether different facets on a single nanoparticle communicate via adsorbate diffusion or not (coupled monofrequential vs. (uncloupled) multifrequential oscillations) [2-5].

In the presented work [6], FEM was applied for real-time *in situ* imaging of H_2 oxidation on a single Rh nanoparticle (mimicked by a nanotip apex with 18 nm radius), revealing self-sustained oscillations at constant external parameters. These "automatic" periodic switches between active and inactive states, together with knowledge of atomic surface structure, provide deep insight into structure sensitivity and the reaction mechanism. The observed spatio-temporal oscillations result from coupling of subsurface oxide formation/depletion with reaction front propagation. A custom-designed method for tracking kinetic transition points allowed identifying the most active nanoparticle regions, which initiate kinetic transitions and

reaction fronts [4]. These so-called “pacemakers” were not simply steps, kinks or adatoms, buth rather specific surface atomic configurations at the interface between strongly corrugated and adjacent flat regions. The first enable oxygen subsurface incorporation, the latter sufficient hydrogen supply, highlighting the importance of interfacet communication via adsorbate diffusion.

Furthermore, the effect of La adatoms on the very same Rh nanotip was examined (Fig. 1a) [6]. Such “additives” are important in catalysis, but atomistic details of their function are often unknown. A La-mediated local catalytic effect was revealed: the presence of La shifts the bistable reaction states, changes the oscillation pattern and deactivates one of two pacemaker types (Fig. 1, bottom left). The experimental observations were corroborated by micro-kinetic model simulations comprising a system of 25 coupled oscillators, as well as density functional theory (DFT), rationalizing that the observed effects originate from La-enhanced oxygen activation on Rh. The novel nanoscale insights in the dynamics of reactants and surfaces, including the identification of active regions, may stimulate new ways of catalyst design and operation.

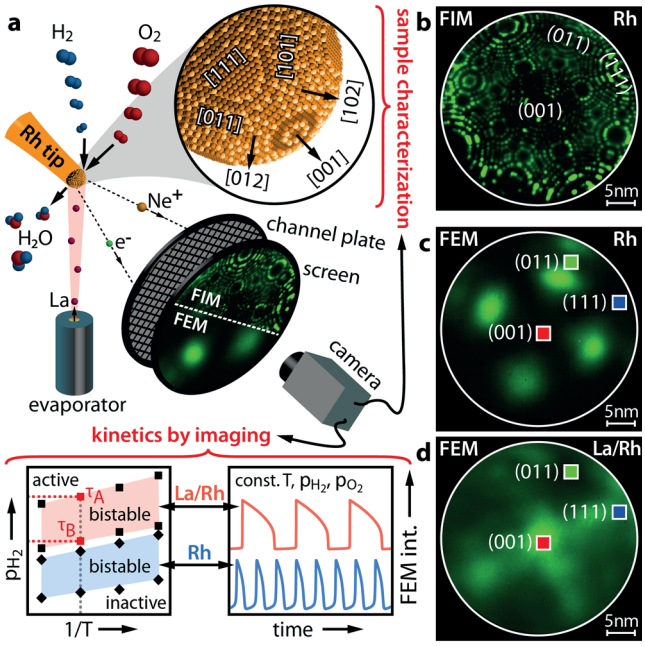

Figure 1. Single particle catalysis: (**a**) Experimental setup: In FIM and FEM, field emitted ions and electrons, respectively, form a point projection image of the sample surface. Benefitting from the adsorbate dependent FEM image intensity, *in situ* kinetic studies can be performed. A La-evaporator produces sub-monolayer La coverages on Rh; (**b**) atomically resolved FIM image of the [001]-oriented Rh nanocrystal, obtained at T = 77 K using Ne^+ ions; (**c**) FEM image of the same field of view as in (**b**) with square ROIs placed on the indicated facets; (**d**) FEM image of the same Rh nanocrystal and field of view as in (**b, c**), but with additionally 0.2 ML La. The effect of La on H_2 oxidation is illustrated on the bottom left.

Support by the Austrian Science Fund (FWF; SFB TACO F81-P08 und P32772-N) is gratefully acknowledged.

[1] G. Rupprechter, Small 2004289 (2021)
[2] J. Zeininger et al., ACS Catalysis 12, 11974 (2022)
[3] Y. Suchorski et al., Science 372, 1314 (2021)
[4] J. Zeininger et al., ACS Catalysis, 1110020 (2021)
[5] Y. Suchorski and G. Rupprechter, Surface Science 643, 52 (2016)
[6] M. Raab et al., Nature Communications 13, 282 (2023)

Simulating high-pressure surface reactions with molecular beams

Amjad Al Taleb[1], Frederik Schiller[2], Denis V. Vyalikh[3,4], J. María Pérez[1], Sabine V. Auras[5], Daniel Farías[1,6,7], and J. Enrique Ortega[2,3,5]

[1]*Facultad de Ciencias, Universidad Autónoma de Madrid, Madrid, Spain*

[2]*Centro de Física de Materiales CSIC/UPV-EHU-Materials Physics Center, San Sebastián, Spain*

[3]*Donostia International Physics Center, San Sebastián, Spain*

[4]*IKERBASQUE, Basque Foundation for Science, Bilbao, Spain*

[5]*Universidad del País Vasco, Dpto. Física Aplicada, San Sebastian, Spain*

[6]*Instituto "Nicolás Cabrera", Universidad Autónoma de Madrid, Madrid, Spain*

[7]*Condensed Matter Physics Center (IFIMAC), Universidad Autónoma de Madrid, Madrid, Spain*

Using a reactive molecular beam with high kinetic energy (E_{kin}) it is possible to speed gas-surface reactions involving high activation barriers (E_{act}), which would require elevated pressures (P_0) if a random, Maxwell-Boltzmann gas is used. By simply computing the number of molecules that overcome the activation barrier in a random gas at P_0 and in a molecular beam at $E_{kin}=E_{act}$ (Fig. 1a), we establish a $P_0(E_{kin})$ equivalence curve (Fig. 1b). Based on this curve, we postulate that molecular beams are ideal tools to investigate gas/surface reactions that involve high E_{act}, such as the activation of greenhouse gases (CH_4 and CO_2) on metal catalysts. In particular, we foresee the use of molecular beams to simulate the industrial-range in such reactions (>10 bar) while making use of X-ray photoemission spectroscopy (XPS). To test this idea, we revisit the oxidation of Cu(111) combining O_2 molecular beams and XPS [1]. By tuning the kinetic energy of the O_2 beam in the range 0.24-1 eV we achieve the same sequence of surface oxides obtained in Ambient Pressure Photoemission (AP-XPS) experiments, in which the Cu(111) surface was exposed to a random O_2 gas up to 1 mbar. Moreover, we observe the same surface oxidation kinetics as in the random gas, but with a much lower dose, close to the expected value derived from the equivalence curve in Fig. 1.

We deeply acknowledge Prof. Clemens Laubschat (TU Dresden), who willingly donated the XPS instruments used in this collaboration. This work has been partially supported by the Spanish Ministerio de Ciencia e Innovación under project TED2021-130446B-I00. The COST Action CA21101 is also acknowledged. D.F. acknowledges financial support from the Spanish Ministry of Economy and Competitiveness, through the "María de Maeztu" Programme (CEX2018-000805-M). SVA acknowledges funding from the European Union's Horizon Europe Programme under the Marie Skłodowska-Curie grant (101066965 CURVEO).

[1] A. Al Taleb et al. DOI: 10.1039/D3CP05071H.

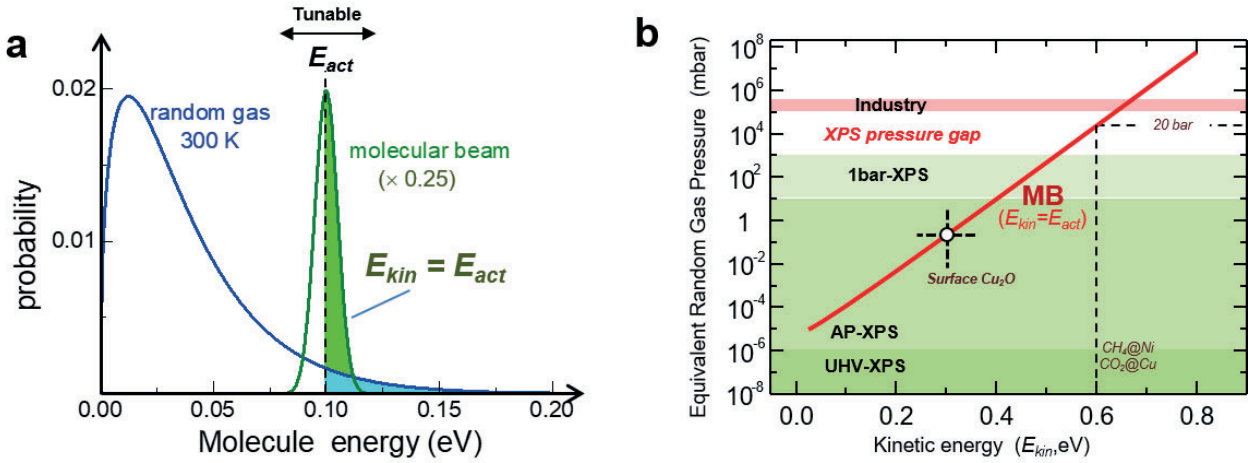

Figure 1. **(a)** Probability distribution curves for molecules in a random, Maxwell-Boltzmann gas at 300 K (blue), and within a molecular beam tuned to E_{kin}=E_{act} = 0.1 eV (green). The area under the curve is normalized to 1 in both cases. The shaded areas mark the number of molecules *n* that are active in each case, being $n_{molecular\text{-}beam} = 20 \times n_{random\text{-}gas}$. **(b)** Molecular-beam/random-gas equivalence curve (red) for molecular reactions of activation energy E_{act}=E_{kin}, assuming a molecular beam of standard flux (10^{15} mol/cm^2·s). The equivalence line has been satisfactorily proved in the oxidation of the Cu(111) surface [1].

Post deadline contributions

Towards understanding interfacial thermodynamics: visualising and quantifying competitive adsorption on muscovite mica with AFM

M. Olgiati[1,2], A. T. Celebi[1], J. Dziadkowiec[1,3], L. L. E. Mears[1], M. Valtiner[1,2]

[1] *Vienna University of Technology, Institute of Applied Physics, Wiedner Hauptstrasse 8-10, 1040 Vienna, Austria*

[2] *CEST (Centre for Electrochemical Surface Technology), Viktor-Kaplan-Strasse 2, 2700 Wiener Neustadt, Austria*

[3] *NJORD Centre, Department of Physics, University of Oslo, Oslo 0371, Norway*

Given its peculiar crystal structure and inherent surface charge, the (001) plane of muscovite mica has served as an excellent model system to study the hydration and electric double layer (EDL) forces at solid-liquid interfaces [1]. So far, force spectroscopies, which measure along the direction perpendicular to the surface, as well as molecular dynamics (MD) simulations, have demonstrated a certain ion-specificity towards the strength of hydration forces on mica surfaces [2-5]. These deviations are mainly attributed to the different properties of individual ions (e.g., hydration shell, size, valency, etc.), which ultimately determine their adsorption character on mica, as well as the interfacial hydration structure [5]. Nevertheless, lateral distribution and arrangement of cations adsorbed on mica was experimentally investigated only to a lesser extent [6], although unravelling the ions' organisation directly at the surface is crucial to elucidate the structure and properties of EDLs.

In the present contribution, we discuss how high-resolution atomic force microscopy (AFM) imaging enables us to visualize the lateral distribution of individual mono- and multi-valent ions on the surface of mica. Thanks to this approach, we are able not only to resolve the crystal structure of mica immersed in aqueous solution, but also to transiently picture the population of adsorbed ions from the salt-rich solutions at different concentrations. By using an automated triangulation algorithm, the ion adsorption coverage as a function of concentration can be quantified in a first order approximation. This methodology highlights the possibility to outline a certain competitive behaviour of charged species at the surface. Understanding such competition as a function of type and concentration of ions allows us to unravel the interfacial thermodynamics directly from AFM data, which has been so far mainly exclusive to MD simulations. To further support our findings, we use surface force apparatus and MD simulations to characterise the structure and mechanical properties of EDLs on mica for different cation species.

References:

[1] R. M. Pashley, Journal of Colloid and Interface Science 83, 2, 531-546 (1981).

[2] T. Baimpos, B. R. Shrestha, S. Raman and M. Valtiner, Langmuir 30, 4322-4332 (2014).

[3] Z. Zachariah, R. M. Espinosa-Marzal and M. P. Heuberger, Journal of Colloid and Interface Science 506, 263-270 (2017).

[4] I. C. Bourg, S. S. Lee, P. Fenter and C. Tournassat, The Journal of Physical Chemistry C 121, 9402-9412 (2017).

[5] S. R. van Lin, K. K. Grotz, I. Siretanu, N. Schwierz and F. Mugele, Langmuir 35, 5737-5745 (2019).

[6] M. Ricci, P. Spijker and K. Voitchovsky, Nature Communications 5, 4400 (2014).

Author Index

USM1400 UHV LT-SPM & Optics

USM1500 2K & affordable magnets

USM1300 400mK high field magnets

USM1600 The milli Kelvin SPM

USM1800 *DryCool*
~5K, no LHe consumption

USM1200 LT-STM
< 5K, low LHe consumption

NEW: USM1200-JT LT-STM
<1K, 3T magnet option

UNISOKU
TII Group

NEW!
USM1200 and
USM1800 now available
with **flag** style sample
holders!

USM1200: Ultimate STM/STS Resolution

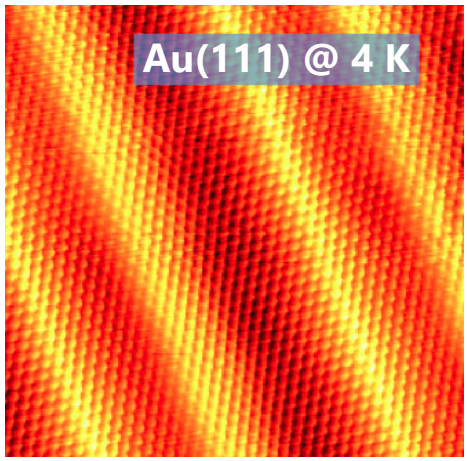

USM1200/ USM1200-JT

Excellent cooling performance
JT stage operated with ^{3}He gas

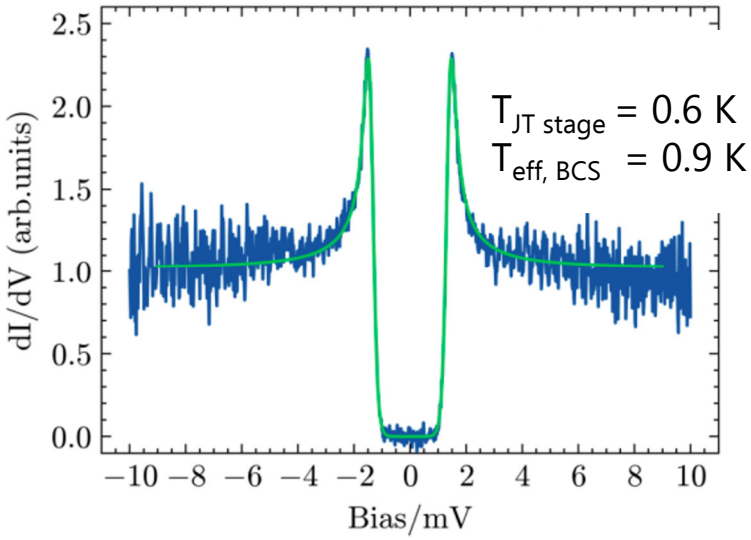

T < 1K proven by SC gap of Pb

3S'24

SYMPOSIUM ON SURFACE SCIENCE 2024
St. Christoph am Arlberg, Austria
March 10 - 16, 2022

Friedrich Aumayr, Ulrike Diebold and Markus Valtiner, organizers
Institute of Applied Physics, TU Wien, Vienna, Austria

Sunday, 10 Mar. 2024

16:00 - 18:30	REGISTRATION
18:30 - 19:30	DINNER
20:00 - 20:20	OPENING

chair: AUMAYR

20:25 - 20:45	MAIER
20:45 - 21:05	MAGNUSSEN
21:05 - 21:25	BARTH

Monday, 11 Mar. 2024

07:15 - 08:00	BREAKFAST

chair: NETZER

08:00 - 08:20	REUTER
08:20 - 08:40	LUNDGREN
09:15 - 12:00	SKIING INSTRUCTIONS
12:00 - 13:00	LUNCH
13:30 - 15:30	SKIING INSTRUCTIONS

chair: DIEBOLD

16:40 - 17:00	SCHNEIDER W D
17:00 - 17:20	ODOBESKO
17:20 - 17:40	SANCHEZ-PORTAL
17:40 - 18:00	VAZQUEZ DE PARGA
18:00 - 18:20	DIL
18:30 - 19:30	DINNER

chair: BLIEM

19:30 - 19:50	MORGENSTERN
19:50 - 20:10	GIESSIBL
20:10 - 20:30	MORESCO
20:30 - 20:50	BRUNE
20:50 - 21:10	ZAIATS

Tuesday, 12 Mar. 2024

07:15 - 08:00	BREAKFAST

chair: LEMELL

08:00 - 08:20	WILLINGER
08:20 - 08:40	STARKE
09:15 - 12:00	SKIING INSTRUCTIONS
12:00 - 13:00	LUNCH
13:30 - 15:30	SKIING INSTRUCTIONS

chair: NIGGAS

16:40 - 17:00	CHESNYAK
17:00 - 17:20	JUGOVAC
17:20 - 17:40	YUHARA
17:40 - 18:00	MOLLE
18:00 - 18:20	AKINWANDE
18:30 - 19:30	DINNER

chair: MITTENDORFER

19:30 - 19:50	LIU
19:50 - 20:10	DE OTEYZA
20:10 - 20:30	VESTERGAARD
20:30 - 20:50	BALJOZOVIC
20:50 - 21:10	BUCK

Wednesday, 13 Mar. 2024

07:15 - 08:00	BREAKFAST

chair: DECURTINS

08:00 - 08:20	VONK
08:20 - 08:40	JAKUB
09:15 - 12:00	SKIING INSTRUCTIONS
12:00 - 13:00	LUNCH
13:30 - 15:30	SKIING INSTRUCTIONS

chair: MIANO

16:40 - 17:00	RATH
17:00 - 17:20	PAVELEC

chair: JELINEK

17:25 - 18:25	POSTER INTRODUCTION
18:30 - 19:30	DINNER
19:30 - 21:30	POSTERSESSION

Thursday, 14 Mar. 2024

07:15 - 08:00	BREAKFAST

chair: SILKIN

08:00 - 08:20	ERNST
08:20 - 08:40	VONBUN-FELDBAUER
09:15 - 12:00	SKIING INSTRUCTIONS
12:00 - 13:00	LUNCH
13:30 - 15:30	SKIING INSTRUCTIONS

chair: CELEBI

16:40 - 17:00	KUNZE-LIEBHÄUSER
17:00 - 17:20	LARSSON
17:20 - 17:40	MESSING
17:40 - 18:00	IBANEZ-AZPIROZ
18:00 - 18:20	MÜLLER
18:30 - 19:30	DINNER

chair: VALTINER

19:30 - 19:50	BERGHAUS
19:50 - 20:10	MIRABELLA
20:10 - 20:30	ALTMANN
20:30 - 20:50	BRÖTZNER
20:50 - 21:10	KOGLER

Friday, 15 Mar. 2024

07:15 - 08:00	BREAKFAST

chair: KOCAN

08:00 - 08:20	SETVIN
08:20 - 08:40	LIBUDA
09:15 - 12:00	GIANT SLALOM RACE
12:00 - 13:00	LUNCH
13:30 - 15:30	SKIING INSTRUCTIONS

chair: HELLBERG

16:30 - 16:50	SCHNEIDER A
16:50 - 17:10	SJÖ
17:10 - 17:30	SIKOLA
17:30 - 17:50	ZAMBORLINI
17:50 - 18:10	BARANOWSKI

chair: SWIECH

18:30 - 18:50	RUPPRECHTER
18:50 - 19:10	ORTEGA
19:10 - 19:40	GIANT SLALOM RACE AWARD CEREMONY
20:00	CONFERENCE DINNER